Defense Nuclear Agency
Alexandria, VA 22310-3398

DNA-TR-94-113

Design, Construct and Test the Hi-Therm Simulator

Peter D. Zavitsanos, et al.
General Sciences, Incorporated
205 Schoolhouse Road
Souderton, PA 18964-2416

February 1998

Technical Report

CONTRACT No. DNA 001-90-C-0089

DESTRUCTION NOTICE:

Destroy this report when it is no longer needed.
Do not return to sender.

PLEASE NOTIFY THE DEFENSE SPECIAL WEAPONS AGENCY, ATTN: CSTI, 6801TELEGRAPH ROAD, ALEXANDRIA, VA 22310-3398, IF YOUR ADDRESS IS INCORRECT, IF YOU WISH IT DELETED FROM THE DISTRIBUTION LIST, OR IF THE ADDRESSEE IS NO LONGER EMPLOYED BY YOUR ORGANIZATION.

DISTRIBUTION LIST UPDATE

This mailer is provided to enable DSWA to maintain current distribution lists for reports. (We would appreciate your providing the requested information.)

☐ Add the individual listed to your distribution list.

☐ Delete the cited organization/individual.

☐ Change of address.

NOTE:
Please return the mailing label from the document so that any additions, changes, corrections or deletions can be made easily. For distribution cancellation or more information call DSWA/IMAS (703) 325-1036.

NAME: _____

ORGANIZATION: _____

OLD ADDRESS	CURRENT ADDRESS
_____	_____
_____	_____
_____	_____

TELEPHONE NUMBER: ( ) _____

DSWA PUBLICATION NUMBER/TITLE	CHANGES/DELETIONS/ADDITIONS, etc.) *(Attach Sheet if more Space is Required)*
_____	_____
_____	_____
_____	_____

DSWA OR OTHER GOVERNMENT CONTRACT NUMBER: _____

CERTIFICATION OF NEED-TO-KNOW BY GOVERNMENT SPONSOR (if other than DSWA):

SPONSORING ORGANIZATION: _____

CONTRACTING OFFICER OR REPRESENTATIVE: _____

SIGNATURE: _____

CUT HERE AND RETURN

DEFENSE SPECIAL WEAPONS AGENCY
ATTN: IMAS
6801 TELEGRAPH ROAD
ALEXANDRIA, VA 22310-3398

DEFENSE SPECIAL WEAPONS AGENCY
ATTN: IMAS
6801 TELEGRAPH ROAD
ALEXANDRIA, VA 22310-3398

REPORT DOCUMENTATION PAGE

Form Approved
OMB No. 0704-0188

1. AGENCY USE ONLY (Leave blank)	2. REPORT DATE	3. REPORT TYPE AND DATES COVERED
	980201	Technical 910116 - 940531

4. TITLE AND SUBTITLE
Design, Construct and Test the Hi-Therm Simulator

5. FUNDING NUMBERS
C - DNA 001-90-C-0089
PE - 62715H
PR - RG
TA - RE
WU - DH304630

6. AUTHOR(S)
Peter D. Zavitsanos, Michael C. Matthews, L. D. DeDominicis, Howard Semon, and Kenneth Lerner

7. PERFORMING ORGANIZATION NAME(S) AND ADDRESS(ES)
General Sciences, Incorporated
205 Schoolhouse Road
Souderton, PA 18964-2416

8. PERFORMING ORGANIZATION REPORT NUMBER
GSI-DNA-59

9. SPONSORING/MONITORING AGENCY NAME(S) AND ADDRESS(ES)
Defense Special Weapons Agency
6801 Telegraph Road
Alexandria, VA 22310-3398
ESA/O'Shaughnessy

10. SPONSORING/MONITORING AGENCY REPORT NUMBER
DNA-TR-94-113

11. SUPPLEMENTARY NOTES
This work was sponsored by the Defense Special Weapons Agency under RDT&E RMC Code B4662D RG RE 10044 TDTR 5200A 25904D.

12a. DISTRIBUTION/AVAILABILITY STATEMENT
Approved for public release; distribution is unlimited.

12b. DISTRIBUTION CODE

13. ABSTRACT *(Maximum 200 words)*

The technical effort described in this report represents a continuation of the work conducted for the Defense Special Weapons Agency (DSWA) by General Sciences, Incorporated (GSI), under a Small Business Innovative Research (SBIR) Phase I effort, contract number DNA001-87-C-0152, and an SBIR Phase II effort, contract DNA001-85-C-0338, both entitled "Nuclear Effects Simulation - Thermal Effects." Under the previous SBIR programs, GSI investigated the application of highly exothermic intermetallic reactions with the most energetic of these reactions constituting the basis for the Hi-Therm Simulator.

The objective of the technical effort pursued under this effort was to develop and demonstrate a thermal source simulator prototype which is capable of uniformly irradiating a 30-foot by 10-foot area with a target plane peak flux of 150 cal/cm^2/sec (628 W/cm^2). At the 150 cal/cm^2/sec peak flux capability, the simulator must be capable of providing a predetermined thermal fluence level in the range of 50 to 450 cal/cm^2 (209 to 1883 J/cm^2). The thermal simulator must be designed so that it will not interfere with the blast effects of a DNA High Explosive full field test. This report summarizes the developmental effort conducted at GSI and the two sets of demonstration tests conducted at the DNA Thermal Radiative Source Test Site, Coyote Canyon, Kirtland AFB, NM, in April and November 1992.

14. SUBJECT TERMS
Simulators
Weapon Effects
Thermal Radiation
Nuclear Explosion Simulation
Heat Flux (Thermal)

15. NUMBER OF PAGES
142

16. PRICE CODE

17. SECURITY CLASSIFICATION OF REPORT	18. SECURITY CLASSIFICATION OF THIS PAGE	19. SECURITY CLASSIFICATION OF ABSTRACT	20. LIMITATION OF ABSTRACT
UNCLASSIFIED	UNCLASSIFIED	UNCLASSIFIED	SAR

CLASSIFIED BY:

N/A since Unclassified.

DECLASSIFY ON:

N/A since Unclassified.

SUMMARY

The program pursued under this effort addressed the application of utilizing reactive intermetallic compositions, configured as a flat panel, as fieldable thermal radiation source to simulate the thermal radiation output of a nuclear explosion. Encouraging results were recorded on subscale tests with recorded emittance values of 108-155 cal/cm^2/sec [452-648 W/cm^2] of radiative thermal output with little or no discernible particulate throw at a distance of five feet from the radiating panel. However, the final scale-up configurations of the thermal radiation source simulator did not meet DNA operational requirements due to excessive particulate ejecta against the test material being irradiated and due to flux and fluence levels at too low a level for compositions which did not produce a particulate fireball when used. This report describes the development effort pursued, the design of the thermal radiation simulator and the results of the field tests at the DNA Permanent High Explosive Test Site, White Sands Missile Range, NM.

Fabrication of higher density panels of the reactive intermetallic composition, having minimal porosity with elimination of volatile constituents, is recommended as a means of meeting the DNA objectives using the radiating panel approach.

PREFACE

This Technical report covers the work conducted by General Sciences, Incorporated (GSI), under the Defense Nuclear Agency (DNA) contract number DNA001-90-C-0089, entitled "Design, Construct and Test the Hi-Therm Simulator," from January 16, 1991, to May 31, 1994. This effort is a continuation of the work conducted by GSI under a Small Business Innovative Research (SBIR) Phase I effort, contract number DNA001-87-C-0152, and an SBIR Phase II effort, contract DNA001-85-C-0338, both entitled "Nuclear Effects Simulation - Thermal Effects."

The developmental and small scale testing performed under this effort was conducted at GSI with main offices in Souderton, PA, under the direction of Dr. Peter D. Zavitsanos. The DNA Technical Point of Contact was Ms. Ellice Patinak/TDTR.

Special thanks to Ellice Patinak, DNA/TDTR, Ed Martinez, DNA/FCTD, and SMSgt Michael Yoas, TRS Test Site, Coyote Canyon, Kirtland AFB, for their support in coordinating and conducting the Hi-Therm demonstration tests which were conducted at Kirtland AFB, NM.

The findings in this effort are not to be considered as official DNA position, unless designated by other authorizing documents.

Mention of any trade names or manufacturer(s) in this report shall not be considered as advertising nor as an official endorsement or approval of such products or companies by the United States Government.

CONVERSION TABLE

MULTIPLY — BY — TO GET TO GET — BY — DIVIDE		
Calorie (cal)	4.184	Joule (J)
Calorie/centimeter^2/second (cal/cm^2/sec)	4.184	Watts/centimeter^2 (W/cm^2)
Joules/second (J/sec)	1	Watts (W)
Meters (m)	3.2808	Feet (ft)
Rankine (R)	0.555556 (5/9)	Kelvin (K)

TABLE OF CONTENTS

TABLE OF CONTENTS (Continued)

FIGURES

FIGURES (Continued)

FIGURES (Continued)

FIGURES (Continued)

TABLES

SECTION 1

INTRODUCTION

1.1 GENERAL.

The technical effort described in this report represents a continuation of the work conducted for the Defense Nuclear Agency (DNA) by General Sciences, Incorporated (GSI), under a Small Business Innovative Research (SBIR) Phase I effort, contract number DNA001-87-C-0152, and an SBIR Phase II effort, contract DNA001-85-C-0338, both entitled "Nuclear Effects Simulation - Thermal Effects."

The immediate phenomena associated with a nuclear explosion are shock and air blast, thermal radiation, and nuclear radiation. In order for a military asset to remain effective in a modern battlefield, it must be capable of surviving in a nuclear environment. DNA has been given the responsibility for ensuring that military equipment be tested under simulated nuclear explosion conditions in order to estimate the effects of a nuclear explosion on the equipment and the degree of nuclear survivability. The effects of combined shock and air blast, and thermal radiation, resulting from a nuclear explosion, necessitate a test methodology by which these combined effects can be simulated. The methodology pursued by DNA is to simulate the shock and air blast with either a mass of high explosives in full field evaluations or with a shock tube in smaller scale tests, with a separate device to provide the thermal radiation transfer to the material or equipment being evaluated.

Currently, for full scale thermal effects simulation, DNA employs a Thermal Radiation Source (TRS) comprised of a linear array of upwardly directed nozzles which produce a high temperature flame/plume from a chemical reaction between flowing liquid oxygen and aluminum powder (TRS Brochure - LBTS units 80 & 800). The TRS can produce target fluxes of up to 70 cal/cm^2/sec (293 W/cm^2). The spectral emission of the TRS is roughly equivalent to that produced by a blackbody emitter at 2800 K (for a surface emittance of approximately 83 cal/cm^2/sec [349 W/cm^2]). The TRS is a cooler source than the fireball produced by a nuclear explosion which produces an effective radiating temperature of 6000 - 7500 K (DA PAM 50-3) with the TRS producing a spectral profile shifted towards longer (infrared) wavelengths.

The goal of this program was to develop an alternative to the liquid oxygen and aluminum used in the TRS unit. Under the previous SBIR Phase I and II contract efforts, referenced above, GSI investigated the application of highly exothermic solid state intermetallic reactions with the most energetic of these reactions constituting the basis for the GSI Hi-Therm Simulator. Intermetallic reaction systems are formed from mixtures of two or more elemental powders which, when ignited, form an intermetallic alloy. These reactive compositions (labeled "Hi-Therm") can be highly exothermic with the reaction proceeding as a condensed phase steady state reaction (self-propagating high-temperature synthesis) according to the following general relationship:

$$\text{Metal A} + \text{Element B} \rightarrow \text{Intermetallic Alloy} + \text{Energy}$$

where 'A' metals are typically of Groups IV and V of the periodic table and the 'B' elements are typically aluminum, boron, carbon, nitrogen and silicon. Intermetallic reactions proceed

pyrotechnically without requiring an outside oxidizer source (such as atmospheric oxygen). Energy levels released by these types of reactions can reach 4.2 kcal/cm^3 (17.6 kJ/cm^3), which compares favorably to the energy release from the detonation of explosives (1.7 kcal/cm^3 [7.1 kJ/cm^3] for TNT and 2.8 kcal/cm^3 [11.9 k/J/cm^3] for HMX). The temperature increase produced by intermetallic reactions can exceed 3500K with reaction products ranging from hot solid radiating particulates and sintered surfaces, to molten intermetallic alloys, to vaporized atoms, to combinations of these products. These reaction products can further react with atmospheric oxygen to form oxides with the energy release of an additional 11.8 kcal/cm^3 (49.3 kJ/cm^3). The titanium plus boron reaction (i.e., $Ti + 2B \rightarrow TiB_2$) has an intrinsic heat of reaction of 1.15 kcal/gram (4.81 kJ/gram) with this reaction forming the basis for the Hi-Therm panel development.

The previous GSI contractual effort towards the development of a Hi-Therm Simulator culminating with a four foot by four foot (16 - one square foot panels) Hi-Therm test at Aberdeen Proving Ground, MD, on April 13, 1989 (Zavitsanos, 1989). Photos of this test (before, during, after) are shown in Figure 1-1. Three Schmidt-Boelter heat flux gauges, equipped with bandpass filters at 2.1 - 2.7 micron (μm), 3.0-5.0 μm and 1.56-1.72 μm (supplied by Science Applications International Corporation [SAIC]) were located 10 feet in front of the Hi-Therm panel. A 0.4 - 30 μm radiometer and a 0.4 - 0.7 μm light probe were located at 100 feet from the panel. The initiation of the Hi-Therm panel resulted in a high flux density fireball projecting a particulate plume extending approximately 10 feet in front of the panel. This particulate plume impacted the three heat flux gauges located at 10 feet, producing heat flux densities characterized by a combination of thermal radiation, conduction and convention, rather than just thermal radiation. The formation of a particulate fireball resulted in a change in the source to detector distance and the resulting effective radiating area used to calculate source emittance values. The emittance values reported below represent those produced from a 16 square foot (4 foot x 4 foot) panel at the original thermal source to detector distance and neglects the effects of the expanding particulate fireball. Table 1-1 summarizes the results of this test. The Hi-Therm intermetallic reaction system material used for this test was 62 wt.% Ti + 28 wt.% B + 10 wt.% CaS04, with the Hi-Therm panels fabricated by slurrying the reactive mixture, pouring into 1 foot x 1 foot aluminum trays and drying. Ignition for each panel was accomplished by running an electrical current through an ignition wire embedded in the reactive mixture.

The particulate fireball formed by the 16 square foot Hi-Therm panel was unexpected as testing conducted with one square foot panels, using the same configuration and materials, did not produce any appreciable particulate plume. The particulate plume produced by the 16 square foot Hi-Therm panel may be attributed to effects linked to scale-up to the larger dimension. The results of the previous efforts, including the results of the 16 square foot panel, and DNA thermal radiation simulator and test requirements, form the basis for the objectives discussed below. The details of the Hi-Therm material development are presented in Appendix A.

1.2 OBJECTIVES.

The objective of the technical effort pursued under this effort was to develop and demonstrate a thermal source simulator prototype which is capable of uniformly irradiating a 30 foot by 10 foot area with a target plane peak flux of 150 cal/cm^2/sec (628 W/cm^2). At the 150 cal/cm^2/sec peak flux capability, the simulator must be capable of providing a predetermined

Panel assembly prior to ignition	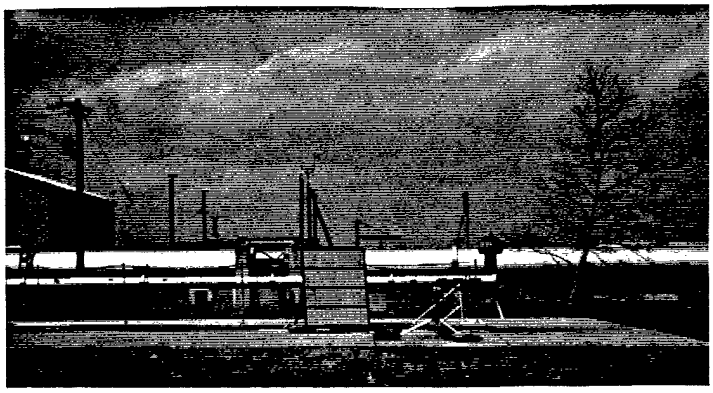
During Hi-Therm reaction	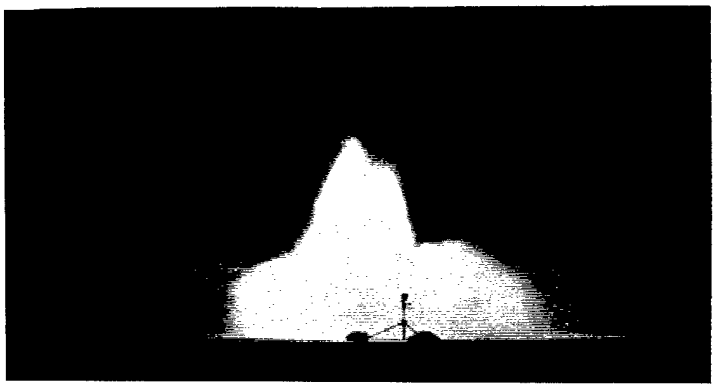
Following reaction, during cool down	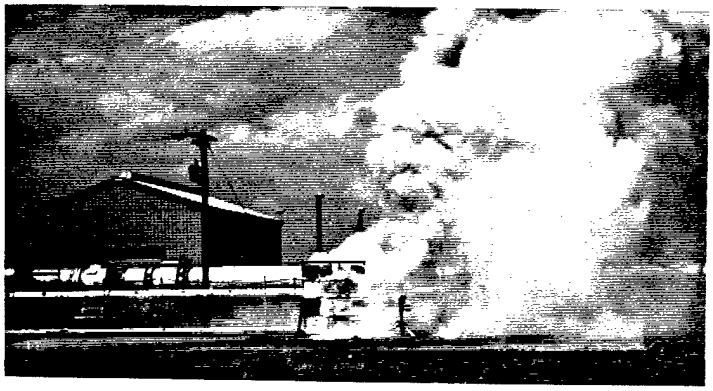

Figure 1-1. Hi-Therm Thermal Simulation (4 foot x 4 foot array).

thermal fluence level in the range of 50 to 450 cal/cm^2 (209 to 1883 W/cm^2). The thermal simulator must be designed so that it will not interfere with the blast effects of a DNA High Explosive full field test. Specific technical objectives which were determined at program inception, or which evolved during the course of the effort, follow:

(1) Maximize peak thermal flux on target with a goal of 150 cal/cm^2/sec (628 W/cm^2) and a controlled fluence of between 50 to 450 cal/cm^2 (209 to 1883 W/cm^2). However, peak fluxes down to 20 cal/cm^2/sec (84 W/cm^2) would be acceptable for some targets given that the only thermal transfer mechanism is radiative and that a uniform source is generated.

Table 1-1. Summary of heat flux data, Hi-Therm Thermal Simulation (4 foot x 4 foot array).

Sensor Number	Sensor Type	Bandwidth (micron)	Distance (ft)	Distance (m)	Maximum Heat Flux Before Fireball Impact (cal/cm^2/sec)	Maximum Heat Flux Before Fireball Impact (W/cm^2)	Maximum Heat Flux After Fireball Impact (cal/cm^2/sec)	Maximum Heat Flux After Fireball Impact (W/cm^2)
1	Schmidt-Boelter	2.1 - 2.7	10	3.05	0.566	2.37	1.83	7.65
2	Schmidt-Boelter	3.0 - 5.0	10	3.05	1.230	5.13	2.45	10.26
3	Schmidt-Boelter	1.56 - 1.72	10	3.05	0.416	1.74	1.26	5.27
4	Radiometer	0.4 - 30	100	30.5	0.0982	0.411	n/a	n/a
5	Light Probe	0.4 - 0.7	100	30.5		6200 lux	n/a	n/a

Sensor Number	Effective Blackbody Temperature Before Fireball Impact (K)	After Fireball Impact (K)	After Fireball Impact (cal/cm^2/sec)	Effective Source Emittance Before Fireball Impact (cal/cm^2/sec)	Before Fireball Impact (W/cm^2)	After Fireball Impact (cal/cm^2/sec)	After Fireball Impact (W/cm^2)
1	Average of 1, 2 & 3 2700	4200	301	72	301	421	1761
2							
3							
4	3450	n/a	n/a	192	803	n/a	n/a
5	2450	n/a	n/a	49	204	n/a	n/a

(2) Minimize the particulate ejecta formed during the ignition and reaction of the Hi-Therm material while maintaining the required high flux and fluence levels.

(3) Reduce the amount of smoke (Hi-Therm material oxides and obscuring reaction products) generated between the Hi-Therm Thermal Simulator and the target to be irradiated.

(4) Design a supporting frame for the Hi-Therm Thermal Simulator which is capable of being removed from the path of the high explosive shock and air blast wave. The simulator panel and frame must be capable of being lowered into a ditch or trough no more then 2 feet across (which is normal to the advancing high explosive shock front) and have a final position such that no part of the simulator is above grade level. The drop time requirements are 1/2 seconds desired and 1 (one) second required. A mechanical assist may be used, if required, to meet the drop time requirements.

(5) Develop an improved ignition system of the Hi-Therm Thermal Simulator panels which ensures multipoint initiation of the panels to produce a more uniform (spatially and temporally) radiating panel. The ignition system must also be shown to be insensitive to the electrostatic and electromagnetic field conditions found at the TRS Test Site, Coyote Canyon, Kirtland AFB, and the DNA Permanent High Explosive Test Site, White Sands Missile Range, NM.

(6) Develop a Hi-Therm panel production process such that the Hi-Therm reactive intermetallic composition and panels could be prepared at a location near the test site.

(7) Develop documentation required to support site operation procedures for the Hi-Therm Thermal Simulator and the support package detailing required DNA mission support to fielding the Hi-Therm Simulator.

To meet these objectives the following experimental program was conducted.

SECTION 2

EXPERIMENTAL

2.1 HI-THERM SIMULATOR PANEL FABRICATION.

The panels used throughout this program were fabricated using the reactive Hi-Therm powder slurry casting process developed in prior programs with modifications made to enhance panel initiation and timing.

The reactive Hi-Therm material powders are first mixed in a V-blender or drum rolled to achieve a homogeneous powder mix. Acetone is added to the dry powder to form a slurry. The resultant slurry is then poured into aluminum panel trays, the acetone evaporated, and the panels sealed. The panels consisted of a 12 inch by 12 inch aluminum tray with 1/2 inch high walls. An insulator is placed in the bottom of the tray (Fiberfax) and the initiation system installed. The reactive Hi-Therm slurry mixture is poured into the tray, and after drying, the panel is sealed in aluminum foil and placed in a plastic bag to minimize water absorption during storage. The initiation system consisted of a coupling through the rear of the Hi-Therm panel tray which allowed attachment of the initiation system to the Hi-Therm panel firing line. To ensure propagation of the cast reactive powder throughout the panel, a Pyrofuze ignition train was wound within the panel and attached to the rear connector. Pyrofuse is a palladium cladded aluminum wire which, when ignited, reacts rapidly with an adiabatic release of 327 cal/gram (1368 J/gram) to form a hot liquid palladium aluminide intermetallic alloy. The adiabatic reaction temperature is 2655 K (Pyrofuse Corp.), well in excess of the initiation temperature of 1000 K for the titanium/boron reaction which is the heart of the Hi-Therm reaction system. The rear of the aluminum tray is fitted with rotating locking clips which are used to secure the panel to the Hi-Therm simulator frame. The Hi-Therm Simulator Drop Frame design is discussed in Paragraph 2.6, below. Figure 2-1 shows a sketch of a Hi-Therm Panel.

2.2 HI-THERM MATERIAL DEVELOPMENT TESTS.

Past work has yielded Hi-Therm intermetallic reactions offering high fluxes along with the ejection of particulates from the radiating surface. This phase of the program attempted to increase the radiative output, decrease throw and explore alternate intermetallic reactions offering modified temporal characteristics.

Initial tests consisted of reduced scale analysis, reproducing earlier work and laying the groundwork for radiative enhancement, and selected approaches to particulate ejection control. Also, processing parameters were evaluated and tailored to simplify the final processing procedure. Results covering a wide range of emittance values and temporal profiles were obtained. The most promising chemistries and configurations were chosen for intermediate scale (1 foot x 1 foot) testing. Thirty-eight tests were conducted using the intermediate scale Hi-Therm Panels leading into an intermediate scale test of the optimal Hi-Therm formulation developed with minimum particulate ejection and with a 9 square foot (3 foot by 3 foot) test of the Hi-Therm formulation developed for maximum thermal output. These first two demonstration tests, designated DNA 92-39 and DNA 92-40 are discussed below. Additional information relating to the 38 initial, and two final tests (DNA 92-39 and DNA 92-40) is presented in Appendix A, Hi-Therm Development Test Detail. The GSI development tests

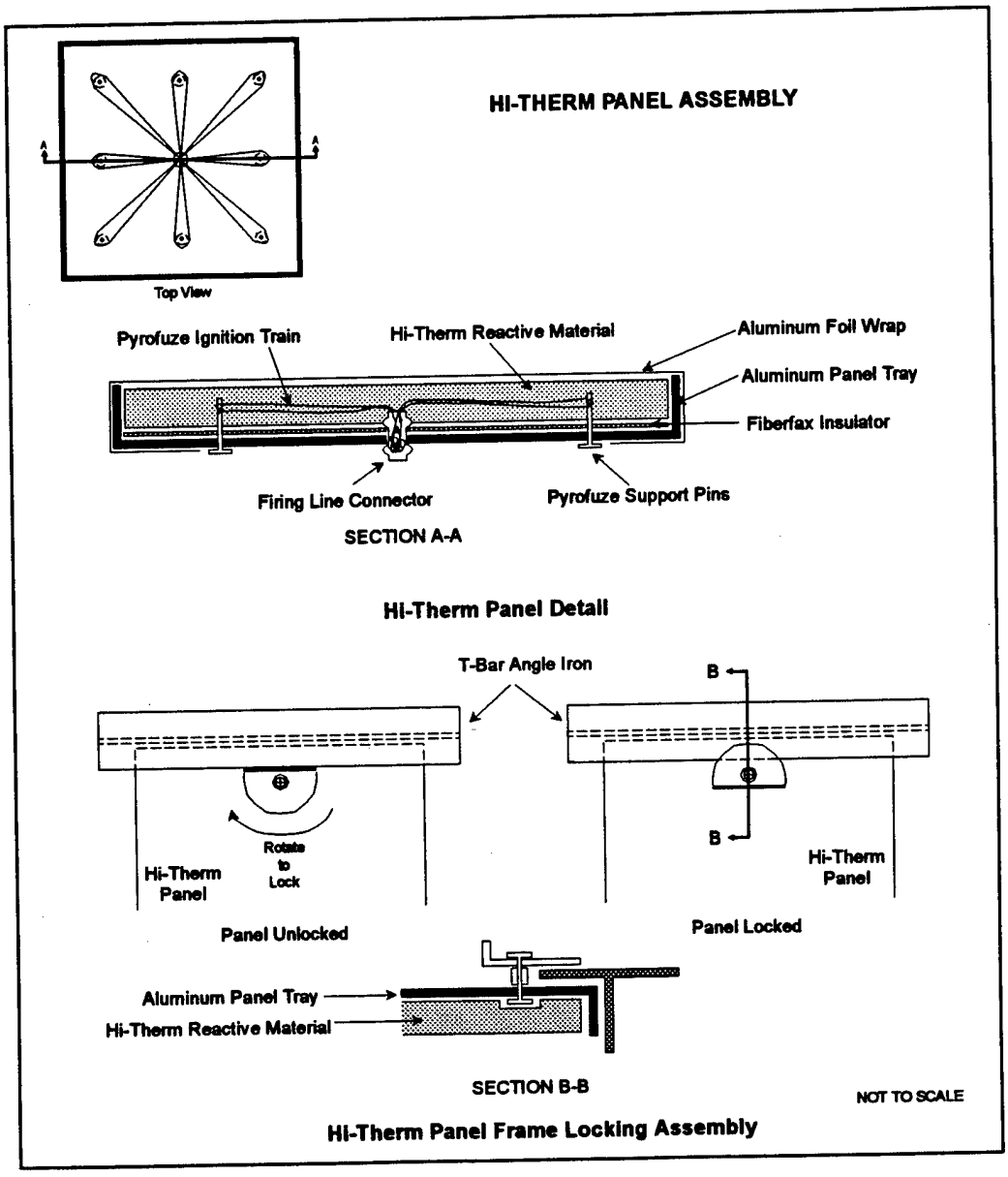

Figure 2-1. Hi-Therm panel assembly.

yielded two candidate compositions (DNA 92-39 and DNA 92-40) which were selected for final in-house assessment. The results of the assessment of these two candidates are discussed in the following paragraphs.

2.2.1 Minimal-Throw Hi-Therm Panel (DNA 92-39).

The minimal throw formulation developed utilized a combination of highly exothermic intermetallic reactants and used fiberglass fibers as a reinforcing aide. This formulation is represented as

71.1 wt.% Ti + 18.1 wt.% B + 7.8 wt.% C + 3 wt.% Fiberglass

and was prepared using the slurry cast process. When initiated, a rise time of approximately 1.2 seconds, and a pulse duration of approximately 2.2 seconds, was observed. From the total radiometer located 100 ft from the panel, the surface emittance was calculated as 78 cal/cm^2/sec (326 W/cm^2) for an effective surface temperature of 2755 K. Some masking of the Hi-Therm source resulted from the set-up of calorimeters located between the radiometer and the Hi-Therm panel. This masking may have contributed to a lower source emittance value for the radiometer when compared to the calorimeter results. The calorimeters were located at distance of 3, 5, 10 and 10 feet from the Hi-Therm panel and recorded emittance values of 155, 124, 108 and 109 cal/cm^2/sec (648, 519, 452 and 456 W/cm^2), respectively. There were little or no discernible particulates ejected at a distance of 5 feet from the panel.

2.2.2 High Flux Hi-Therm 9 Square Foot Panel Test (DNA 92-40).

The formulation developed under this effort which demonstrated the highest flux output is represented as

62.0 wt.% Ti + 28.0 wt.% B + 10 wt.% Al.

Nine panels of this formulation were prepared slurry casting and tested as a 3 foot by 3 foot array. Test instrumentation was set up in the same locations as in the DNA 92-39 test. Photos of the test set-up are shown in Figures 2-2 and 2-3.

Radiometric analysis of this test yielded a rise time to peak flux of approximately 0.65 seconds with a pulse duration of approximately 1.3 seconds. Upon initiation of the 9 panel array, a particulate fireball approximately 10 feet in diameter was formed, which entrained particulates to the calorimeters at 10 feet within a hot radiating cloud. Figures 2-4 through 2-11 show photos of this test at a framing rate of 6 frames per second (0.167 seconds between frames). The calorimeters produced detector fluxes of 46, 19.7 and 20.9 cal/cm^2/sec (192, 82.4 and 87.4 W/cm^2) at 5, 10 and 10 feet respectively (note - these calorimeters were engulfed by the particulate fireball produced during this test). The radiometer located 35 feet from the Hi-Therm panel array measured a maximum detector flux of 0.302 cal/cm^2/sec (1.26 W/cm^2) which roughly corresponds to a surface temperature of 3125 K. The radiometer at 100 feet yielded a detector flux of 0.068 cal/cm^2/sec (0.28 W/cm^2) which corresponds to a surface emittance of 237 cal/cm^2/sec (992 W/cm^2) and an effective surface temperature of 3638 K. The surface emittance calculations for the radiometers with 35 and 100 feet assumes that the panel has an effective surface area of 9 square meters (i.e., no fireball formation). Assuming a 10 foot diameter fireball, the emittance of the surface of the fireball from the data recorded at 35 feet is 25 cal/cm^2/sec (105 W/cm^2) and from the 100 foot radiometer location is also 25 cal/cm^2/sec (105 W/cm^2).

The high flux formulation was selected for the demonstration test conducted in April, 1992, at the TRS Site, Kirtland AFB, NM. These tests are described in paragraph 2.3, below.

2.2.3 Radiometric Equations.

The radiometric equations used to estimate the surface emittance and effective blackbody temperature of the Hi-Therm simulator are summarized below.

Figure 2-2. Test DNA 92-40 setup overview.

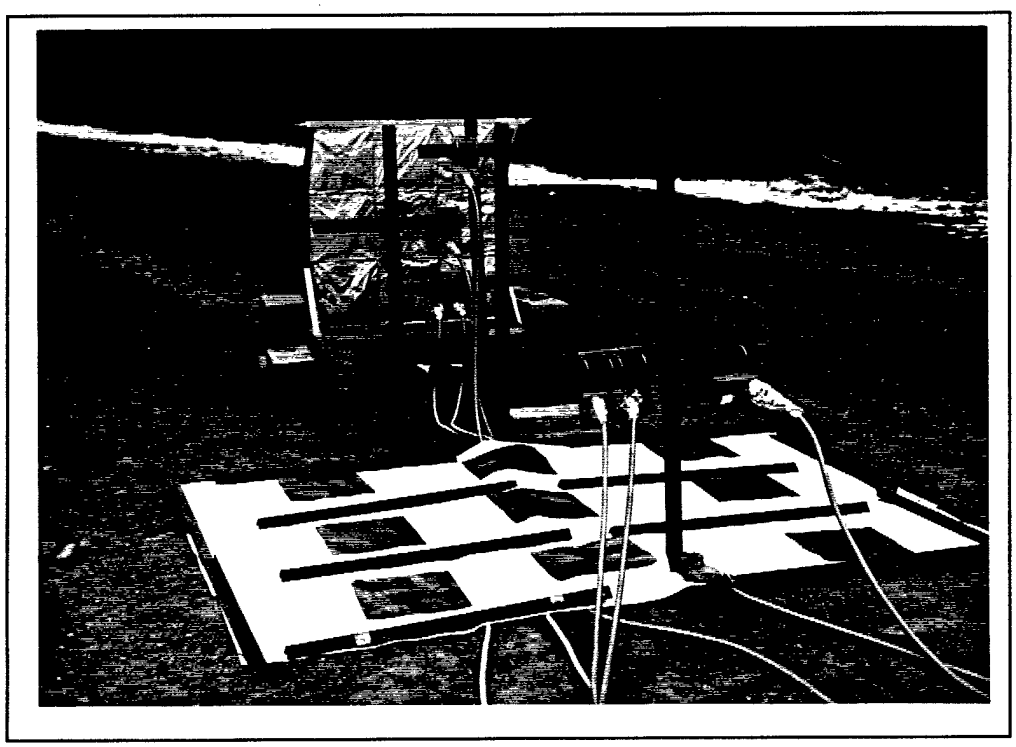

Figure 2-3. Test DNA 92-40 setup close-up.

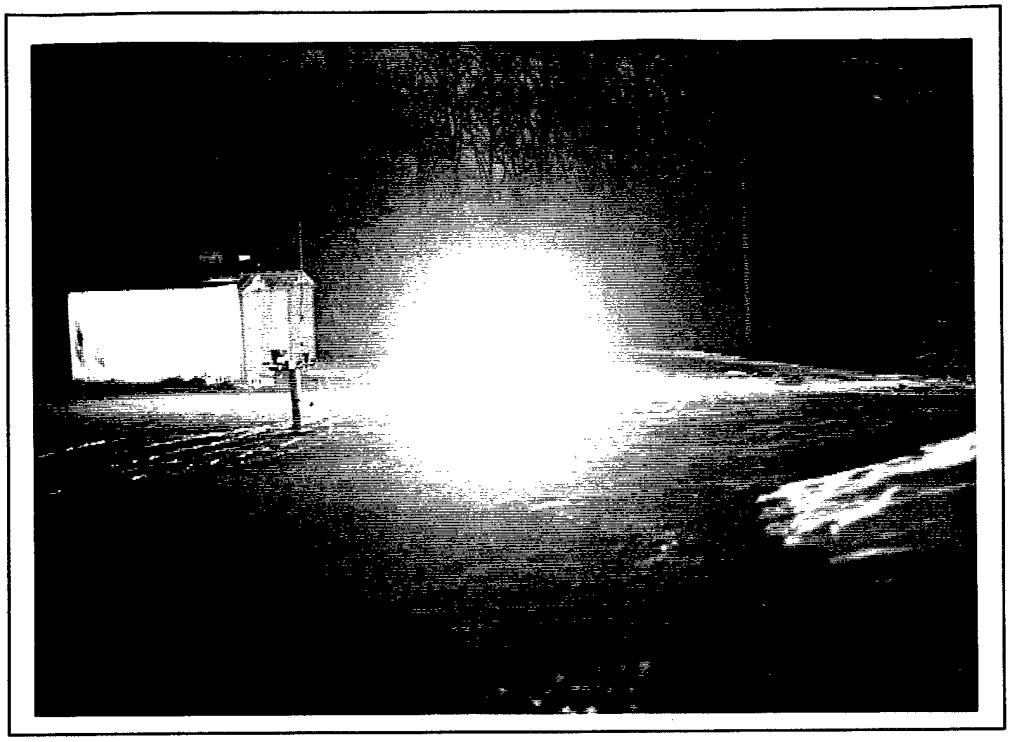

Figure 2-4. Test DNA 92-40 photo #1.

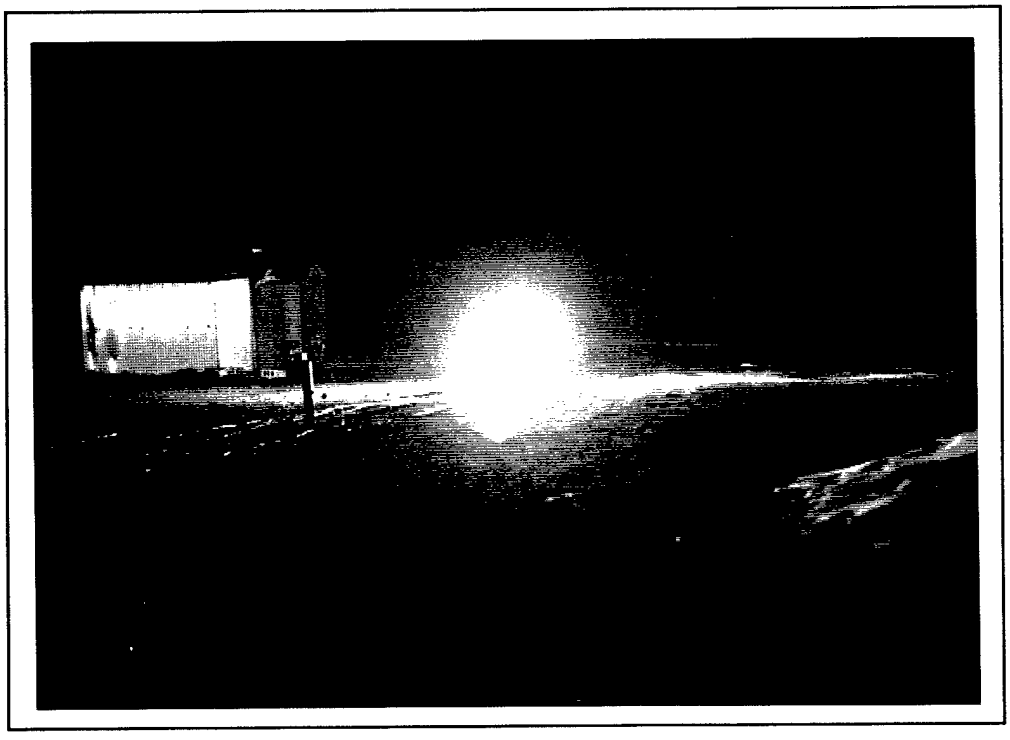

Figure 2-5. Test DNA 92-40 photo #2.

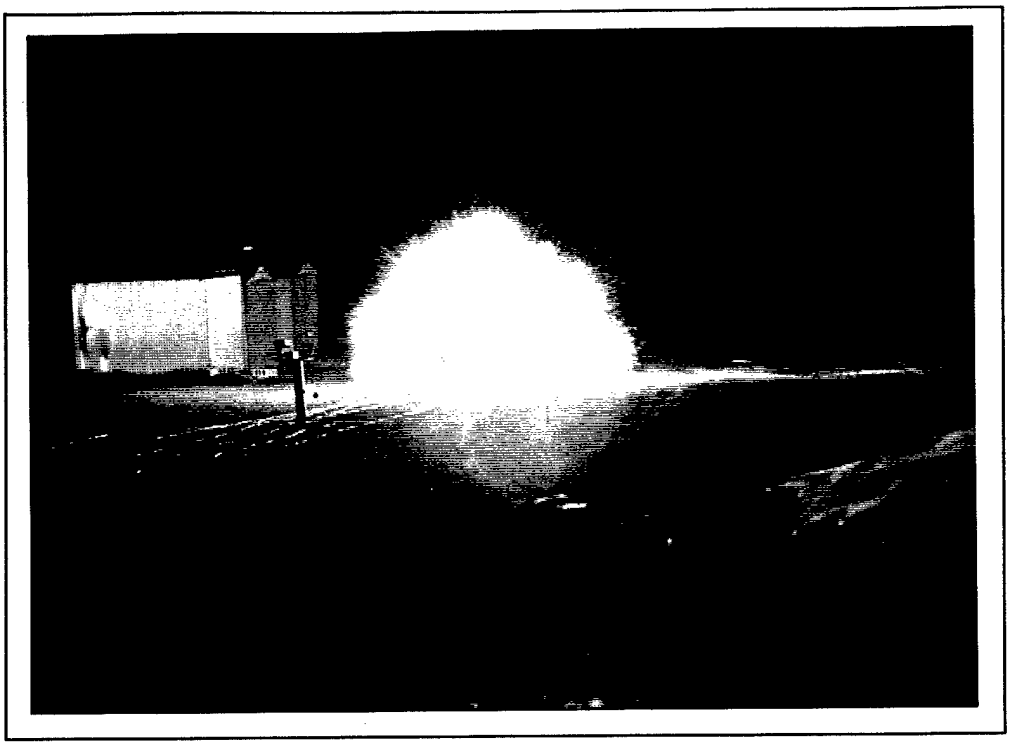

Figure 2-6. Test DNA 92-40 photo #3.

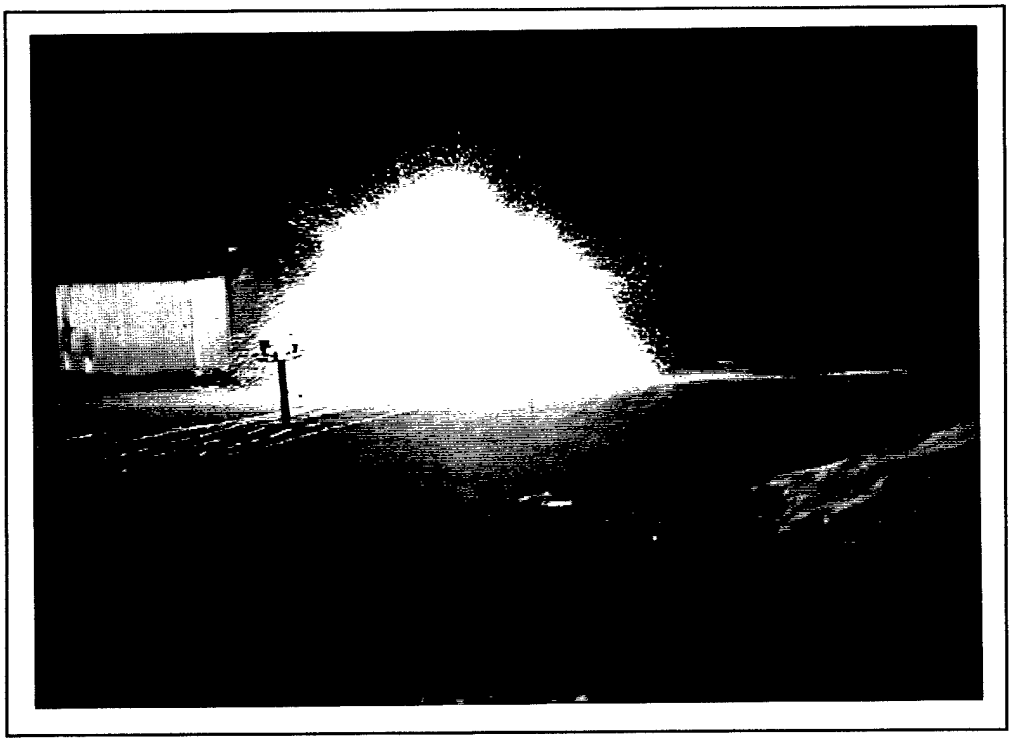

Figure 2-7. Test DNA 92-40 photo #4.

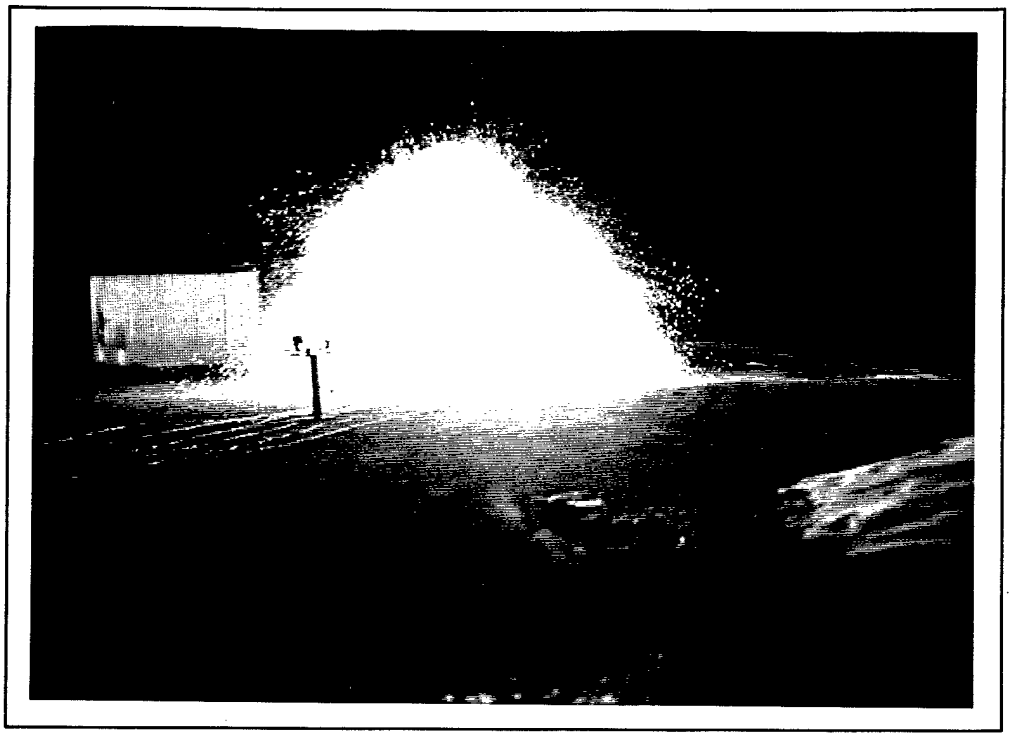

Figure 2-8. Test DNA 92-40 photo #5.

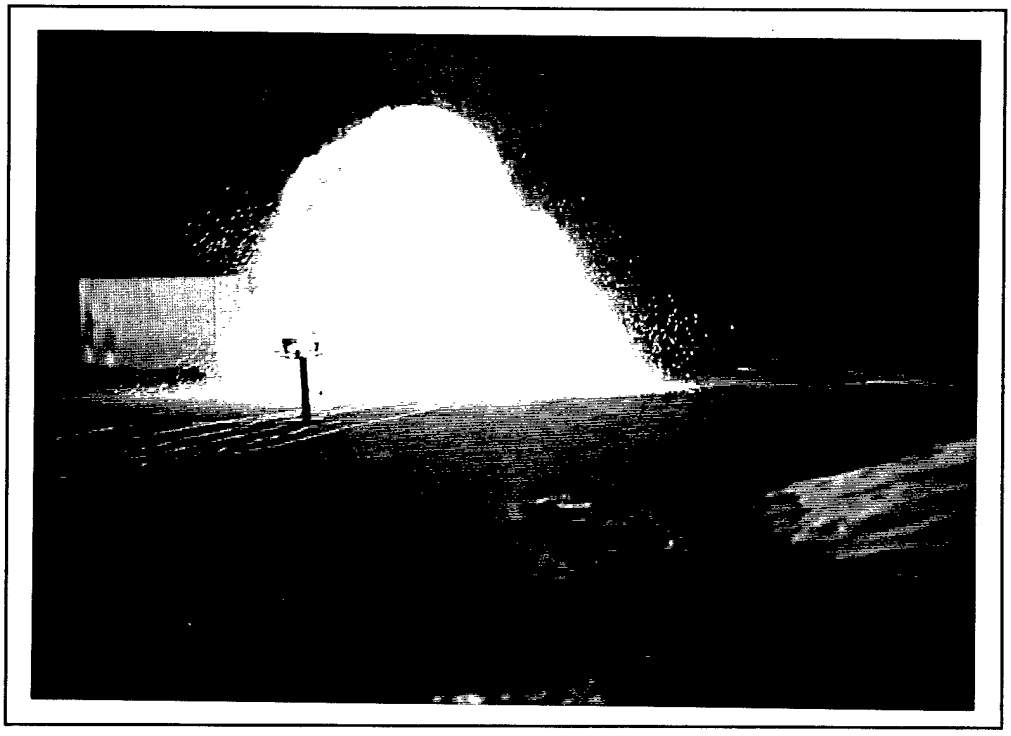

Figure 2-9. Test DNA 92-40 photo #6.

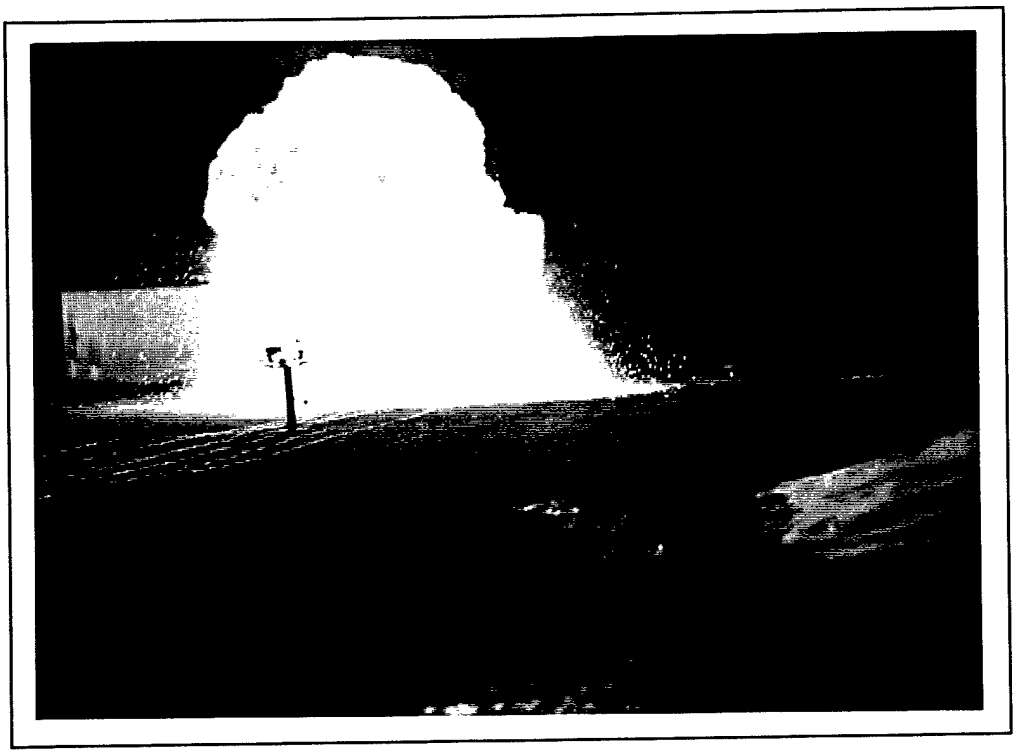

Figure 2-10. Test DNA 92-40 photo #7.

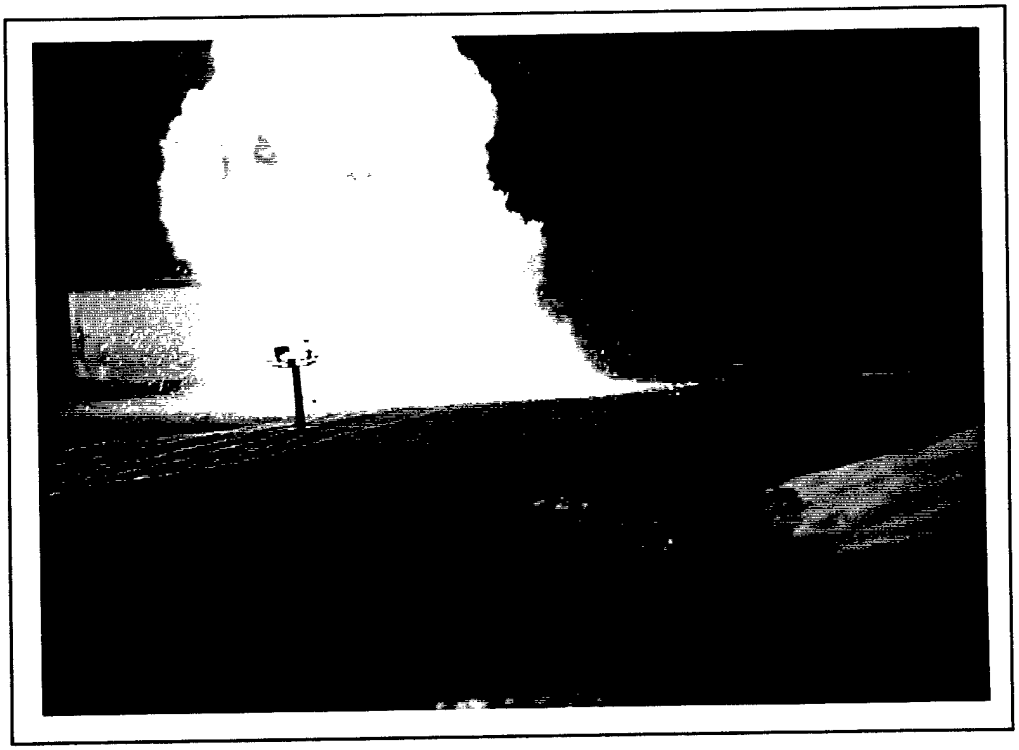

Figure 2-11. Test DNA 92-40 photo #8.

The total emittance of a blackbody radiator can be expressed as;

$$E = \sigma T^4 \tag{1}$$

where;

E = Surface emittance (W/cm^2)
σ = Stefan-Boltzmann constant (5.66997 x 10^{-12} W·cm^2·K^4)
T = Temperature (K)

This relationship assumes that the emissivity of the radiating source is equal to 1.0. For a graybody, or non-ideal, radiator and for determine the radiating emittance of surface for a fixed bandwidth, equation (1) becomes;

$$E_{\Delta\lambda} = \int_{\lambda_1}^{\lambda_2} E(\lambda)\varepsilon(\lambda)\, d\lambda$$

where;

$E_{\Delta\lambda}$ = Surface emittance over bandwidth (W/cm^2)
$E(\lambda)$ = Spectral emittance as a function of wavelength (W/cm^2·micron)
$\varepsilon(\lambda)$ = Emissivity of radiating body as a function of wavelength (0→1.0)
λ = Wavelength (micron)
λ_1 = Starting wavelength (micron)
λ_2 = Ending wavelength (micron)

As the spectral emissivity of a radiating body can change greatly as a function of wavelength and temperature, and given the difficulty of obtaining emissivity of a material as a function of temperature and wavelength, surface emittance calculations are made where the emissivity is assumed to be equal to 1.0 and the apparent blackbody temperature reported.

The surface emittance and apparent blackbody temperature of a radiating body can be determined experimentally by measuring the heat flux on a detector at some known distance from the radiating body from;

$$\phi_{\Delta\lambda} = \frac{I}{d^2} = \frac{AE_{\Delta\lambda}\varepsilon_{\Delta\lambda}}{d^2\pi} \tag{2}$$

where;

$\phi_{\Delta\lambda}$ = Detector flux over bandwidth (W/cm^2)
I = Source Intensity (W/cm^2·sr)
d = Distance from source to detector (cm)
A = Radiating area (cm^2)

For a radiating sphere, assuming an emissivity of 1.0, equation 2 becomes;

$$\phi_{\Delta\lambda} = \frac{E_{\Delta\lambda} r^2}{d^2 + r^2} \tag{3}$$

where;

r = Source radius (cm)

For a flat radiating circular plate, or where the distance to the detector is much greater the source radius (i.e., $d >> r$), equation 3 simplifies to;

$$\phi_{\Delta\lambda} = \frac{E_{\Delta\lambda} r^2}{d^2}$$

For a rectangular emitting surface, the detector flux is related to the surface emittance by;

$$\phi = \frac{E}{2\pi}\left[\frac{x_1 \arctan\left(\frac{y_1}{\sqrt{d^2+x_1^2}}\right)}{\sqrt{d^2+x_1^2}} + \frac{x_2 \arctan\left(\frac{y_1}{\sqrt{d^2+x_2^2}}\right)}{\sqrt{d^2+x_2^2}} + \frac{y_1 \arctan\left(\frac{x_1}{\sqrt{d^2+y_1^2}}\right)}{\sqrt{d^2+y_1^2}} + \frac{y_1 \arctan\left(\frac{x_2}{\sqrt{d^2+y_1^2}}\right)}{\sqrt{d^2+y_1^2}} + \right.$$

$$\left. \frac{x_1 \arctan\left(\frac{y_2}{\sqrt{d^2+x_1^2}}\right)}{\sqrt{d^2+x_1^2}} + \frac{x_2 \arctan\left(\frac{y_2}{\sqrt{d^2+x_2^2}}\right)}{\sqrt{d^2+x_2^2}} + \frac{y_2 \arctan\left(\frac{x_1}{\sqrt{d^2+y_2^2}}\right)}{\sqrt{d^2+y_2^2}} + \frac{y_2 \arctan\left(\frac{x_2}{\sqrt{d^2+y_2^2}}\right)}{\sqrt{d^2+y_2^2}}\right]$$

where x_1, x_2, y_1 and y_2 are rectangular coordinates of the radiating surface shown in Figure 2-12.

The surface emittance and apparent blackbody temperature equations shown above are dependent upon assigning a detector to source distance and an area for the radiating surface. In the case of the Hi-Therm simulator tests, the reactive material produced a particulate fireball which change the effective distance and surface area, and if not included in the data reduction, produced values higher than actual.

2.3 DEMONSTRATION TESTS, APRIL 1992.

Three (3) Hi-Therm Thermal Simulator demonstration tests were conducted at the TRS Test Site, Coyote Canyon, Kirtland AFB, NM. The tests consisted of 2 single panel tests (test numbers TRS-HT1 and TRS-HT2) and an 80 (8 foot by 10 foot) panel test (test number TRS-HT3).

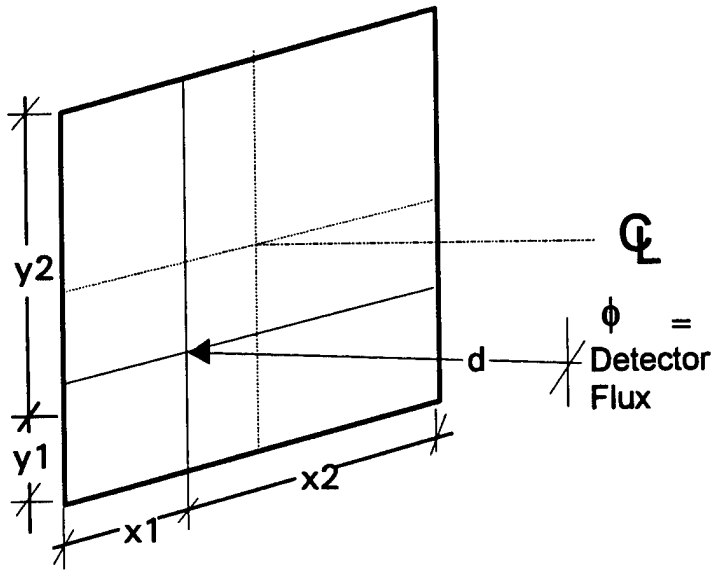

Figure 2-12. Rectangular coordinate system.

A detailed review of these demonstration tests is attached as Appendix B. A short summary of these tests follows.

2.3.1 TRS-HT1 and TRS-HT2 Test Summary.

For both of these tests, a single panel of the 62.0 wt.% Ti + 28.0 wt.% B + 10 wt.% Al Hi-Therm formulation was initiated with an instrument array set up to characterize the resultant event. Instrumentation for these tests consisted of 2 video cameras fitted with PLZT windows, 2 motorized 35 mm cameras fitted with neutral density filters and an 80B tungsten correction filter; spectrometers were positioned 10 feet in front of the panel and two 7° field of view Medtherm radiometers were located 10 feet in front of the panel. The output of the Hi-Therm material in both of these tests was similar. Peak emittance flux measurements from the radiometers were 22.2 and 26.3 cal/cm^2/sec (92.9 and 110 W/cm^2) for TRS-HT1 and 24.1 and 29.2 cal/cm^2/sec (101 and 122 W/cm^2) for TRS-HT2. The spectrometer data for these tests yielded an effective blackbody temperature of 2000 K for TRS-HT1 and 2350 K for TRS-HT2. The emittance calculated from these temperatures is 21.7 cal/cm^2/sec (90.7 W/cm^2) and 41.3 cal/cm^2/sec (173 W/cm^2), respectively. There is good correlation between the radiometers and spectrometer data for test TRS-HT1 with some variance in the data from TRS-HT2.

2.3.2 TRS-HT3 Test Summary.

An 8 foot wide by 10 foot tall matrix was constructed to form an 80 square foot panel. A steel mesh particle catcher was mounted one foot in front of the matrix to assist in reducing particulate ejection. Instrumentation consisted of 2 video cameras fitted with PLZT windows, 4 high speed 16 mm cameras, 2 motorized 35 mm cameras, 6 radiometers at 10 feet, 9 DNA Medtherm calorimeters at 10 feet, 1 calorimeter at 20 feet, 2 calorimeters at 30 feet and a spectrometer at 10 feet. Upon initiation, the 80 square foot Hi-Therm panel produced an expanding particulate fireball, with the fireball surface expanding at approximately 50 feet per

second. The expanding fireball rapidly engulfed the instrumentation out to 30 feet resulting in erroneous emittance values. The data presented below represents the peak measurements made before being engulfed by the expanding fireball.

2.3.3 TRS-HT3 Test Results.

The peak flux recorded before fireball impact for the 6 radiometers at 10 feet was 30, 36, 38 and 44 cal/cm^2/sec (125, 150, 160, 125, 151 and 184 W/cm^2). In all cases, the radiometers showed a sharp increase in flux values following particulate fireball impact with post fireball impact flux measurements of greater than 765 cal/cm^2/sec (3200 W/cm^2) achieved. For the 9 calorimeters at 10 feet, the one calorimeter at 20 feet and the two calorimeters at 30 feet, peak flux readings between 14 cal/cm^2/sec (58 W/cm^2) at 30 feet to 40 cal/cm^2/sec (167 W/cm^2) at 20 feet were recorded. Again, these values represent the peak flux measured before fireball impact. Due to the fast fireball growth, only one valid spectral curve was obtained from the spectrometer. The curve gave an effective blackbody fireball surface temperature of 2350 K for an approximate surface emittance of 41 cal/cm^2/sec (172 W/cm^2). A considerable amount of particulate ash was ejected from the panels during the test. A heavy layer of ash was found between 20 to 30 feet from the Hi-Therm array with light ash found out to 100 feet.

As a result of the large particulate fireball generated during this test, it was determined that this particular formulation and configuration was unacceptable as a nuclear explosion thermal radiation simulator source. In order to function as a thermal source simulator, the target material must be subjected to only thermal radiation. Thermal transfer by convection (from the hot fireball gases) and conduction (from the hot particulates) are unacceptable. It is postulated that the large fireball was the result of several factors. While some particulate generation was observed in smaller scale tests, it believed that the larger test array reduced "edge-effects" resulting in higher temperatures which in turn generated more vapor species (from the aluminum, as well as any water, trapped gasses or impurities, in the composition and vaporization of the test frame). Additionally, the Hi-Therm panel was situated over a concrete test pit (approximately 12 feet deep x 10 feet across and 30 feet long) at the beginning of the test. When the Hi-Therm reaction occurs, the reacting composition loses structural strength and slumps or falls off the individual panels. The dropping of 40 kilograms of hot reacting titanium and boron into the concrete pit may have caused the air within the pit to heat up and rise, thereby contributing to the fireball growth.

Following the review of the data generated during this test, GSI was directed to revisit the candidate formulations which produced little or no particulate ejecta, even though a lower thermal output was produced. These investigations are discussed below.

2.4 HI-THERM MINIMAL-THROW DEVELOPMENT TESTS.

In order to minimize the amount of particulate ejecta resulting from the initiation and reaction of a large scale Hi-Therm panel matrix, the minimal throw formulations were revisited for possible use. Following the first set of demonstration test at the TRS test site in April, 1992 (TRS-HT1 through TRS-HT3), 18 tests were conducted at GSI with variations on the minimal or no-throw chemistries previously developed. Table 2-1 shows a summary of the minimal throw Hi-Therm formulations and test results. The preparation of these test panels was the same as previous tests except that the pyrofuze ignition train was moved to the front surface of the Hi-Therm

Table 2-1. Summary of minimal throw Hi-Therm formulations.

Test No.	Chemistry	Radiometer Peak Flux		Thermogauge Peak Flux		Time to Peak (sec)	Particle Throw (see note)
		($cal/cm^2 \cdot sec$)	(W/cm^2)	($cal/cm^2 \cdot sec$)	(W/cm^2)		
1	58.2 wt.% Ti/2B + 38.9 wt.% Ti/C + 2.9 wt.% carbon fibers	1.30	5.44	1.43	6.00	1.15	1
2	62.6 wt.% Ti/2B + 33.7 wt.% Ti/C + 3.7 wt.% carbon fibers	1.66	6.93	1.55	6.49	1.18	1
3	58.4 wt.% Ti/2B + 39.0 wt.% Ti/C + 1.1 wt.% carbon fibers + 1.5 wt.% fiberglass fibers	1.61	6.75	1.55	6.49	1.12	1
4	58.2 wt.% Ti/2B + 38.9 wt.% Ti/C + 2.9 wt.% carbon fibers	1.29	5.40	1.64	6.85	0.75	1
5	62.6 wt.% Ti/2B + 33.7 wt.% Ti/C + 3.7 wt.% carbon fibers	1.69	7.07	1.55	6.50	1.02	1
6	58.4 wt.% Ti/2B + 39.0 wt.% Ti/C + 1.1 wt.% carbon fibers + 1.5 wt.% fiberglass fibers	1.45	6.08	1.44	6.03	0.77	1
7	63.1 wt.% Ti/2B + 34.0 wt.% Ti/C + 2.9 wt.% carbon fibers	1.53	6.40	1.66	6.96	0.77	1
8	63.1 wt.% Ti/2B + 34.0 wt.% Ti/C + 2.9 wt.% carbon fibers	1.77	7.43	1.99	8.35	0.62	1
9	64.1 wt.% Ti + 34.9 wt.% AlB_{12} + 1.0 wt.% carbon fibers	2.42	10.13	4.20	17.6	0.86	2
10	62.6 wt.% Ti/2B + 33.7 wt.% Ti/C + 3.7 wt.% carbon fibers	1.64	6.85	3.10	12.98	0.96	2
11	62.6 wt.% Ti/2B + 33.7 wt.% Ti/C + 3.7 wt.% carbon fibers	no data	no data	no data	no data	no data	3
12	62.6 wt.% Ti/2B + 33.7 wt.% Ti/C + 3.7 wt.% carbon fibers	saturated detector	saturated detector	1.77	7.40	1.05	2
13	63.1 wt.% Ti/2B + 34.0 wt.% Ti/C + 2.9 wt.% carbon fibers	1.66	6.93	2.33	9.74	0.78	1
14	63.1 wt.% Ti/2B + 34.0 wt.% Ti/C + 2.9 wt.% carbon fibers	1.91	8.00	2.21	9.27	0.85	2
15	63.1 wt.% Ti/2B + 34.0 wt.% Ti/C + 2.9 wt.% carbon fibers	1.71	7.16	no data	no data	0.50	3
16	62.6 wt.% Ti/2B + 33.7 wt.% Ti/C + 3.7 wt.% carbon fibers	1.02	4.26	1.77	7.42	0.73	1
Note on Particle Throw: 1 ≡ insignificant particle throw; 2 ≡ Modest particle throw; 3 ≡ Significant particle throw							

material. Total radiometers and Thermogauge heat flux gauges were used to measure the thermal output of these tests. Appendix C complies these panel output curves. From these tests the formulation designated as

45.9 wt.% Ti + 19.6 wt.% B + 0.6 wt.% C + 2.9 wt.% Carbon Fibers

produced detector fluxes of 1.66 $cal/cm^2/sec$ (6.9 W/cm^2) for the radiometer and 2.33 $cal/cm^2/sec$ (9.7 W/cm^2) for the Thermogauge flux gauge. This corresponds to a surface emittance of 132 $cal/cm^2/sec$ (553 W/cm^2) and an effective surface temperature of 3140 K for the radiometer data. This formulation was selected for the second series of demonstration tests held at the TRS Test site, Coyote Canyon, Kirtland AFB, NM.

2.5 DEMONSTRATION TESTS, NOV 1992.

Three minimal-throw Hi-Therm Simulator demonstration tests were conducted at the TRS test site, Coyote Canyon, Kirtland AFB, NM. These tests consisted of 2 tests of the 9 panel matrix

and a 28 panel test (tests numbers TRS-HITH-4, TRS-HITH-5 and TRS-HITH-6, respectively). Appendix D contains the instrumentation traces form these tests. A short summary of these follows.

2.5.1 TRS-HITH-4 Test Summary.

This test consisted of 9 (3 foot by 3 foot matrix) minimal-throw Hi-Therm panels. Instrumentation for this test consisted of 6 DNA Medtherm calorimeters located at varying distances and locations around the Hi-Therm panel, 3 restricted field of view radiometers and a GSI Thermogauge heat flux gauge, light probe and radiometer. A summary of the test data as presented in Table 2-2.

Table 2-2. Summary of test TRS-HITH-4.

Instrument(1)	Location(2)			Peak Flux		Total Fluence	
	X	Y	Z	(cal/cm^2/sec)	(W/cm^2)	(cal/cm^2)	(J/cm^2)
Medtherm Calorimeter	0	10	5.25	no data		no data	
Medtherm Calorimeter	0	10	2.75	2.31	9.66	6.62	27.7
Medtherm Calorimeter	0	10	3.75	2.23	9.33	6.27	26.2
Medtherm Calorimeter	-1.5	10	3.75	2.11	8.83	6.72	28.1
Medtherm Calorimeter	1.5	10	3.75	2.1	8.79	6.06	25.4
Medtherm Calorimeter	0	-10	3.75	1.36	5.69	2.61	10.9
GSI Radiometer	0	20	3.75	6.63	27.7	11.32	47.4
GSI Radiometer	0	-10	3.75	12.03	50.3	60.5	253
GSI Radiometer	-10	1	3.75	8.06	33.7	10.3	76.6

(1) Medtherm Calorimeters were supplied by DNA
(2) Location: 'X' is distance to the left (-) or right (+) of center line
'Y' is distance in front (+) or back (-) of panel
'Z' is distance above ground

2.5.2 TRS-HITH-5 Test Summary.

This test consisted of a 9 (3 foot by 3 foot) panel matrix of the minimal-throw Hi-Therm panels. Instrumentation for this test consisted of 6 DNA Medtherm calorimeters, 4 restricted field of view radiometers and a GSI Thermogauge, light probe and radiometer. The test set up was similar to that used in TRS-HITH-4. A summary of the test data is presented in Table 2-3.

2.5.3 TRS-HITH-6 Test Summary.

This test consisted of a 28 panel (4 foot by 7 foot) array matrix of the minimal-throw Hi-Therm panels. Instrumentation for this test consisted of 14 DNA Medtherm calorimeters, 4 restricted field of view radiometers, 2 GSI Thermogauge heat flux gauges and a GSI light probe. A summary of the test data is presented in Table 2-4.

Following review of the data from these tests, the projected on-target fluxes did not meet the minimum criteria for use as a DNA Thermal Simulator. At this point in the program, further development was halted.

Table 2-3. Summary of test TRS-HITH-5.

Instrument[1]	Location[2]			Peak Flux		Total Fluence	
	X	Y	Z	(cal/cm^2/sec)	(W/cm^2)	(cal/cm^2)	(J/cm^2)
Medtherm Calorimeter	0	6	5.25	4.98	20.8	12.9	54.0
Medtherm Calorimeter	0	6	3.75	5.00	20.9	14.0	58.4
Medtherm Calorimeter	0	6	2.75	5.02	21.0	14.0	58.5
Medtherm Calorimeter	-1.5	6	3.75	4.49	18.8	12.2	51.2
Medtherm Calorimeter	1.5	6	3.75	4.20	17.6	11.5	48.2
Medtherm Calorimeter	0	-6	3.75	2.05	8.6	4.07	17.0
GSI Radiometer	0	10	3.75	4.63	19.4	9.62	40.2
GSI Radiometer	0	-10	3.75	11.60	48.5	42.9	180
GSI Radiometer	-10	1	3.75	7.50	31.4	21.7	91.0
GSI Radiometer	-10	1	3.75	9.59	40.1	21.4	89.4

(1) Medtherm Calorimeters were supplied by DNA
(2) Location
'X' is distance to the left (-) or right (+) of center line
'Y' is distance in front (+) or back (-) of panel
'Z' is distance above ground

Table 2-4. Summary of test TRS-HITH-6.

Instrument[1]	Location[2]			Peak Flux		Total Fluence[3]	
	X	Y	Z	(cal/cm^2/sec)	(W/cm^2)	(cal/cm^2)	(J/cm^2)
Medtherm Calorimeter	0.5	6	6.5	8.04	33.6	7.93	33.2
Medtherm Calorimeter	0.5	6	4.5	7.52	31.5	8.17	34.2
Medtherm Calorimeter	0.5	6	2.9	8.31	34.7	8.37	35.0
Medtherm Calorimeter	2	6	6.4	7.39	30.9	6.87	28.7
Medtherm Calorimeter	2	6	4.7	6.33	26.5	6.74	28.2
Medtherm Calorimeter	2	6	2.9	5.62	23.5	5.74	24.0
Medtherm Calorimeter	-0.5	8	8.2	4.79	20.0	4.29	17.9
Medtherm Calorimeter	-0.5	8	7.25	4.44	18.6	4.16	17.4
Medtherm Calorimeter	-0.5	8	5.5	4.16	17.4	4.34	18.2
Medtherm Calorimeter	-0.5	8	3.75	1.92	8.0	1.98	8.3
Medtherm Calorimeter	-2	8	8.2	2.53	10.6	2.53	10.6
Medtherm Calorimeter	-2	6	7.25	2.61	10.9	2.74	11.5
Medtherm Calorimeter	-2	8	5.5	2.95	12.3	3.15	13.2
Medtherm Calorimeter	-2	8	3.5	3.31	13.8	3.35	14.0
GSI Radiometer	-2	-10	4.7	2.05	8.6	1.13	4.7
GSI Radiometer	0	20	4.5	10.7	44.6	11.4	47.9
GSI Radiometer	0	-10	4.7	7.73	32.3	7.81	32.7
GSI Radiometer	-10	20	4.7	9.62	40.2	10.9	45.5
GSI Thermogauge	0	10	4.7	11.9	50.0	13.4	55.9
GSI Thermogauge	-3	1	4.7	9.79	41.0	10.4	43.3

(1) Medtherm Calorimeters were supplied by DNA
(2) Location
'X' is distance to the left (-) or right (+) of center line
'Y' is distance in front (+) or back (-) of panel
'Z' is distance above ground
(3) Data at late times during this tests are corrupted and the Total Fluence values represent minimal Total Fluences

2.6 HI-THERM THERMAL SIMULATOR DROP FRAME.

As part of the design effort, which was conducted prior to the tests at the TRS Site, Coyote Canyon, Kirtland AFB, a method to remove the Hi-Therm Simulator from the line of sight of the shockwave from a high explosive shockwave and air blast event was required for fielding at the DNA Permanent High Explosive Test Site, White Sands Missile Range, NM. The drop frame requirements were to drop the Hi-Therm frame below grade level in less than 1 second required, 0.5 second desired, into a pit no more than 2 feet across normal to the shockwave travel direction. A subcontract was let to Kaman Sciences Corporation to design a drop frame for use with the Hi-Therm Simulator. The drop frame design has been transmitted to DNA under separate cover (Kaman, KA-TN-212).

2.7 TECHNICAL SUPPORT PLAN AND SAFETY OPERATING PROCEDURES.

A Technical Support Plan (TSP) was assembled during this effort in order to identify the level of effort required from DNA, upon successfully meeting program technical objectives, to field a Hi-Therm Simulator(s) at the DNA Permanent High Explosive Test site located at White Sands Missile Range, NM. The TSP describes test objectives, required diagnostic and control instrumentation, data collection system(s), safety, site outlay, security, weather restrictions, support requirements and other appropriate measures for a safe and successful test execution. The initial version of the TSP was developed based, in part, on the standard operating procedure and site requirements to support the testing at TRS Site, Coyote Canyon, Kirtland AFB.

SECTION 3

CONCLUSIONS

The following conclusions were reached as a result of this program:

(1) The flux and fluence requirements stated in the original objectives were unable to be obtained from a Hi-Therm Thermal Simulator using the materials and panel fabrication process explored in this effort. A major disadvantage of the explored formulations, processing techniques and configurations, is the generation of an excessive hot radiating particulate plume or fireball which restricts the placement of target materials, which is to be exposed to a thermal environment, close enough to the Hi-Therm simulator to achieve the desired heat flux and fluences levels. We believe that this is primarily due to the high level of porosity of the Hi-Therm composition and the inclusion of volatile metals within the composition, as applicable. A process technique which produces a higher density (i.e., lower porosity) in the intermetallic composition will greatly reduce or eliminate the particulate ejecta effects.

(2) A drop frame was developed which would allow for a gravity driven drop time of approximately 0.8 seconds and which meets the other requirements of the Hi-Therm Thermal Simulator drop frame fielding requirements.

(3) An improved initiation system was developed and demonstrated which allowed for multiple panel ignition with initiation of each panel occurring in the millisecond range. To achieve this a commercially available blasting system (designed for quarry blasting) was used.

(4) The fabrication procedure developed for construction and loading of the Hi-Therm panels avails itself to fixed site field operations using conventional materials and chemical processing hardware.

SECTION 4

RECOMMENDATIONS

Theoretically, the formulations investigated were capable of meeting the required surface emittance values. A review of the material processing techniques, panel configuration and test results indicate two major areas for substantial improvement of the Hi-Therm Thermal Radiation Simulator Concept.

These areas are:

- Remove reactive components which vaporize upon reaction initiation and progression.
- Remove residual porosity and volatile processing contaminates (e.g., water and organic liquids).

It is recommended that if additional effort is deemed beneficial to DNA, that powder metallurgy processing techniques which produce low porosity dry pressed powder greenbodies be pursued.

SECTION 5

REFERENCES

Army Pamphlet No. 50-3, The Effects of Nuclear Weapons (U) , March 1977, UNCLASSIFIED.

Kaman Sciences Division, Design and Analysis of a Retractable Hi-Therm Frame Structure (U), KA-TM-212, UNCLASSIFIED

Pyrofuze Engineering Catalog (U), Pyrofuze Corporation, Mount Vernon, NY, UNCLASSIFIED.

TRS Brochure, Description of the Thermal Radiation Source Test Facility Field Command (U), Defense Nuclear Agency, Kirtland AFB, NM 87115, UNCLASSIFIED.

Zavitsanos, P.D., Nuclear Effects Simulation - Thermal Effects (U), Contract DNA001-87-C-0152, July 7, 1989, UNCLASSIFIED.

APPENDIX A

HI-THERM MATERIAL DEVELOPMENT TEST DETAIL

A.1 BACKGROUND.

General Sciences, Incorporated, has been involved in studies to develop a new class of nuclear thermal simulants based upon intermetallic reactants. Briefly, these materials provide their thermal energy through an exothermic reaction which takes place between two or more metal particles, in the process of forming a new intermetallic alloy or ceramic product. These reactions (over 250) are capable of producing energies on the order of 1.15 kcal/g and temperatures in excess of 3500 K. The early stages of the DNA efforts examined several intermetallic mixtures and developed a concept of a modular heat source in the form of a solid radiating wall. Unlike other current simulant techniques, the thermal wall is capable of producing a uniform thermal flux across the dimensions of the wall. Current systems produce their thermal flux by injecting a metal/oxygen mixture from a ground based nozzle. The resultant flame produces a strong thermal gradient from the flame base to its peak, resulting in a non-uniform flux projected upon the target.

The GSI studies to date have resulted in a 1 foot x 1 foot panel of reactive intermetallic material, which is mounted into a frame, to create a wall of the required dimensions. Each panel is individually wired for ignition producing a uniform thermal rise time across the wall. The GSI materials, known as Hi-Therm, have been previously evaluated in wall configurations up to 4 feet by 4 feet and have involved material masses in excess of 40 pounds. Previous tests have identified specific areas of improvement before the Hi-Therm system can be scaled up to full size in conjunction with shock wave experiments. For those tests, the Hi-Therm system has been designed to be mounted on a retractable wall which will not interfere with shock wave passage. The main obstacles to overcome for the Hi-Therm concept, constitute the focus of this current effort and are as follows:

- Particle Throw: To date, the Hi-Therm chemistries, mounted vertically, tend to eject particulates from the wall when they are ignited. This ejection results in the dispersion of very hot ceramic particle at distances up to 8 feet. While these particles are very fine (< 1 mm average), it is possible that their direct impingement upon a sensitive test article could result in undesirable damage. Moreover, particle impingement produces a non-uniform thermal flux distribution upon the target.

- Increased Reaction Time: Current Hi-Therm devices produce a thermal profile consisting of a 0.5 second rise, followed by a 1 second decay. While this thermal profile is a very good match for most simulation requirements, a longer pulse chemistry is also desired. The goal of this second chemistry is to produce a minimum 2 second pulse.

- Process Parameter Evaluation: It is planned to scale up the production of the 1 foot x 1 foot panels for very large arrays to be tested at the present Permanent High Explosive Test Site at White Sands Missile Range (WSMR), NM. To accomplish this, the most economic path for Hi-Therm production involves setting up a pilot processing facility on-site at WSMR, NM. The role of this pilot plant would be to blend all reactants and process individual panels which could then be stored for upcoming tests. This investigation will focus on low cost rapid processing techniques for a safe, repeatable method of panel fabrication.

A.2 HI-THERM MATERIAL DEVELOPMENT TEST.

A.2.1 Small Scale Reactant Evaluation & Particle Throw.

Intermetallic systems were investigated with the emphasis on reducing the particle throw from the panels during ignition. The most promising methods for accomplishing this are (1) binder additions and (2) chopped fiber additions. The key distinction between the two is that the binders are conventional organic additives of the ceramic industry while the chopped fibers (carbon and fiberglass) are standards of the composite industry. Inherent in a study which limits the particle throw is a further evaluation to increase the total thermal flux of the chemistry. While it is acknowledged that the primary energy source from the Hi-Therm system is the intermetallic reaction, it has also been demonstrated that once ignited, the particles that eject themselves from the wall react with ambient air and produce additional energy by the rapid oxidation of the hot ceramic/intermetallic particles.

Also in this study, new chemical formulations were investigated which would produce a lower overall flux, but would do so for a longer time; the goal being a 2 second pulse.

Initial tests DNA92-# 1 through #32 were panels cast into aluminum weighing pans, area = 31.16 cm^2 and a thickness = 1.75 cm. Sensors were at a distance of 15 feet. The sensor setup is shown in Figure A-1.

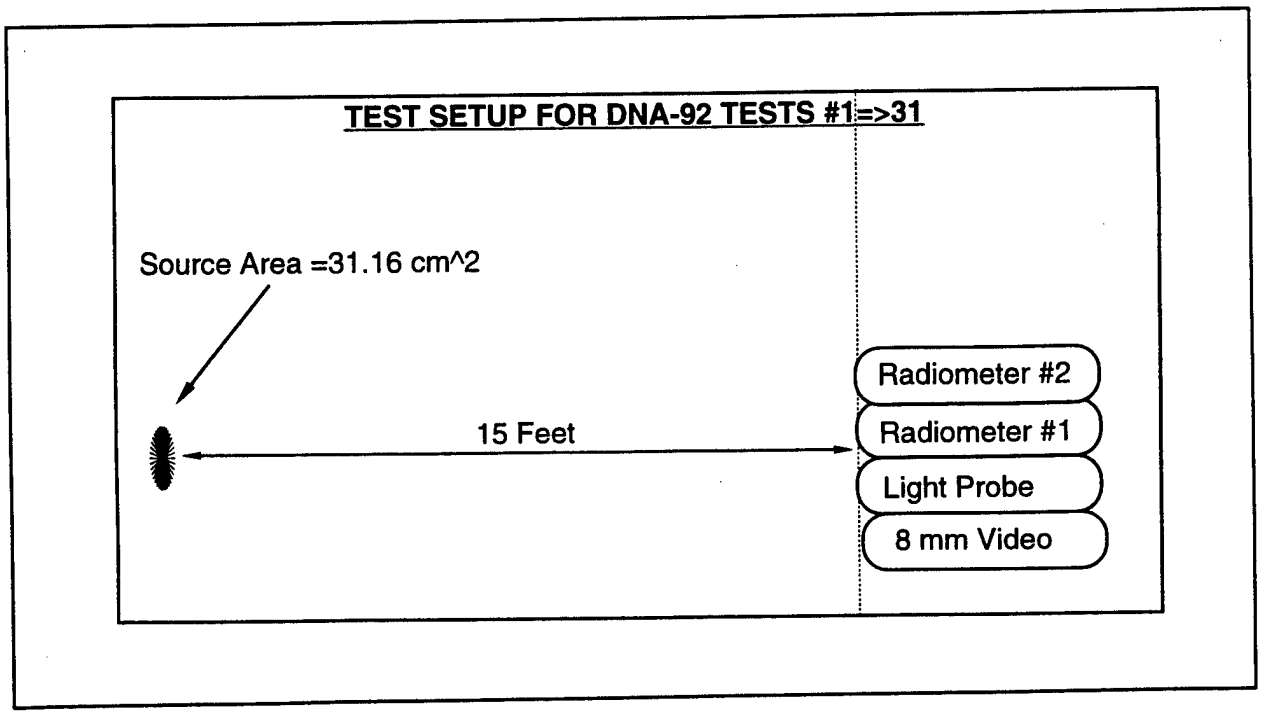

Figure A-1. Test set-up for DNA-92, tests 1-31.

Materials tested in this first series exhibited excessive particle throw in comparison to previous testing. This artificial oversized area yields exaggerated emittance values for the source. The use of the original source area, prior to reaction, is the only uniform means of comparing tests with wider varying degrees of particle ejection. (i.e., the observation and analysis is dependent

upon the application of the starting area as a reference for surface emittance determination). Note that the detector flux values reported are the actual fluxes received at the specific distance from the source. Both of these values, detector flux and emittance, need to be evaluated in determining the efficiency of a particular chemistry. The flux at the detector yields the actual energy seen by the detector. The surface emittance yields the means of comparing each chemistry on the basis of the geometry of the particle cloud formation and the secondary reaction effects due to particle combustion in air. The interaction of this particle cloud with air has been explored and confirmed by GSI to enhance the energy of this type of reacting system.

The methodology relating to increasing thermal output consisted of oxidizers additions and combinations of intermetallic reactions exhibiting superior fluxes with reference to the current system. Potential future processing parameters (overall simplicity, safety, economy, etc.) were considered in process design and chemical component selections.

In addition to the Titanium/Boron reaction, the Hafnium/Carbon (Hf/C) intermetallic reaction was also explored. This reaction yields an adiabatic reaction temperature of ≈3800 K, several hundred degrees higher than the adiabatic reaction temperature of Ti/2B (≈3200 K). In direct comparison between the Hf/C and the Ti/2B systems, the overall emittance and potential flux yields are higher for the Hf/C chemistry as well as the UV contribution. Potential drawbacks of this material are high cost and handling complications. For economic reasons thin coatings of Hf/C and Hf/C oxidizer were explored as thermal enhancers to existing chemistries This thin coating, or appliqué, is expected to increase performance at acceptable cost escalation.

The experimental methodology relating to restraining particle throw consisted of two major approaches. The first approach utilized conventional binders form the pyrotechnics and intermetallics industries. The second approach is fiber reinforcement. Fiberglass fibers were examined in addition to previously tested carbon fibers as a means keeping the reacting solid as an interconnected mass. Both the fiber and binder additives offer a convenient means of diluting or moderating the reaction. Thus extended the duration of the thermal pulse as well as reducing particulate ejection.

A.2.2 Processing Parameter Study.

Processing parameters were studied with the goals of improved processing efficiency simplicity, safety and cost. The implications of decreasing slurry viscosity via increased acetone to powder ratio was explored. Acetone is used as a slurrying agent because of its inherent volatility (to aid in quick drying) and its interaction from a surface energy standpoint readily forming a low viscosity slurry without decreasing safety via powder surface activation. A slurry with a lower viscosity permits the gravity delivery of material into the panels. Previous work optimized an acetone weight percent of ≈33 wt.%; but the range can be extended to ≈45 wt.%. The increased quantity of acetone allows the slurry to flow via gravity and greatly aids in the handling and transfer of the slurry. The alternative is a mechanized system capable of handling pyrotechnic slurries.

Material homogeneity was improved by modification of the drying process. Test panels were previously air dried, sealed and packaged with desiccant. It was determined that more efficient water removal from the panels yielded superior panel performance in terms of reduced particle throw. The processing procedure was changed to permit the unsealed panels to be fully

desiccated prior to sealing. This modification was added as a result of abnormal material behavior in tests 92-11 through 92-31. This will be discussed in detail in the analysis section of this report.

A.2.3 Test Series DNA #92-1 through #92-10.

The downselected chemistries from previous testing, (i.e., large scale 4' x 4' and the 1' x 1' "Minimal Throw" tests at GSI) were reproduced in this test series (#92-1 and #92-2). The "Minimal Throw" chemistry #92-1 yielded results consistent with previous testing. The maximum thermal pulse chemistry (#92-2 - henceforth the reference chemistry) yielded excessive particle throw and an artificially exaggerated surface emittance. Oxidizers binders and alternate Hi-Therm chemistries were explored in this test series. The Reference Chemistry #92-2 was modified with addition of binders (test # 92-4, 5, and 9). The use of high energy coatings in conjunction with the Reference Chemistry was explored in tests # 92-7 and 92-8. An oxidizer additive to the "Minimal Throw" chemistry (i.e., an attempt to increased panel output) was explored in test #92-6. Hf and C reaction enhancement was attempted via both oxidizer and binder additives in tests #92-3 and #92-10 respectively.

A.2.4 Test Result Overview.

The results of this series are summarized in Table A-1, where the emittance values range from 63 to 349 cal/cm^2/sec.

Table A-1. Summary of test results for DNA 92-1 through DNA 92-10.

Test No.	Chemistry	Mass (grams)	Emittance (cal/cm^2/sec)	Peak Visible (Lux)	Mix to Acetone Ratio	Particle Throw (1)
92-1	60 parts Ti/2B + 40 parts Ti/C + 3 parts excess carbon fiber	40.21	63.0	1087	40/70	4
92-2	80 parts ti/2B + 20 parts Al	44.39	315	6815	30/70	7
92-3	98 parts Hf/C + 2 parts $KClO_4$	39.72	78.7	728	40/65	2
92-4	78 parts Ti/2B + 20 parts Al + 2 parts PMMA	34.26	no test	no test	50/50	no test
92-5	80 parts Ti/2B + 20 parts Al + 2 parts Acacia	27.55	211.4	518	40/70	3
92-6	60 parts Ti/2B + 40 parts Ti/C + 30 parts carbon fiber + 2 parts $KClO_4$	36.15	59.0	1264	50/50	1
92-7	60 parts Ti/2B + 20 parts Al + 20 parts Hf/C	60.66	349	15800	40/70	7
92-8	30 parts Ti/2B + 20 parts Al + 30 parts Hf/C + 20 parts Al	57.61	280	12350	40/70	7
92-9	80 parts Ti/2B + 20 parts Al + 1 part PMMA	29.31	no test	no test	50/50	no test
92-10	100 parts Hf/C + 1 part Acacia	24.08	no test	no test	50/50	no test
(1) Particle Throw: 0 (no particle throw) → 10 (most or all material ejected)						

The details for individual runs are as follows:

92-1. Previous "Minimal Throw" chemistry -- consistent
92-2. Previous high output chemistry -- excessive particle throw
92-3. Oxidizer enhanced Hi-Therm II -- high output, excessive throw
92-4. Reference 2 -- excessive binder, no reaction
92-5. Reference 2 -- moderate output acceptable particle throw
92-6. Oxidizer enhanced "Minimal Throw" chemistry -- low output, minimal particle throw
92-7. Hi-Therm II based coating on Reference Chemistry -- high output, excessive throw
92-8. Hi-Therm II based coating on Reference Chemistry -- high output, excessive throw
92-9. Reference Chemistry with binder -- excessive binder, no reaction
92-10. Hi-Therm II + Binder -- excessive binder, no reaction

The radiometer based emittance date for tests #91-1, 2, 5, and 7 follows in Figures A-2 through A-5.

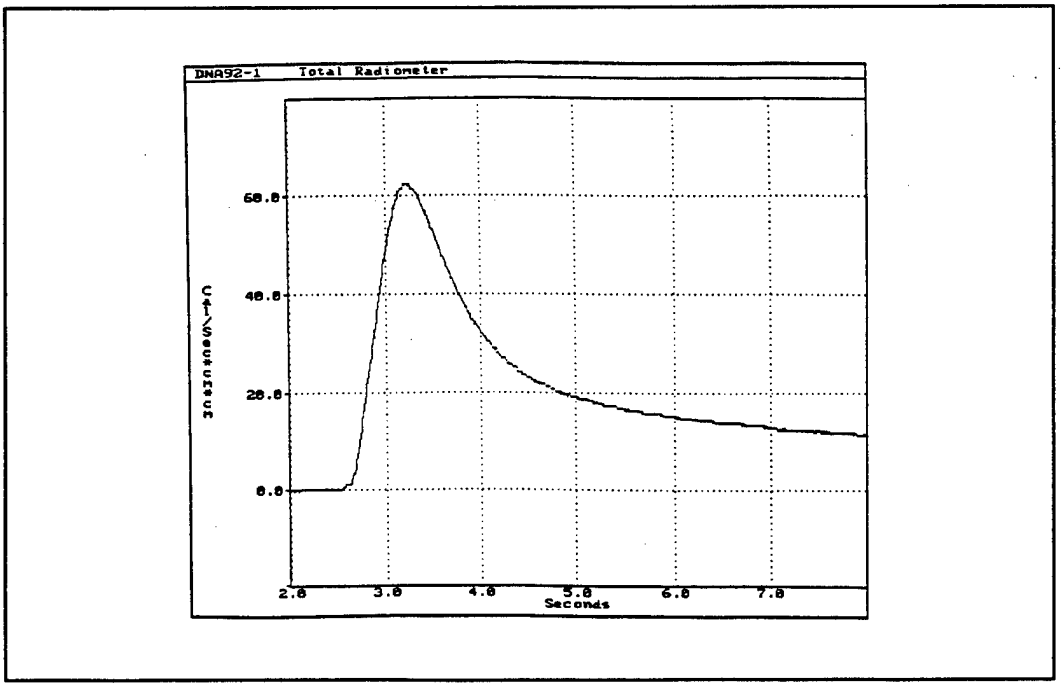

Figure A-2. Test DNA 92-1, total radiometer.

A.2.5 Test Series DNA #92-11 through #92-21.

Repeat tests on previous formulations and variations on these chemistries were tested in this series. Also, fiberglass fibers were evaluated as a substitute for C-Fibers in the "Minimal Throw" panels. These test results are presented in Table A-2 where calculated emittance values range from 112 to 826 cal/cm^2/sec. Excessive particle throw occurred in these tests (i.e., in excess of 15 feet from the small panels). An example of the artificially elevated radiometric emittance determination is shown in Figure A-6 for sample 92-11.

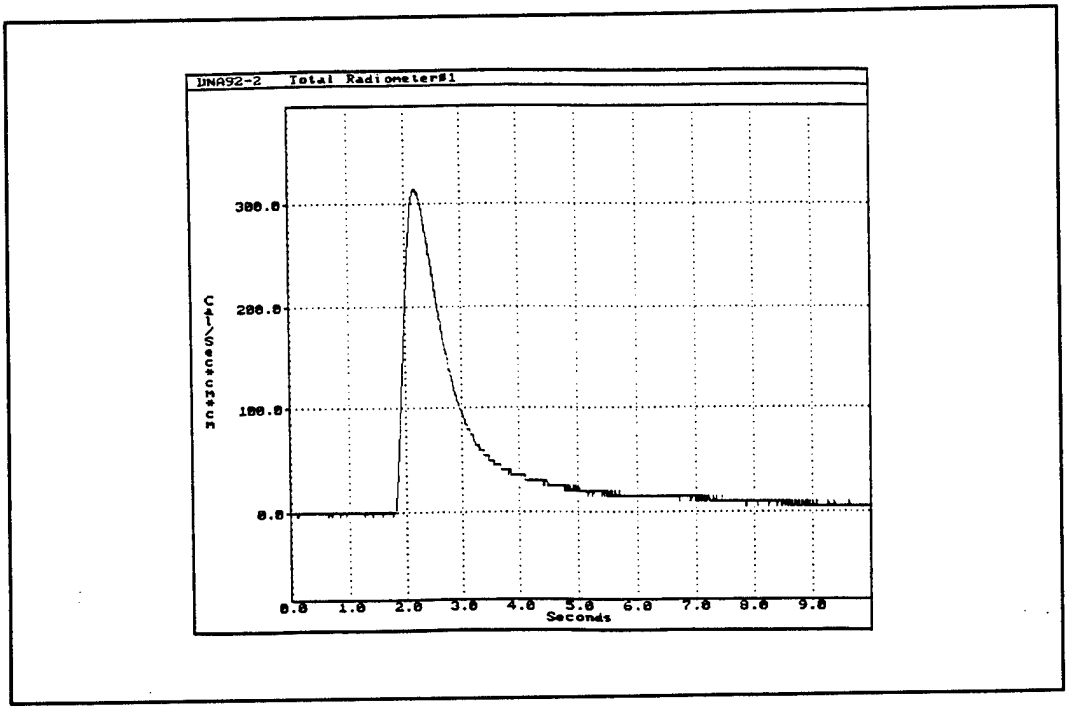

Figure A-3. Test DNA 92-3, total radiometer.

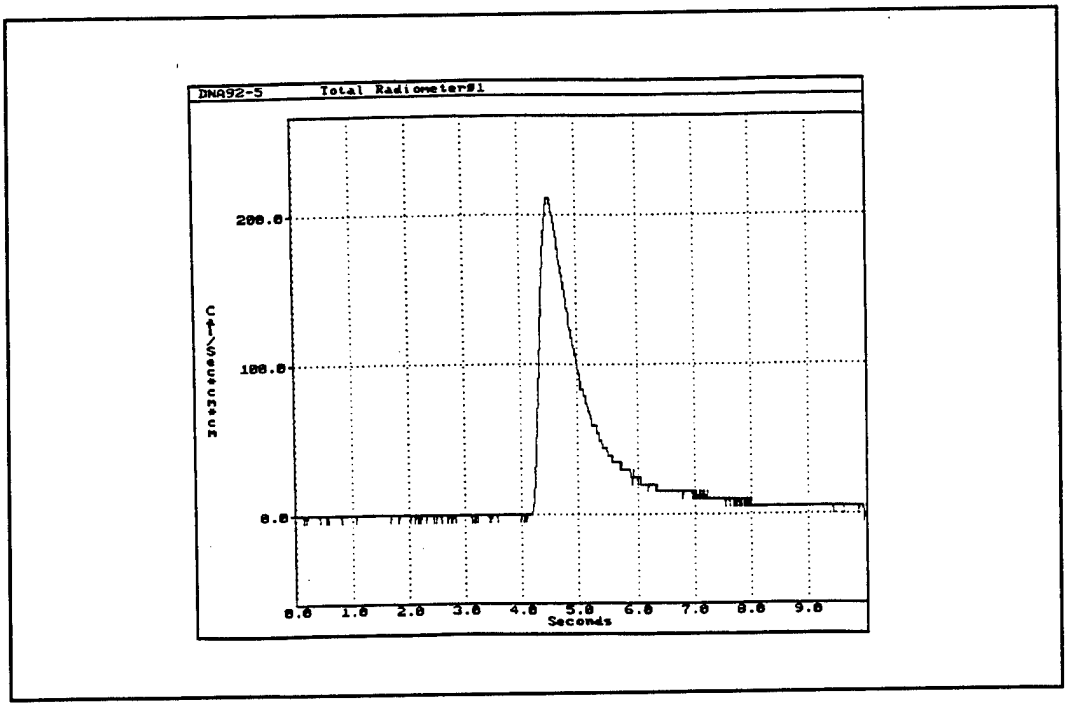

Figure A-4. Test DNA 92-5, total radiometer.

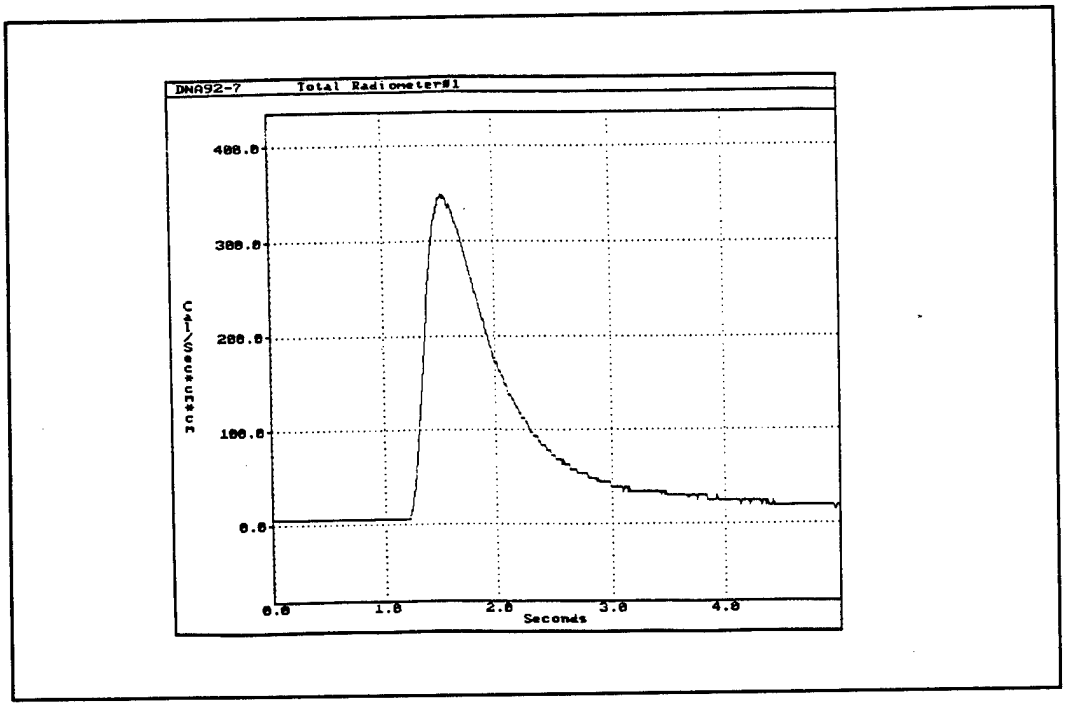

Figure A-5. Test DNA 92-7, total radiometer.

Table A-2. Summary of test results for DNA 92-11 through DNA 92-21.

Test No.	Chemistry	Mass (grams)	Emittance ($cal/cm^2/sec$)	Peak Visible (Lux)	Mix to Acetone Ratio	Particle Throw (1)
92-11	80 parts Ti/2B + 20 parts Al	53.66	767	21976	45/60	10
92-12	90 parts Ti/2B + 10 parts Al	51.09	826	44940	40/60	10
92-13	80 parts Ti/2B + 10 parts Al + 2 parts Acacia	59.97	792	43211	50/50	10
92-14	80 parts Ti/2B + 10 parts Al + 0.1 parts PMMA	48.13	565	20495	30/70	9
92-15	90 parts Ti/2B + 10 parts Al + 50 parts Hf/C	57.65	472	22717	50/80	8
92-16	90 parts Ti/2B + 30 parts Al + 80 parts Hf/C	55.35	546	22717	50/80	10
92-17	150 parts Ti/2B + 10 parts Al + 40 parts Ti/C+ 3 parts carbon fiber	57.07	683	26421	50/90	10
92-18	90 parts Ti/2B + 10 parts Al + 1 part $KClO_4$	50.47	728	23704	40/70	10
92-19	210 parts Ti/2B + 80 parts Ti/C + 10 parts Al + 3 parts fiberglass	75.19	664	26424	35/70	10
92-20	90 parts Ti/2B + 10 parts Al + 3 parts fiberglass	49.92	644	22223	40/70	9
92-21	60 parts Ti/2B + 40 parts Ti/C + 3 parts fiberglass	47.33	112	3210	45/60	1
(1) Particle Throw: 0 (no particle throw) → 10 (most or all material ejected)						

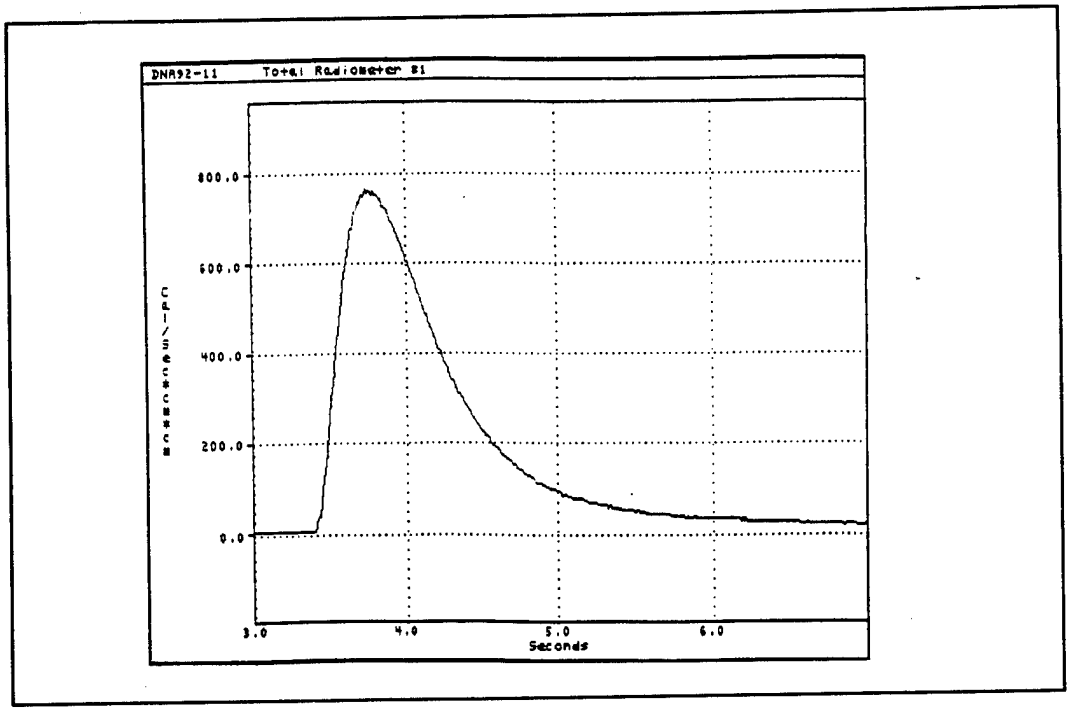

Figure A-6. Test DNA 92-11, total radiometer.

Test # 92-21 (Fiberglass fibers substituted for carbon fibers in the "Minimal Throw" chemistry) performed very well; particle throw was minimal and the surface emittance (112 cal/cm2/sec) was nearly double that of previous "Minimal Throw"

A.2.6 Test Series DNA #92-22 through #92-32.

The chemistries and configurations evaluated in this test series were essentially a repeat of the previous test series and are shown in Table A-3. The goal being to determine whether any extraneous test conditions such as wind was affecting the test results. This test series exhibited the excessive particle throw as seen in the previous test series (a particle containment screen was still not being used). Tests # 92-24 through 30 yielded emittance values representative of an emitting area larger than the initial panel area. The utility of the measurements is that a relative comparison can be made as to the total energetic output of specific chemistries and configurations. Tests # 92-22, 23, 31 and 32 yielded results that approach standard predicted emittance values; although #92-22 and 23 still exhibit fluxes predicative of slightly increased radiating areas (i.e., particulate cloud moderately larger than the original panel area). Test # 92-32 was undertaken with a modification to the standard test procedure. A light probe was placed 1 inch from the "Minimal Throw" panel in the hopes that a technique for "minimum" emittance values could be developed. The complete filling of the field of view of the light probe would permit a true emittance determination for that position. Any portion of the event not captured by this field of view would not be accounted for in an analysis by this technique.

Table A-3. Summary of test results for DNA 92-11 through DNA 92-21.

Test No.	Chemistry	Mass (grams)	Emittance ($cal/cm^2/sec$)	Peak Visible (Lux)	Mix to Acetone Ratio	Particle Throw (1)
92-22	80 parts Ti/2B + 40 parts Al + 80 parts Hf/C	105.8	369	10499	120/73	7
92-23	80 parts Ti/2B + 20 parts Al	57.07	349	16893	20/9	6
92-24	90 parts Ti/2B + 10 parts Al	55.22	654	saturated	70/30	9
92-25	90 parts Ti/2B + 10 parts Al + 2 parts Acacia	56.75	787	saturated	70/35	9
92-26	90 parts Ti/2B + 10 parts Al + 0.1 parts PMMA	56.35	762	saturated	80/35	9
92-27	80 parts Ti/2B + 30 parts Al + 80 parts Hf/C	117.6	497	24284	140/63	7
92-28	150 parts Ti/2B + 10 parts Al + 40 parts Ti/C + 3 parts carbon fibers	96.4	521	24341	80/37	7
92-29	90 parts Ti/2B + 10 parts Al + 1 part $KClO_4$	53.6	757	4863	30/24	9
92-30	90 parts Ti/2B + 10 parts Al + 3 parts fiberglass	54.65	669	saturated	80/35	8
92-31	60 parts Ti/2B + 40 parts Ti/C + 3 parts fiberglass	55.85	137	4517	80/35	no data
92-32	60 parts Ti/2B + 40 parts Ti/C + 3 parts carbon fibers	40.79	32	saturated	80/35	0
(1) Particle Throw: 0 (no particle throw) → 10 (most or all material ejected)						

The excessive particle throw of tests #92-2 and #92-11 through #20 was investigated. The integrity of the starting # 92-24 through #30 lots was confirmed via standard powder quality control methods. The common denominator between these chemistries is the presence of Aluminum and/or Boron Powder. Both these powders are hygroscopic to a degree such that the adsorbed and absorbed water can be deleterious to the gas evolution character of energetic reactions. The vaporization of this entrained moisture was sufficiently energetic to increase the kinetic energy associated with particle ejection.

It was determined that the simplest means of verifying the hypothesis was to subject the cast panels to a desiccating step as the final chemical processing step. Also the completed panels would be stored in desiccant prior to their usage.

The emittance curves based on radiometric analysis for tests DNA 92-22, 23, 31 and 32 follow in Figures A-7 through A-10.

A.2.7 Test Series DNA #92-33 Through #38.

This test series (conducted as shown in Figure A-11) evaluated 12"x12" panels with an 1/8"x1/8" mesh metal particle restraint system was used for these tests. Also, a witness plate of quartz fabric is placed from 5 to 11 feet in front of the panels to aid in the determination of the degree of particle throw. The distance from the test panels to the sensors was 60 feet. A ballistic radiometer is used in place of one of the "nominal" radiometers used in the earlier test

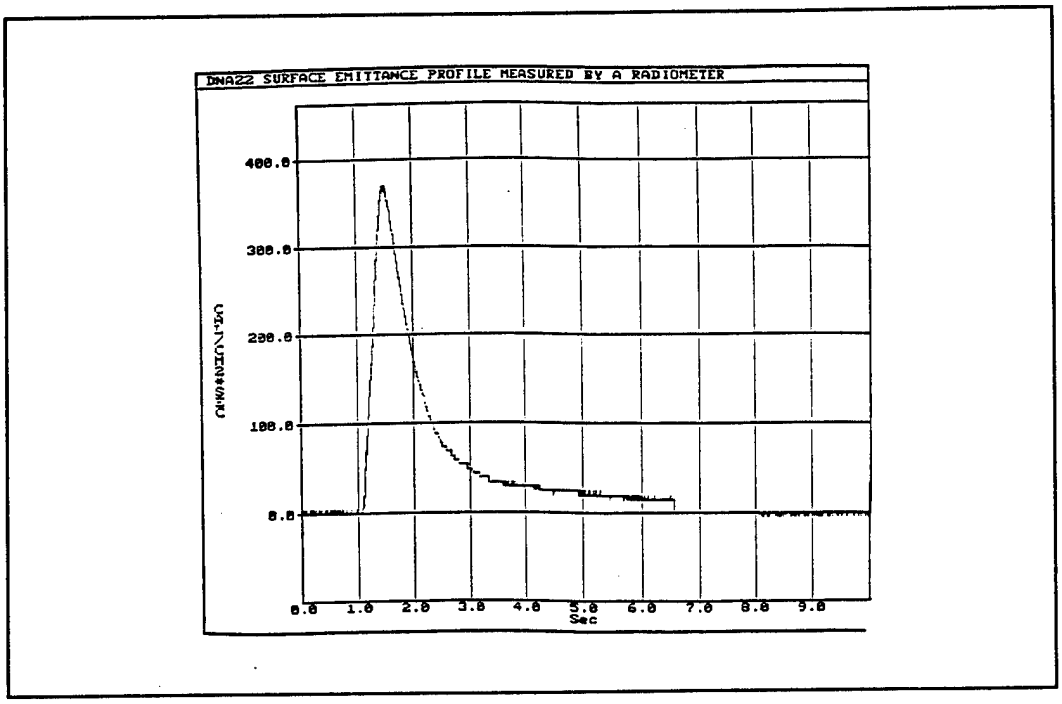

Figure A-7. Test DNA 92-22, total radiometer.

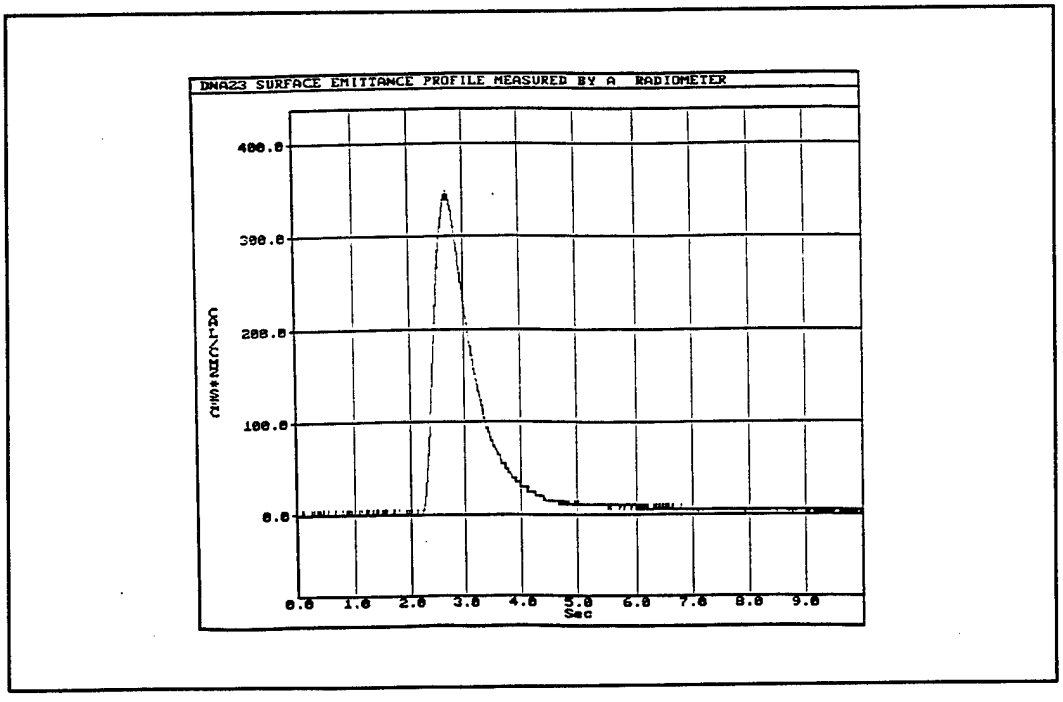

Figure A-8. Test DNA 92-23, total radiometer.

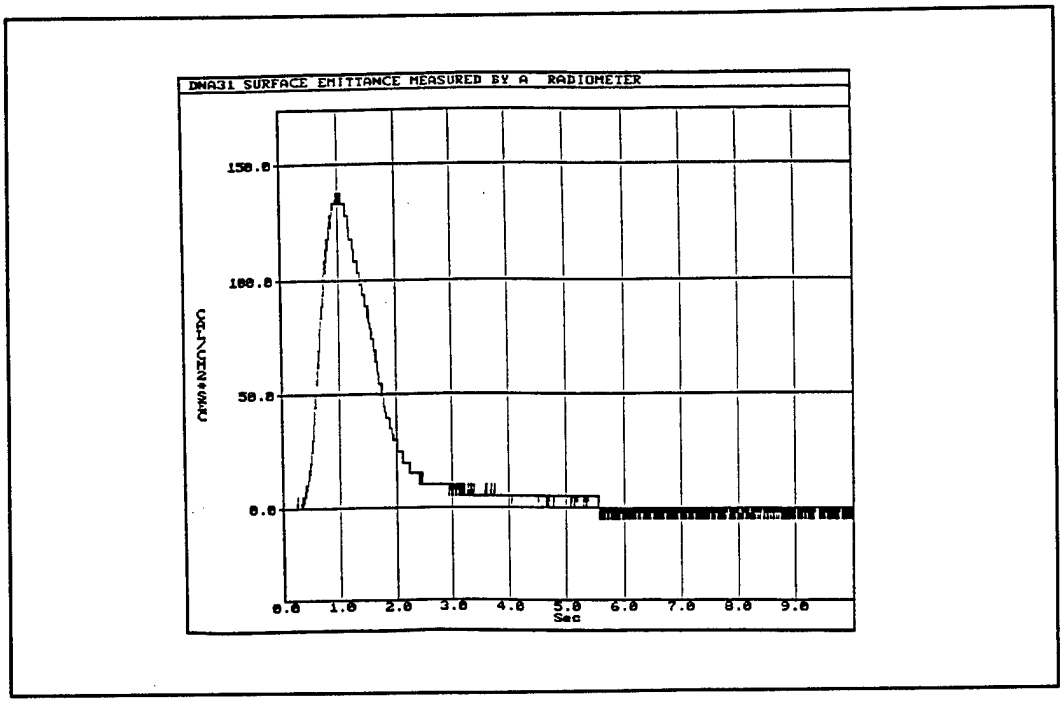

Figure A-9. Test DNA 92-31, total radiometer.

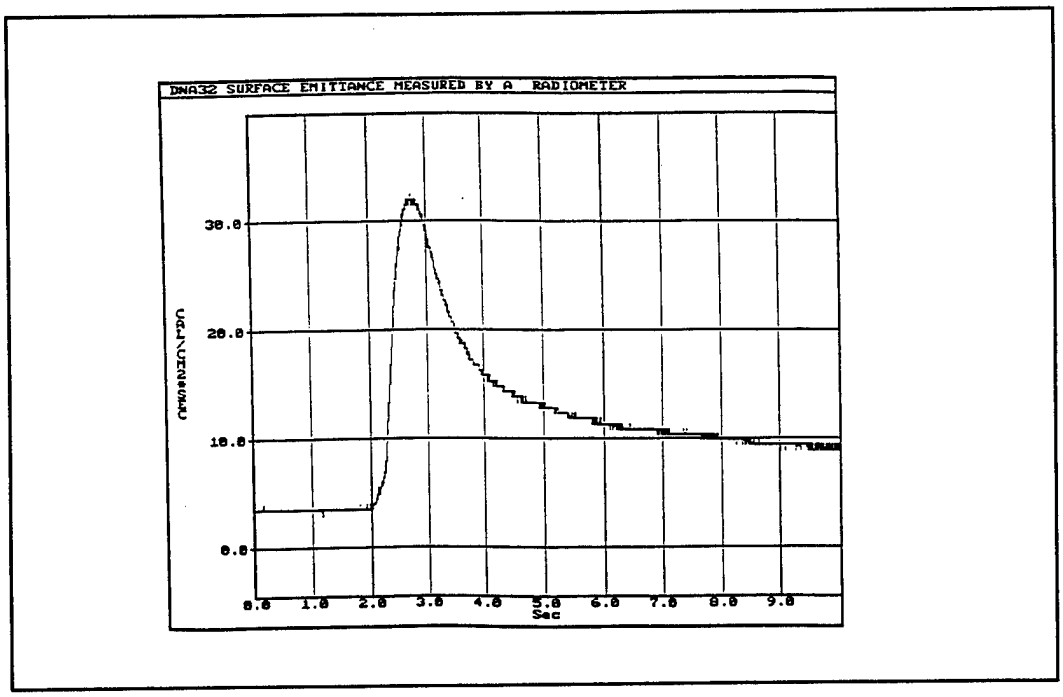

Figure A-10. Test DNA 92-32, total radiometer.

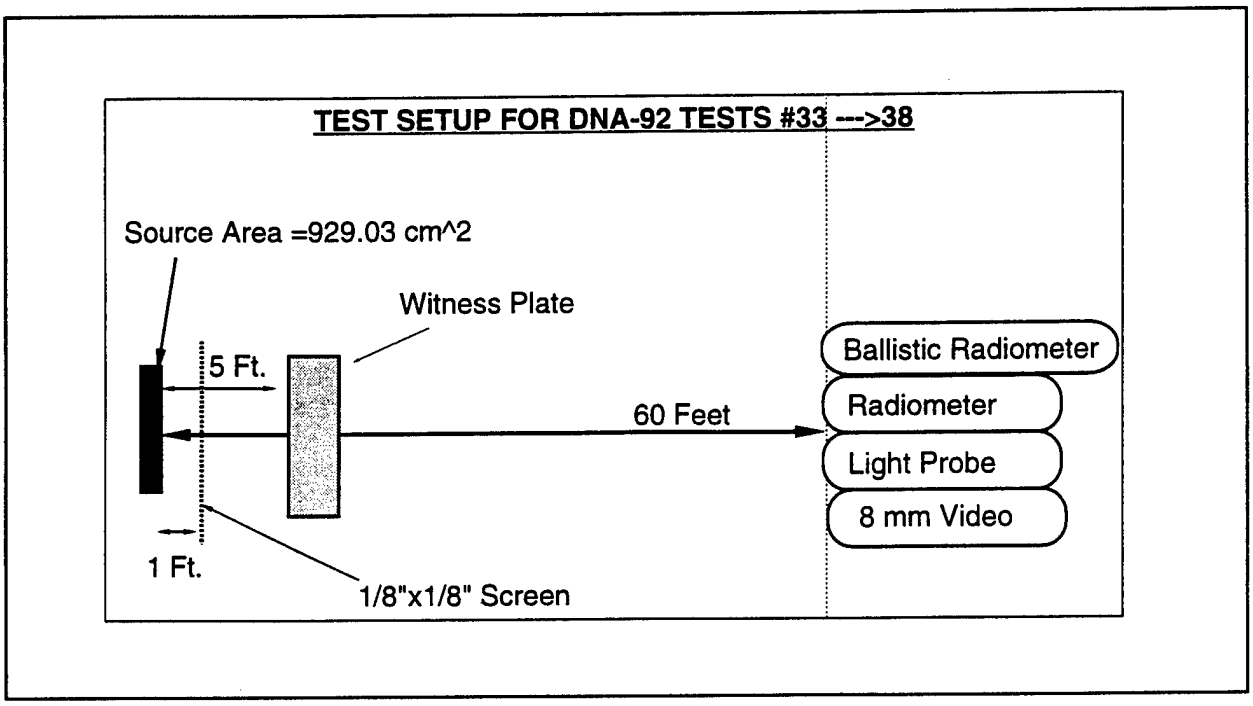

Figure A-11. Test set-up for DNA-92, tests 33-38.

series. This ballistic radiometer normally yields emittance values slightly lower than the nominal radiometer due to the devices inability to observe steady state events. The nominal radiometer provides a more precise analysis of the relatively long lived simulant event (in comparison to the short lived initial ignition pulse). The panels were fabricated using the refined drying procedure, air dried for 24 hours, then stored in desiccant for 24 hours prior to testing.

The results of the next series of tests are summarized in Table A-4 where emittance values range from 73 to 258 cal/cm^2/sec.

Table A-4. Summary of test results for DNA 92-11 through DNA 92-21.

Test No.	Chemistry	Mass (grams)	Emittance (cal/cm^2/sec)	Peak Visible (Lux)	Mix to Acetone Ratio	Particle Throw (1)
92-33	90 parts Ti/2B + 10 parts Al	1144.8	311	15968	22/10	4
92-34	90 parts Ti/2B + 10 parts Al	1139.9	258	11727	22/10	4
92-35	80 parts Ti/2B + 20 parts Al	1186.3	176	4924	23/10	2
92-36	60 parts Ti/2B + 40 parts Ti/C + 3 parts fiberglass	1204.0	73	3466	22/10	0
92-37	80 parts Ti/2B + 20 parts Al	1254.6	242	6334	23/10	2
92-38	60 parts Ti/2B + 40 parts Ti/C + 3 parts fiberglass	1208.9	78	2699	22/10	0
(1) Particle Throw: 0 (no particle throw) → 10 (most or all material ejected)						

Test #92-33 and #34 were both a modification of the reference chemistry. The weight percent of aluminum was decreased by 1/2 in the hope that particle throw could be decreased by decreasing the available expanding aluminum vapor. It was also hypothesized that less aluminum would not dilute the basic Ti/2B reaction, thus increasing the reaction temperature. The results for these two tests were promising. The rise times were approximately 0.60 seconds and the pulse duration was about 1.6 seconds. The emittance values were at a high level ≈300 cal/cm2/sec and the particle throw extended to a distance of 10 feet. These particles were on the order of a millimeter or less. The degree of particle throw, although much less relative to the small panel tests, still contributed to a small artificial increase in the emittance levels.

Test #92-35 and #37 were the reference chemistry. The rise times were about 0.50 seconds and the pulse duration was approximately 1.5 seconds. The surface emittance for #92-35 was 176 cal/cm^2/sec as measured by the nominal radiometer, and 137 cal/cm^2/sec, as measured by the ballistic radiometer. Although these levels are somewhat lower than desired under these conditions, there were no particulates expelled to a distance greater than five feet from the source. The surface emittance for #92-37 was 242 cal/cm^2/sec as measured by the nominal radiometer and 176 cal/cm^2/sec as measured by the ballistic radiometer. This level is considered to be both desirable and acceptable. However, there were fine particulates (sub-millimeter) extending to a distance of 8 feet from the source. The only conclusion that has been drawn for the output difference between two identical panels is the difference in particle throw and its effect on emittance measurement. It is obvious that a trade off between emittance and particle throw is required in order to optimize this system for its final production form.

Tests #92-36 and #38 were the modified "Minimal Throw" chemistry. Previous tests have shown that the fiberglass fiber substitution for carbon fibers offer enhanced flux performance at little or no penalty in particle throw. These panels will be referred to as the "Glass Reinforced" panels. The rise times were about 1.2 seconds and the pulse duration was approximately 2.2 seconds. There were no discernible particles collected on the witness plates from these tests. The surface emittance for #92-36 was 73 cal/cm^2/sec and the surface emittance for #92-38 was 78 cal/cm^2/sec, as measured by the nominal radiometer. The ballistic radiometer yields values approximately one half of the nominal radiometer. This difference is due to the manner in which these sensors view an event. The ballistic radiometer is capable of millisecond resolution but is limited to pulsed events (i.e., for this chemistry with a relatively slow rise time and pulse, the ballistic radiometer senses only a portion of the event). These emittance values are an increase of 10-20 cal/cm^2/sec over the previous minimal throw chemistry utilizing carbon fibers as a reinforcement.

The emittance values as determined by radiometric analysis for tests DNA 92-33 through DNA 92-38 following in figures A-12 through A-17.

A.2.8 Test DNA #92-39, Single Minimal Throw Panel.

This test (as shown in Figure A-18) was a single 12"x12" panel representing the "minimal throw" chemistry as downselected by the previous test series. A witness plate of quartz fabric was placed in front of the panel (extending from 5 to 8 feet in front of the panel).

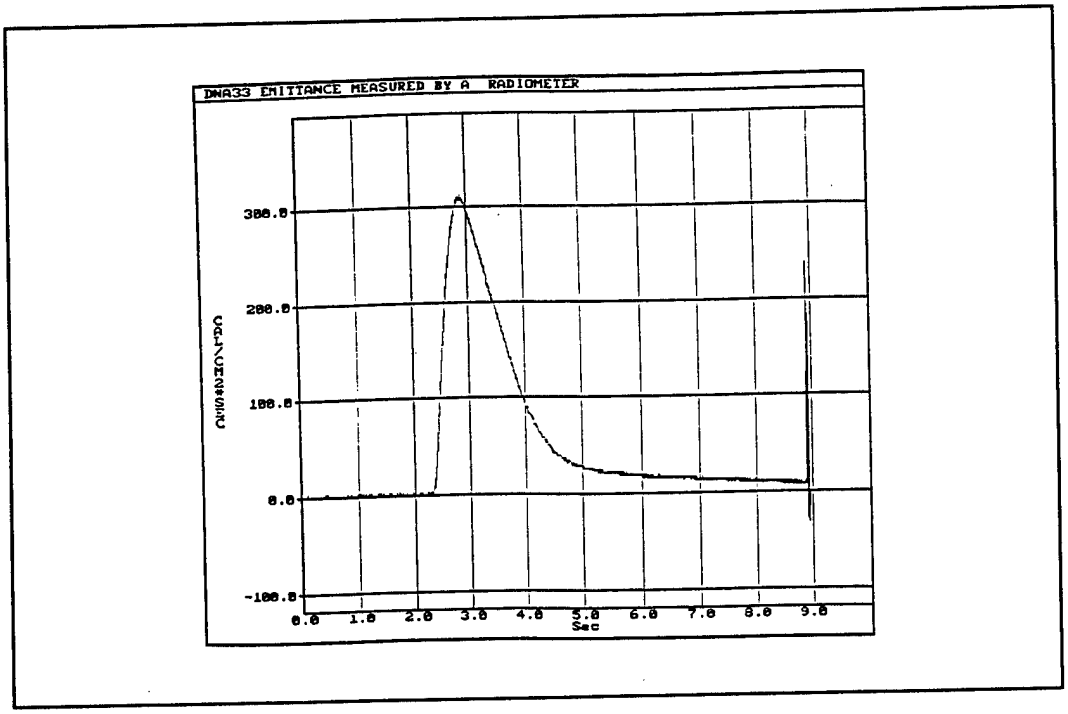

Figure A-12. Test DNA 92-33, total radiometer.

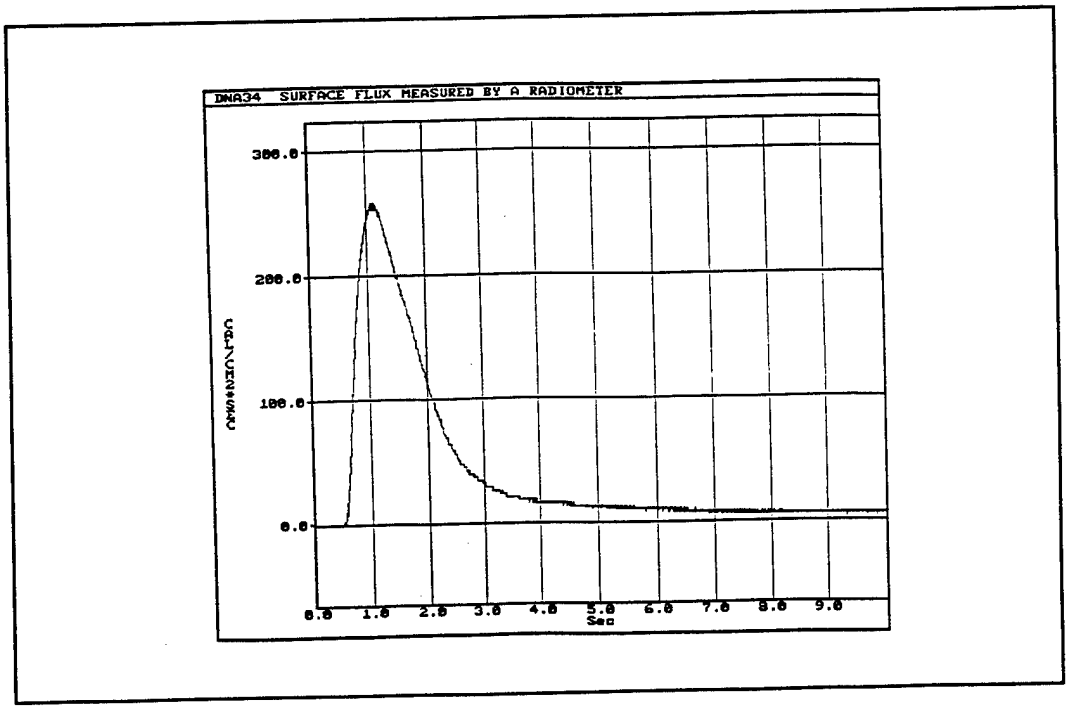

Figure A-13. Test DNA 92-34, total radiometer.

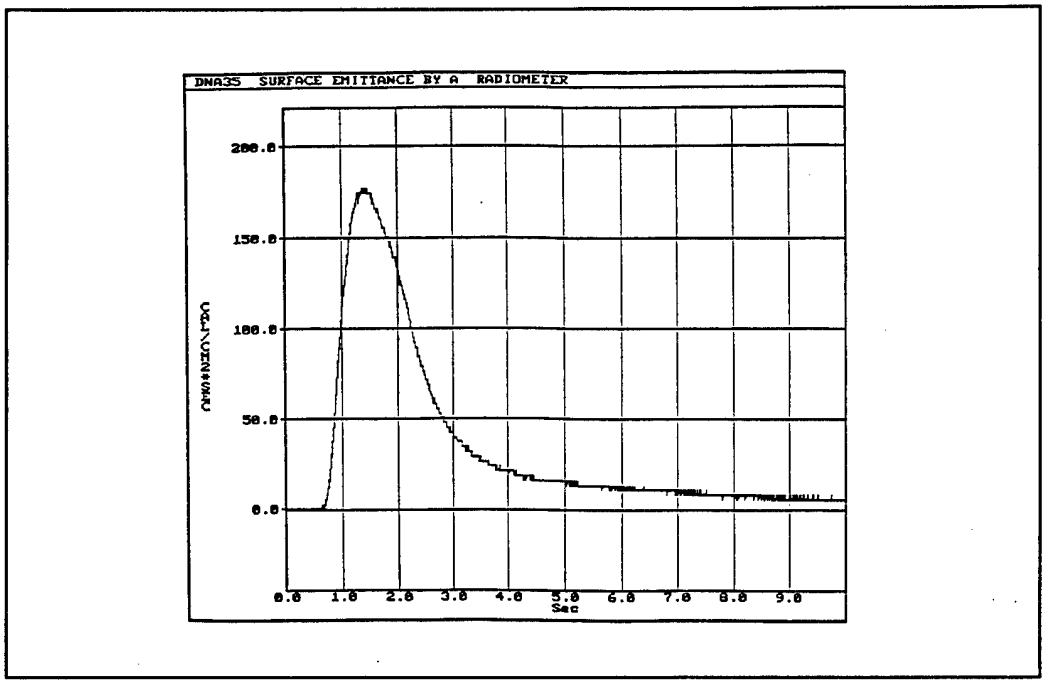

Figure A-14. Test DNA 92-35, total radiometer.

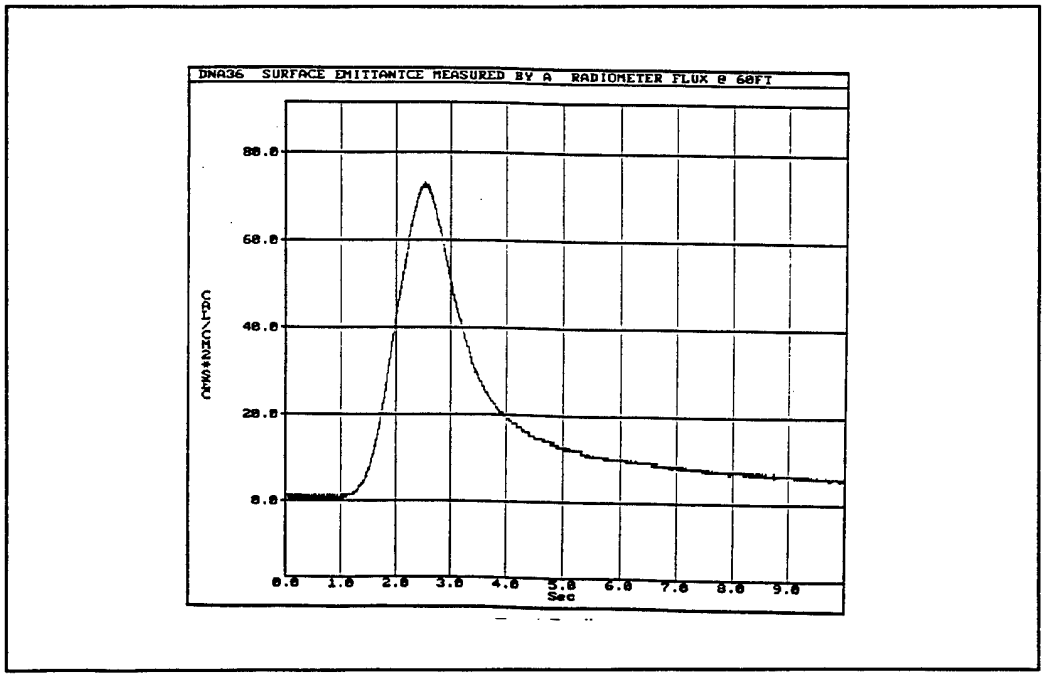

Figure A-15. Test DNA 92-36, total radiometer.

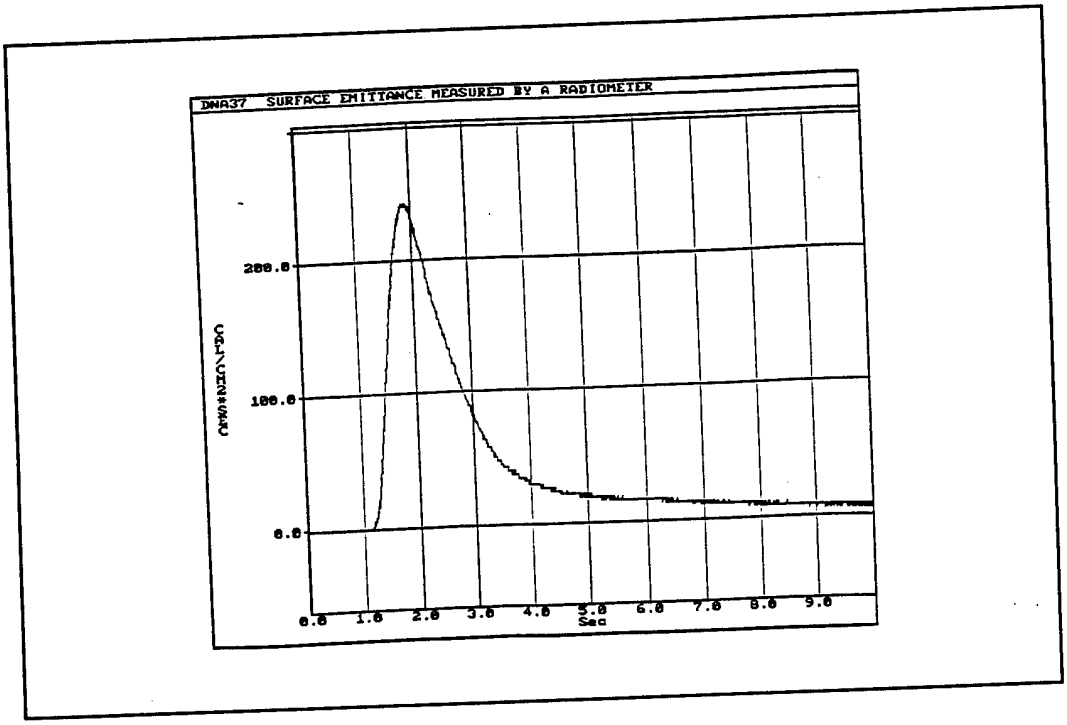

Figure A-16. Test DNA 92-37, total radiometer.

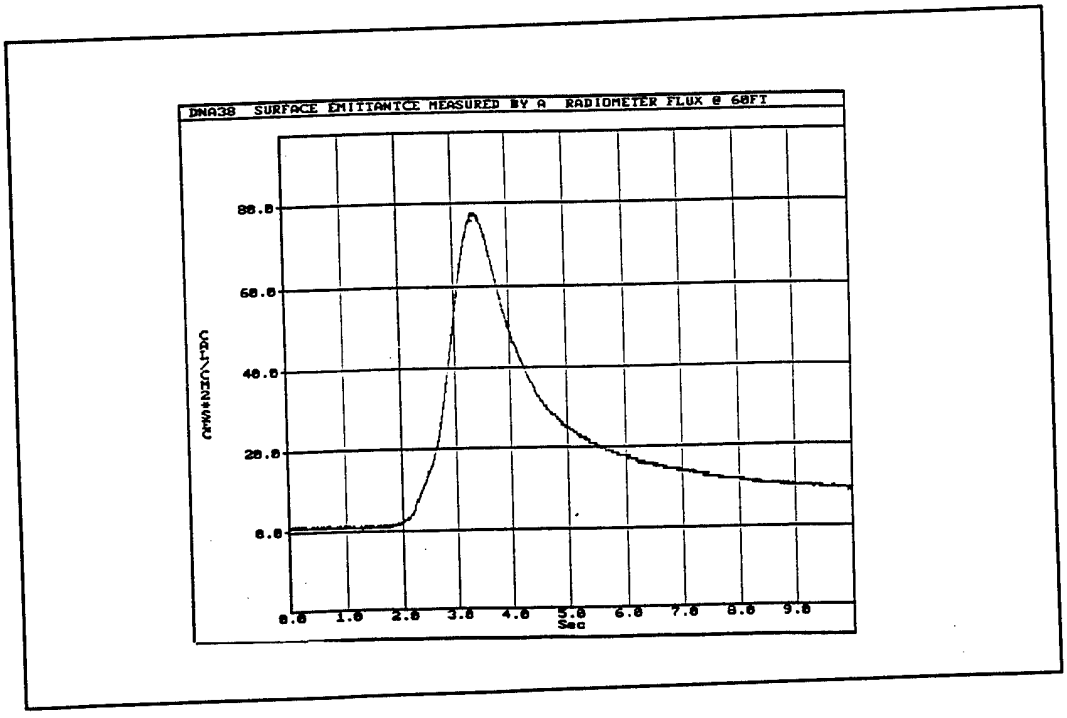

Figure A-17. Test DNA 92-37, total radiometer.

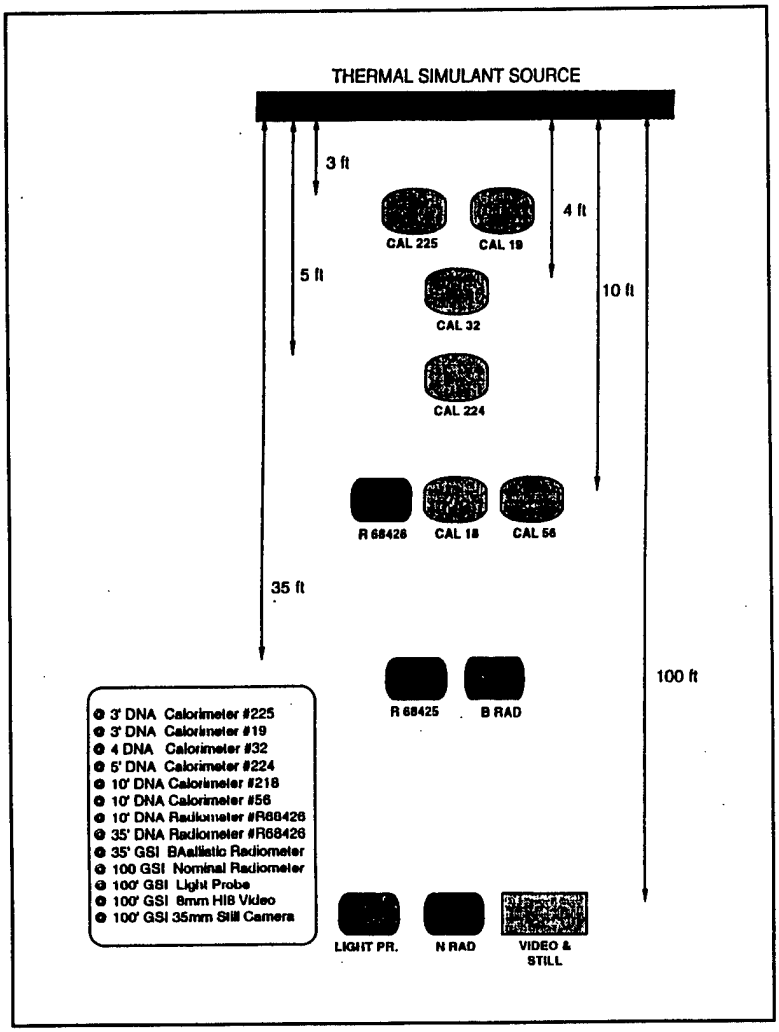

Figure A-18. Test DNA 92, tests 39 and 40.

A.2.8.1 Instrumentation. Instrumentation for this test provided by DNA consisted of two slug calorimeters at 3 feet, one at 4 feet, one at 5 feet, and two at 10 feet. Also, radiometers were at 10 feet and 35 feet. GSI supplied instrumentation consisted of a ballistic radiometer at 35 feet a light probe at 100 feet and a nominal radiometer at 100 feet. An 8mm Hi 8 video system was also at 100 feet. The linear disposition of sensors is shown in Figure A-18, and the projection (cross section at the panel surface) of the fields of view of sensors with fields of view less than 60 degrees are shown in Figure A-19.

Data acquisition was as follows:

- The first calorimeter's signal (#225), was amplified and recorded on a Digital Audio Tape (DAT) data recording system
- The second and third calorimeters (#19 and 32), signal were recorded on the DAT system

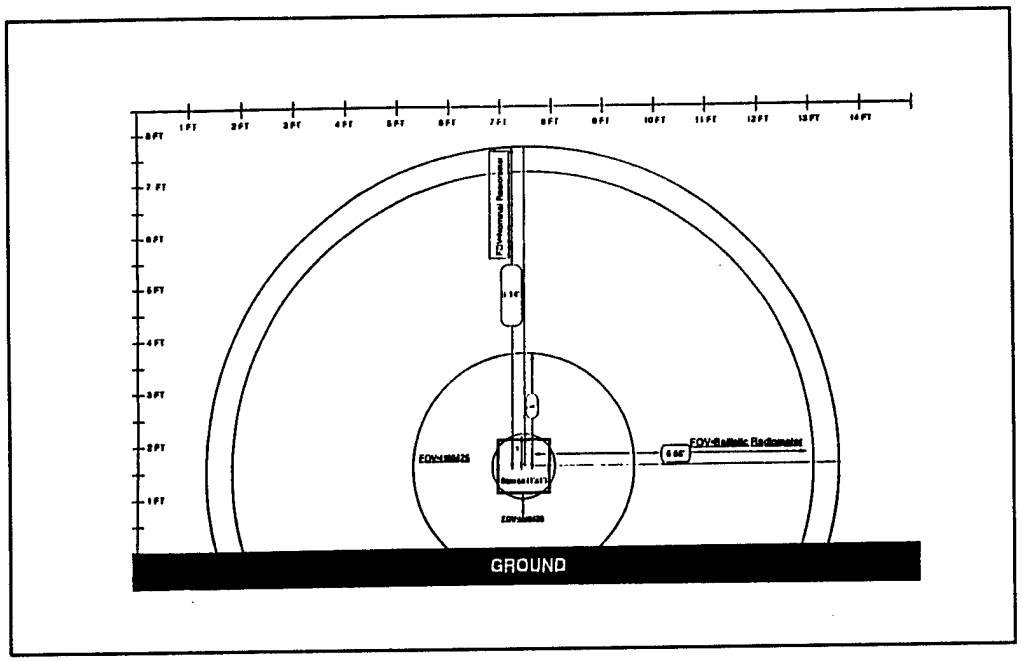

Figure A-19. Instrumentation field of view for test DNA 92-39.

- The fourth through sixth calorimeters signals were recorded on a chart recorder and were manually transposed into a digital format for analysis purposes
- The two DNA supplied radiometers signals (#68426 and 68425) were amplified and recorded on the DAT system
- The ballistic radiometer signal was amplified and recorded on the DAT system
- The signals from the nominal radiometer and the light probe were recorded directly by the DAT system

A.2.8.2 Panel Preparation. The panel was prepared by placing the following materials into a nalgene container:

1. Titanium, -325 mesh, 99.9%, Atlantic Equipment Eng.	953.2 g ± 0.1 g
2. Boron, Atlantic, BO -250, 2-3μm, 95-97%	242.5 g ± 0.1 g
3. Carbon Graphite, ConAstro, 41 A, 2μm, 99%	104.2 g ± 0.1 g
4. Fiberglass, Manville, #728, 3/16" x 13μm	39.0 g ± 0.1 g
5. Acetone, Fisher Scientific, Histological Grade	585.8 g ± 1.0 g

This mixture is designated 58.2 wt.% Ti/2B + 38.8 wt.% Ti/C + 3 wt.% excess Fiberglass.

A mesh screen mechanical mixing aid was added to the container. The container was then rolled on a standard powder rolling table for two hours. The resulting slurry was then cast (poured) into the prepared panel and permitted to dry for 24 hours. After air drying for 24 hours the panel was placed in a sealed polyethylene bag along with 200 grams of -8 mesh Drierite desiccant. The panel was maintained in this desiccating environment for 24 hours

after which the panel was sealed with 1 mil thick aluminum foil and then returned to the polyethylene bag for long-term storage. The initial empty weight of the panel was 532.6 grams. After casting and drying of the thermal simulant composition, the total weight of the panel was 1767.7 grams. Thus, the weight of the thermal simulant in this panel was 1235.1 grams.

A.2.8.3 Test Execution. The panel was initiated using a 5 volt-35 amp firing power supply applied across a 130' firing line. There were no ignition anomalies.

A.2.8.4 Results and Analysis. Table A-5 shows the results for this test. Radiometric analysis yields a rise time of approximately 1 second and a pulse duration of approximately 1.9 seconds for this test.

Table A-5. Summary of test results for DNA 92-39.

Detectors	Cal 225	Cal 19	Cal 32	Cal 224	Cal 18	Cal 50	Rad 68426	Bal Rad	Rad 88426	N Rad
Distance (ft)	3	3	4	2	10	10	10	35	35	100
Distance (cm)	91	91	121	152	304	304	304	1067	1067	3048
Field of View (degrees)	180	180	180	180	180	180	7	17.9	7	7
Area (cm^2)	n/a	n/a	n/a	n/a	n/a	n/a	1100	93247	13475	110003
Cal Factor ($cal/sec \cdot cm^2 \cdot mV$)	11.3	6.76	5.50	10.28	6.9	7.59	0.114	39.9	0.113	4.8
Signal Amplification	50	4	4	0	0	0	400	0.1	400	4
Detector Flux ($cal/cm^2/sec$)	5.53	low	low	1.59	0.345	0.349	0.053	0.012	0.0136	0.00049
Intensity (kW/sr)	191	low	low	154	134	135	20	56	65	19
Emittance (cal/cm^2)	155	low	low	127	108	109.6	16.5	45	52	15.4

It is of interest to note that the relatively small area of the source panel versus the cross sectional area of the sensors and their mounts led to an unavoidable cumulative obscuration of the source panel by each successive sensor and mount. It was impossible to spatially orient the instrumentation to completely negate the obscuration of the thermal event by instruments in front of one another. Therefore, each measured value obtained from the sensors at a distance of 4 feet and greater is a minimum value. No attempt was made to calculate the individual and cumulative effect of the "blocking" of each successive sensor. It is felt that this approach will not seriously degrade the integrity of the obtained data but will merely yield a conservative analysis.

One calorimeter at 3 feet (#225) measured a source emittance of 155 $cal/cm^2/sec$. The other calorimeter at 3 feet (#19) and the calorimeter at 4 feet (#32) did not yield data. The data were not obtained for these devices because insufficient signal amplification yielded a signal amplitude indistinguishable from background noise. The calorimeters at 5, 10, and 10 feet (#224, 18, 56) measured a surface emittance of 124 $cal/cm^2/sec$, 108 $cal/cm^2/sec$, and 108.9 $cal/cm^2/sec$, respectively. It is highly probable that this slight drop off with distance is due to the obscuration effects of preceding detectors. These values correlate with previously

obtained radiometric emittance values. The emittance curves for calorimeters #18, 56, 224, and 225 follow in Figures A-20 through A-23.

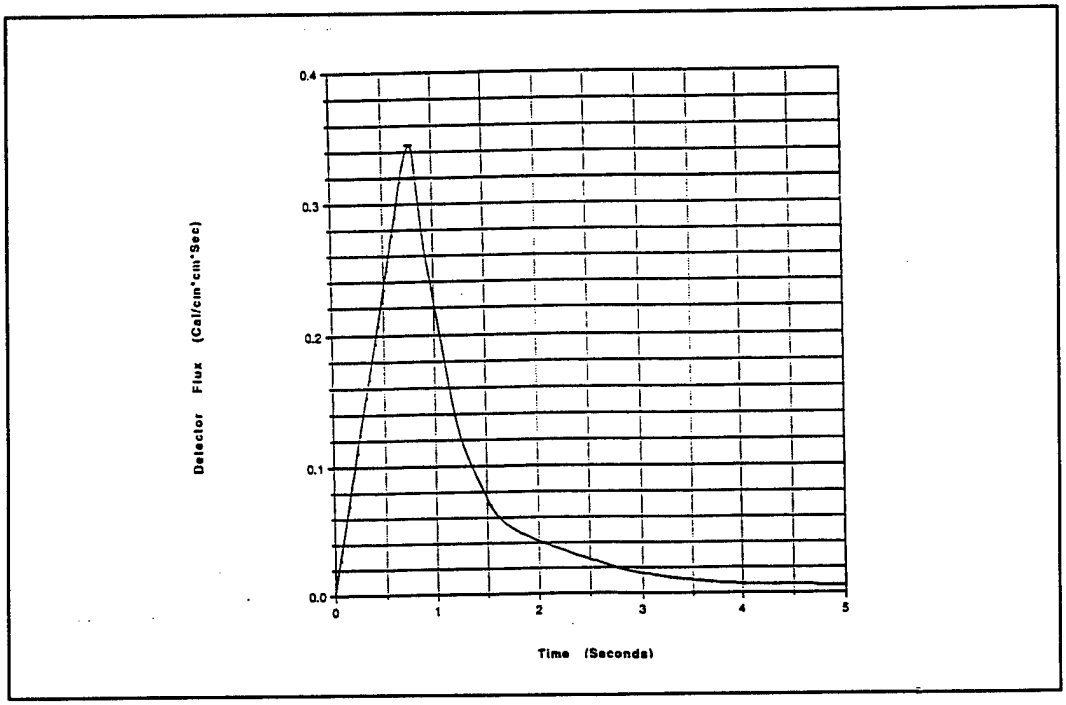

Figure A-20. Test DNA 92-39, slug calorimeter at 10 feet.

The radiometer at 10 feet yielded a surface emittance value of 16.5 cal/cm^2/sec. Possible explanations offered for this low result are: improper calibration, improper alignment, data acquisition error, obscuration by preceding sensors, or a combination of the above. The radiometer at 35 feet (#68425), yielded a surface emittance value of 52 cal/cm^2/sec. This value supports the hypothesis that with increasing distance, the masking effects of closer instrumentation and support hardware effects the field of view of sensors at a greater distance. It was anticipated that all sensors would yield emittance values that fell within a range dictated by acceptable experimental error. It should be noted that it was not feasible (due to the late modifications to the number and types of sensors) to design and fabricate a sensor array support system that would have mitigated the observed masking effects. The emittance curves for these radiometers are shown in Figures A-24 and A-25.

GSI Instrumentation other GSI instrumentation such as the ballistic radiometer at 35 feet yielded a surface emittance of 45 cal/cm^2/sec. This detector experienced the same degree of sensor masking as DNA radiometer #68425. It is expected that the ballistic radiometer would yield a slightly lower value than a non-ballistic device because the ballistic device would not be able to measure the steady state portion of the thermal simulant event. Thus, there is good correlation between the two radiometers at 35 feet.

The nominal radiometer (or sometimes referred to as "radiometer"), yielded a surface emittance of 15.4 cal/cm^2/sec. It is believed that sensor masking has significantly contributed to this artificially low value as well.

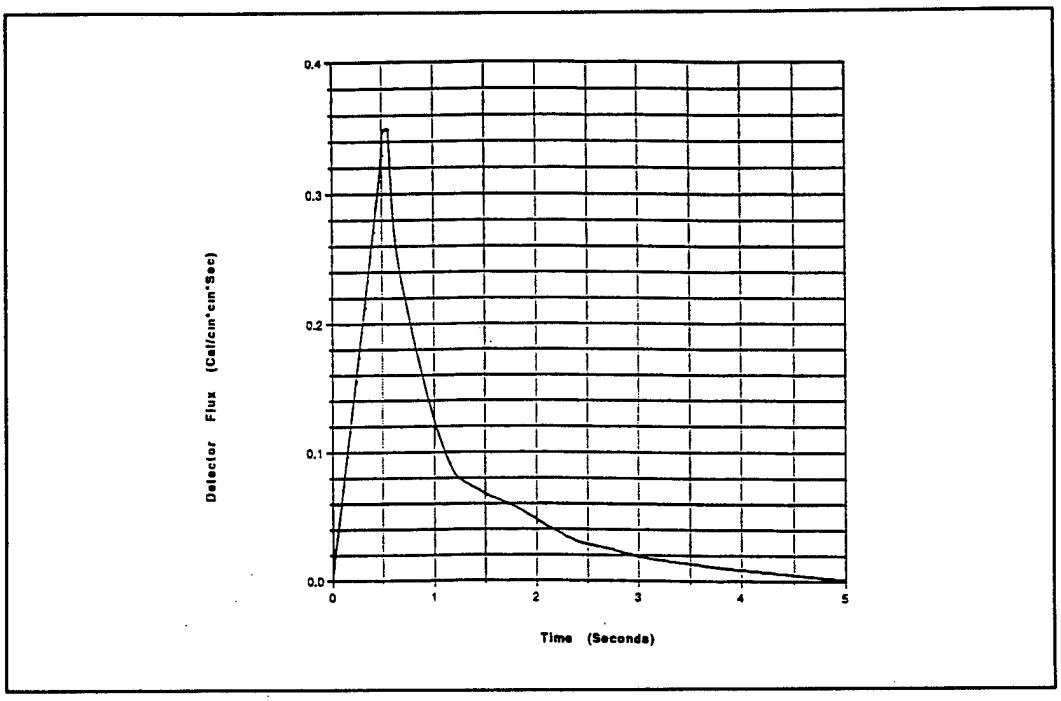

Figure A-21. Test DNA 92-39, slug calorimeter #56 at 10 feet.

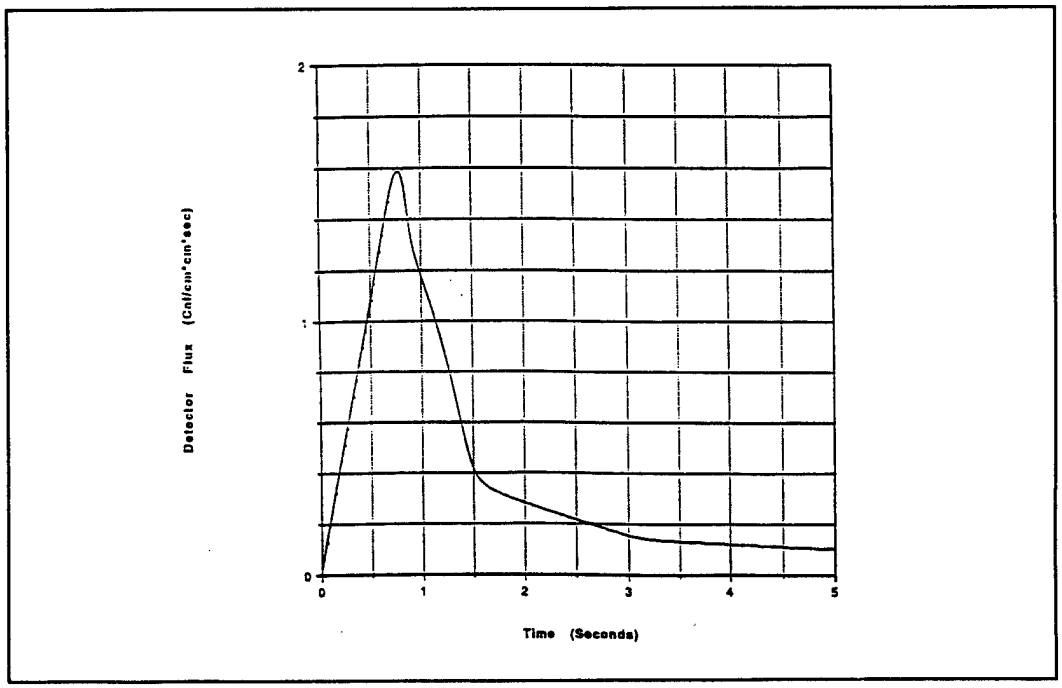

Figure A-22. Test DNA 92-39, slug calorimeter #22 at 5 feet.

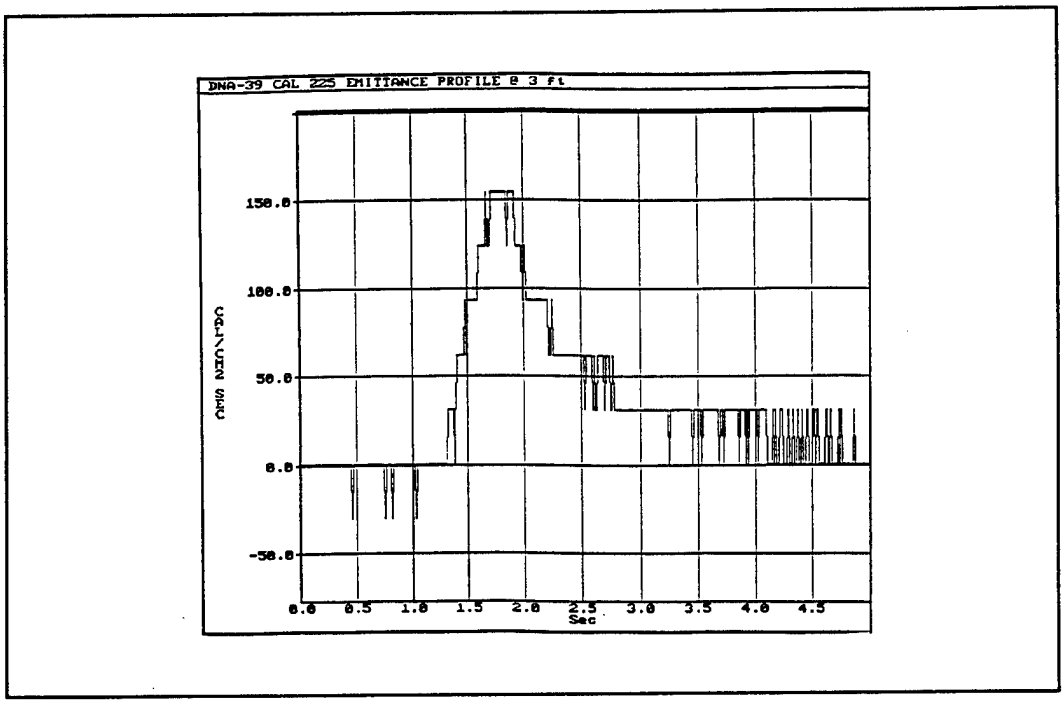

Figure A-23. Test DNA 92-39, calorimeter #225 at 3 feet.

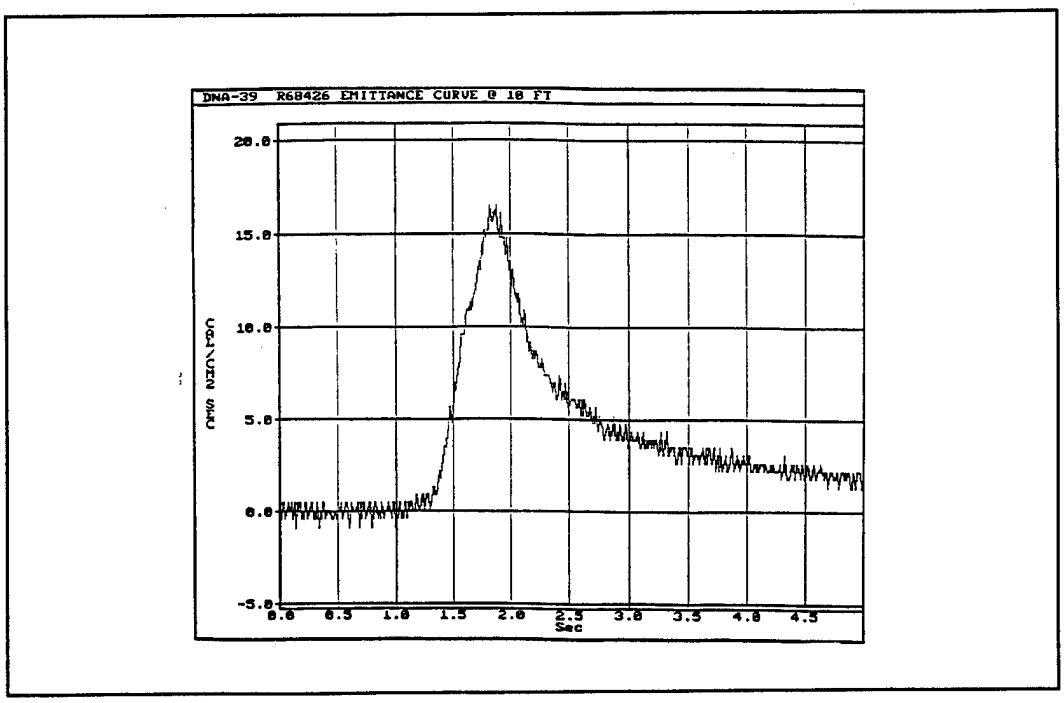

Figure A-24. Test DNA 92-39, total radiometer at 10 feet.

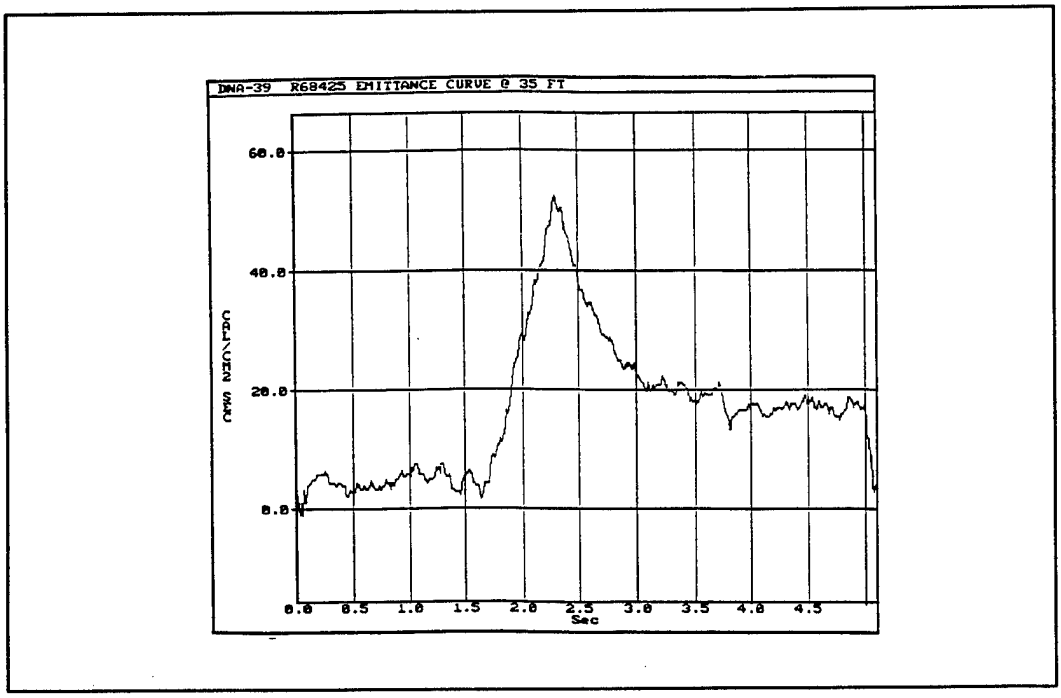

Figure A-25. Test DNA 92-39, total radiometer at 35 feet.

The light probe experienced a peak detector flux of 703 Lux. This measurement is used as a means of comparing similar test runs and will be held for future comparisons of similar tests. The emittance curves for these radiometers and the detector flux for the light probe are shown in Figures A-26 through A-28.

As far as particle throw is concerned there were little or no discernible particulates at a distance of 5 feet prom the panel. A small quantity of sub-millimeter particulates did fall off to the side of the panel (in the same plane). This sideways motion of some particles may have been the result of a slight cross wind that was blowing at the time of the test. In conclusion it is felt that this test demonstrated a thermal simulant with little or no particle throw.

A.2.9 Test DNA #92-40-9 Panel Array.

This test involved the simultaneous ignition of (9) 12"x12" panels arranged in a 3 feet x 3 feet array. A witness plate of quartz fabric was placed in front of the panel (extending from 5 to 11 feet in front of the panels).

A.2.9.1 Instrumentation. Instrumentation for this test provided by DNA consisted of two slug calorimeters at 3 feet, one at 4 feet, one at 5 feet, and two at 10 feet. Also, radiometers were at 10 feet and 35 feet. GSI supplied instrumentation consisted of a ballistic radiometer at 35 feet, a light probe at 100 feet and a nominal radiometer at 100 feet. An 8mm Hi 8 video system was also at 100 feet. The linear disposition of sensors were the same as for test DNA 92-39 as shown Figure A-18. The projection (cross section at the panel surface) of the fields of view of sensors with fields of view less than 60 degrees is shown in Figure A-29.

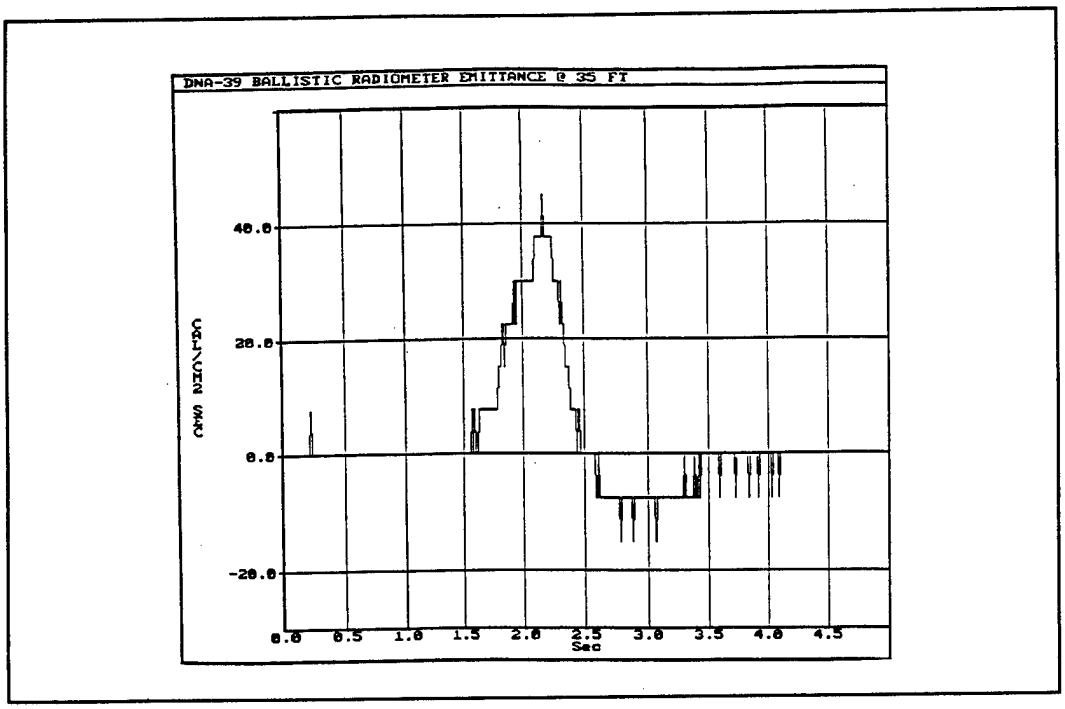

Figure A-26. Test DNA 92-39, ballistic radiometer at 25 feet.

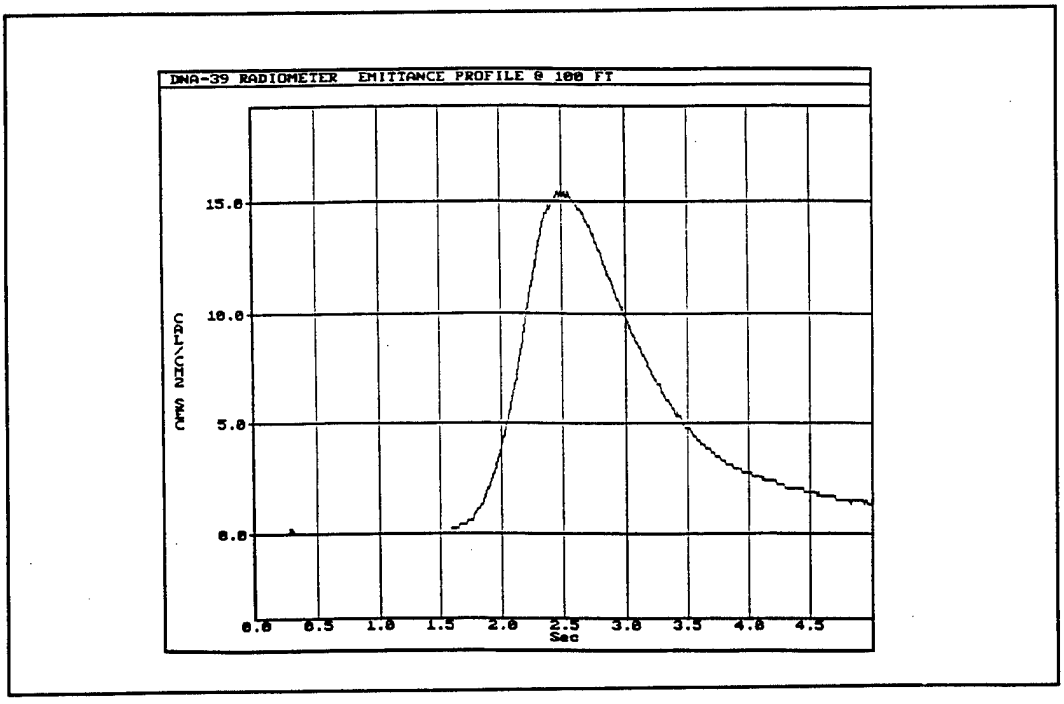

Figure A-27. Test DNA 92-39, total radiometer at 100 feet.

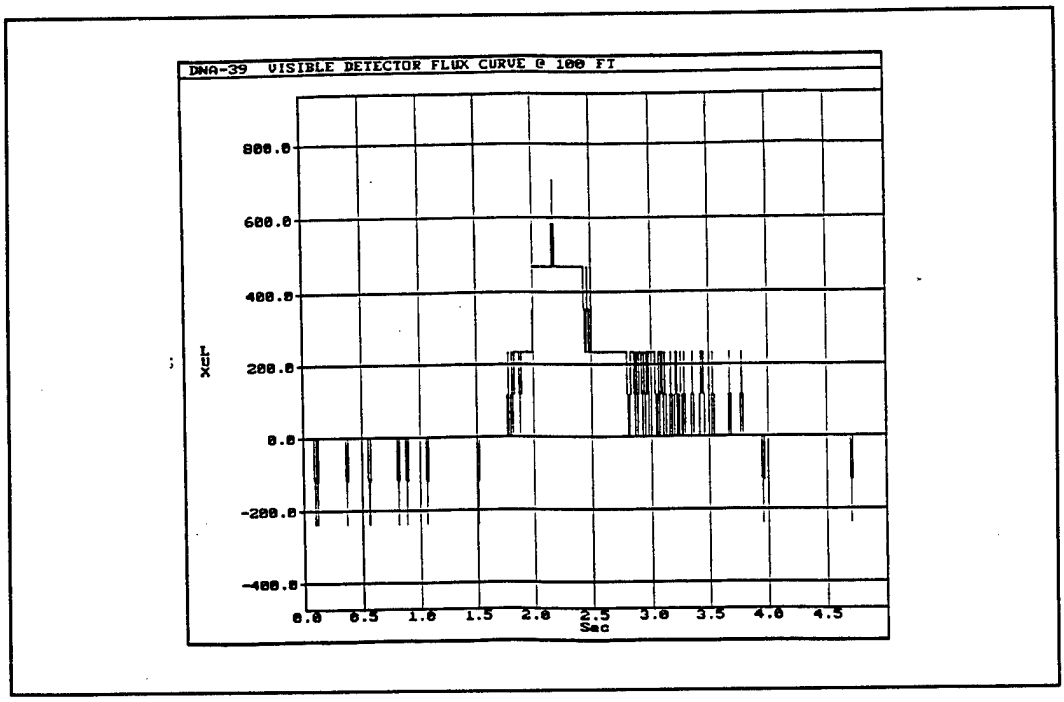

Figure A-28. Test DNA 92-39, light probe at 100 feet.

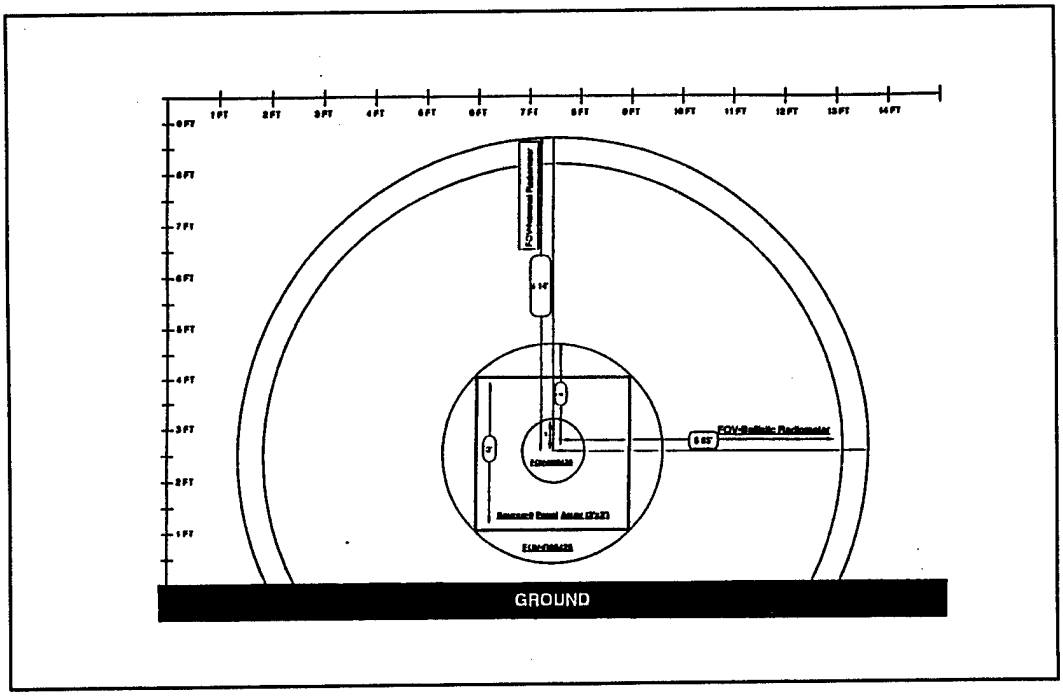

Figure A-29. Test DNA 92-40, instrumentation field of view.

Data acquisition was as follows:

- The first calorimeter's signal (#225), was amplified and recorded on a Digital Audio Tape (DAT) data recording system
- The second and third calorimeters' (#19 and 32), signal were recorded on the DAT system
- The fourth through sixth calorimeters' signals were recorded on a chart recorder and were manually transposed into a digital format for analysis purposes
- The two DNA supplied radiometers' signals (#68426 and 68425) were amplified and recorded on the DAT system
- The ballistic radiometer's signal was amplified and recorded on the DAT system
- The signals from the nominal radiometer and the light probe were recorded directly by the DAT system

The test setup can be seen in Figures 2-2 and 2-3 in the main section of the report.

The panels were prepared by placing the following materials, each into a nalgene containers:

1. Titanium, -325 mesh, 99.9%, Atlantic Equipment Eng., 806.1 g ± 0.1 g
2. Boron, Atlantic, BO -250, 2-3μm, 95-97%, 363.9 g ± 0.1 g
3. Aluminum, Johnson Matthey, -325, 99%, 130.0 g ± 0.1 g
4. Acetone, Fisher Scientific, Histological Grade, 590 g ± 1.0 g

This mixture is designated 90 wt.% Ti/2B + 10 wt.% Al.

A mesh screen mechanical mixing aid was added to each container. The containers were then rolled on a standard powder rolling table for two hours. The resulting slurry was then cast (poured) into the prepared panels and permitted to dry for 24 hours. After air drying for 24 hours the panels were placed in a sealed polyethylene bag along with 200 grams of -8 mesh Drierite desiccant. The panels were maintained in this desiccating environment for 24 hours after which the panels were sealed with 1 mil thick aluminum foil and then returned to the polyethylene bag for long term storage. The initial empty weight of the panels as well as the final weights for the dried panels and the final weight of the thermal simulant in each panel are shown in Table A-6.

Table A-6. DNA 92-40 panel weights and mix weights.

Panel No.	Tare weight (grams)	Lot	Mix weight (grams)	Finished panel weight (grams)
1	535.9	G	1225.0	1760.9
2	534.1	C	1207.9	1742.0
3	533.5	B	1235.3	1768.8
4	538.9	H	1227.2	1766.1
5	535.8	A	1240.9	1776.7
6	535.3	E	1251.2	1786.5
7	536.3	F	1261.0	1797.3
8	537.3	I	1224.9	1762.2
9	531.5	D	1254.0	1785.5

A.2.9.2 Test Execution. Initiation of the panels was initially attempted using a 5 volt-35 amp firing supply. This voltage applied across a 130 feet firing line was insufficient to ignite the panels due to the voltage drop across the firing line. Subsequently a 20 volt-30 amp firing supply was used to initiate the 9 panel array. Figures 2-4 through 2-11, in the main report, are the 35 mm stills taken of the thermal simulant test. The rear of the panel array showing the igniter hookups and the bus bar system can be seen in Figure A-30. This same hardware is shown after the test in Figure A-31.

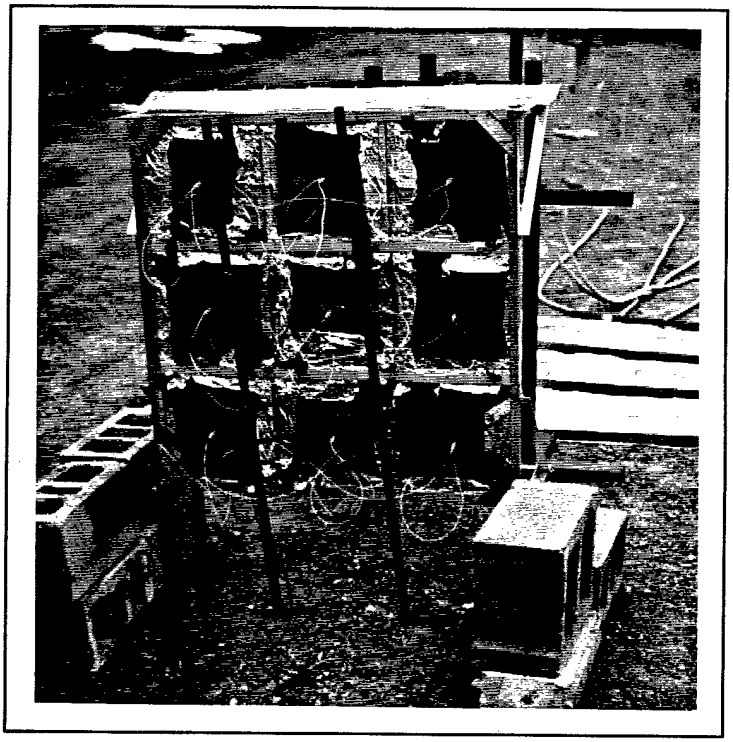

Figure A-30. Rear view of the 9 panel array pre-test.

A.2.9.3 DNA Supplied Calorimeters. The calorimeters at 3 (#225 and 19) and 4 feet (#32) sustained heavy particle impact, while the calorimeters at 5 (#224) and 10 feet (#18 and 56) sustained very little particle impact (see Figures A-32 through A-37). The effect of the particle impact on the calorimeters at 3 feet was to cause an erratic signal with a portion yielding negative values (Figures A-32 and A-33). We feel that the resultant data is unreliable and cannot be used as part of our analysis. The calorimeter at 5 feet peaked the chart recorder and thus provides a minimum detector flux of 46.26 cal/cm^2/sec (Figure 35). The two calorimeters at 10 feet (#18 and 56) measured a detector flux of 19.67 cal/cm^2/sec, and 20.87 cal/cm^2/sec, respectively (Figures 37 and 38). The similarity between these two detectors provides evidence that the values measured are reliable. The detector fluxes measured by the calorimeters are representative of the energy radiated upon these detectors. The fact that the thermal simulant event generated a hot cloud that encompasses the detectors severely complicates the source emittance analysis for these detectors. Ideally, the hot cloud would be geometrically and thermally characterized per unit time. Unfortunately, this cannot be accomplished with the current instrumentation configuration. Therefore an attempt

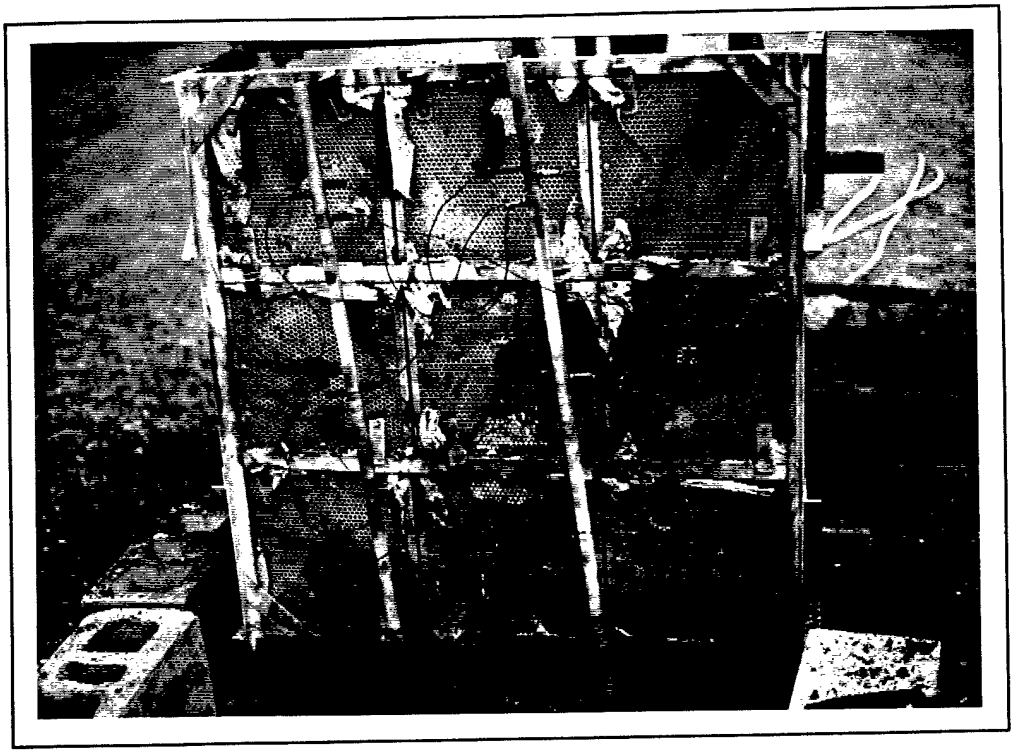

Figure A-31. Rear view of the 9 panel array post-test.

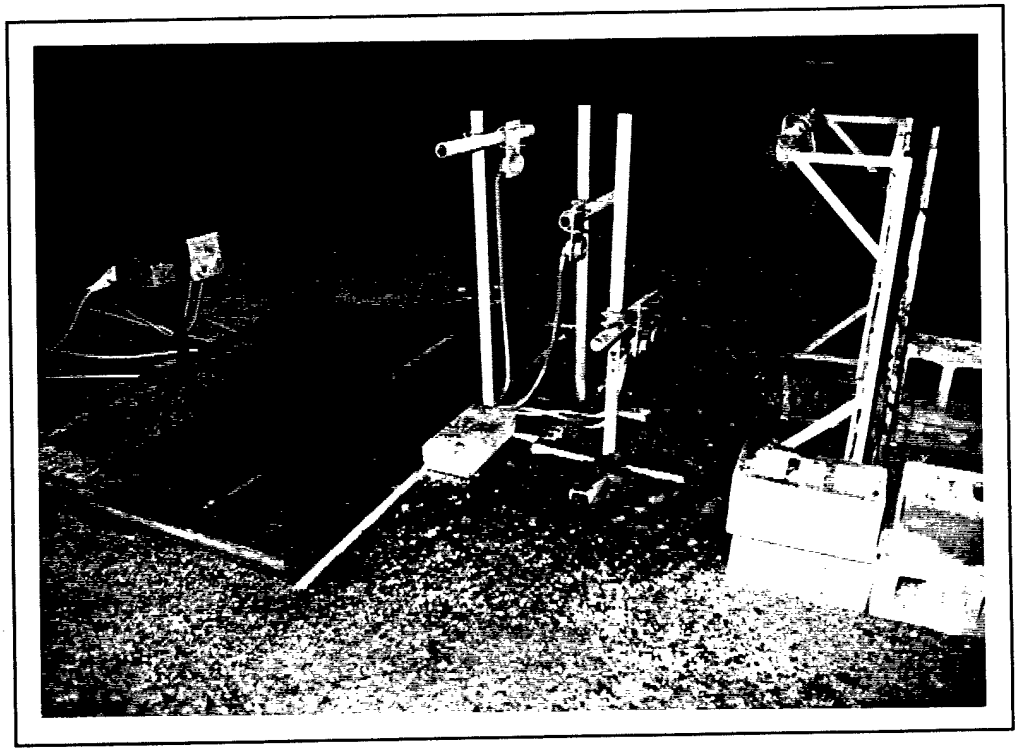

Figure A-32. Calorimeters at 3, 4, 5 and 10 feet, post test.

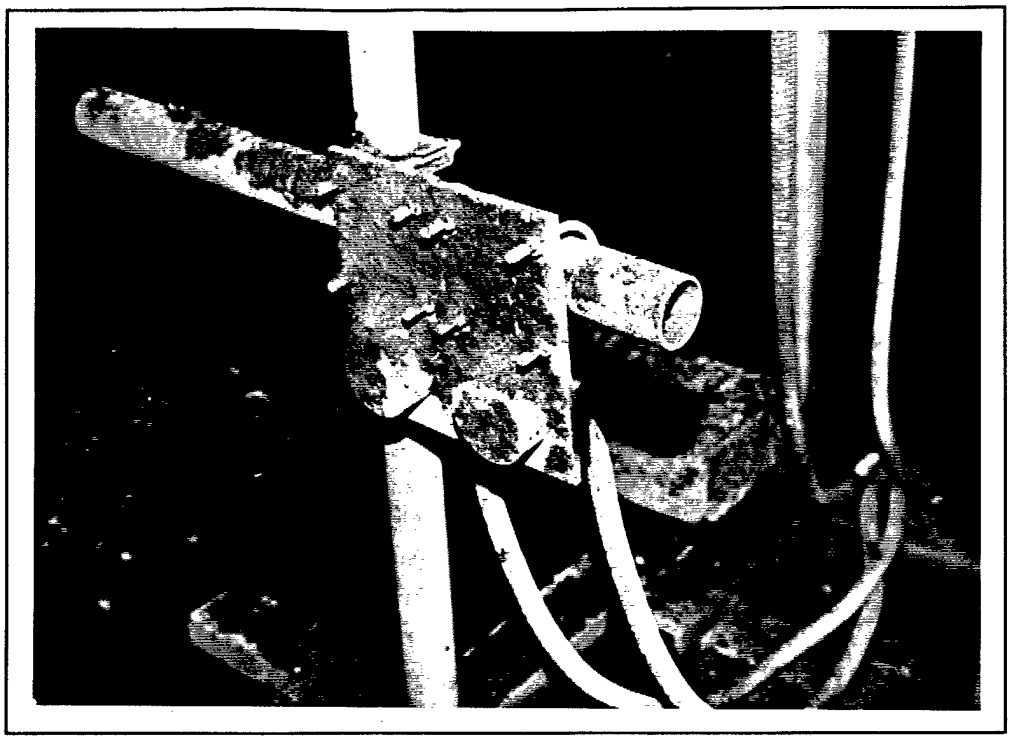

Figure A-33. Calorimeter at 3 feet, post test.

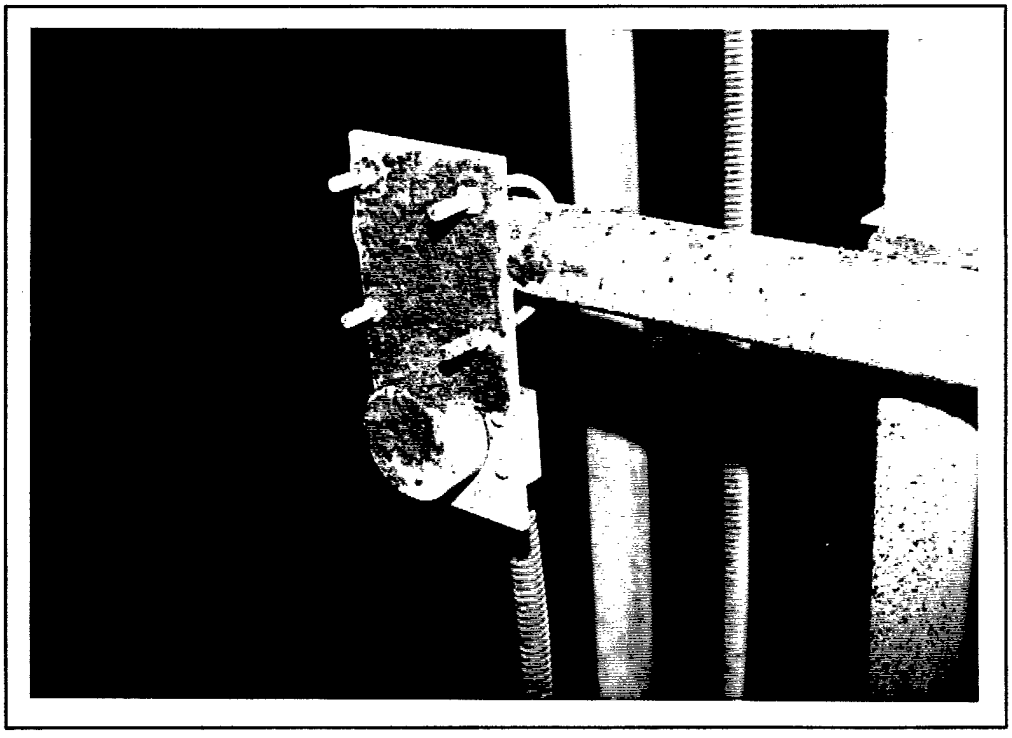

Figure A-34. Calorimeter at 4 feet, post test.

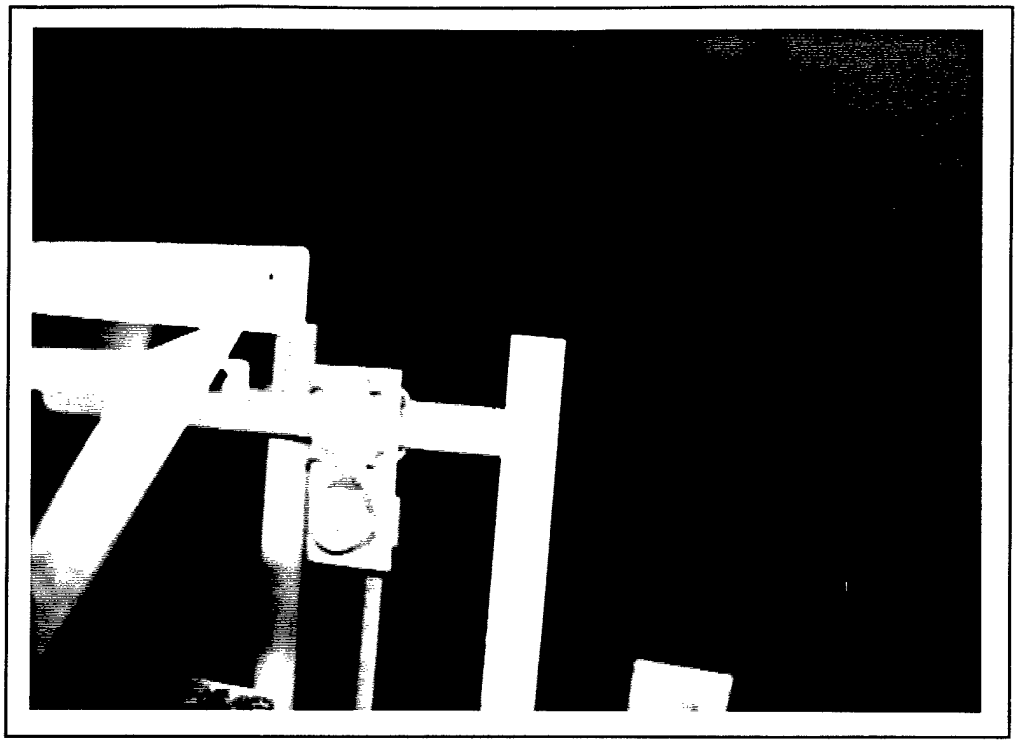

Figure A-35. Calorimeter at 5 feet, post-test.

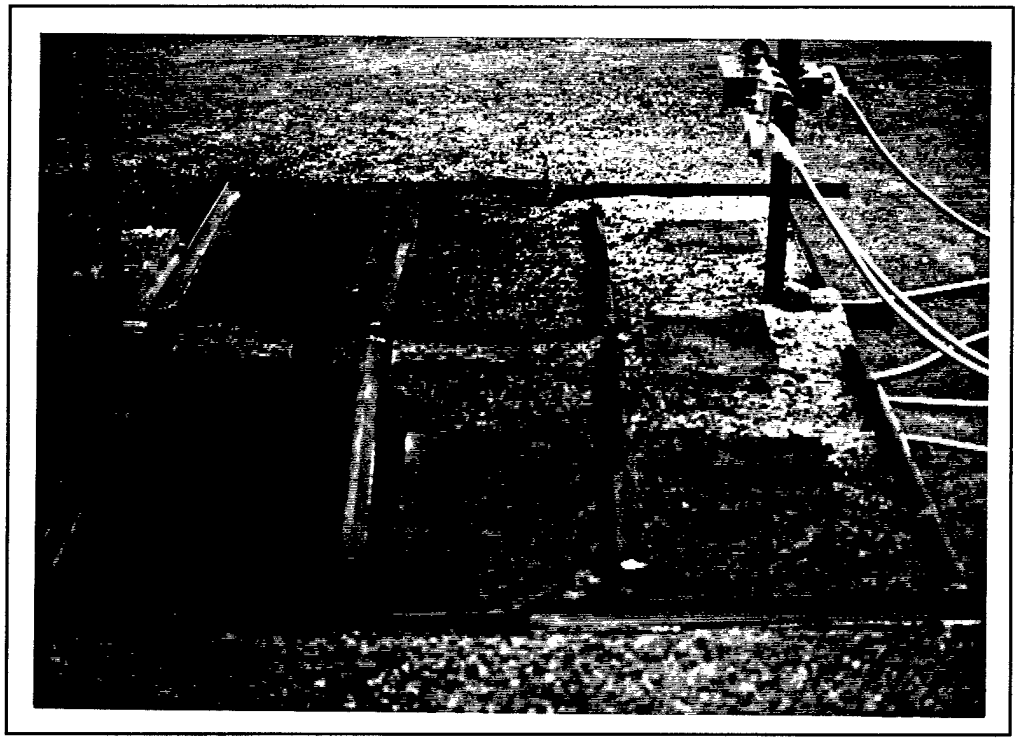

Figure A-36. Calorimeter at 10 feet, post-test.

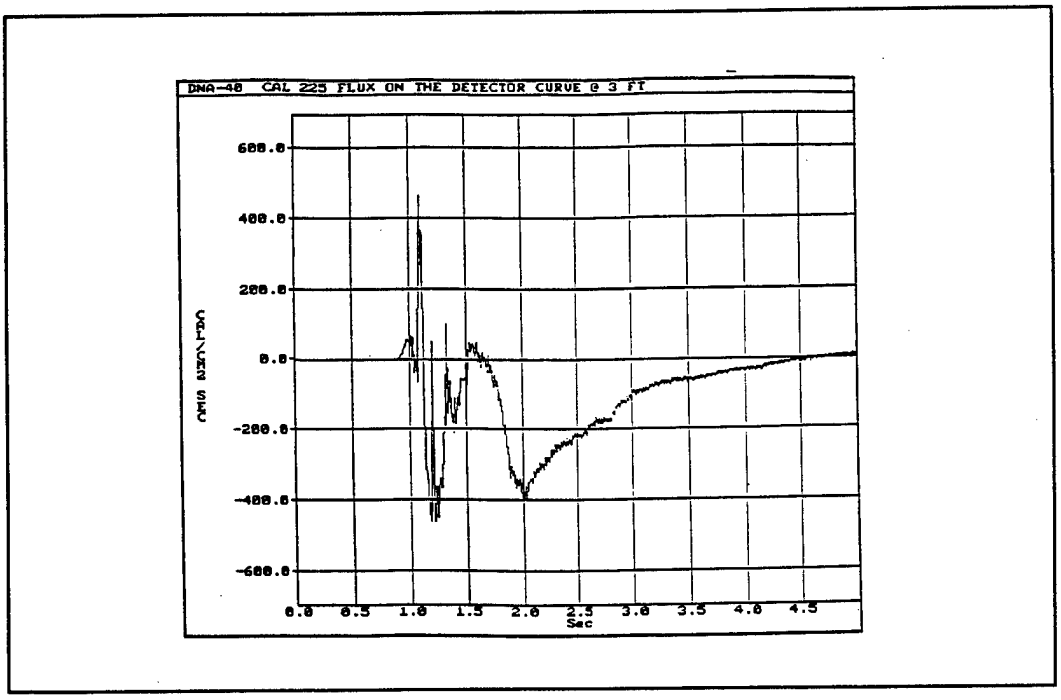

Figure A-37. Test DNA 92-40, calorimeter #225 at 3 feet.

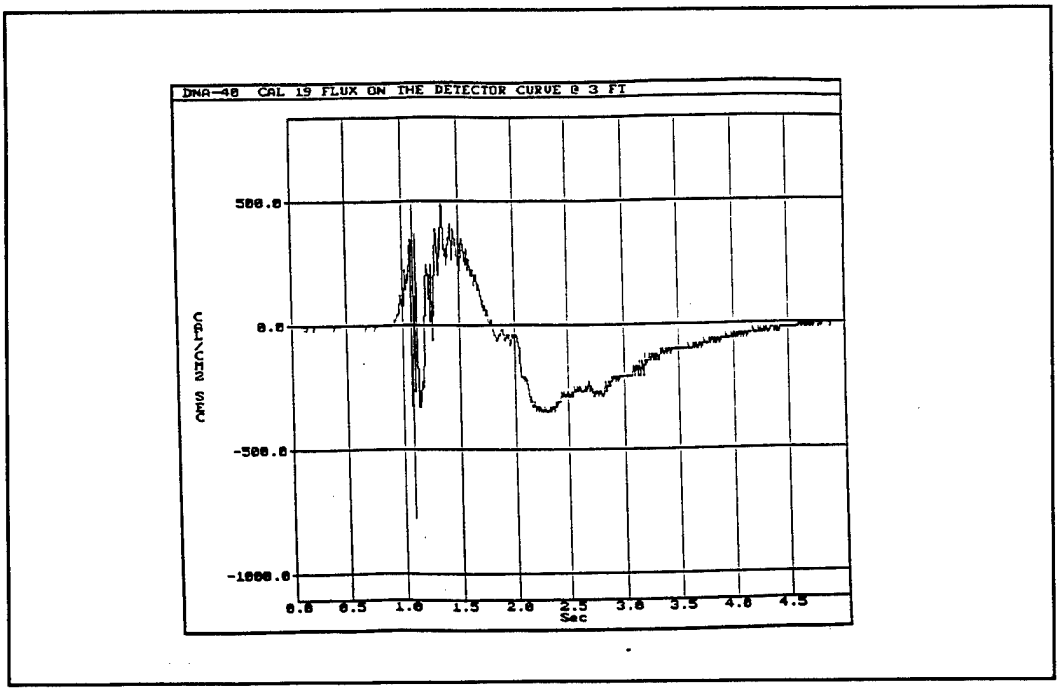

Figure A-38. Test DNA 92-40, calorimeter #19 at 3 feet.

will be made to characterize the surface emittance of the thermal simulant event utilizing sensors not entrained in the hot cloud.

A.2.9.4 DNA Supplied Radiometers. The radiometer at 10 feet (R68426) yielded a detector flux of 0.127 cal/cm^2/sec. This value is much lower than the other detectors at 10 feet. It is highly probable that the restricted field of view of this radiometer verses the wide field of view of the calorimeters mitigates the effects of the hot radiating cloud and permits a surface emittance to be calculated. A surface emittance value of 54.30 cal/cm^2/sec was calculated. The radiometer at 35 feet (R68425) yielded a detector flux of 0.093 cal/cm2/sec. A surface emittance value of 39.76 cal/cm^2/sec was calculated. These values are much lower than the other detector at 35 feet. An explanation for these low values is that the entraining cloud possesses both emissive and attenuating characteristics. The restricted fields of view in combination with entrainment by the cloud (for R68426) can explain the obviously low detector fluxes and surface emittance values. These interpretations will be explored and confirmed utilizing data from other sensors.

A.2.9.5 GSI Instrumentation. The ballistic radiometer at 35 feet yielded a detector flux of 0.302 cal/cm^2/sec and a surface emittance of 129 cal/cm^2/sec (Figure A-39). It is believed that this is an artificially low value due to the previously discussed inability to view steady state events. The ballistic radiometer is invaluable in analyzing the initial initiation pulse that occurs to quickly for any of the other thermal detectors to evaluate (i.e., the ballistic radiometer is seeing a portion of the radiant energy that the other detectors cannot "see" and vice versa).

The nominal radiometer, at 100 feet yielded a detector flux of 0.068 cal/cm^2/sec and a surface emittance of 238 cal/cm^2/sec (Figure A-40). These values correlate with data obtained from the previous single panel test series.

The light probe experienced a peak detector flux of 24375 Lux (Figure A-41). This measurement is used as a means of comparing similar test runs and will be held for comparisons of future tests which possess similar geometrical and thermal parameters.

A.9.1.6 Particle Throw. There was heavy particle throw out to a distance of 9 feet and moderate particle throw to a distance of 11 feet. Beyond this distance up to ≈12 feet there were extremely fine particulates or "fines".

A.2.9.7 Results and Analysis. The results of test DNA 92-40 are shown in Table A-7.

Radiometric analysis yields a rise time of approximately 0.65 second and a pulse duration of approximately 1.3 seconds for this test. The 9 panel array upon reaction increases its area via the formation of a highly emissive particulate cloud. This cloud reacts with ambient air in a highly exothermic fashion. The calorimeters at 3, 4, 5, and 10 feet were entrained in this hot radiating cloud. The relatively large area of the source panels versus the cross sectional area of the sensors and their mounts minimizes the cumulative obscuration (discussed in the previous section; test #92-39) of the source panel by each successive sensor and mount. No attempt was made to calculate the individual and cumulative effect of the "blocking" of each successive sensor; it is felt that this approach will not seriously degrade the integrity of the obtained data but will merely yield a comparatively conservative analysis.

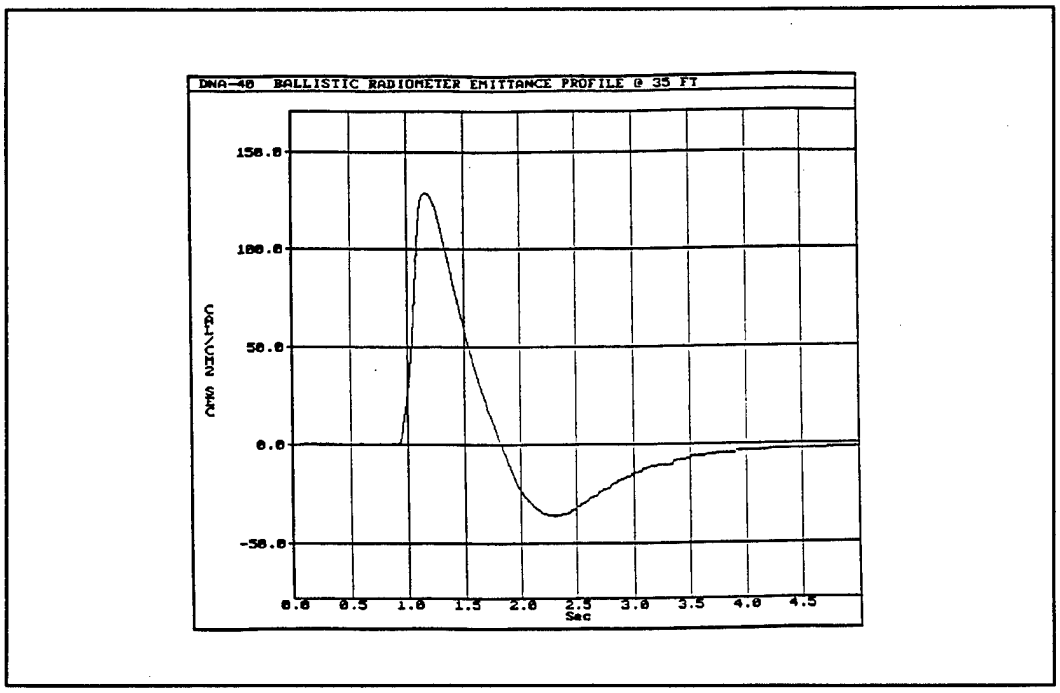

Figure A-39. Test DNA 92-40, ballistic radiometer at 35 feet.

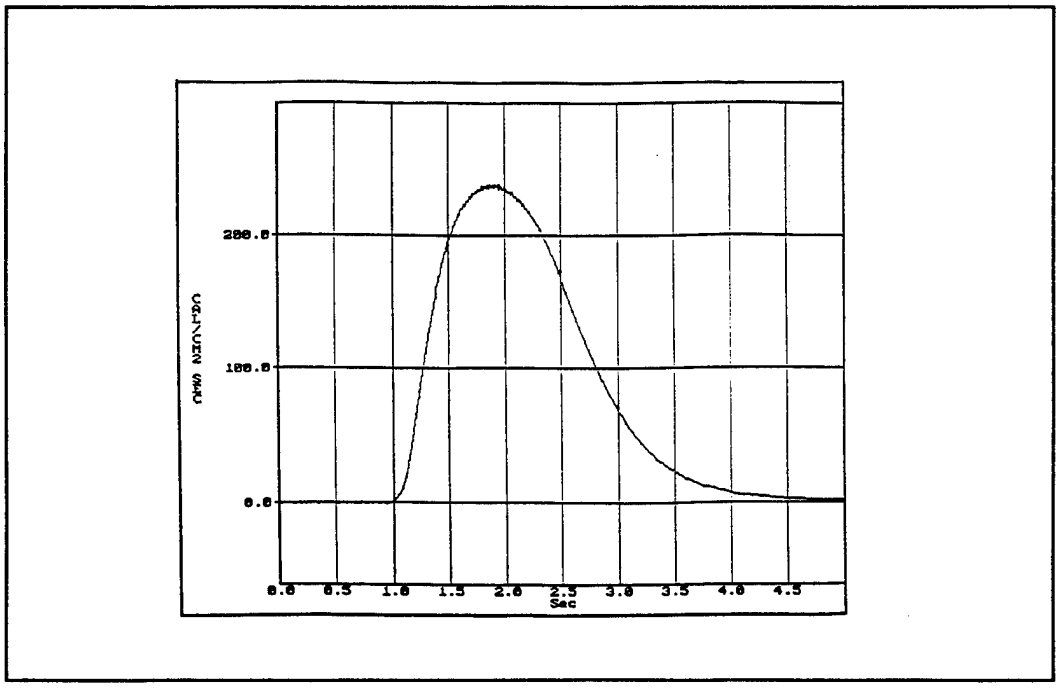

Figure A-40. Test DNA 92-40, total radiometer at 100 feet.

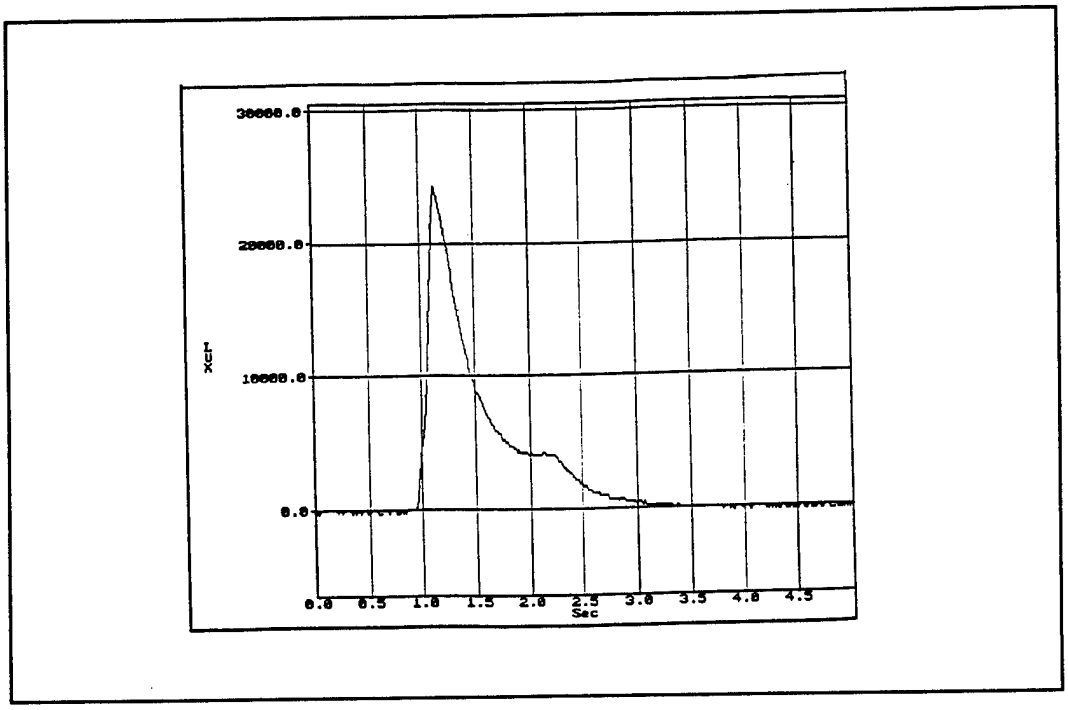

Figure A-41. Test DNA 92-40, light probe at 100 feet.

Table A-7. Summary of test results for DNA 92-40.

Detectors	Cal 225	Cal 19	Cal 32	Cal 224	Cal 18	Cal 50	Rad 68426	Bal Rad	Rad 88426	N Rad
Distance (ft)	3	3	4	5	10	10	10	35	35	100
Distance (cm)	91	91	121	152	304	304	304	1067	1067	3048
Field of View (degrees)	180	180	180	180	180	180	7	17.9	7	7
Area (cm^2)	n/a	n/a	n/a	n/a	n/a	n/a	1100	93247	13475	110003
Cal Factor ($cal/sec \cdot cm^2 \cdot mV$)	11.3	6.76	5.50	10.28	6.9	7.59	0.114	39.9	0.113	4.8
Signal Amplification	50	4	4	0	0	0	400	0.1	400	4
Detector Flux ($cal/cm^2/sec$)	noisy	noisy	400	46.25	19.67	20.87	0.127	0.302	0.093	0.0068
Intensity (kW/sr)	n/a	n/a	n/a	n/a	n/a	n/a	49	1439	444	2649
Emittance (cal/cm^2)	n/a	n/a	n/a	n/a	n/a	n/a	54.3	129	39.76	238

A.2.9.8 Interpretation of GSI Hi-Therm Test Measurement. In evaluating the sensor responses that were generated during the 9 panel test on 3/25/92, the effect of the particle radiating field in addition to the radiation from the panel must be considered.

The flux density received by a sensor can be expressed as,

$$\phi\left(\frac{Power}{Area}\right) = R \cdot \Omega$$

where;

ϕ = Detector flux
R = Source radiance
Ω = Solid angle of the source as "viewed" by the sensor

For circular sources, this can be rewritten as,

$$\phi = R\frac{2\pi \sin^2 \theta_{1/2}}{1+\cos\theta_{1/2}} \qquad \text{(A.1)}$$

where;

$\theta_{1/2}$ = Half-angle of the source as viewed by the detector

If we assume that the source is a Lambertian radiator (i.e., like a black-body source) with,

$$R = \frac{E}{\pi}$$

where;

E = Source emittance

then,

$$\phi = R\frac{2E \sin^2 \theta_{1/2}}{1+\cos\theta_{1/2}}$$

In evaluating, the sensor responses we assume that there is an "equivalent" radiating surface that produces the same flux densities as those recorded by the panel and radiating particle cloud. Consequently, the E that is derived from the sensor is the "effective E".

A.2.9.9 Sensor Results and Analysis. The calorimeter response at 3 and 4 feet produced erratic results and could not be used as valid measurements (see Figures A-37 through A-39).

The calorimeters at 10 feet with field-of-view (FOV) of 180° and the radiometer at 10 feet with FOV of 7° produced valid responses. If we average the two calorimeter responses (see Table A-7), there results a value of 20.3 cal/cm^2/sec whose FOV is such that it must have included the entire source. From the ratio of this value to the radiometer result at 0.13 cal/cm^2/sec with FOV of 7°, we can estimate the "effective source size" using equation (A.1) from,

$$\frac{20.3}{0.13} = \frac{\sin^2\theta_{1/2}(source)}{1+\cos\theta_{1/2}(source)} \frac{1+\cos\theta_{1/2}(sensor)}{\sin^2\theta_{1/2}(source)}$$

Here we assume that the 180° FOV sensors are under filled and the 7° FOV is overfilled. Solving for (source), we obtain that the source size at 10 feet has an angular diameter of 90° or approximately 15.7 feet diameter.

Based on this diameter, the effective emittance as "viewed" at 10 feet is about 69 cal/cm^2/sec.

The detectors at 35 feet with FOV's of 7° and 17.5° would both be overfilled as "viewed" at 35 feet. We can estimate the true response of these detectors if they had larger FOV's by the ratio of detector solid angle and source solid angle.

For the 7° detector, we have that,

$$0.09\left(\frac{0.025\ source}{1.87x10^{-3}\ detector}\right) = 1.20\ cal/cm^2/\sec$$

for the true flux density at 35 feet.

For the 17.5° detector, we have that,

$$0.30\left(\frac{0.025\ source}{0.0116\ detector}\right) = 0.65\ cal/cm^2/\sec$$

Since the two values do not agree, we are led to believe that one or both of the FOV's values are incorrect. It is our belief that the 17.5° FOV degree is closer to 12.5° FOV.

We average both values at 0.925 cal/cm^2/sec to determine the effective emittance from,

$$0.925 = E_{EFFECTIVE}(0.025\ soure)$$

giving E at 35 feet as 37 cal/cm^2/sec.

For the radiometer at 100 feet with a FOV of 7°, the source size is larger then the FOV. Hence, the true value at 100 feet due to the source size is,

$$0.068\left(\frac{0.00308}{0.001865}\right) \cong 0.11\ cal/cm^2/\sec$$

From this value, the effective E becomes 36 cal/cm^2/sec.

As the values at 100 feet and 35 feet agree, it indicates that at least between 35 feet and 100 feet there is no contribution from the particle field.

A.2.9.10 Estimate of the Source Emittance. As we have effective emittance values at only two distances that are different (i.e., 35 feet and 10 feet), an assumption must be made as to the form of the curve of effective emittance as sensor moves closer to the panel.

As a minimum, we can use a linear extrapolation leading to a minimum source emittance of 82 cal/cm^2/sec. If we use an exponential form based on the two points, we arrive at an effective emittance of over 250 cal/cm^2/sec. The true value lies somewhere between these two values.

A.2.9.11 Conclusions and Recommendations. In view of the fact that the sensors at 3 and 4 feet failed, a true picture of the source emittance can not be obtained. Therefore, it is recommended that in the future, those sensors (very close to the source) be shielded better and a window like KCl be used over the calorimeters to reduce the particle impact on the sensors.

In addition, as the video and photographs indicate that the cloud does not extend to 35 feet, additional sensors be used between 10 and 35 feet to help evaluate the contribution of the particle field.

With the available data gathered from this test, and based on previous panel tests, we estimate that the "true" source emittance is somewhere around 200 cal/cm^2/sec. This would correspond to an effective source temperature of around 3485 K.

Finally, it is recommended, that neither the video nor photography of the cloud formation be synchronized with the calorimeter and radiometer responses to determine the effective contribution of the particle field to the overall peak flux density.

APPENDIX B

HI-THERM DEMONSTRATION TEST DETAIL, APRIL 1992

B.1 TEST TRS-HT1 AND TRS-HT2.

B.1.1 Description.

A single Hi-Therm panel was mounted in a four-panel frame with it's axis approximately 30 inches above the concrete pad. A steel mesh particle "catcher" was mounted approximately 12 inches in front of the panel. Photo coverage was provided by 2 DNA video cameras fitted with PLZT windows and by 2 SAIC motorized 35 mm cameras fitted with neutral density filters and 80B tungsten correction filters to allow the daylight film to more accurately record a high intensity 2800 K event. These cameras were arranged to give a side and front view. Spectrometers were positioned on the panel axis 10 feet in from of the panel. Two each 7° Field-of-View (FOV) Medtherm radiometers were mounted in the spectrometer housing.

B.1.2 Results of Tests TRS-HT1 and TRS-HT2.

DNA Radiometers. The output from the two radiometers for test TRS-HT1 is shown in Figures B-1 and B-2. The output of the DNA radiometer is shown in Figure B-3 for comparison. The results from test TRS-HT2 are shown in Figures B-4 through B-6. The DNA radiometers (7° FOV) cover an area with a diameter of 14.6 inches at 10 feet. As we can see from the photograph the FOV is completely filled immediately after ignition.

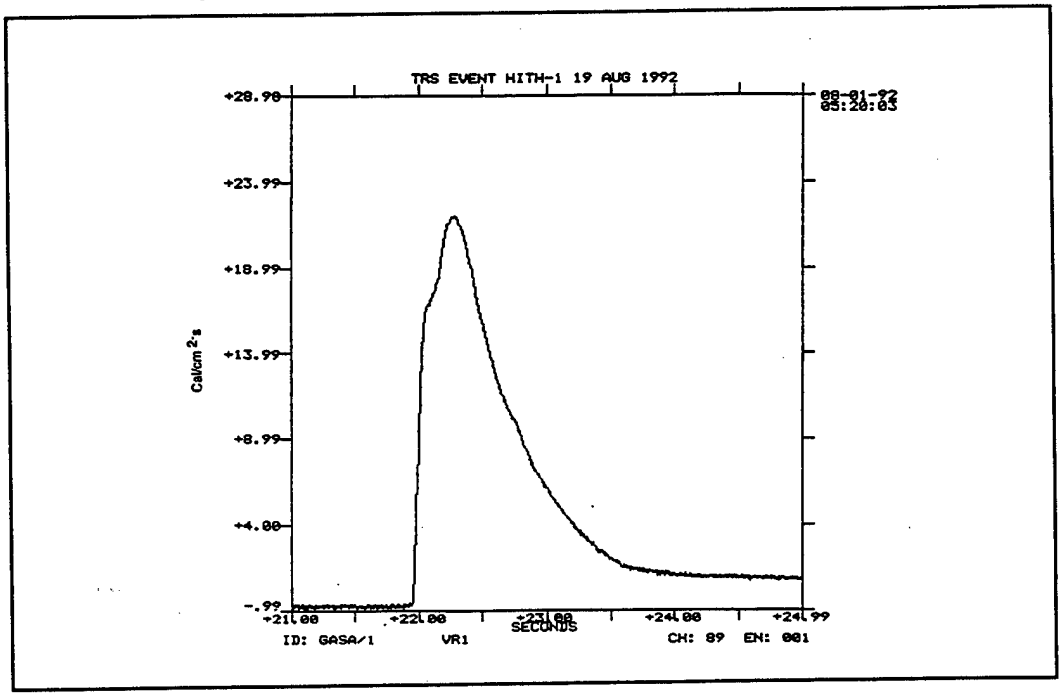

Figure B-1. DNA radiometer at 10 feet.

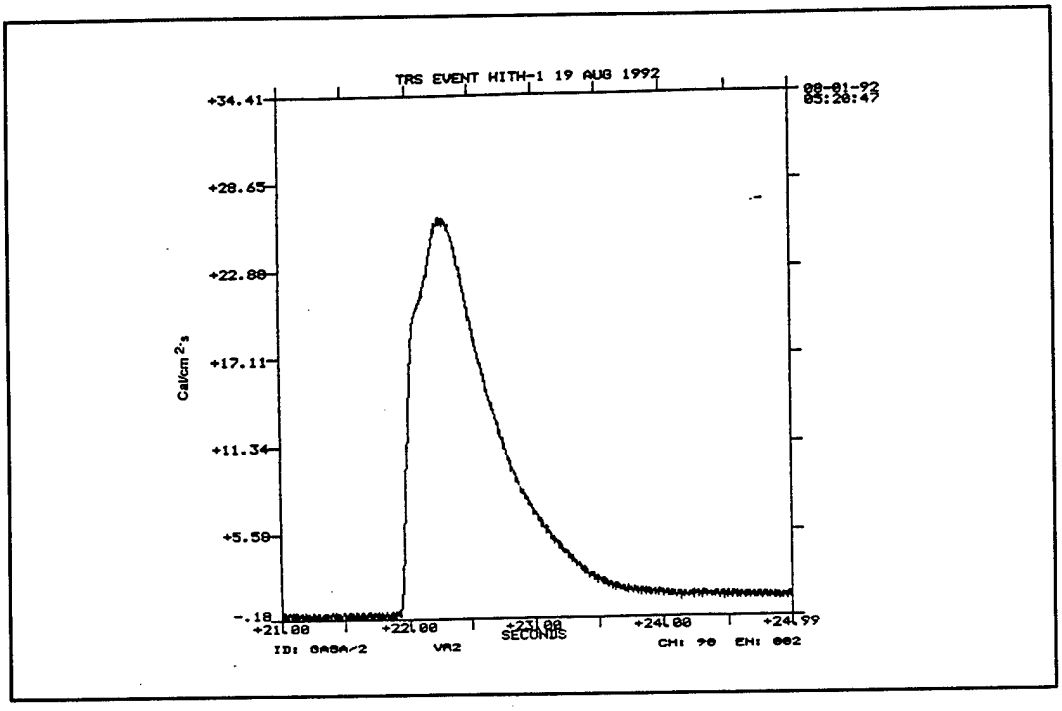

Figure B-2. DNA radiometer at 10 feet.

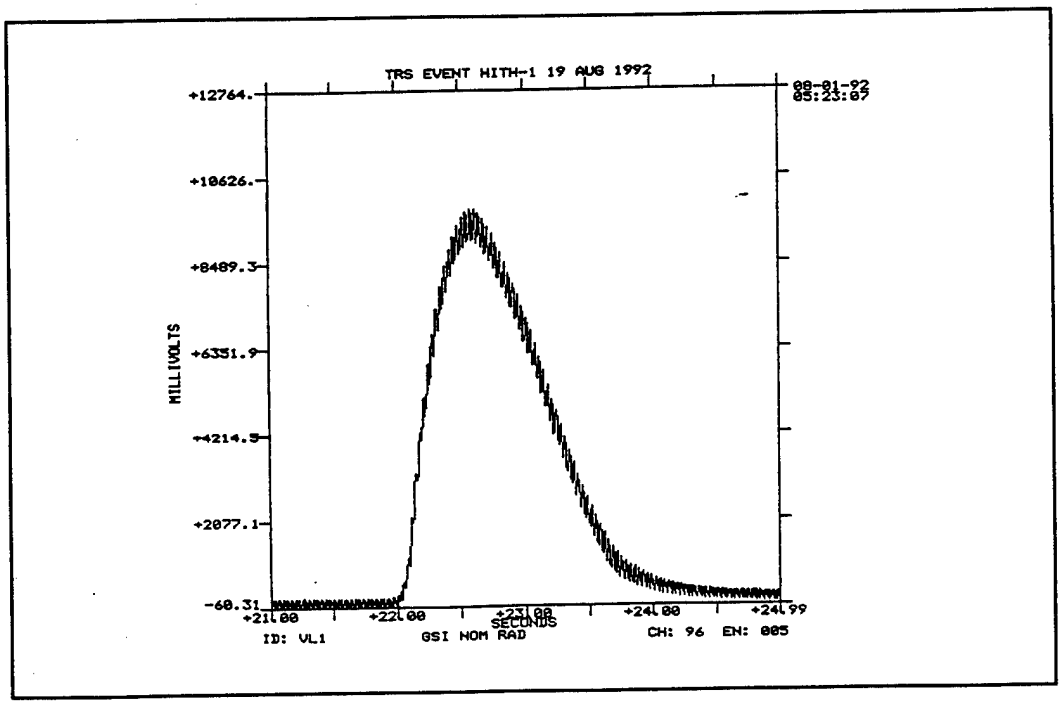

Figure B-3. GSI radiometer.

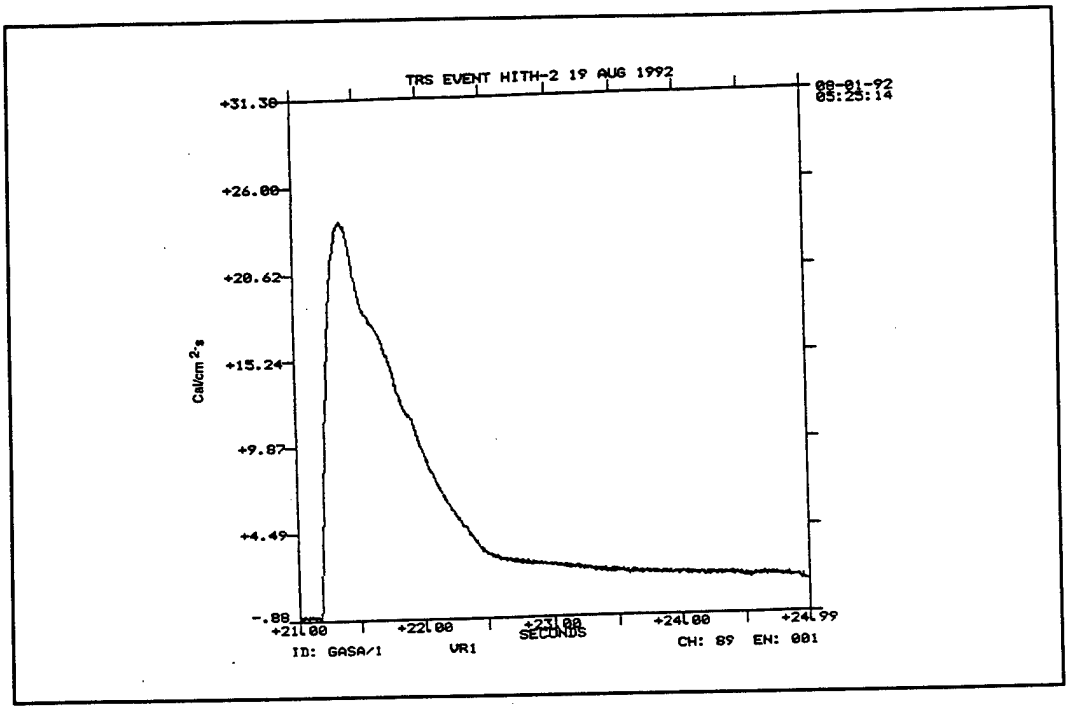

Figure B-4. DNA radiometer at 10 feet.

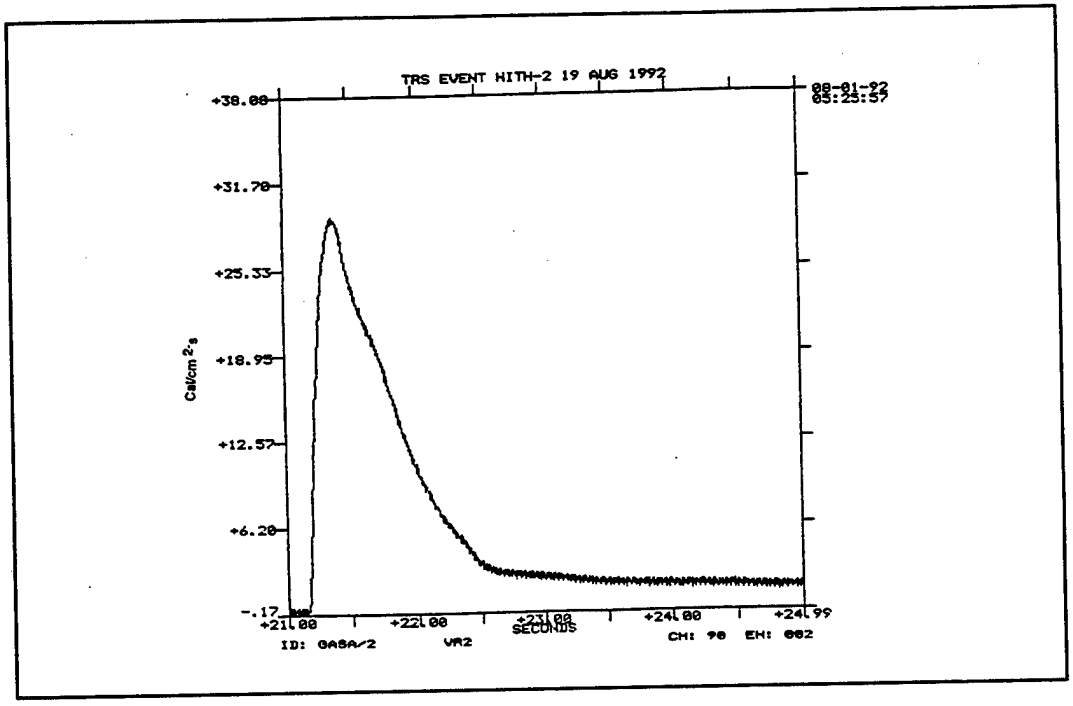

Figure B-5. DNA radiometer at 10 feet.

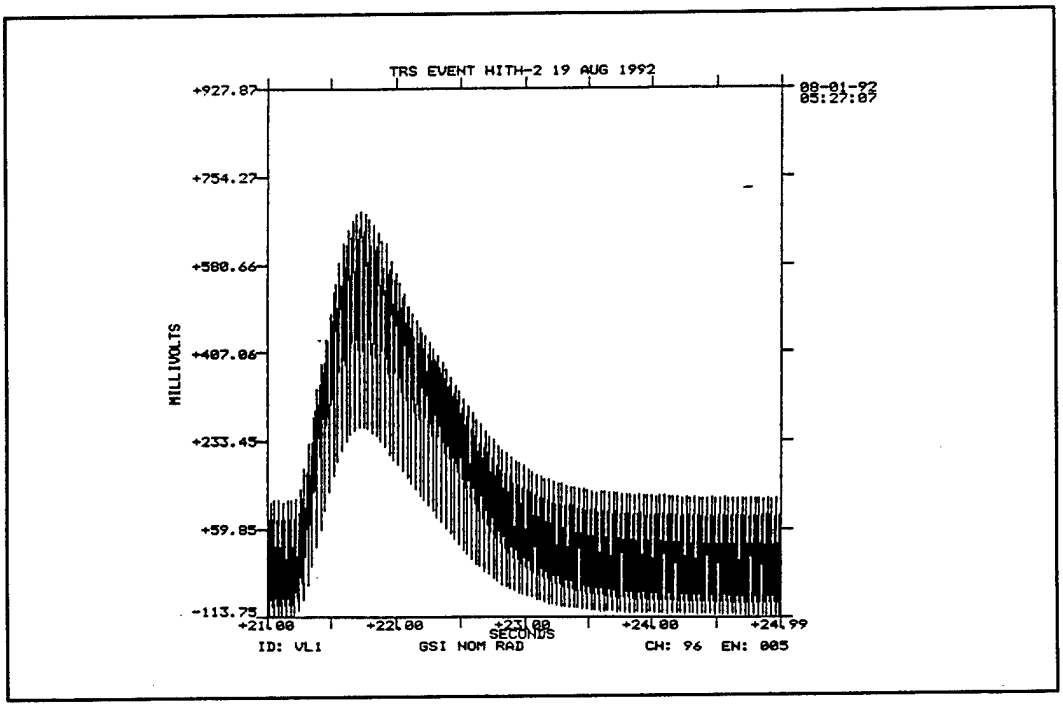

Figure B-6. GSI radiometer.

The rise time (10-90%) as measured on test TRS-HT2 is 115 ms. Peak flux measurements from the SAIC radiometers are 22.2 and 26.3 cal/cm^2/s for TRS-HT1 and 24.1 and 29.2 cal/cm^2/s for TRS-HT2.

B.2 TEST TRS-HT3.

B.2.1 Description.

A total of 80 Hi-Therm panels were mounted in a frame to form an 8 foot wide by 10 foot high matrix. A steel mesh particle "catcher" was mounted approximately one foot in front of this matrix.

Photographic coverage was provided by two DNA video cameras fitted with PLZT windows to the front and rear of the Hi-Therm panels, four high speed 16 mm cameras provided by Base photo covered the front and side views, two motorized 35 mm cameras provided by DNA covered front and side views, and a video camera provided by GSI positioned at approximately 100 feet from the panels provided a view from the east side.

Most of the instrumentation used on this test was mounted in a plane 10 feet in front of the panels. Additionally a single standard Medtherm calorimeter was positioned 20 feet from the panels and two more were mounted at a distance of 30 feet. A complete description of instrumentation location is given in Table B-1. Instrumentation included six DNA radiometers, 12 standard Medtherm calorimeters and the spectrometer system with integrating spheres.

Table B-1. Instrumentation details for TRS-HT3.

Entry	Instrument	Serial No.	Location		
			Distance from centerline X (ft)	Distance from panel Y (ft)	Height above ground Z (ft)
1	7° FOV Radiometer	GASA/1	-2	10	2.5
2	7° FOV Radiometer	GASA/5	2	10	3
3	7° FOV Radiometer	GASA/2	0	10	2.5
4	7° FOV Radiometer	GASA/7	-2	10	5
5	7° FOV Radiometer	GASA/4	2	10	7.5
6	7° FOV Radiometer	GASA/3	-2	10	7.5
7	Calorimeter	215	0	10	1
8	Calorimeter	216	0	10	2.5
9	Calorimeter	105	-4.25	10	2.5
10	Calorimeter	42	-1.58	10	5
11	Calorimeter	46	1	10	5
12	Calorimeter	217	6	10	5
13	Calorimeter	212	4	10	5
14	Calorimeter	96	-4.25	10	7.5
15	Calorimeter	41	0	10	9
16	Calorimeter	218	0	20	5
17	Calorimeter	97	-.05	30	5
18	Calorimeter	98	0.5	30	5
19	Spectrometer Pulse				
20	GSI Radiometer				
21	Spectrometer		0	10	5

B.2.2 Results.

B.2.2.1 DNA Video. The video camera looking at the rear of the panels shows the fireball expanding to double the initial area in approximately 60 ms. The video camera looking at the front of the panels shows ignition at 41.41 seconds, then shows the fireball engulfing the 10 foot calorimeters at 41.68 seconds, the 20 foot calorimeters at 41.93 seconds and the 30 foot calorimeters at 42.33 seconds. Finally, the fireball reaches the video camera (PLZT goes out) at 42.6 seconds. This camera was located at approximately 45 feet. Fireball expansion velocity from the front video is approximately 30-40 feet/second.

B.2.2.2 GSI Video. The GSI video from the east side gave a very good view of the event. A time base was recorded on the tape after the event and this allowed a measurement of flame-front velocity to be made. This was estimated at 50 feet/second.

B.2.2.5 DNA Radiometers. Six radiometers were used distributed across the 10 foot array (see Table B-1 for details). These radiometers were water-cooled and each was mounted in a small aluminum instrument box (approximately 3 x 6 x 8 inches) for convenience of use. (Technical details of these devices are given in Appendix A). In all cases the box was completely destroyed during the event. Figures B-7 through B-12 show the recorded output from the six radiometers. We can see from these records a slowly rising pulse which starts at 20.74 and continues until 20.95 seconds, at which time the signals go violently positive. This

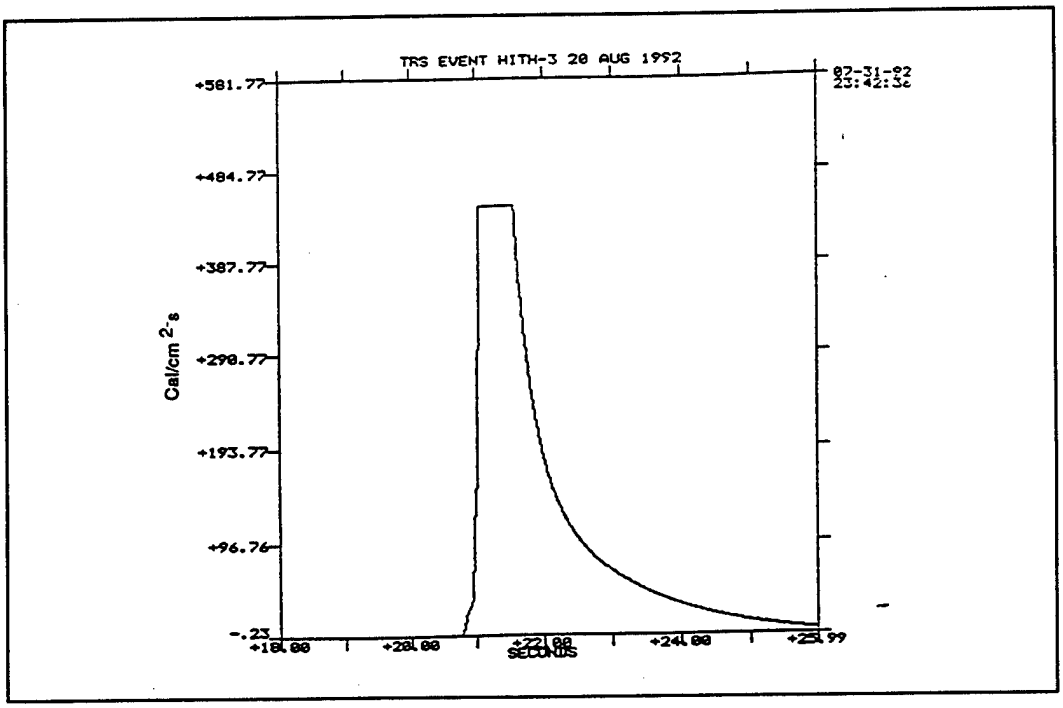

Figure B-7. DNA radiometer at 10 feet.

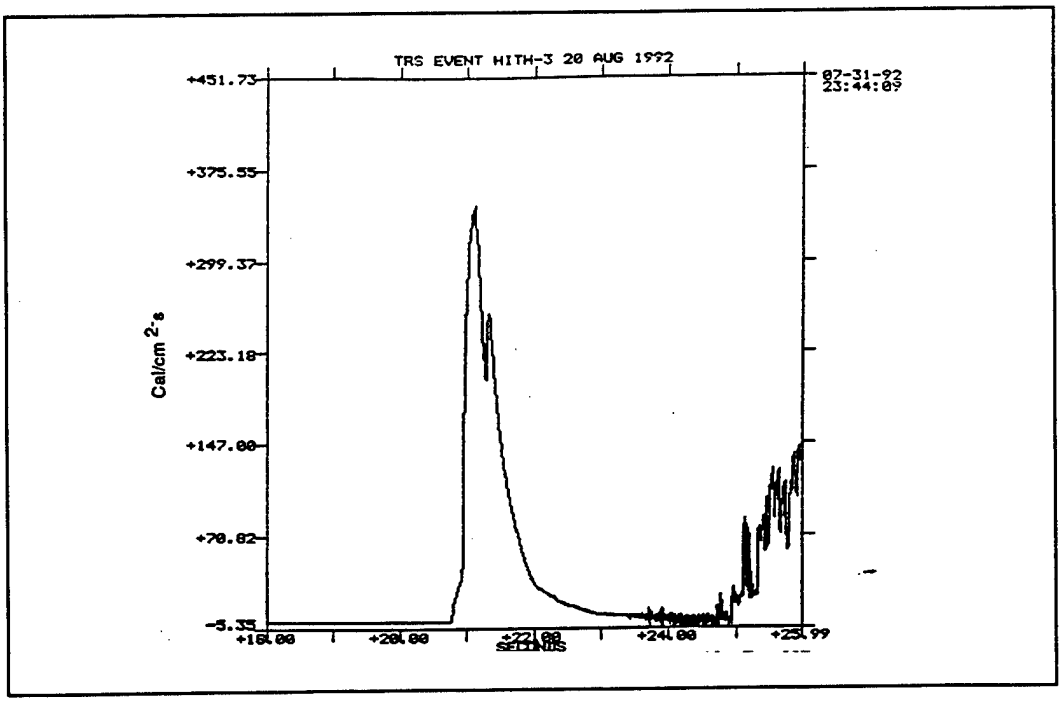

Figure B-8. DNA radiometer at 10 feet.

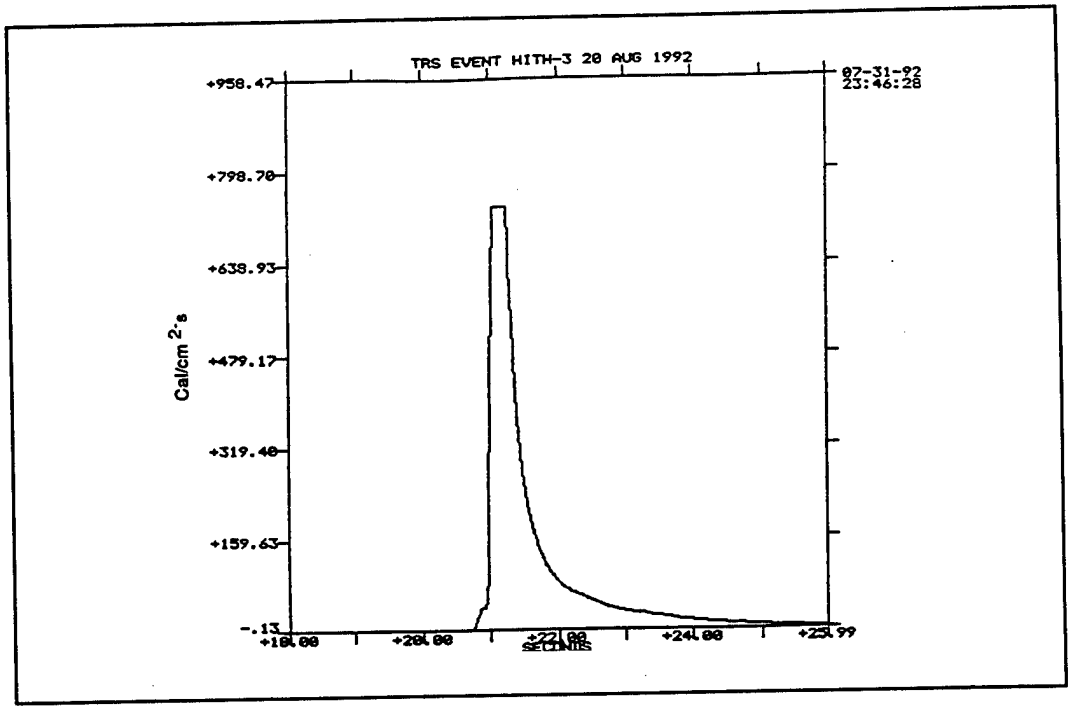

Figure B-9. DNA radiometer at 10 feet.

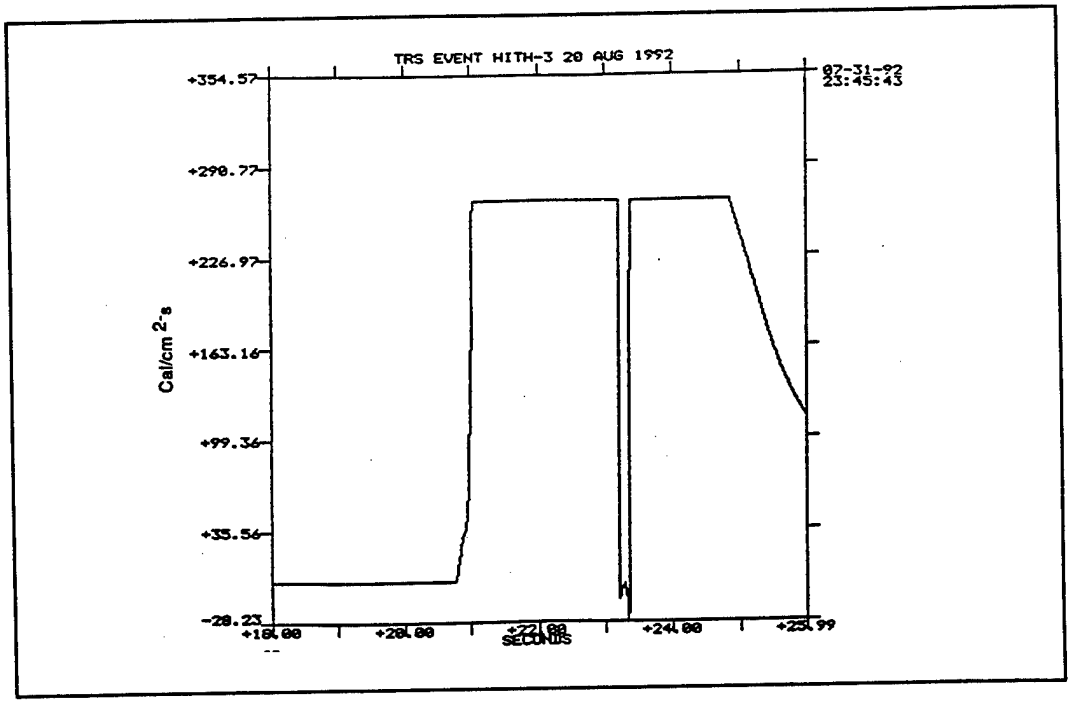

Figure B-10. DNA radiometer at 10 feet.

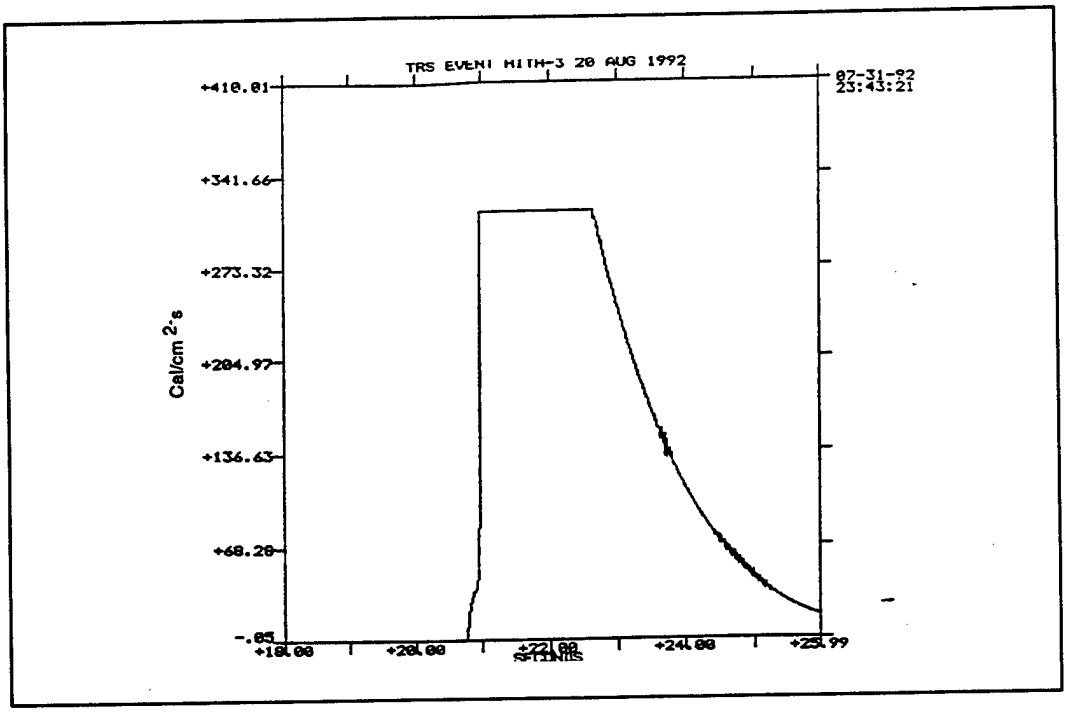

Figure B-11. DNA radiometer at 10 feet.

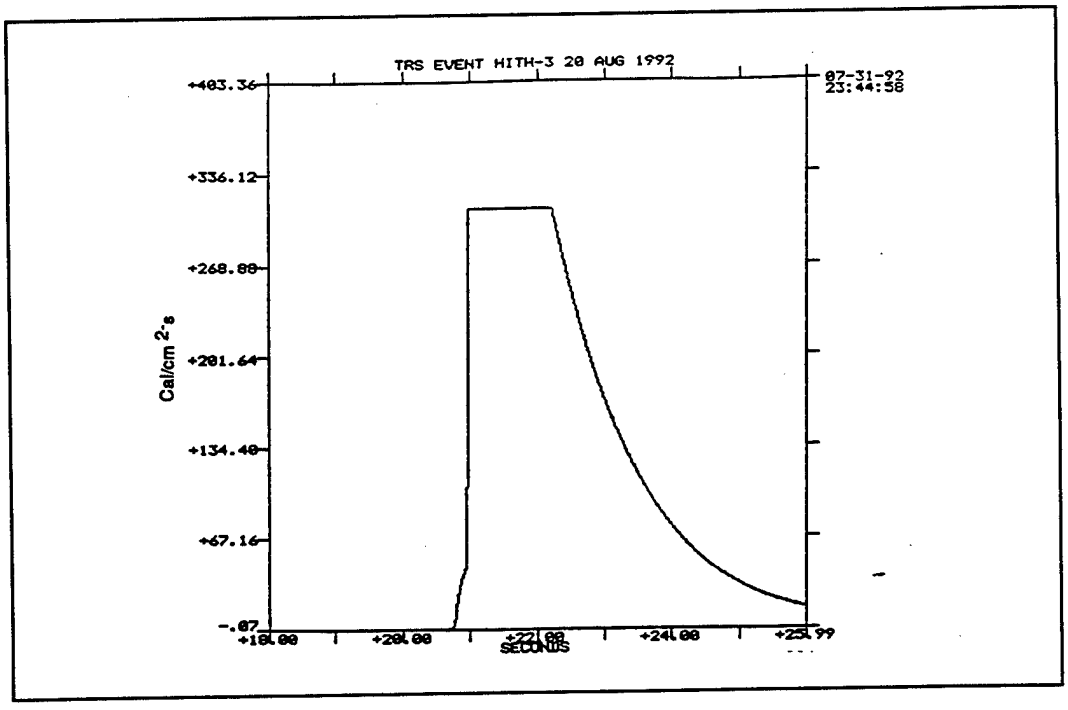

Figure B-12. DNA radiometer at 10 feet.

time coincides with the flame front arriving at the 10 foot array at 50 feet/second. At the time of flame impact maximum flux values are given in Table B-2.

Table B-2. Radiometers peak flux values before flame impact.

Radiometer Number	Location X, Y, Z (ft)	Peak Flux ($cal/cm^2/sec$)
GASA/1	-2, 10, 2.5	30
GASA/2	0, 10, 2.5	36
GASA/3	-2, 10, 7.5	38
GASA/4	2, 10, 7.5	30
GASA/5	2, 10, 3	36
GASA/7	-2, 10, 5	44

B.2.2.6 DNA Calorimeters. Nine calorimeters were distributed across the 10 foot array. Three additional calorimeters were added, one at 20 feet and two at 30 feet. (See Table B-1 for details). All calorimeters except the two at 30 feet were coated with ash during the event. Figures B-12 through B-24 show the recorded output from the 12 calorimeters. Again we see the signal going rapidly positive at first light + 200 ms for those gauges at 10 feet. For the gauge at 20 feet we seen an event on the pulse at first light +0.48 seconds. For the 2 gauges at 30 feet we seen an event at first light +0.59 and 0.78 seconds corresponding to a flame velocity of approximately 40-50 feet/second. Maximum flux valves just before flame impact are given in Table B-3. Note that although the Y distance is given as 10, 20 or 30 feet, this value tending to zero as the flame front approaches the gauge and therefore increasingly fills the FOV. Figure B-25 shows the GSI radiometer which was located at a distance of 45 feet for comparison.

B.3 SPECTROMETER MEASUREMENTS.

B.3.1 Description.

In order to determine the spectral characteristics of the Hi-Therm sources, the DNA spectrometer system was employed for all three of the tests. Using the spectral data obtained from these, a comparison can be made with theoretical blackbody curves to determine the approximate color temperature of the source. This information can also be used to verify the data obtained from the radiometers and calorimeters.

The DNA spectrometer system consists of three optical scanning monochromators, which operate over the wavelength ranges of 200-1100nm (model 6101), 600-1900nm (model 6102), and 1500-5000nm (model 6104). All three monochromators are connected to a controller/data acquisition system which is computer driven. In order to insure that the spectra obtained from the 3 monochromators were synchronized, two of the units were configured to trigger off of the third (the 6101), which in effect acted as a master signal. The software was then set up to acquire data from all three channels simultaneously, at the maximum sampling rate of 6 spectra/second. Normally the maximum sampling rate with this system is 12 spectra/second, but with three channel simultaneous acquisition, the system skins every other spectra. The system would be triggered approximately 1 second before the firing of the test panel, and

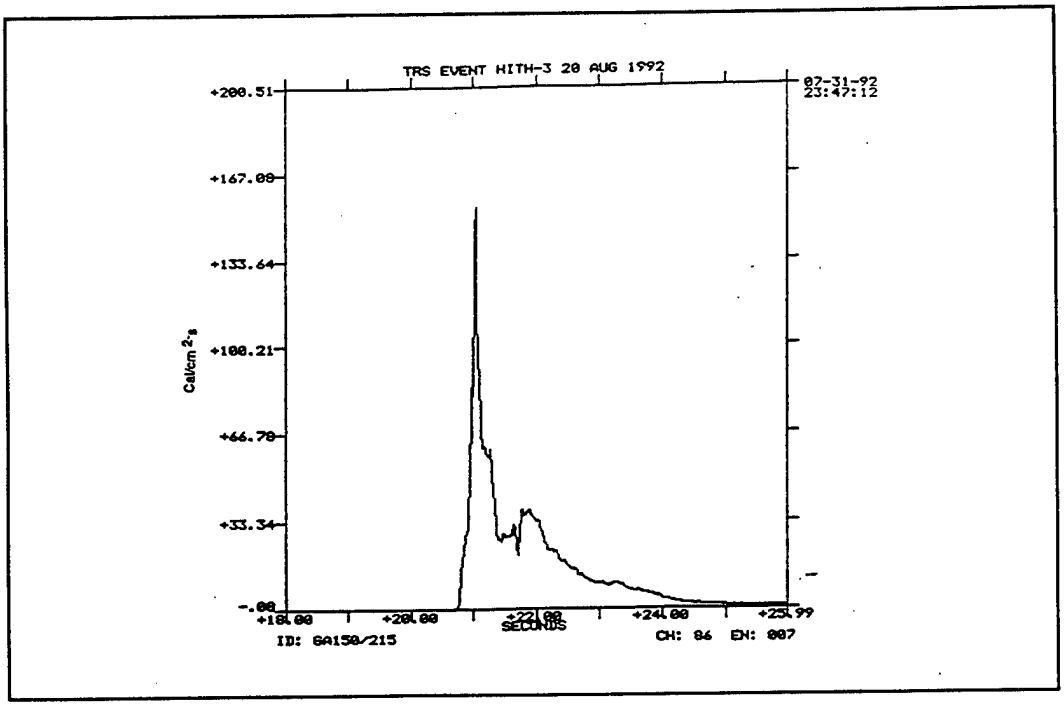

Figure B-13. DNA calorimeter at 10 feet.

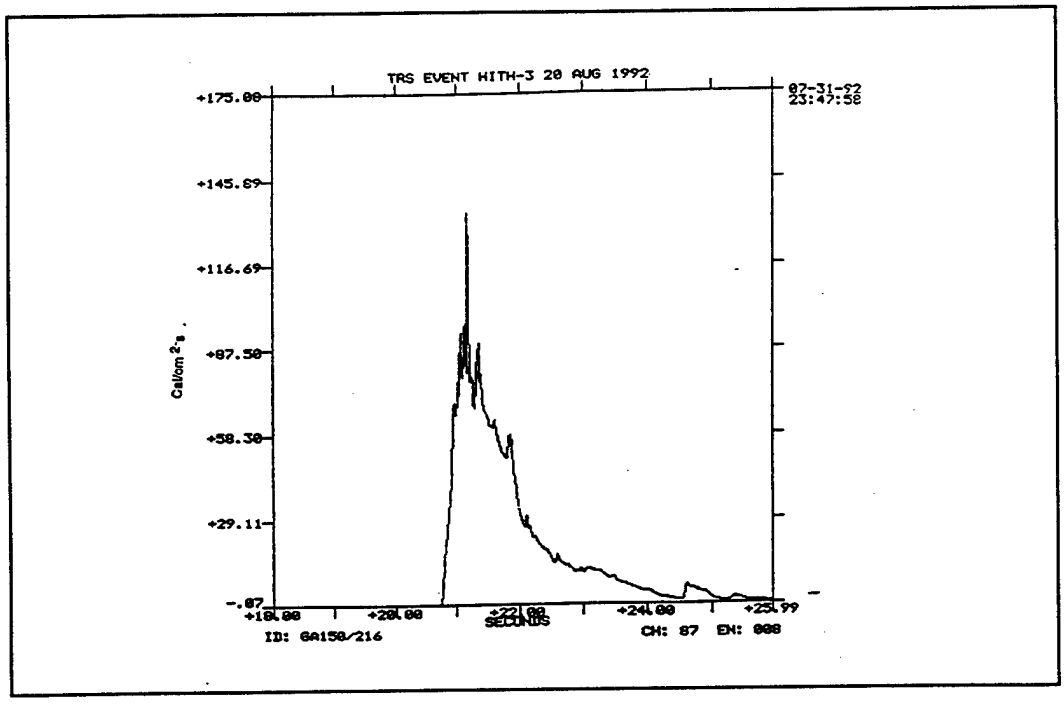

Figure B-14. DNA calorimeter at 10 feet.

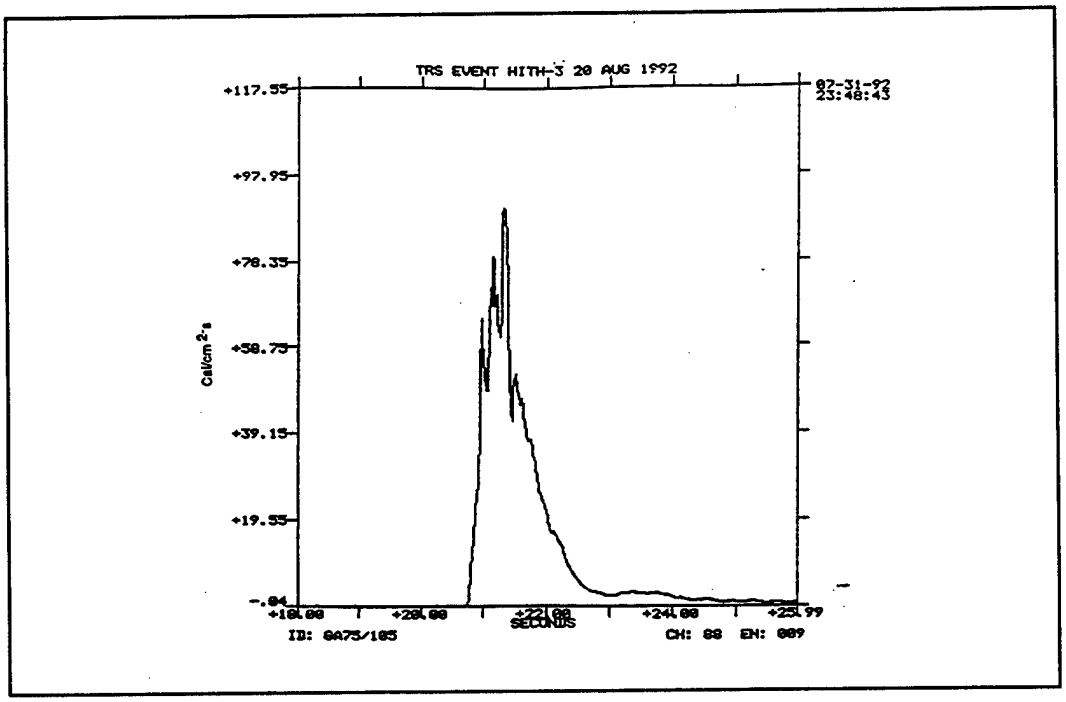

Figure B-15. DNA calorimeter at 10 feet.

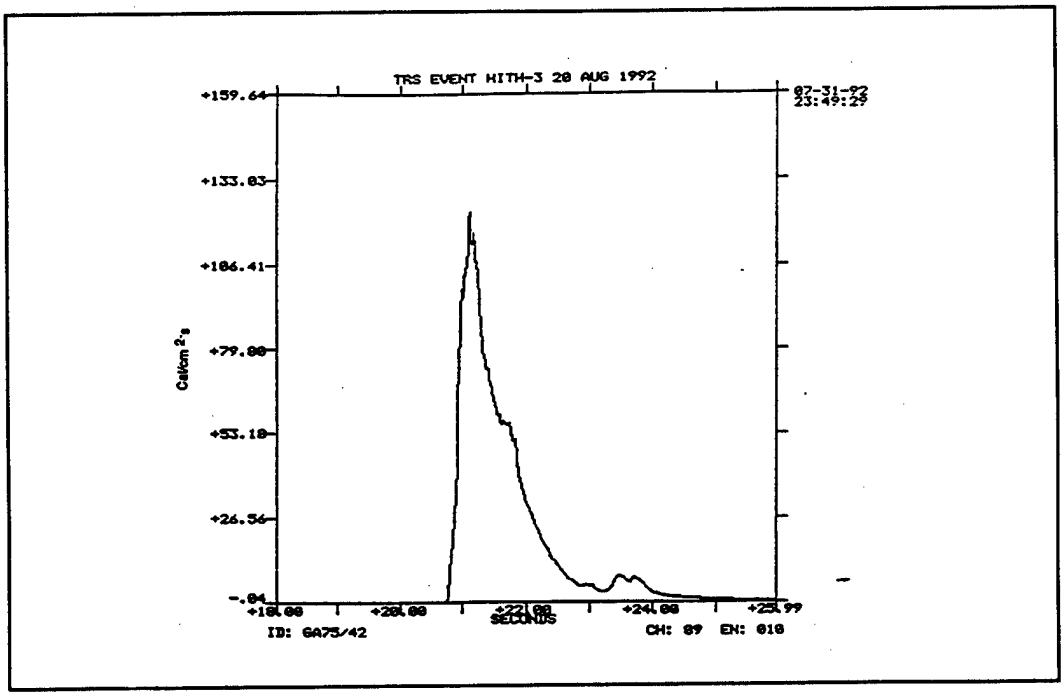

Figure B-16. DNA calorimeter at 10 feet.

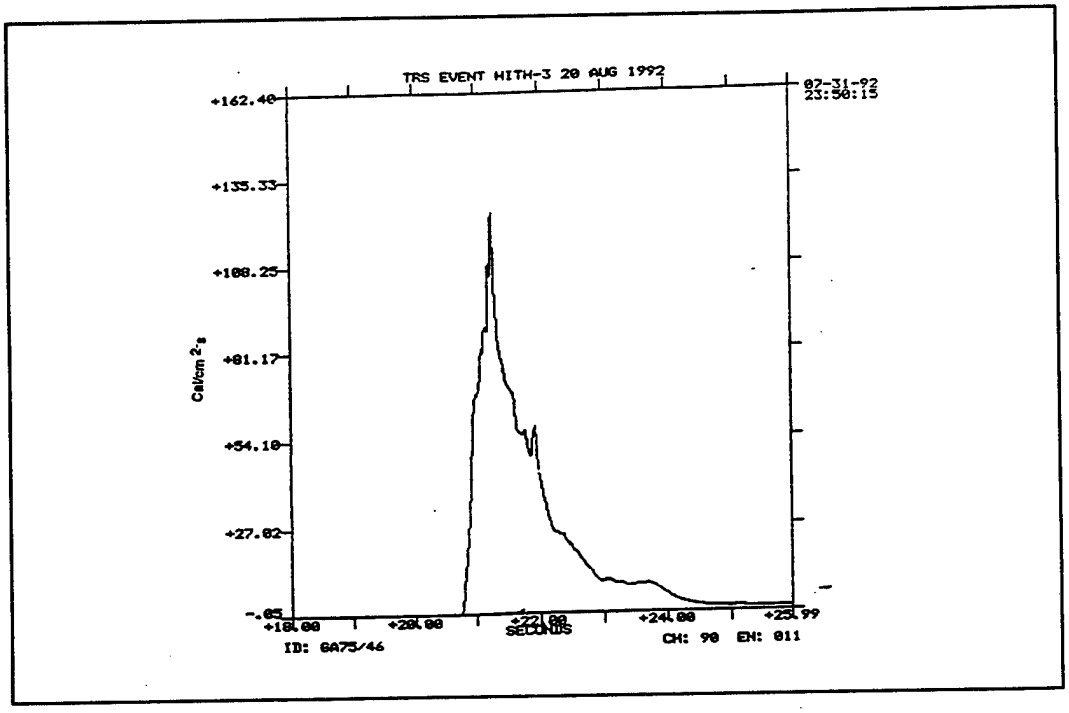

Figure B-17. DNA calorimeter at 10 feet.

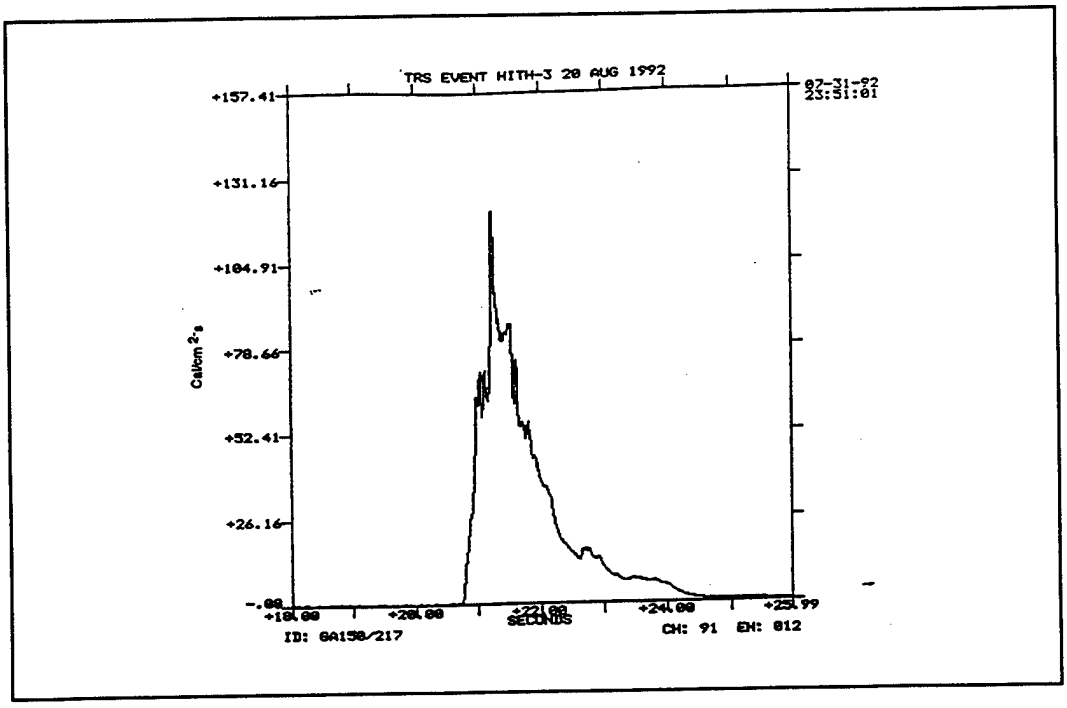

Figure B-18. DNA calorimeter at 10 feet.

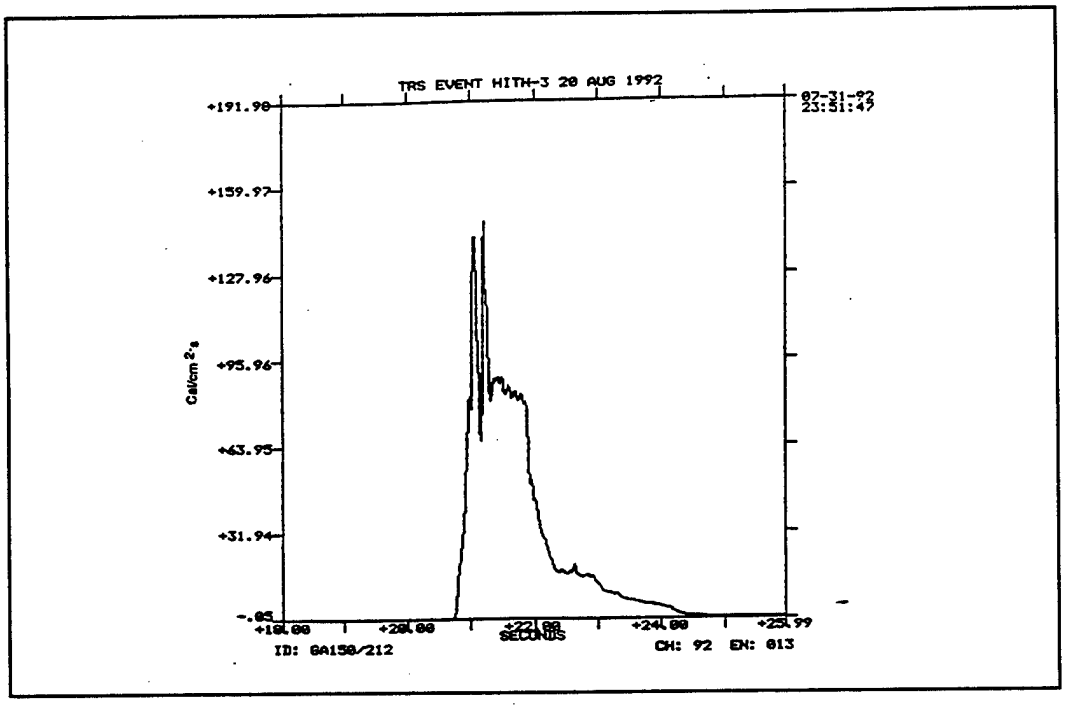

Figure B-19. DNA calorimeter at 10 feet.

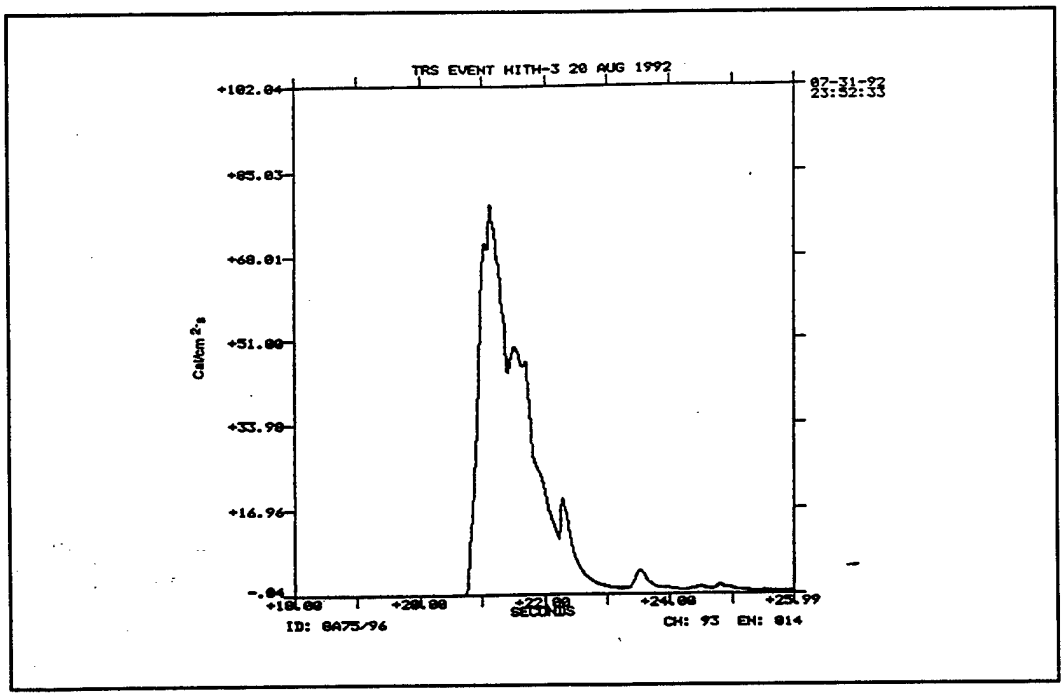

Figure B-20. DNA calorimeter at 10 feet.

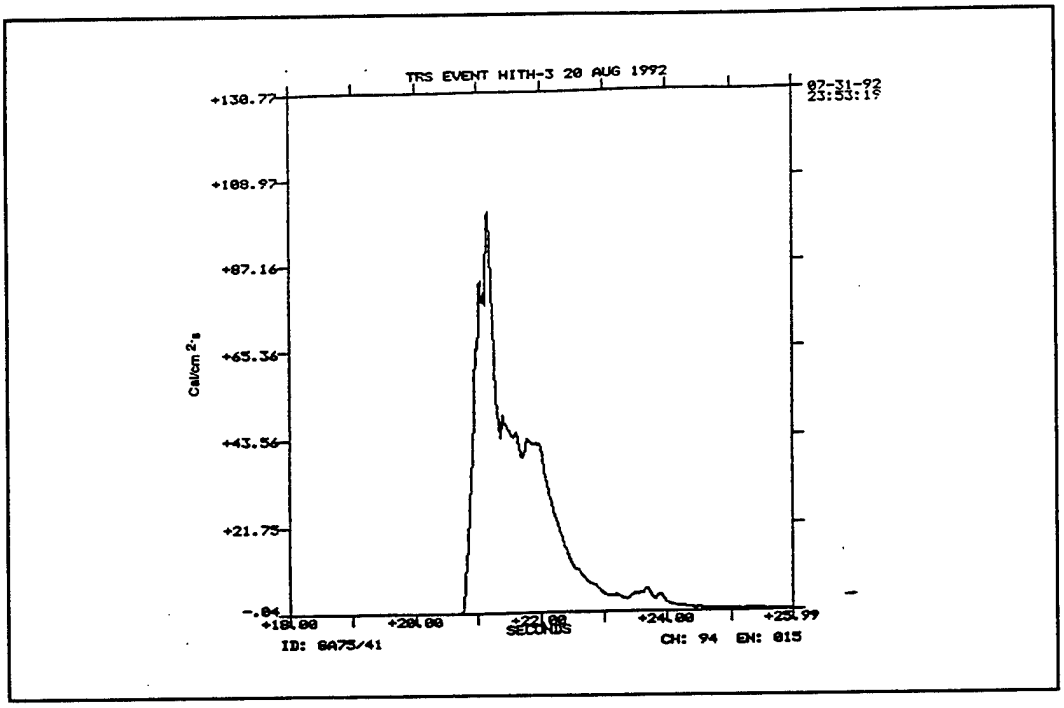

Figure B-21. DNA calorimeter at 10 feet.

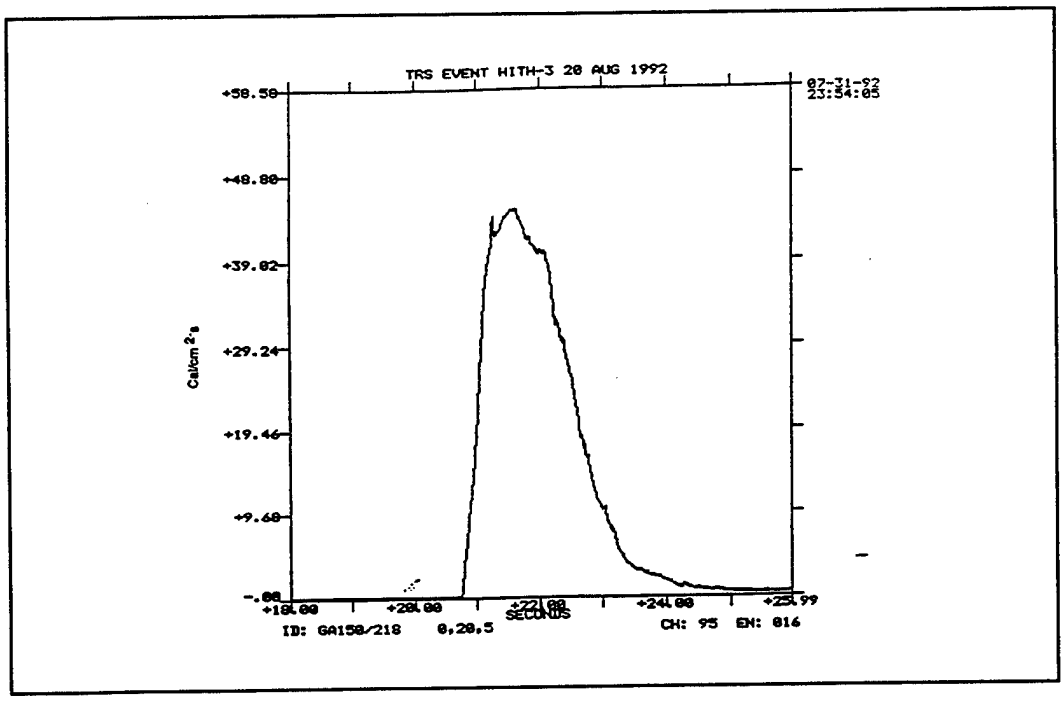

Figure B-22. DNA calorimeter at 20 feet.

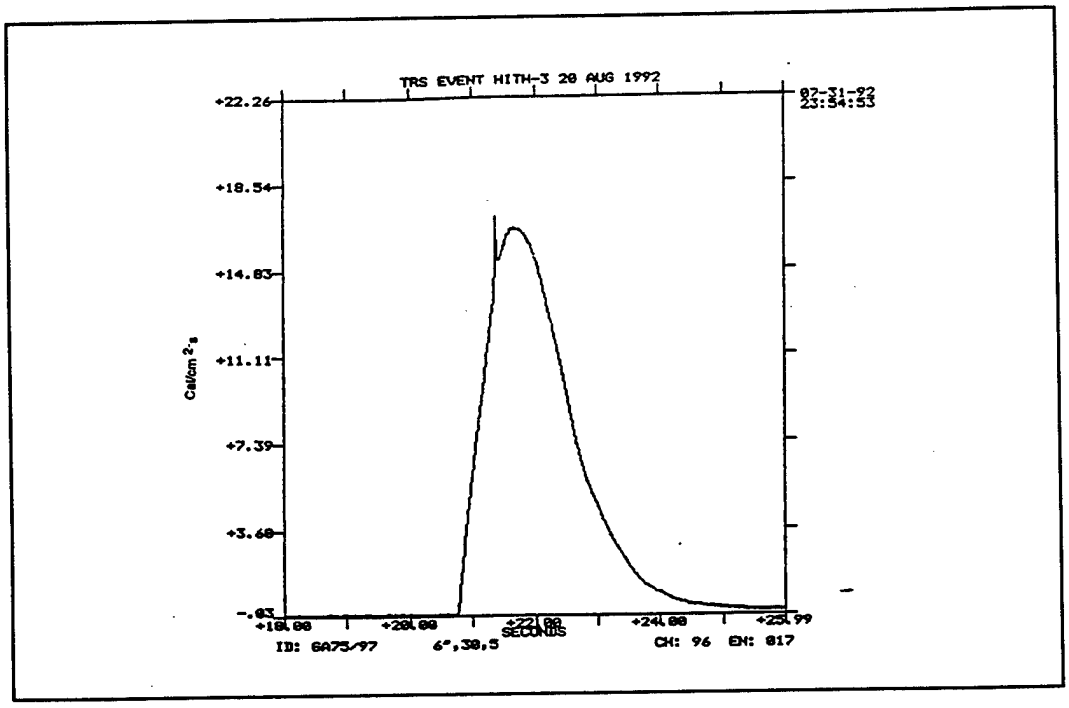

Figure B-23. DNA calorimeter at 30 feet.

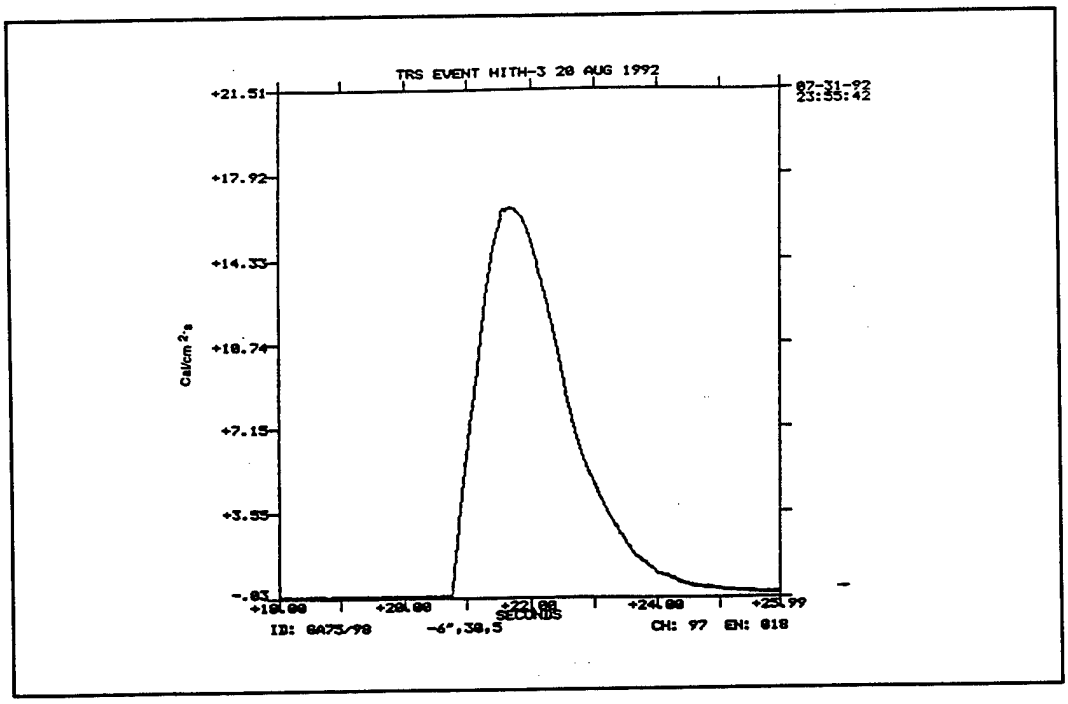

Figure B-24. DNA calorimeter at 30 feet.

Table B-3. Calorimeters peak flux values before flame impact.

Calorimeter Number	Location X, Y, Z (ft)	Peak Flux (cal/cm^2/sec)
215	0, 10, 1	29
216	0, 10, 2.5	37
105	-4.25, 10, 2.5	27
42	-1.6, 10, 5	
46	1, 10, 5	26
217	6, 10, 5	27
212	4, 10, 5	30
96	-4.25, 10, 7.5	
41	0, 10, 9	
218	0, 20, 5	40
97	-0.5, 30, 5	14
98	0.5, 30, 5	16

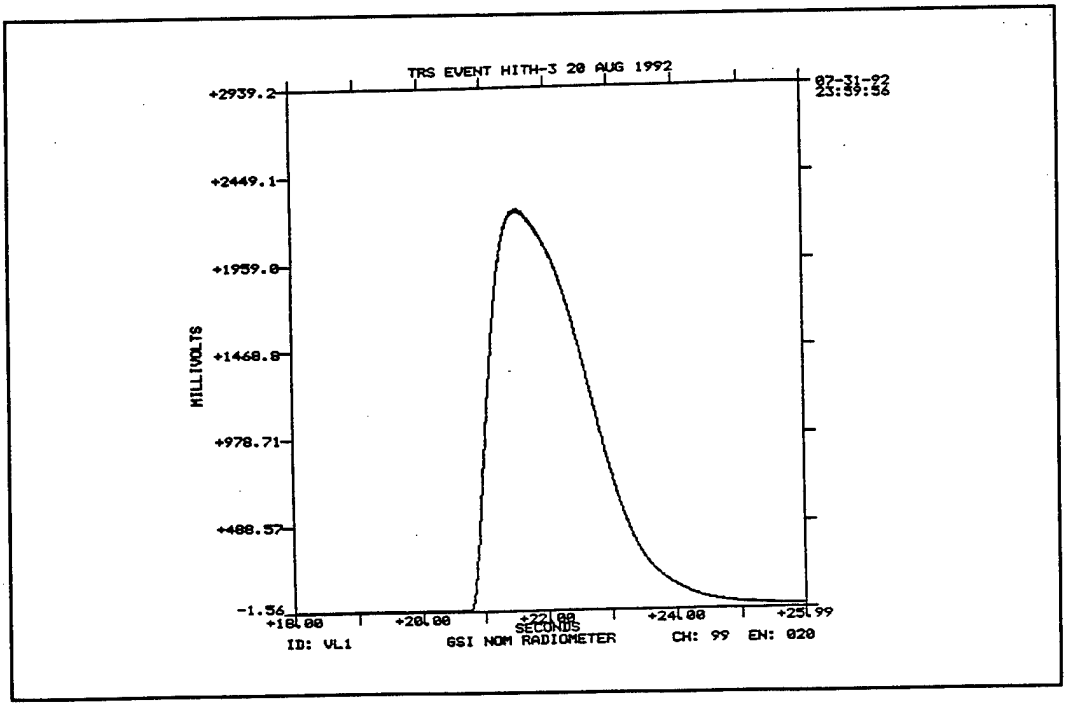

Figure B-25. GSI radiometer.

30 spectra from each channel would be recorded. Two different equipment configurations were used.

B.3.2 Tests TRS-HT1 and TRS-HT2.

B.3.2.1 Instrument Configuration. For tests TRS-HT1 and TRS-HT2, the spectrometers were enclosed in a small steel box, along with two view restricted (7° diameter field of view) radiometers. The 6101 and 6102 monochromators employed glass fiberoptic cables as their

input optics. These fiber cables each had a view restrictor mounted on the input end, so that their field of view was approximately 7° diameter. The 6104 monochromator used only a masking type view restrictor, which also yielded a field of view of approximately 7° diameter.

Since the detector elements of the monochromators do not have a linear response, calibration data was generated for each using a 1000 Watt quartz halogen calibration lamp (obtained from OPTRONICS LABORATORY), which is calibrated over the range of 250-4500nm.

All instruments were mounted on a plate which was to be inserted into the protective housing. The distance from the instruments to the source was to be 10 feet, so the instruments were aimed so that the center of their fields of view all were aligned on the same point at this distance. This was accomplished by using a target lamp, and aiming all of the instruments at this lamp. The instrument package was then mounted in the protective enclosure, and positioned on the test site at the appropriate distance from the test panel holder. The target lamp was again used to align the whole instrument package by locating the lamp in place of the test panel, and observing the signals received. The area viewed by the instruments at the test distance was approximately 14.6 inches in diameter. Even though the test panels were only 1 foot x1 foot, GSI was informed that the radiating source area would be significantly larger, and would fill the field of view of all of the instruments. Calculations were performed using information provided by GSI, as well as previous spectrometer data acquired from the SAIC TRS units, and appropriate amplifier gain settings were determined. Based on these calculations, an ND1 neutral density filter was inserted in the inputs optics of the 6101 monochromator.

B.3.2.2 Data Analysis (TRS-HT1). Test TRS-HT1 yielded a number of spectra of adequate signal strength acquired throughout the duration of the pulse. The first step in reducing the raw data is dividing through by the amplifier gain. A few of these processed spectra (uncorrected for detector response) are shown in Figure B-26, plotted on a log scale. The parallel traces indicate that there is not much variation in the spectral output of the source during the hottest portion of the pulse, although the sampling rate of the system must be taken into account.

Spectrum 10 was identified from this data as the one corresponding to the highest spectral irradiance level recorded by the system. In order to convert this data into a true spectrum, correction factors were generated using the calibration information. For the 6101 monochromator, there was no calibration data which included the ND1 neutral density filter. This filter has been characterized previously as having a relatively flat transmission coefficient over the wavelength range applicable in this instance. Since this translates to an attenuation factor of approximately 10%, the correction factors generated for use without a filter were multiplied by a factor of 10. The curves for the three detectors were then merged, with a slight normalization employed in order to match the curves where they overlapped. This result is shown in Figure B-27.

The data corresponding to the extrements of the wavelength ranges of the monochromators is not generally used for final analysis, as the sensitivity in these areas falls off drastically. This is due to the fact that the monochromators are optimized (i.e., type of detector, blaze wavelength of dispersion grating, etc.) for response in the central portions of their ranges but these areas are included in this figure for completeness. The appropriate ranges to be

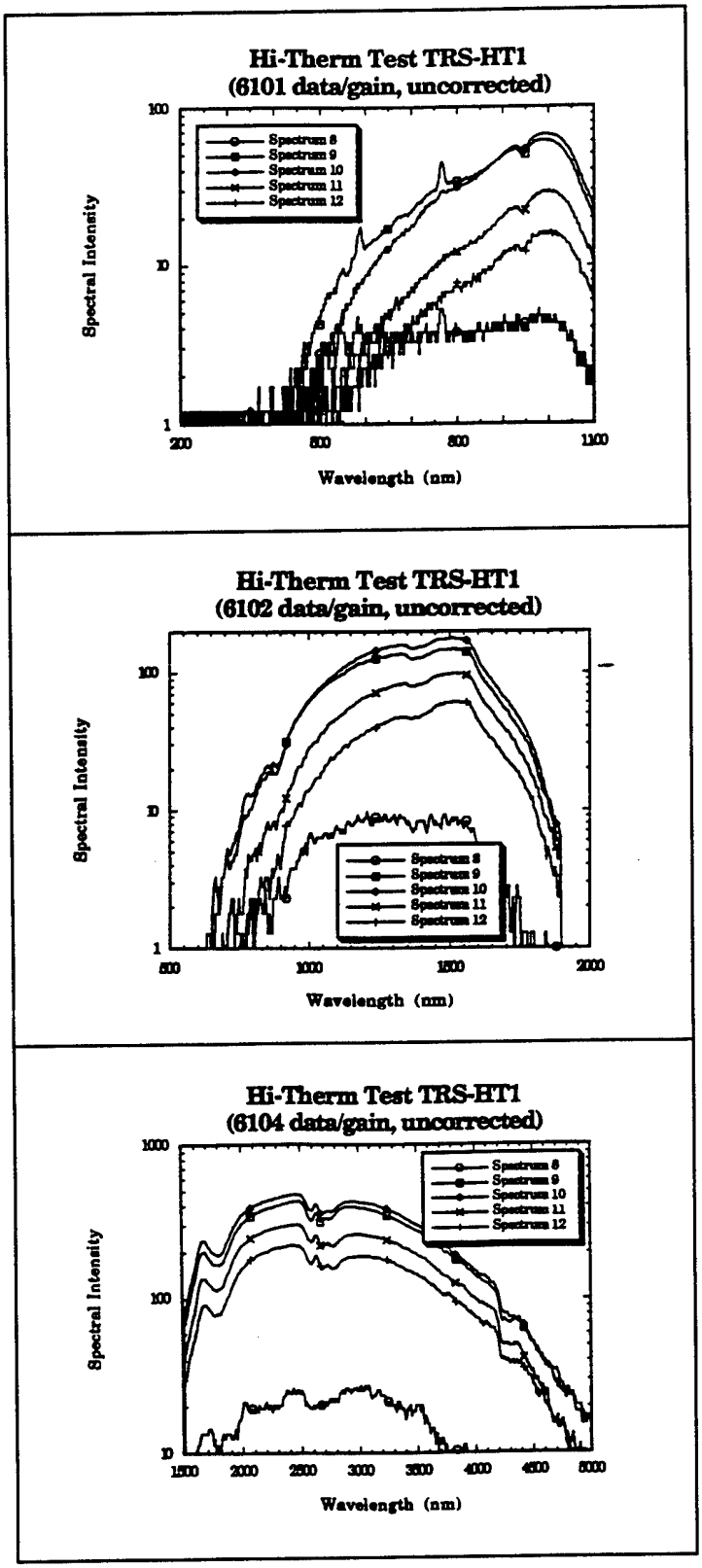

Figure B-26. Representative spectral data for TRS-HT1.

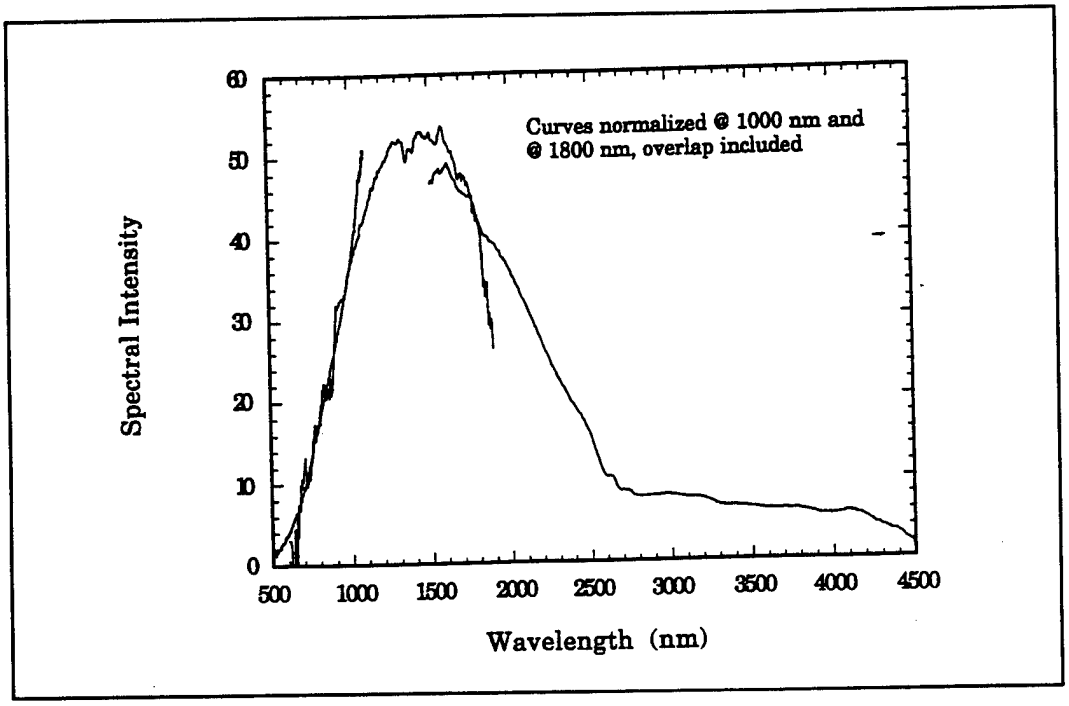

Figure B-27. Merged data for spectrum 10.

considered for final analysis of the data from the monochromators used in these tests are shown in Table B-4.

Table B-4. Wavelength ranges of monochromators.

6101 monochromator	400 - 1000 nm
6102 monochromator	750 - 1750 nm
6104 monochromator	1800 - 4000 nm

A comparison was made with blackbody curves generated using Plank's equation, and it was found that the color temperature of the Hi-Therm source was equivalent to that of a 2000K blackbody. This is shown in Figure 3-28. The spectral power of a blackbody at this temperature (using the Stephan-Boltzman equation) is approximately 22 cal/cm^2/s, which does correlate with the data from the view restricted radiometers. In addition to this, it must be pointed out that the spectra from this test exhibit strong line radiation at about 590 and 870nm, suggesting combustion of the metal reactants.

B.3.2.3 Data Analysis (TRS-HT2). The only difference between test TRS-HT1 and TRS-HT2 is that the ND1 neutral density filter was removed, and the amplifier gain settings changed to reflect anticipated spectral power levels. The raw data was processed by dividing through by the amplifier gain settings. Typical results are shown in Figure 3-29. Again there does not appear to be much variation in the spectral output of the source over the duration of the pulse.

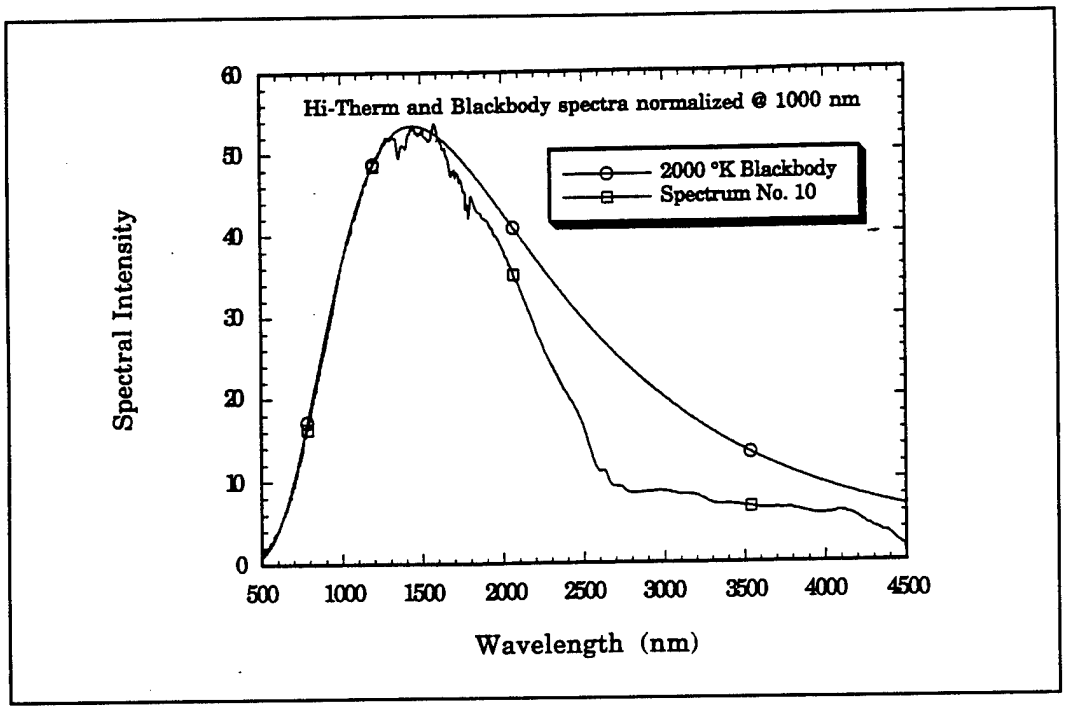

Figure B-28. Spectrum 10 and blackbody comparison.

Spectrum 9 was selected from this set of data as being the one corresponding to the maximum viewed spectral irradiance level during the test. The data for this spectrum was corrected for detector response, and the curves again merged as before. This is shown in Figure 3-30. A comparison made with blackbody curves found that the source appeared to be similar to a 2350 K blackbody, as shown in Figure 3-31. The emissive power of a blackbody at this temperature is approximately 41 cal/cm^2/sec. Again this correlates with the data from the view restricted radiometers.

B.3.3 Test TRS-HT3.

B.3.3.1 Instrument Configuration. The spectrometer instrumentation for test TRS-HT3 was very similar to that used in the previous tests. For this test, the input optics for the monochromators consisted of 4 inch diameter integrating spheres, which gave a field of view equal to that of the calorimeters. Based upon information provided by GSI, and also data from previous tests, neutral density filters were installed in the 6101 (ND2), and the 6102 (ND1). Detector response calibration data was again generated using the OPTRONICS lamp. The instruments were mounted in a protective enclosure, and located approximately 10 feet from the front surface of the Hi-Therm test panels, centered on the 10 foot x 8 foot panel array. No additional alignment was necessary since the instruments had an effective field of view of 2π. The system controller and software were configured in the same manner as in the previous two tests.

B.3.3.2 Data Analysis (TRS-HT3). Actual performance of the test yielded mixed results. When the Hi-Therm panels were ignited, a flame front developed and moved quickly towards

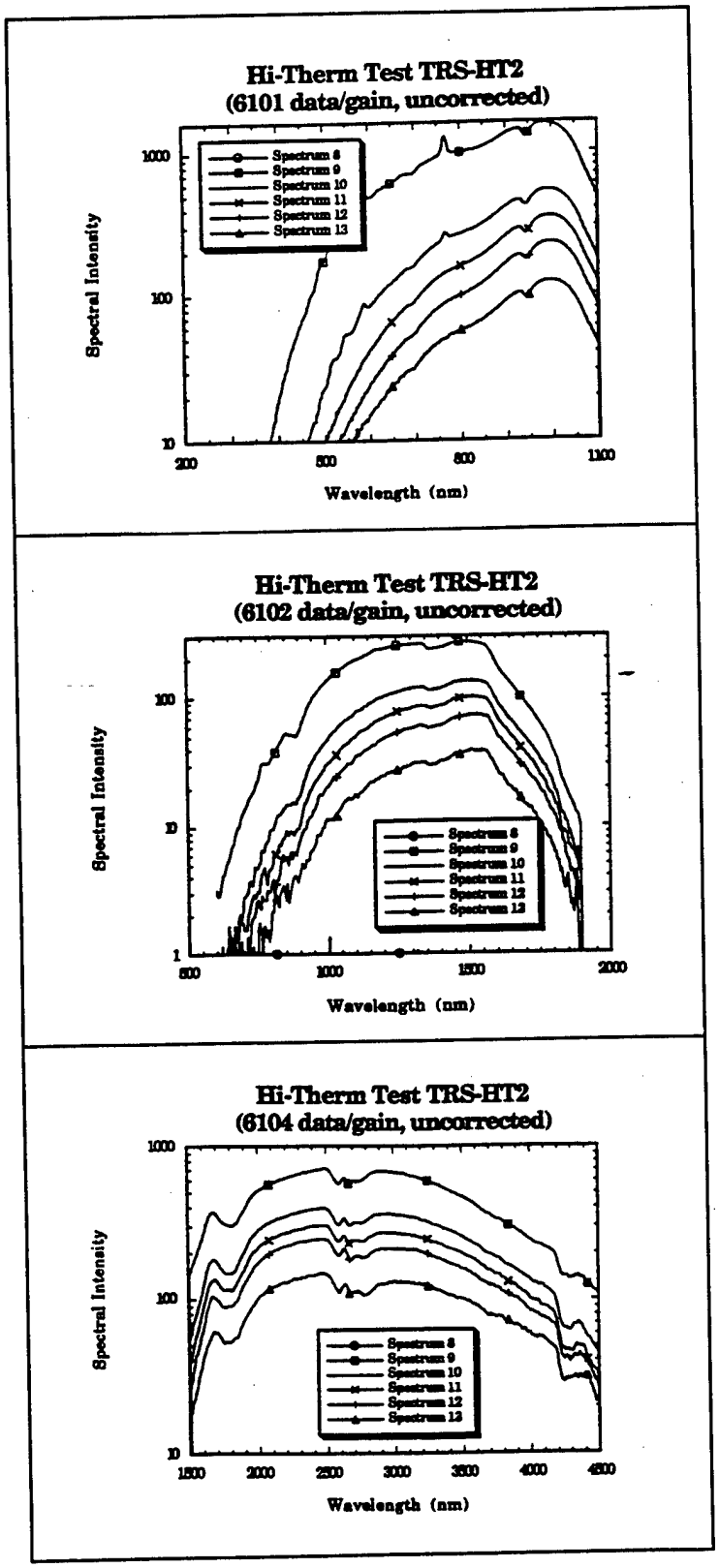

Figure B-29. Representative spectral data for TRS-HT2.

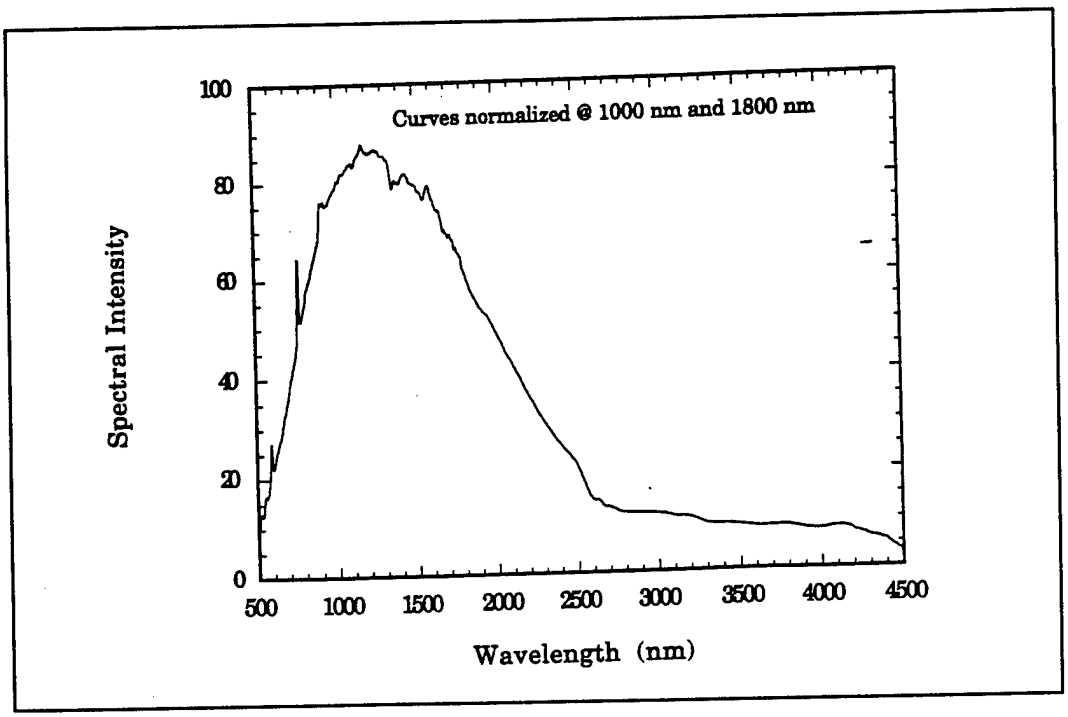

Figure B-30. Merged data for spectrum 9.

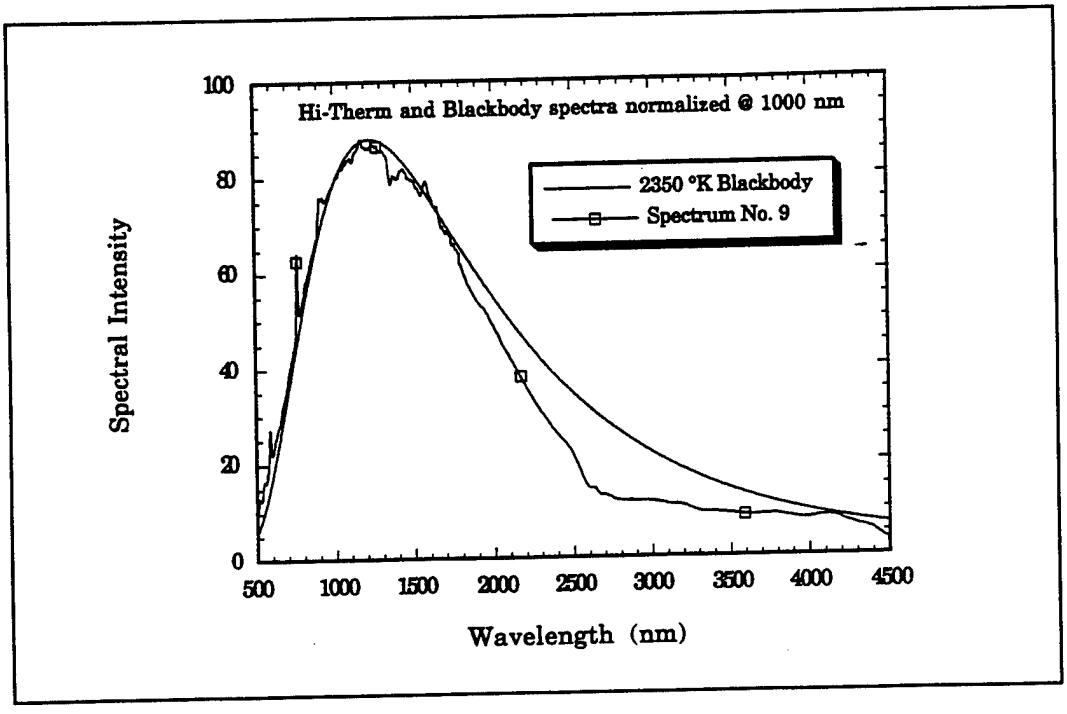

Figure B-31. Spectrum 9 and blackbody comparison.

the instrumentation. Viewing the videotapes of the test indicated that the spectrometer enclosure, being one of the closest instruments, was almost immediately engulfed in the fireball. For this reason, interpretation of the spectrometer data is very difficult.

The peak signals recorded by the system are completely off scale, more than likely corresponding to the time period when the spectrometers were engulfed. In addition, a considerable layer of particulate matter was at some point deposited on the inside of the integrating spheres, which would have a great affect on the response of the instruments. A representative group of spectra are shown in Figure B-32.

The very first spectrum showing any signal level (spectrum 9) may be the only one which can be of any value. Using the same data reduction techniques on spectrum 9, a characterization of the spectral irradiance observed by the instruments can be derived. It must be emphasized again that it is difficult to determine the exact conditions under which spectrum 9 was acquired, since it is possible that the flame front had already engulfed the instruments at this time. In any case, a comparison was made with blackbody curves, and the color temperature of spectrum 9 appears to be similar to that of a 2350K blackbody, as shown in Figure B-33. A blackbody at this temperature has an existence of approximately 41 cal/cm^2/s.

B.4 Data Review.

The data are consistent within the data set. Average peak surface flux from the single panel was 25 cal/cm^2/s and from the 80 panel test was 36 cal/cm^2/s. For the large array test (TRS-HT3) very high outputs were seen on all of the instruments at the 10 ft. location. This was due entirely to convective heating from the hot gas in the fireball or conductive heating from hot particles hitting/condensing on the active elements of the instrumentation, as evidenced by the rapidly fluctuating traces. The calibration of the view restricted radiometers was rendered invalid as their viewing ports were filled with still-reacting materials at about 200 ms, so only data before this time can be used. It is evident that enough data was gathered to completely characterize the performance of the Hi-Therm panels.

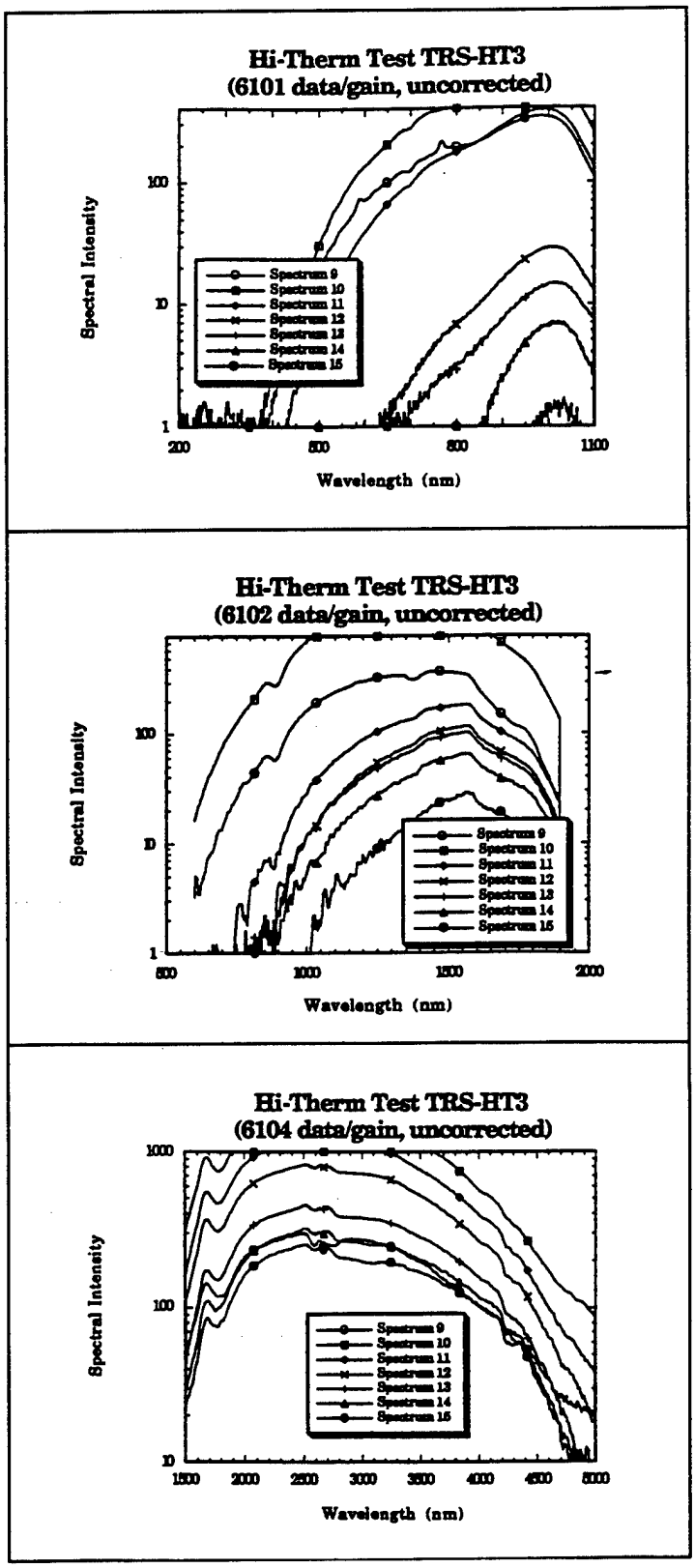

Figure B-32. Representative spectral data for TRS-HT3.

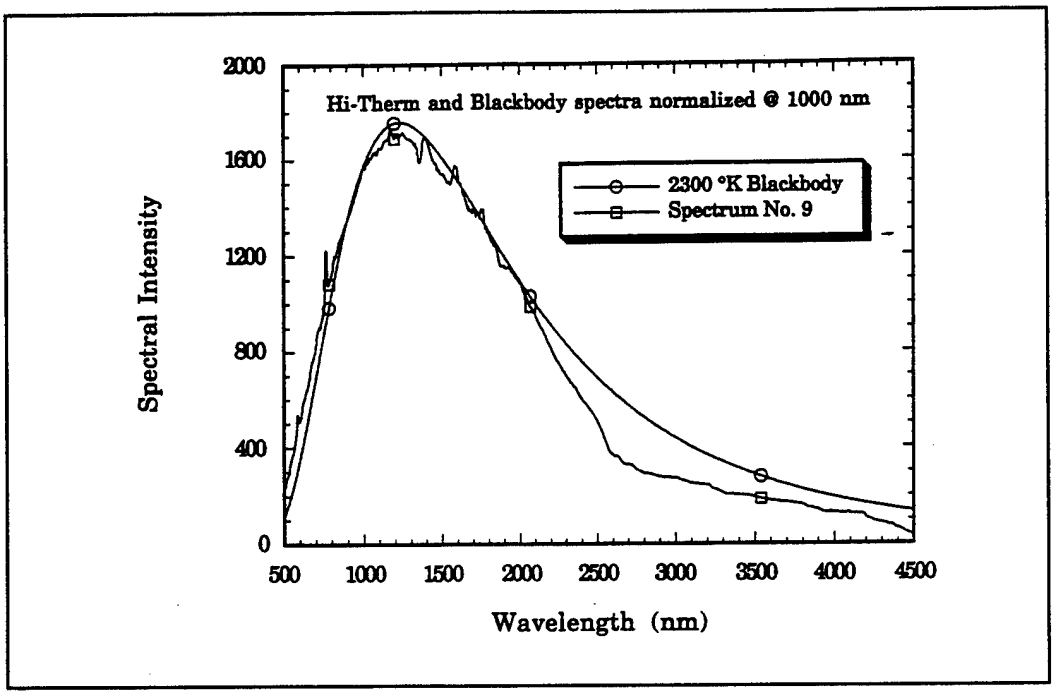

Figure B-33. Spectrum 9 and blackbody comparison.

APPENDIX C

HI-THERM MINIMAL-THROW DEVELOPMENT TEST DATA DETAIL

Attached is a summary (Table C-1), and the flux curves (Figures C-1 through C-28) for the 18 minimal-throw Hi-Therm single panel tests. The curves represent data recorded by a total radiometer and a thermogauge heat flux gauge at 5 feet from the Hi-Therm panel source.

Table C-1. Summary of minimal throw Hi-Therm formulations.

Test No.	Chemistry	Radiometer Peak Flux		Thermogauge Peak Flux		Time to Peak (sec)	Particle Throw (see note)
		($cal/cm^2 \cdot sec$)	(W/cm^2)	($cal/cm^2 \cdot sec$)	(W/cm^2)		
1	58.2 wt.% Ti/2B + 38.9 wt.% Ti/C + 2.9 wt.% carbon fibers	1.30	5.44	1.43	6.00	1.15	1
2	62.6 wt.% Ti/2B + 33.7 wt.% Ti/C + 3.7 wt.% carbon fibers	1.66	6.93	1.55	6.49	1.18	1
3	58.4 wt.% Ti/2B + 39.0 wt.% Ti/C + 1.1 wt.% carbon fibers + 1.5 wt.% fiberglass fibers	1.61	6.75	1.55	6.49	1.12	1
4	58.2 wt.% Ti/2B + 38.9 wt.% Ti/C + 2.9 wt.% carbon fibers	1.29	5.40	1.64	6.85	0.75	1
5	62.6 wt.% Ti/2B + 33.7 wt.% Ti/C + 3.7 wt.% carbon fibers	1.69	7.07	1.55	6.50	1.02	1
6	58.4 wt.% Ti/2B + 39.0 wt.% Ti/C + 1.1 wt.% carbon fibers + 1.5 wt.% fiberglass fibers	1.45	6.08	1.44	6.03	0.77	1
7	63.1 wt.% Ti/2B + 34.0 wt.% Ti/C + 2.9 wt.% carbon fibers	1.53	6.40	1.66	6.96	0.77	1
8	63.1 wt.% Ti/2B + 34.0 wt.% Ti/C + 2.9 wt.% carbon fibers	1.77	7.43	1.99	8.35	0.62	1
9	64.1 wt.% Ti + 34.9 wt.% AlB_{12} + 1.0 wt.% carbon fibers	2.42	10.13	4.20	17.6	0.86	2
10	62.6 wt.% Ti/2B + 33.7 wt.% Ti/C + 3.7 wt.% carbon fibers	1.64	6.85	3.10	12.98	0.96	2
11	62.6 wt.% Ti/2B + 33.7 wt.% Ti/C + 3.7 wt.% carbon fibers	no data	no data	no data	no data	no data	3
12	62.6 wt.% Ti/2B + 33.7 wt.% Ti/C + 3.7 wt.% carbon fibers	saturated detector	saturated detector	1.77	7.40	1.05	2
13	63.1 wt.% Ti/2B + 34.0 wt.% Ti/C + 2.9 wt.% carbon fibers	1.66	6.93	2.33	9.74	0.78	1
14	63.1 wt.% Ti/2B + 34.0 wt.% Ti/C + 2.9 wt.% carbon fibers	1.91	8.00	2.21	9.27	0.85	2
15	63.1 wt.% Ti/2B + 34.0 wt.% Ti/C + 2.9 wt.% carbon fibers	1.71	7.16	no data	no data	0.50	3
16	62.6 wt.% Ti/2B + 33.7 wt.% Ti/C + 3.7 wt.% carbon fibers	1.02	4.26	1.77	7.42	0.73	1
Note on Particle Throw: 1 = insignificant particle throw; 2 = Modest particle throw; 3 = Significant particle throw							

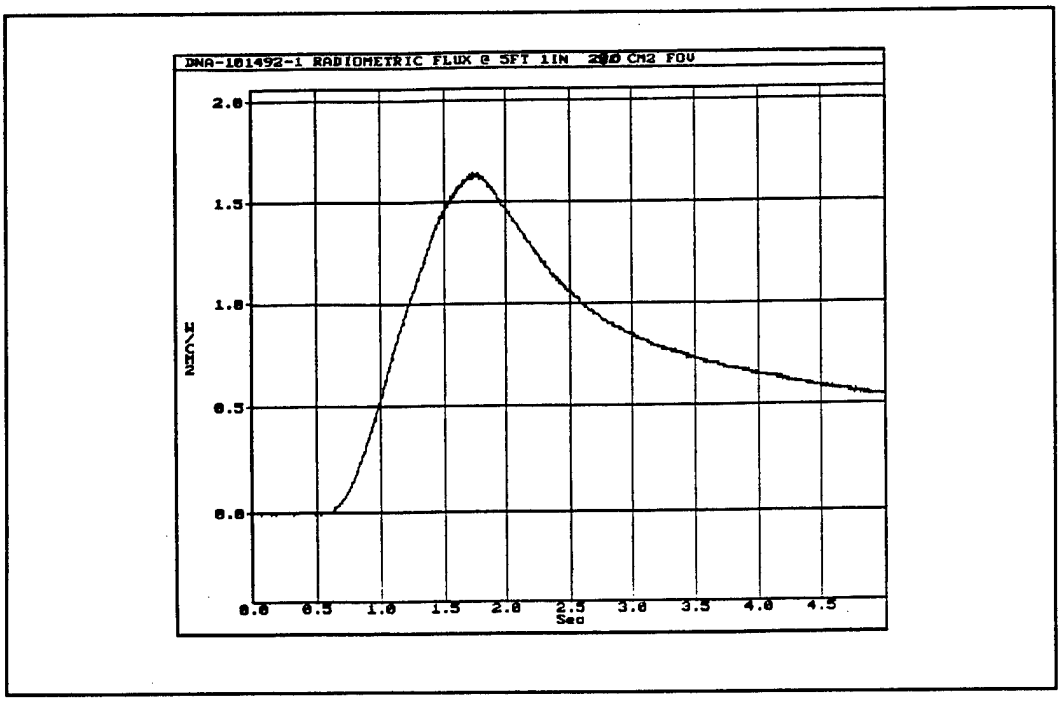

Figure C-1. Radiometer, flux on detector, test #1, uncorrected for FOV.

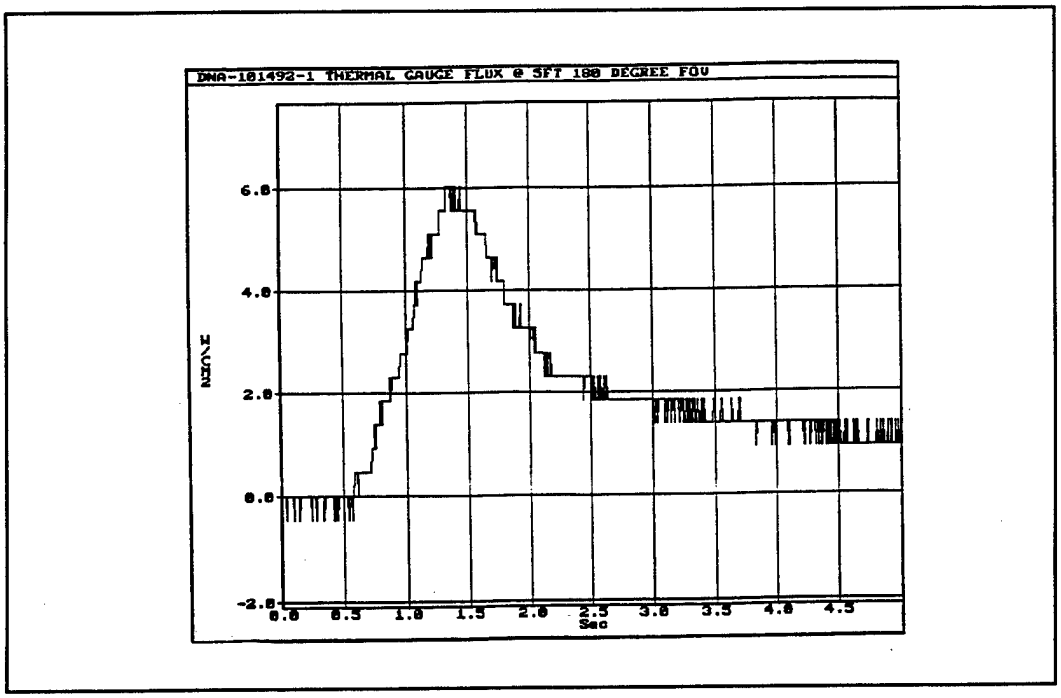

Figure C-2. thermogauge heat flux gauge, flux on detector, test #1.

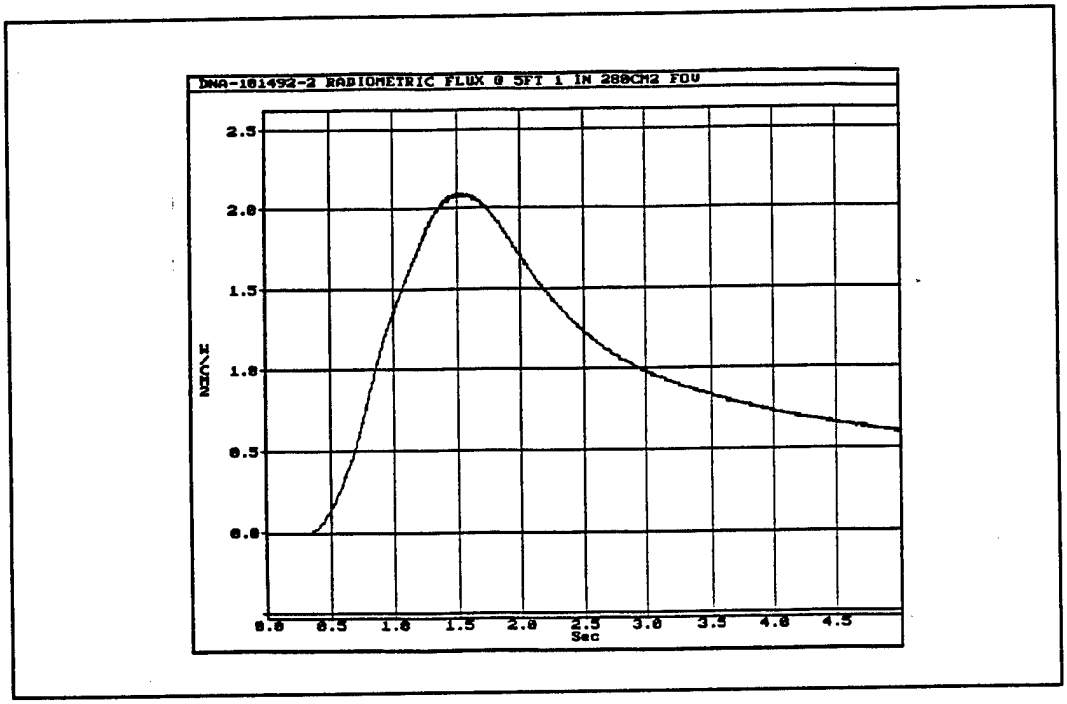

Figure C-3. Radiometer, flux on detector, test #2, uncorrected for FOV.

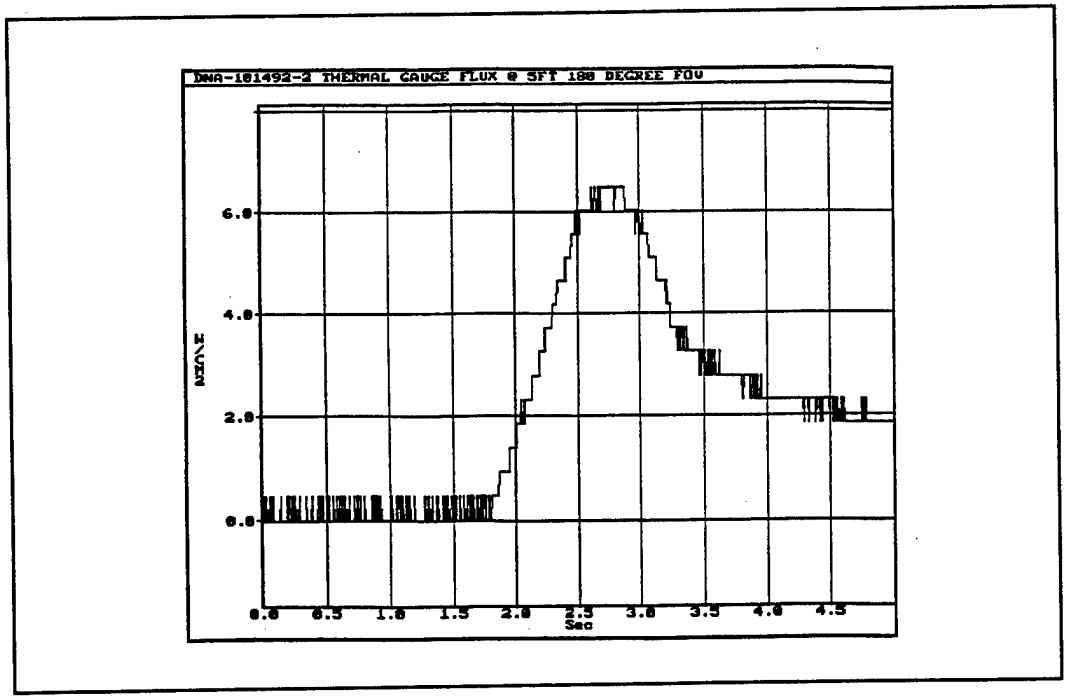

Figure C-4. thermogauge heat flux gauge, flux on detector, test #2.

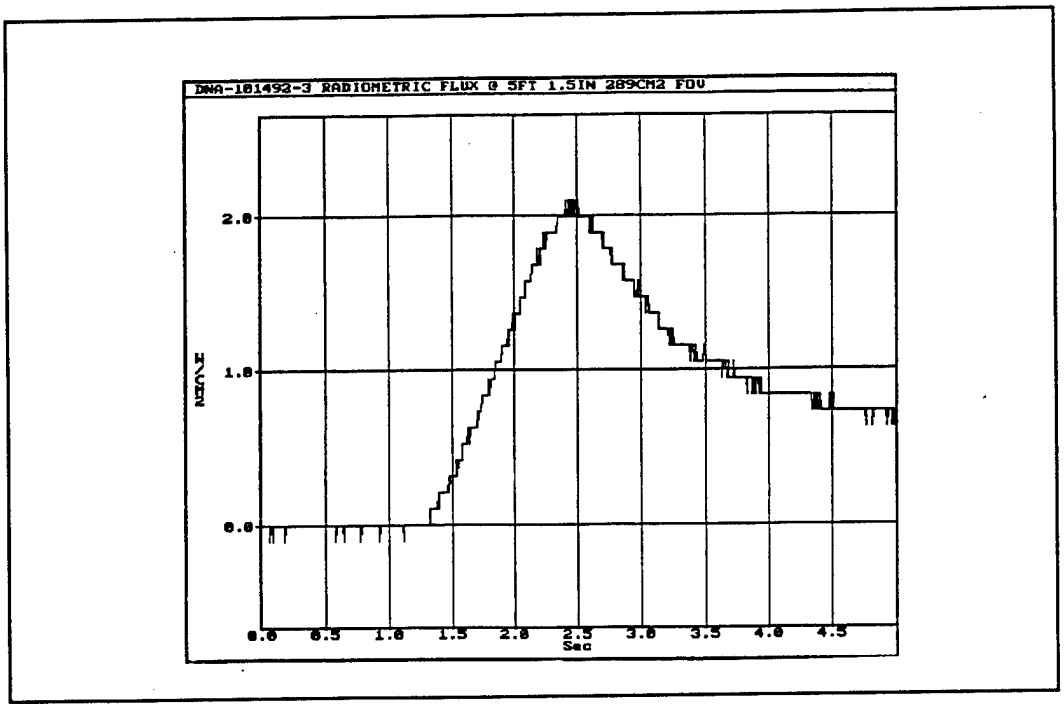

Figure C-5. Radiometer, flux on detector, test #3, uncorrected for FOV.

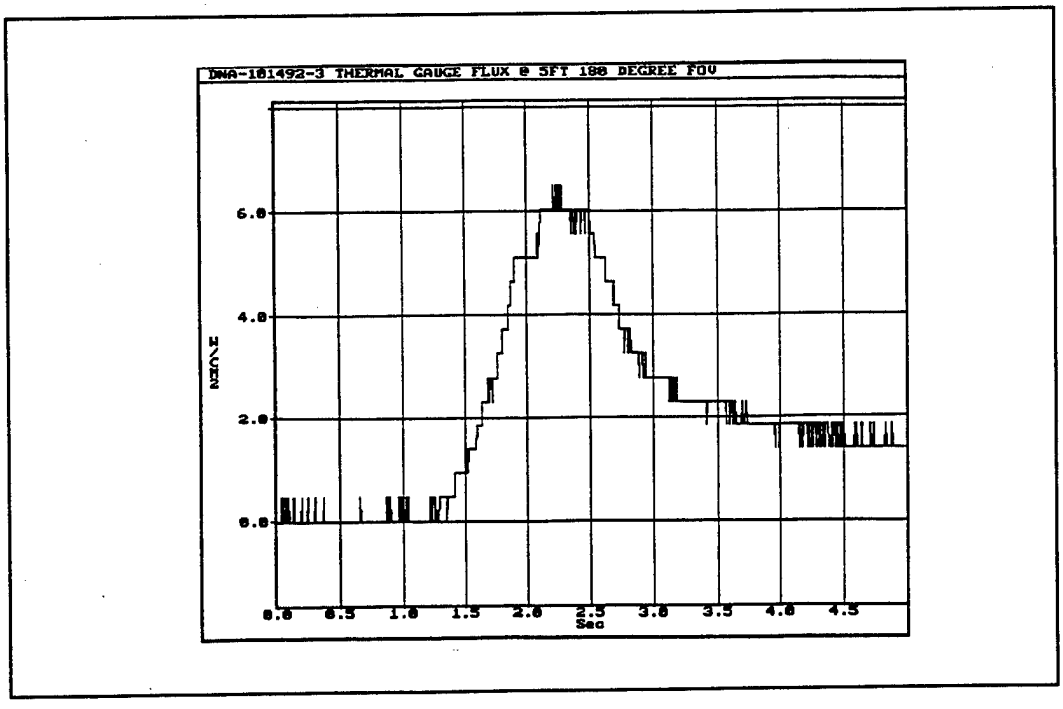

Figure C-6. thermogauge heat flux gauge, flux on detector, test #3.

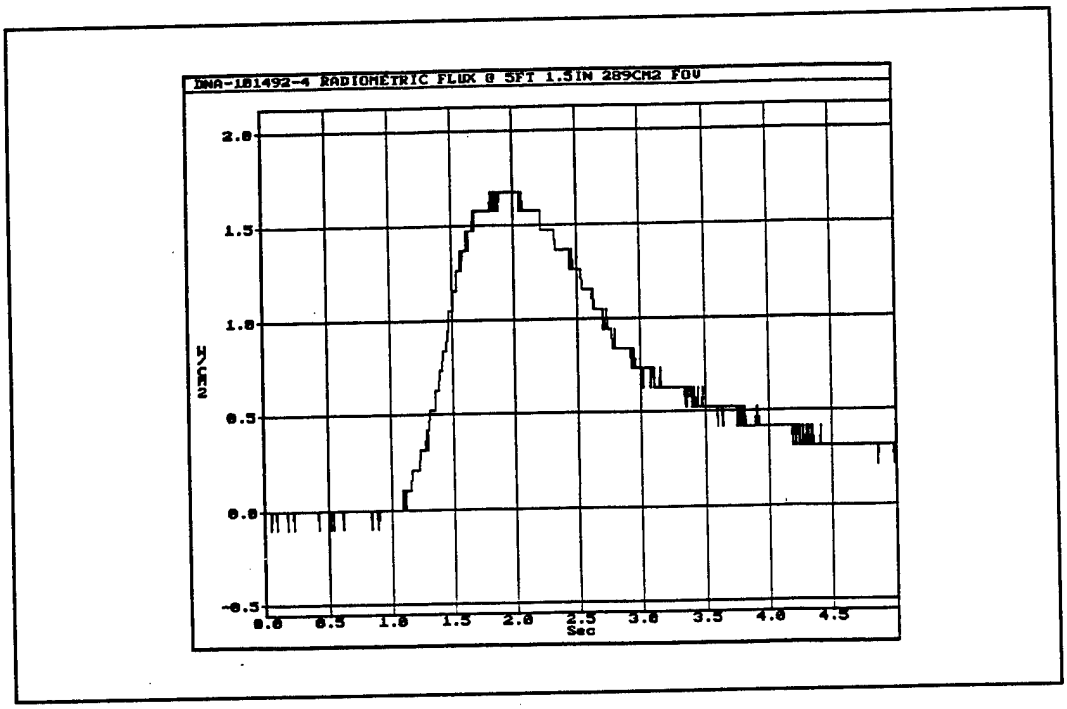

Figure C-7. Radiometer, flux on detector, test #4, uncorrected for FOV.

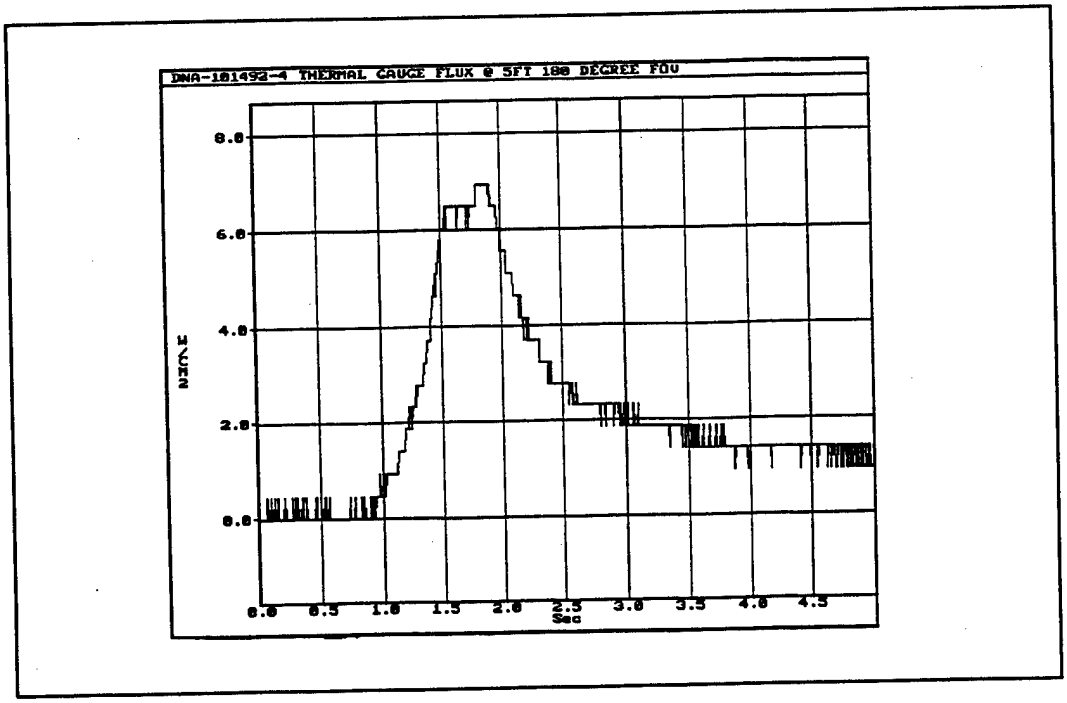

Figure C-8. thermogauge heat flux gauge, flux on detector, test #4.

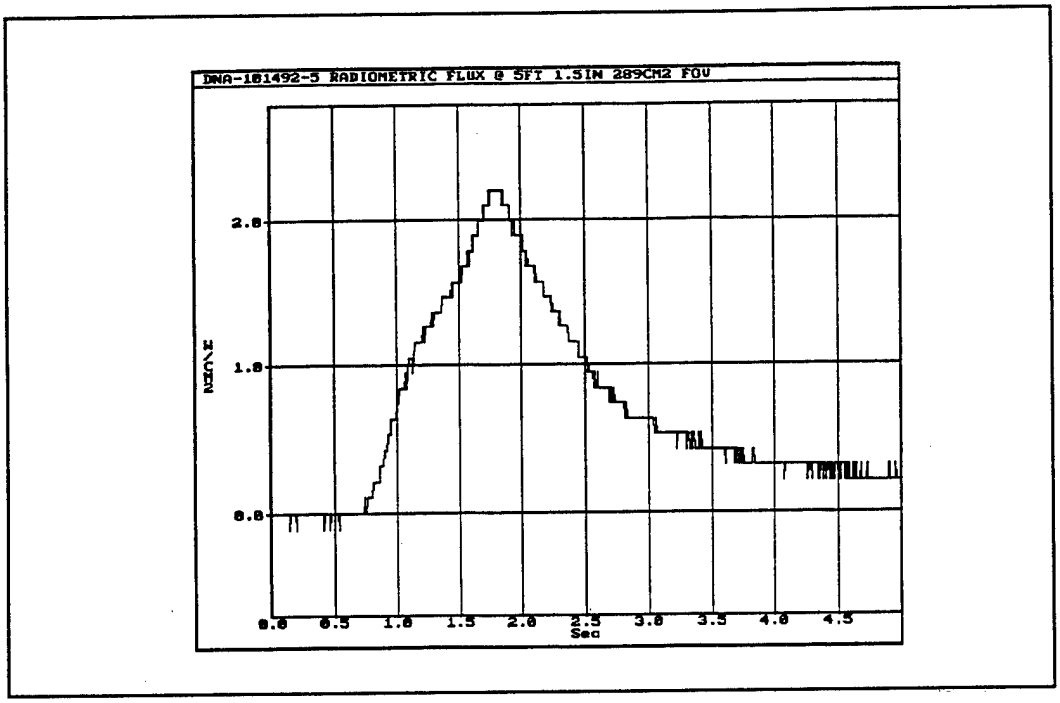

Figure C-9. Radiometer, flux on detector, test #5, uncorrected for FOV.

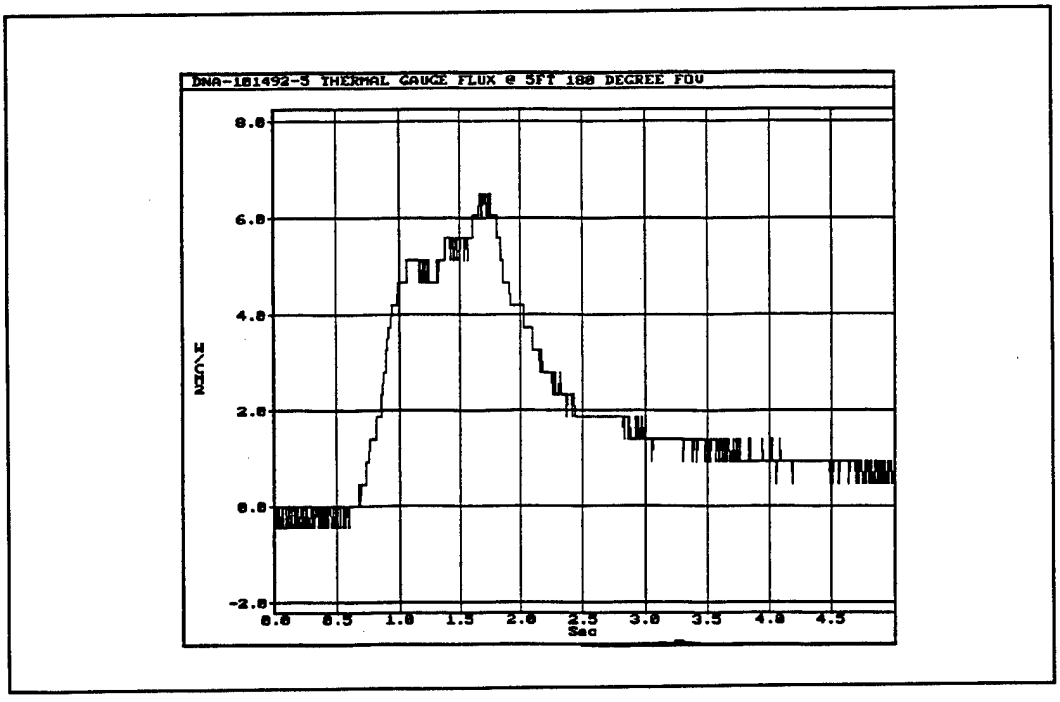

Figure C-10. thermogauge heat flux gauge, flux on detector, test #5.

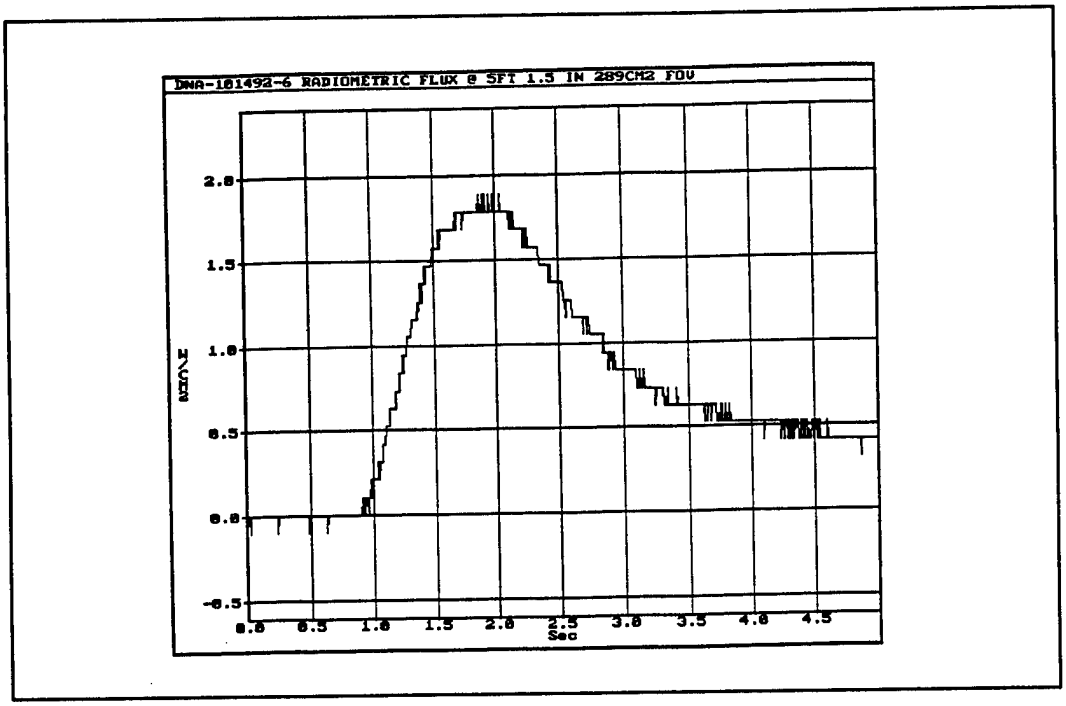

Figure C-11. Radiometer, flux on detector, test #6, uncorrected for FOV.

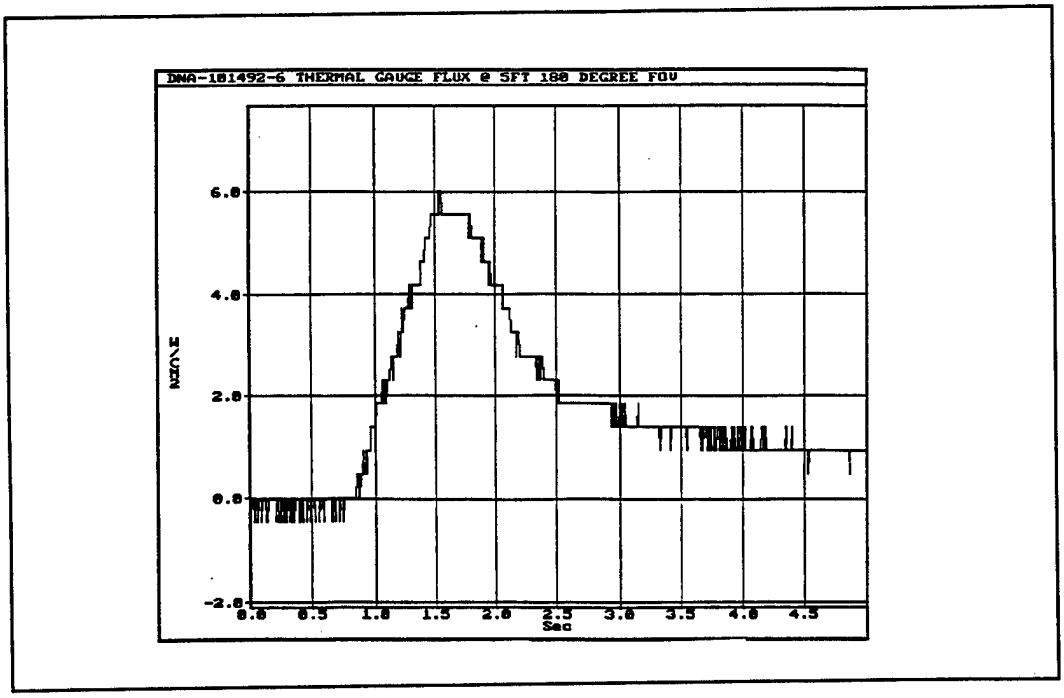

Figure C-12. thermogauge heat flux gauge, flux on detector, test #6.

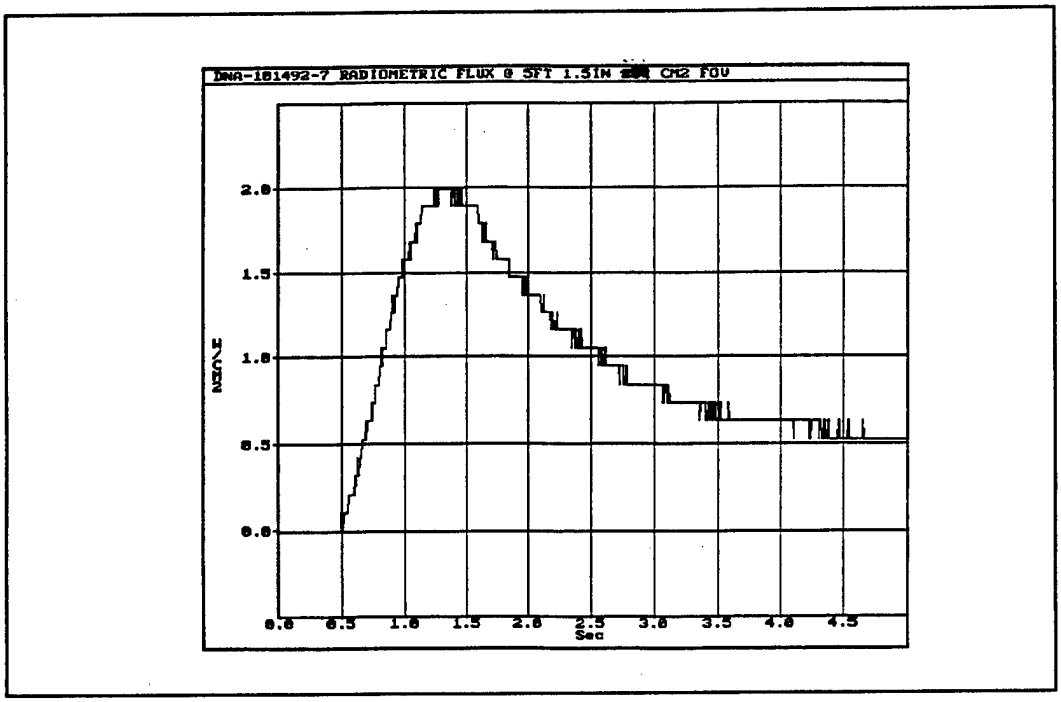

Figure C-13. Radiometer, flux on detector, test #7, uncorrected for FOV.

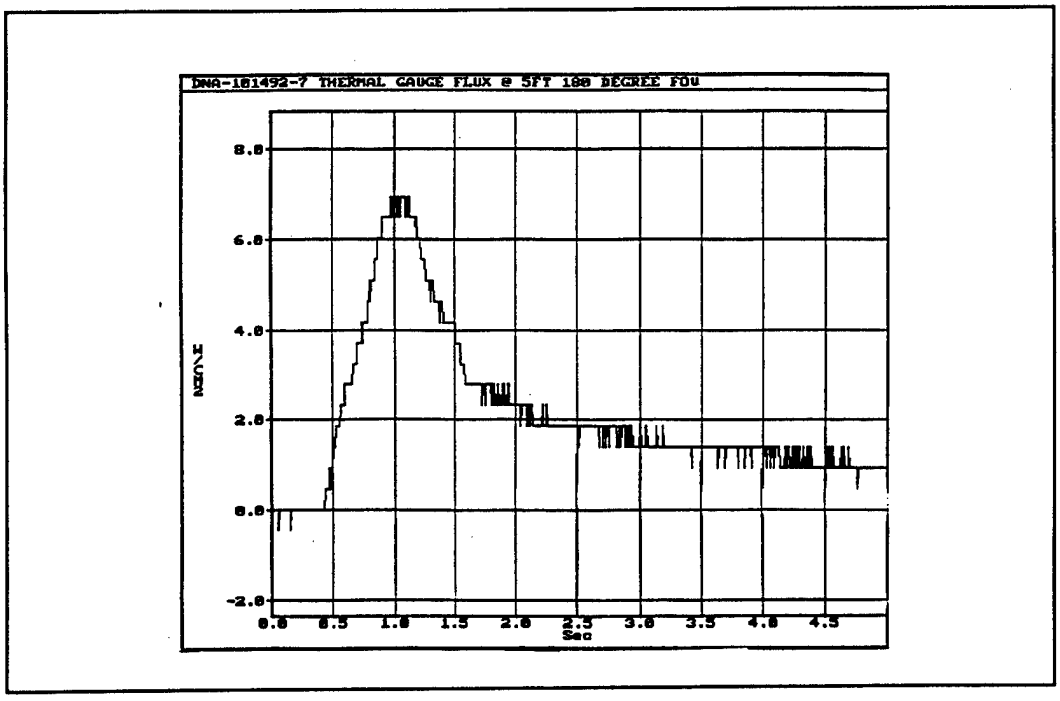

Figure C-14. thermogauge heat flux gauge, flux on detector, test #7.

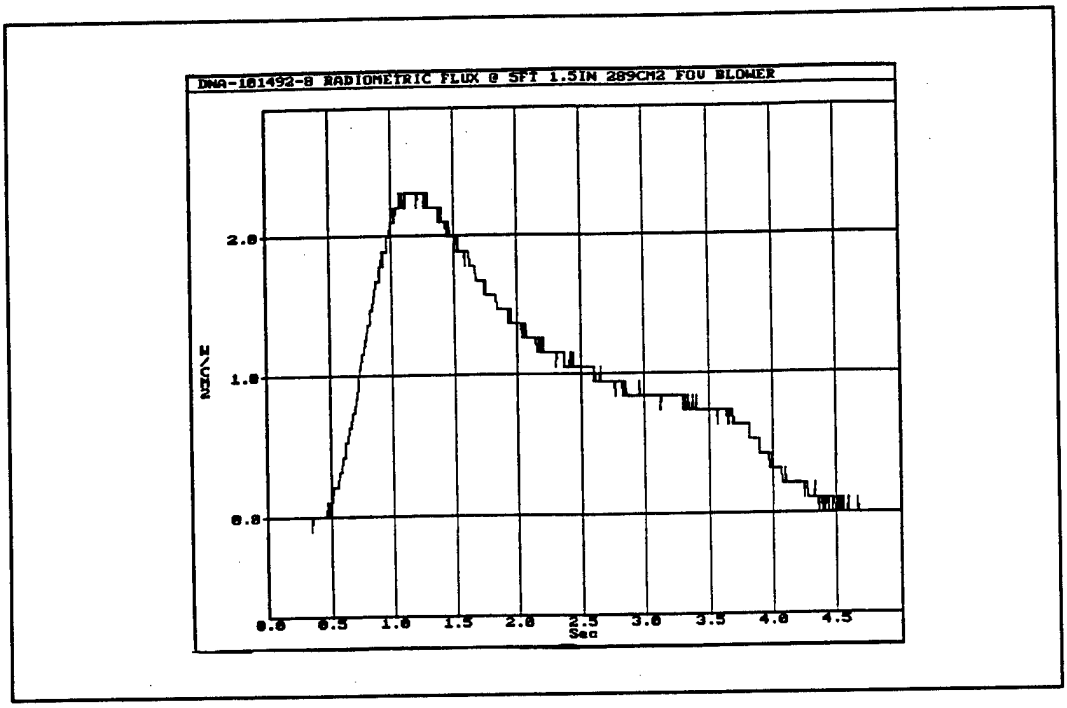

Figure C-15. Radiometer, flux on detector, test #8, uncorrected for FOV.

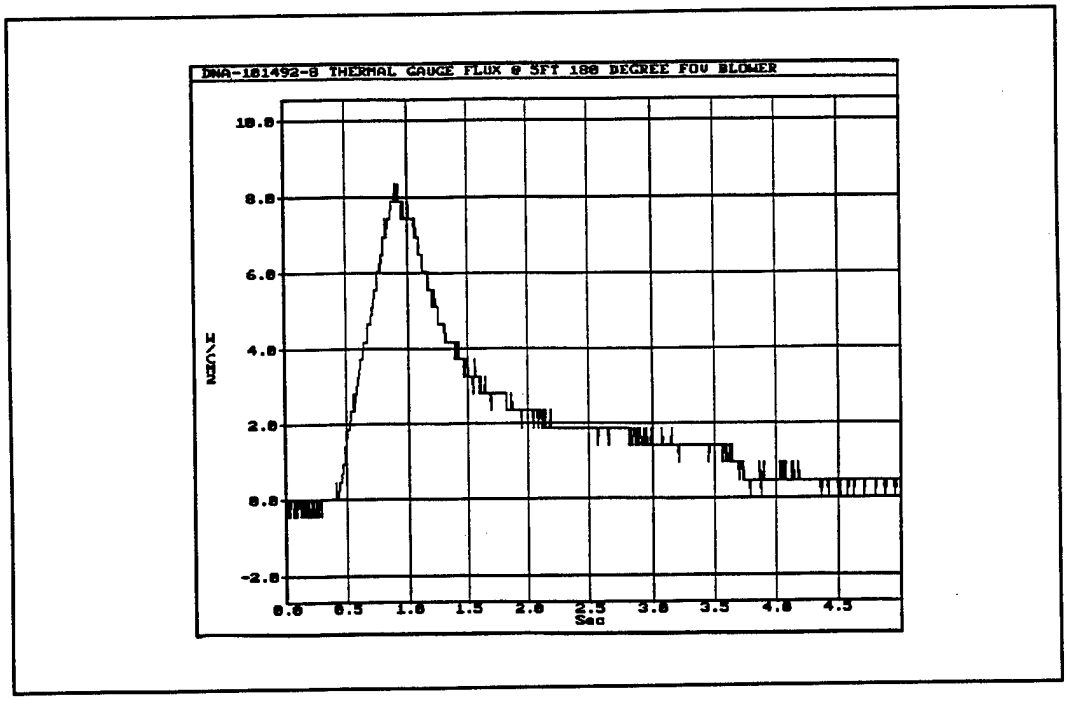

Figure C-16. thermogauge heat flux gauge, flux on detector, test #8.

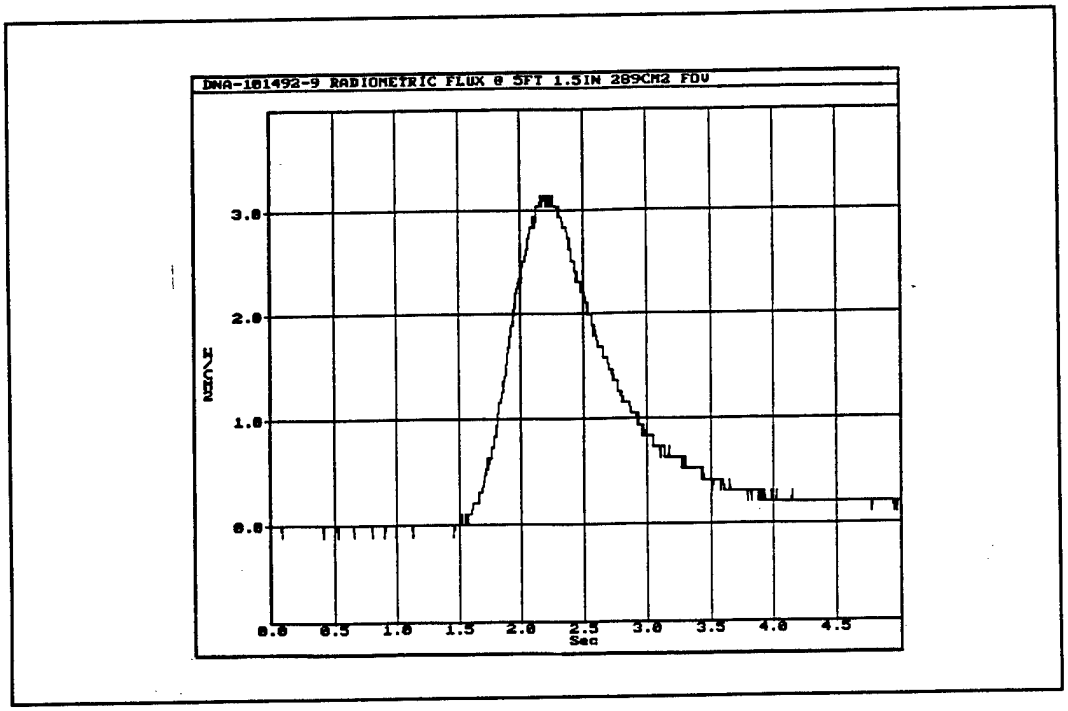

Figure C-17. Radiometer, flux on detector, test #9, uncorrected for FOV.

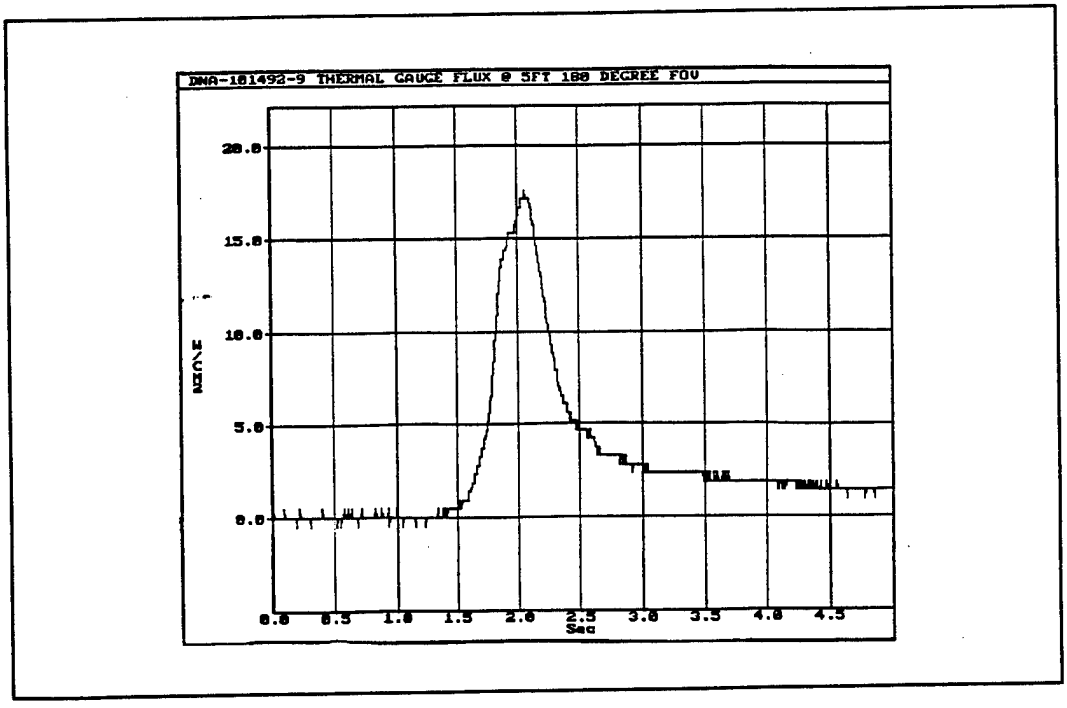

Figure C-18. thermogauge heat flux gauge, flux on detector, test #9.

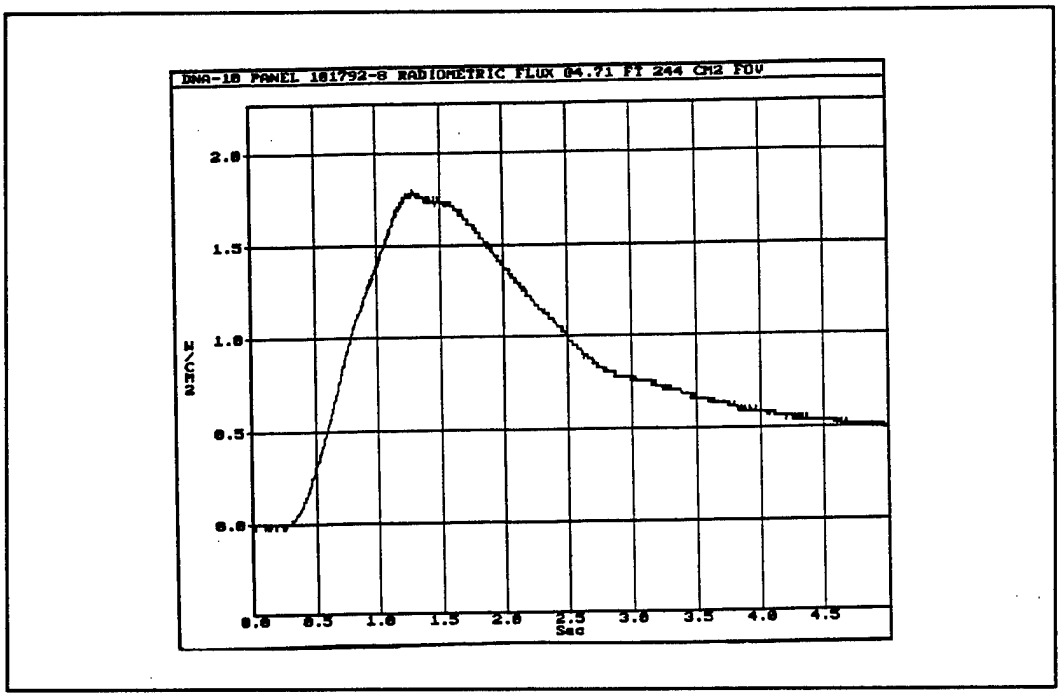

Figure C-19. Radiometer, flux on detector, test #10, uncorrected for FOV.

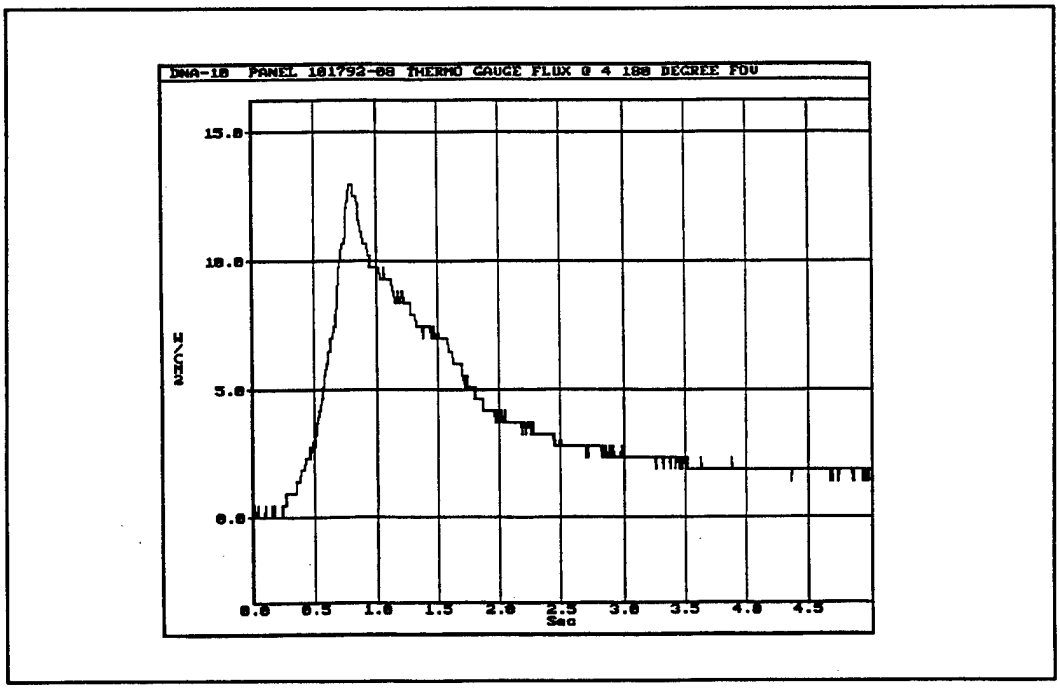

Figure C-20. thermogauge heat flux gauge, flux on detector, test #10.

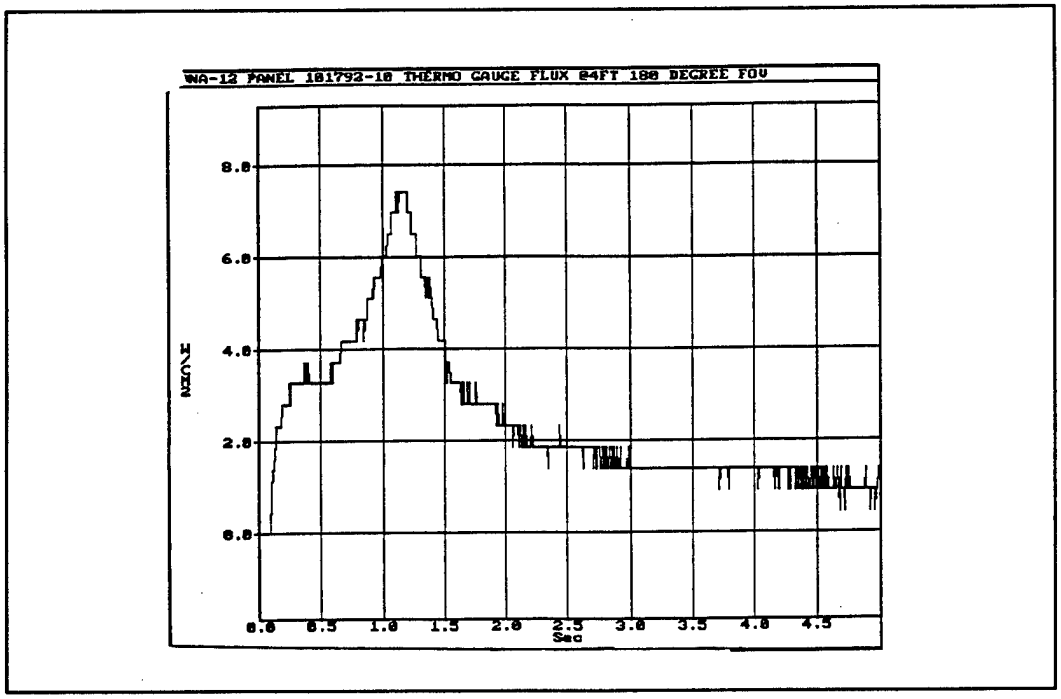

Figure C-21. Radiometer, flux on detector, test #12, uncorrected for FOV.

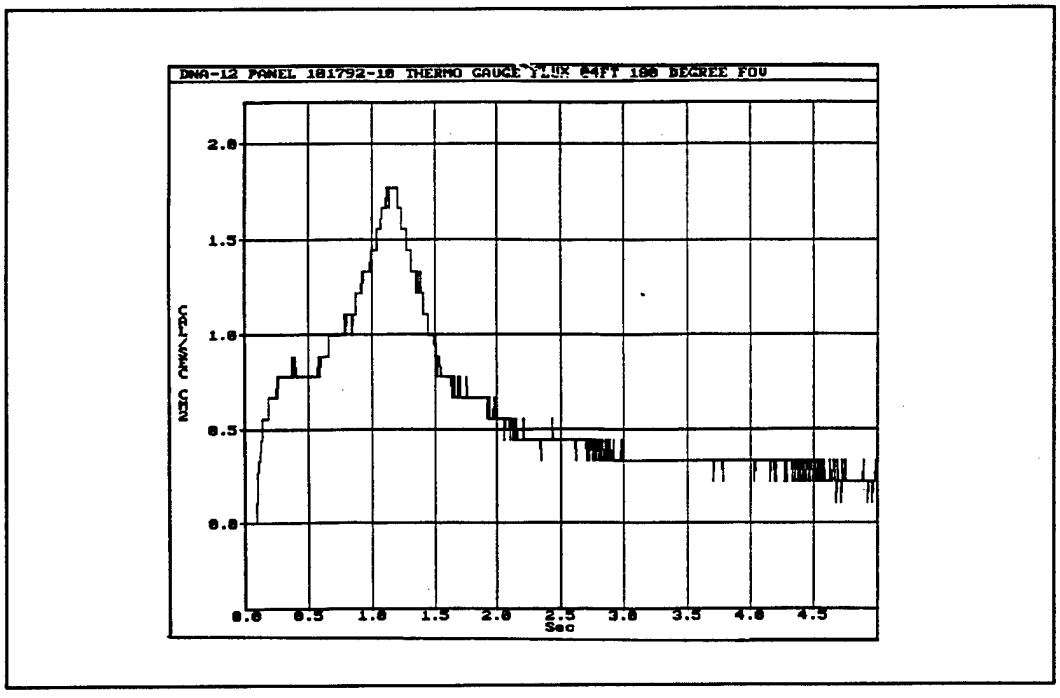

Figure C-22. thermogauge heat flux gauge, flux on detector, test #12.

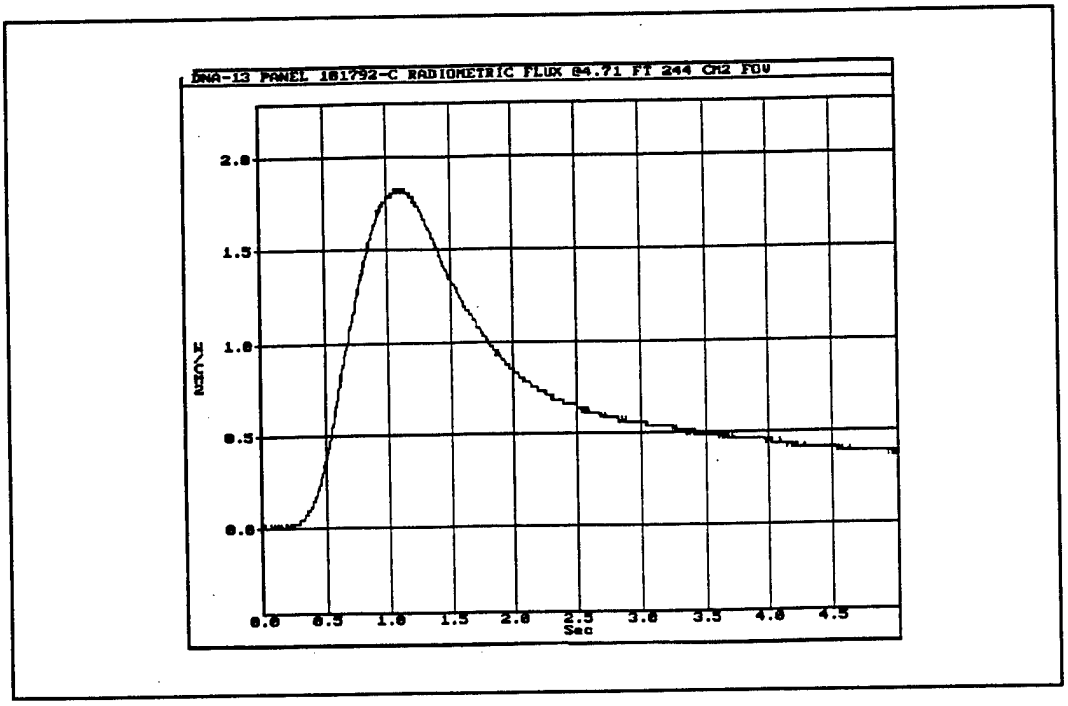

Figure C-23. Radiometer, flux on detector, test #13, uncorrected for FOV.

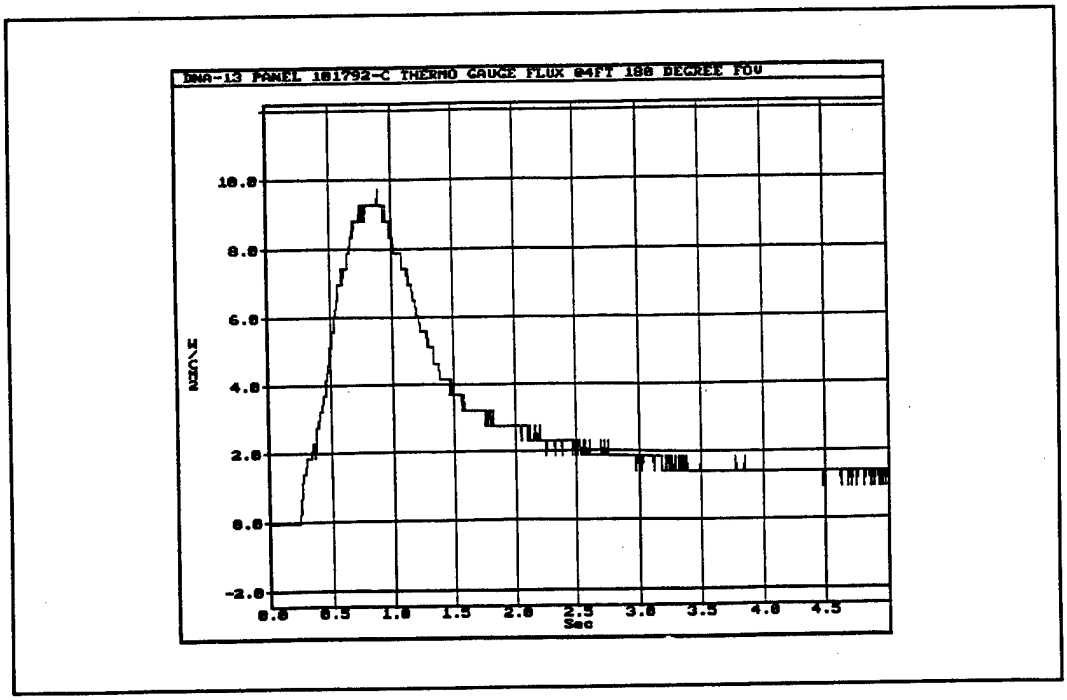

Figure C-24. thermogauge heat flux gauge, flux on detector, test #13.

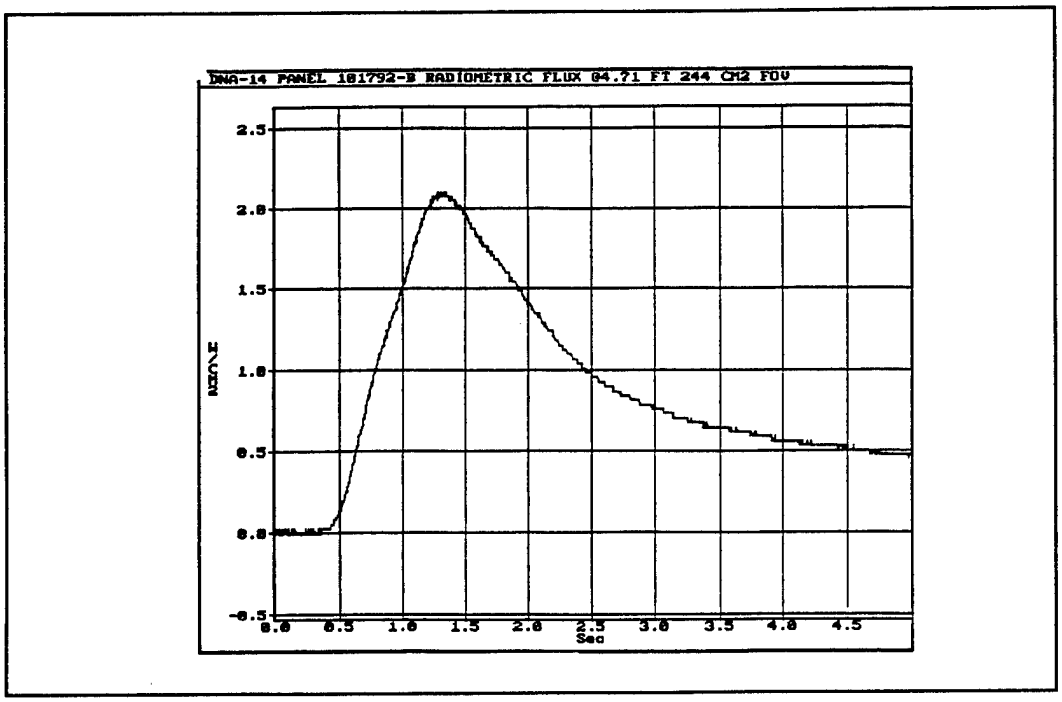

Figure C-25. Radiometer, flux on detector, test #14, uncorrected for FOV.

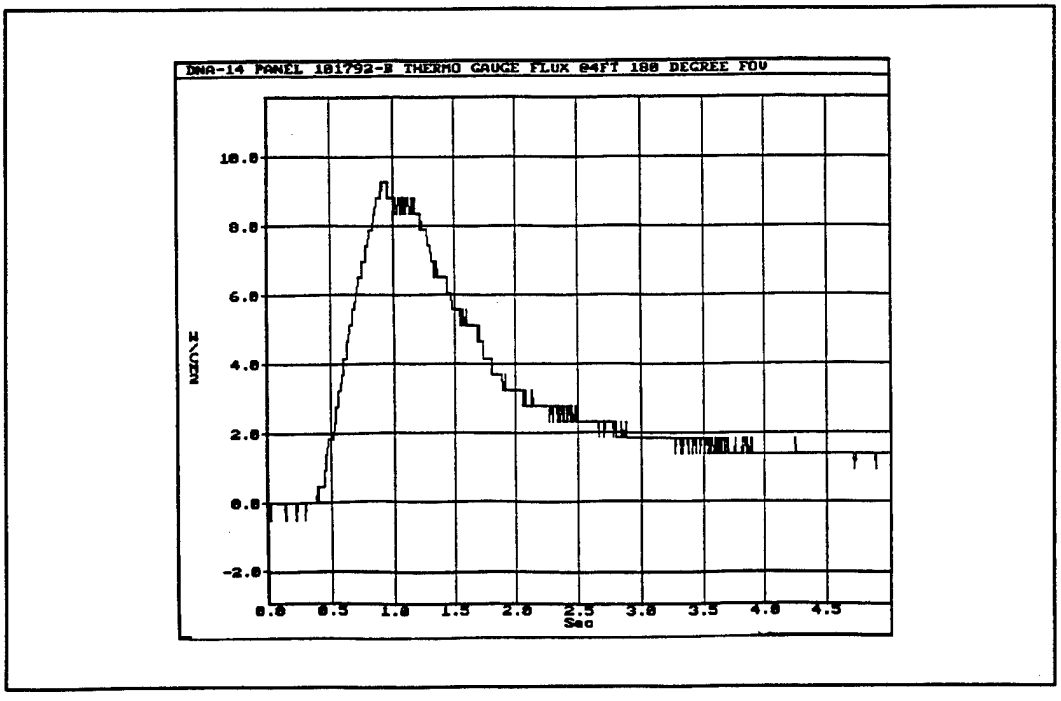

Figure C-26. thermogauge heat flux gauge, flux on detector, test #14.

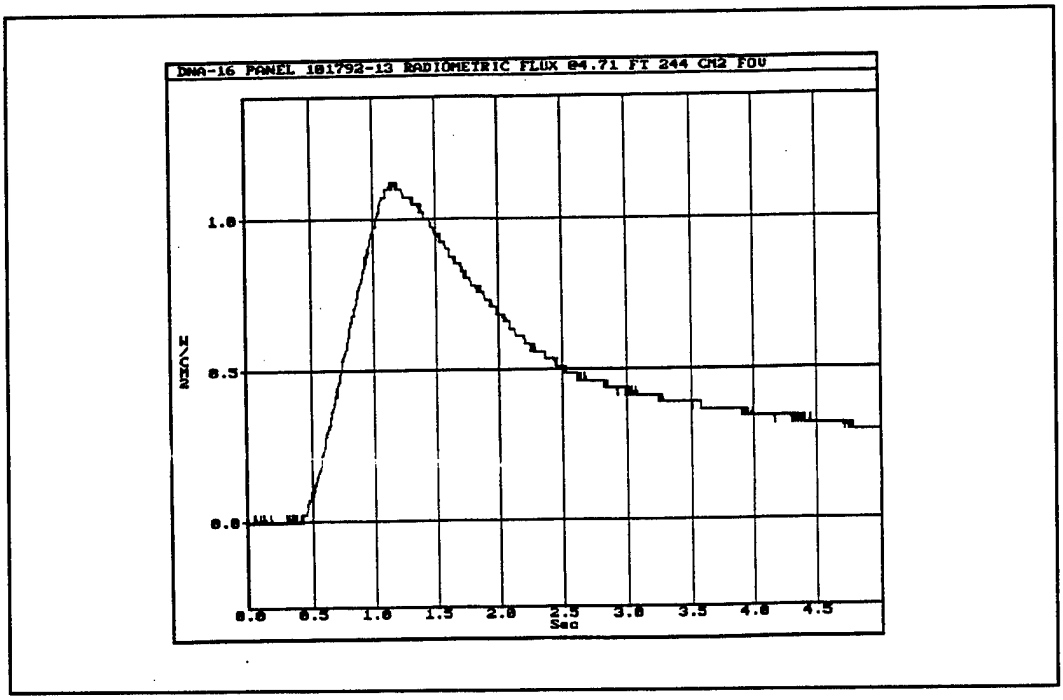

Figure C-27. Radiometer, flux on detector, test #16, uncorrected for FOV.

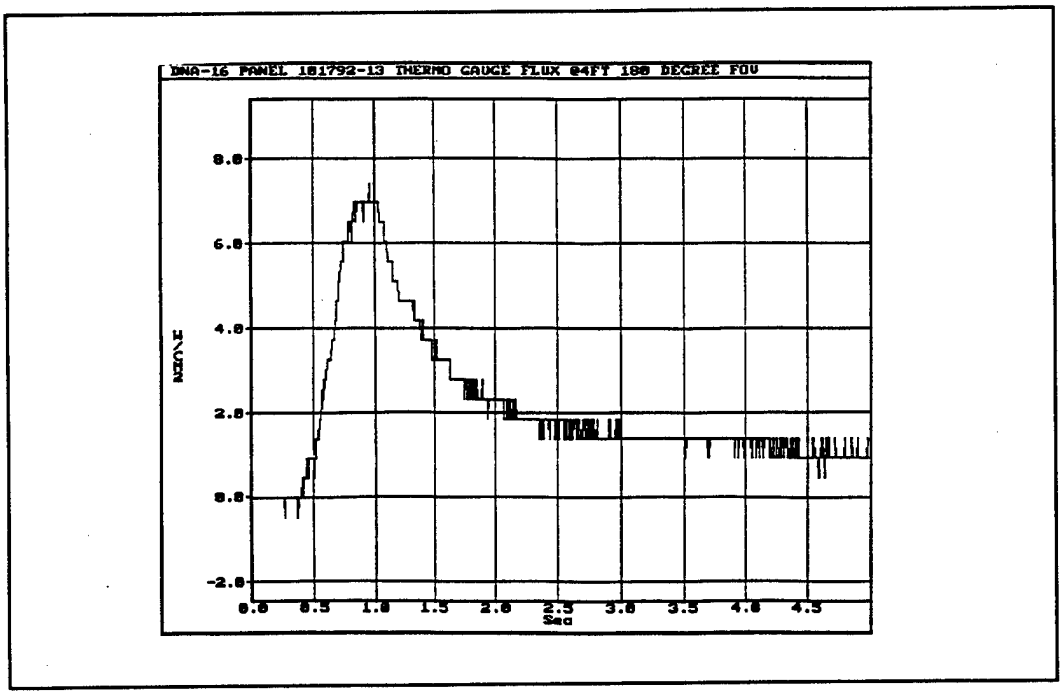

Figure C-28. thermogauge heat flux gauge, flux on detector, test #16.

APPENDIX D

HI-THERM DEMONSTRATION TEST DETAIL, NOVEMBER 1992

A summary of the test data (Figures D-1 through D-43) for the demonstration tests conducted at the TRS test site, Coyote Canyon, Kirtland AFB, NM, during November 1992, follows. The tests conducted were two 9 panel tests (TRS-HITH-4 and TRS-HITH-5) and one 28 panel test (TRS-HITH-6). The sensor location is given in the figure title and is in the format (X, Y, Z) [ex., (0, 10, 5.25]) when X is defined as the distance to the left (-) and right (+) of the center line of the panel, Y is defined as the distance in front (+) or in back (-) of the front face of the panel and Z is defined as the height above ground. The X, Y, Z dimensions are in feet.

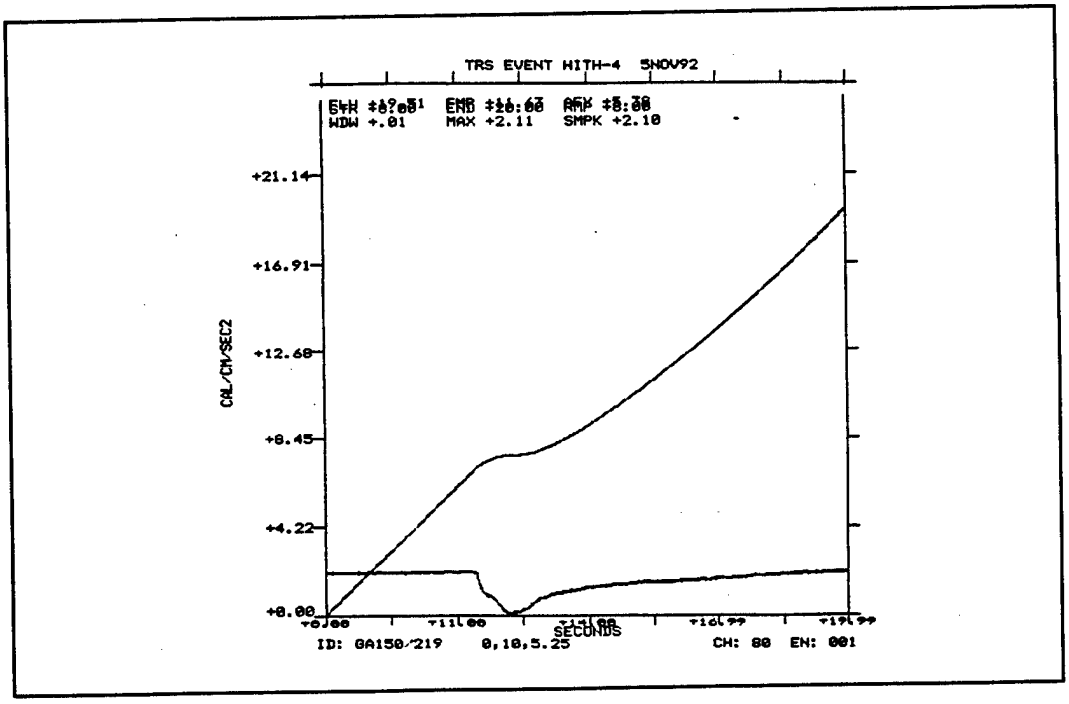

Figure D-1. Test TRS-HITH-4, Medtherm calorimeter at (0, 10, 5.25).

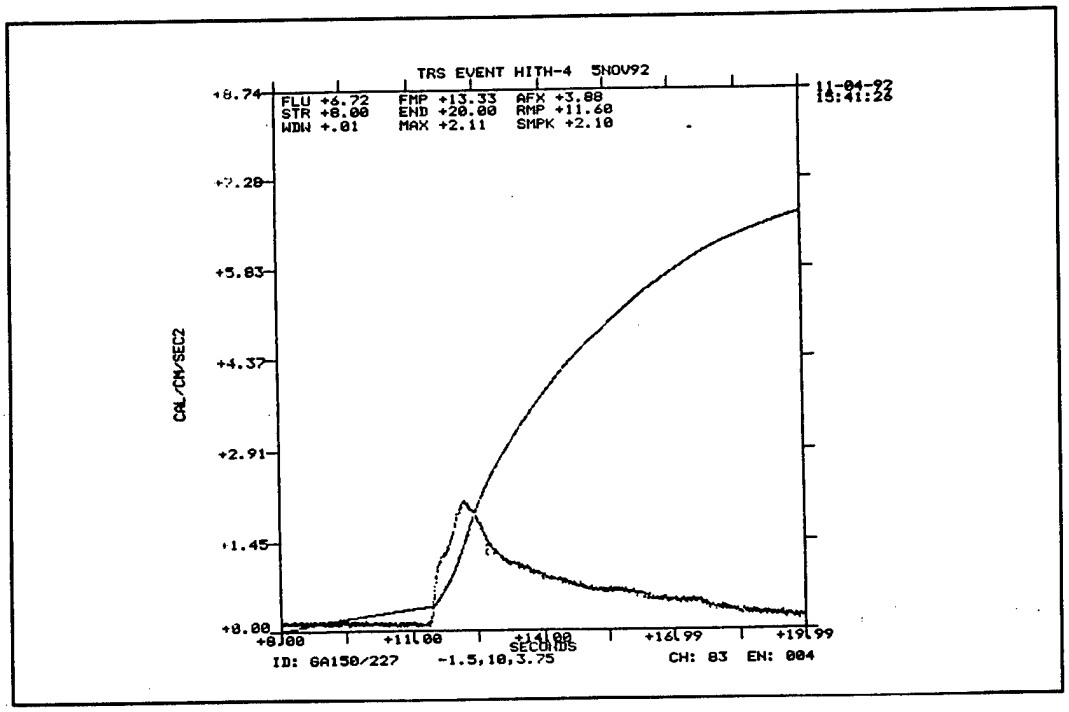

Figure D-2. Test TRS-HITH-4, Medtherm calorimeter at (0, 10, 3.75).

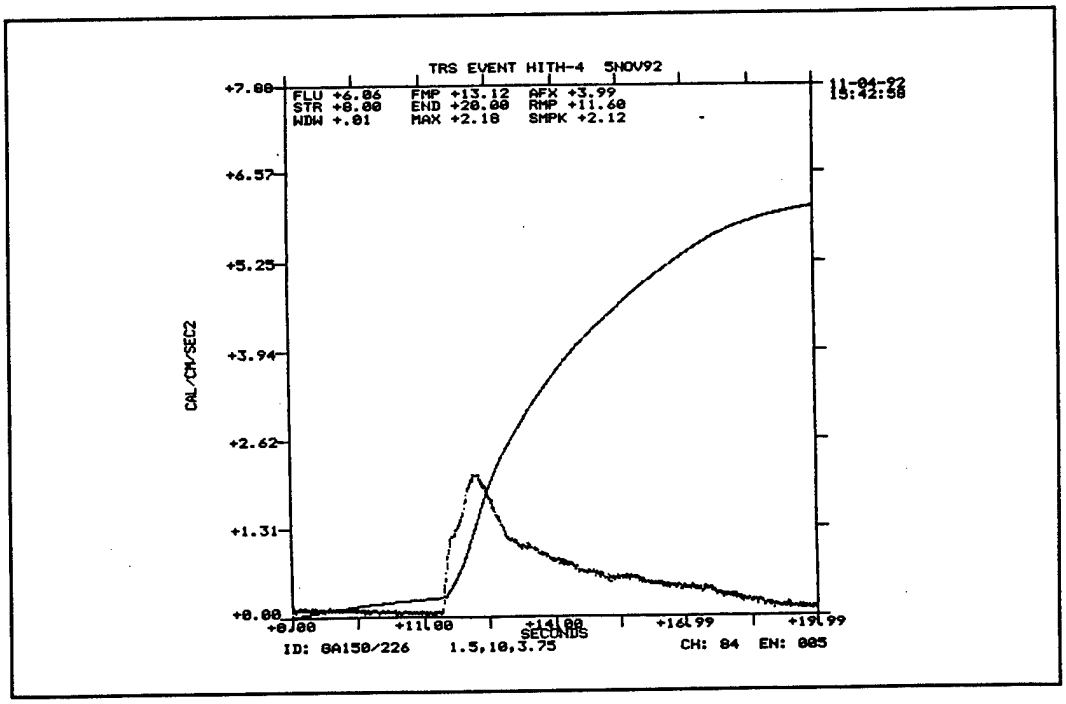

Figure D-3. Test TRS-HITH-4, Medtherm calorimeter at (0, 10, 2.75).

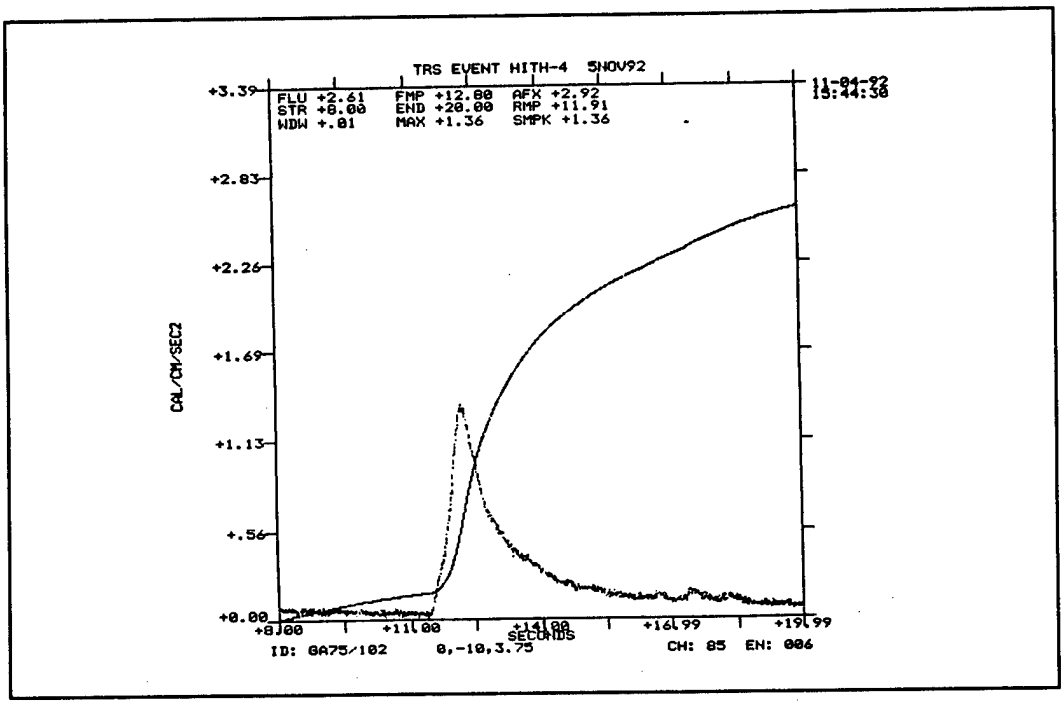

Figure D-4. Test TRS-HITH-4, Medtherm calorimeter at (-1.5, 10, 3.75).

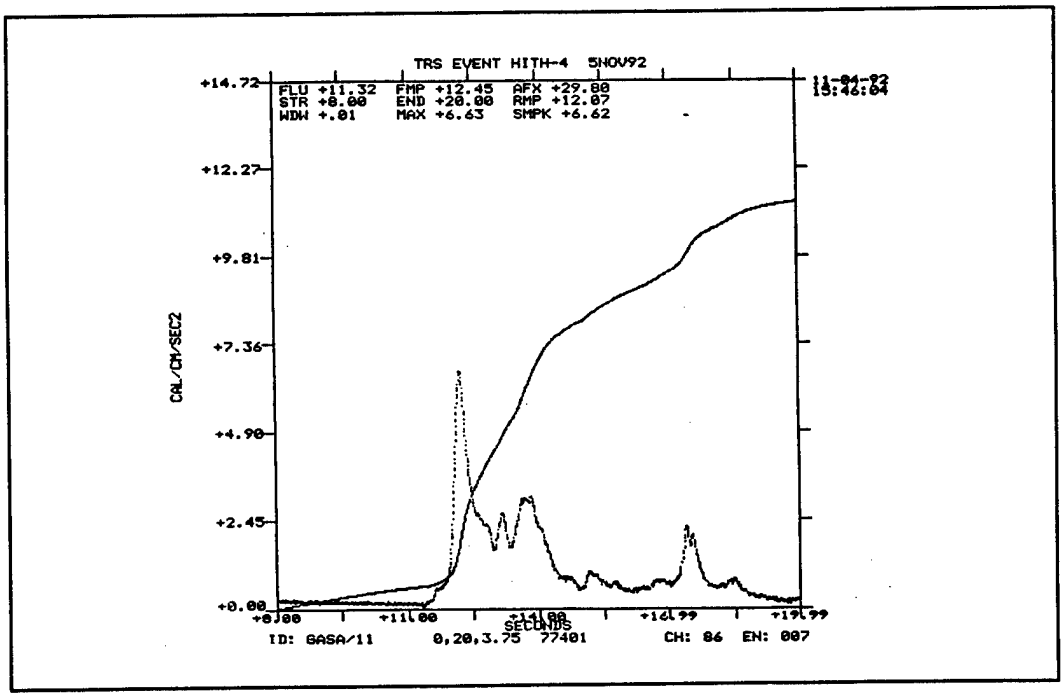

Figure D-5. Test TRS-HITH-4, Medtherm calorimeter at (1.5, 10, 3.75).

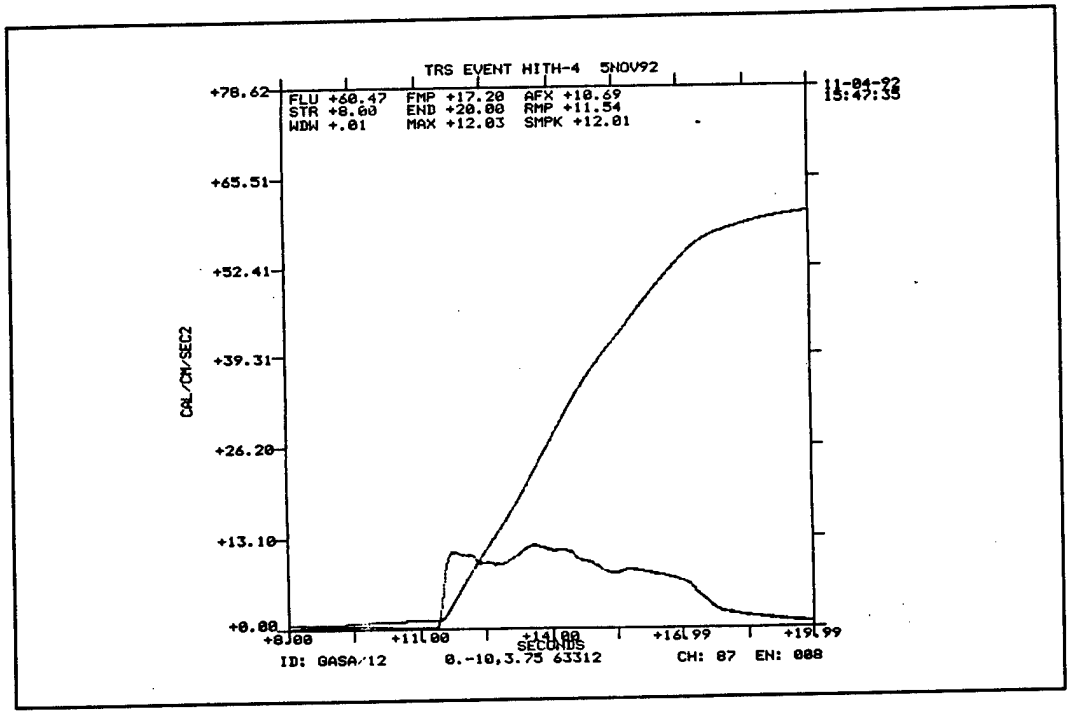

Figure D-6. Test TRS-HITH-4, Medtherm calorimeter at (0, 10, 3.75).

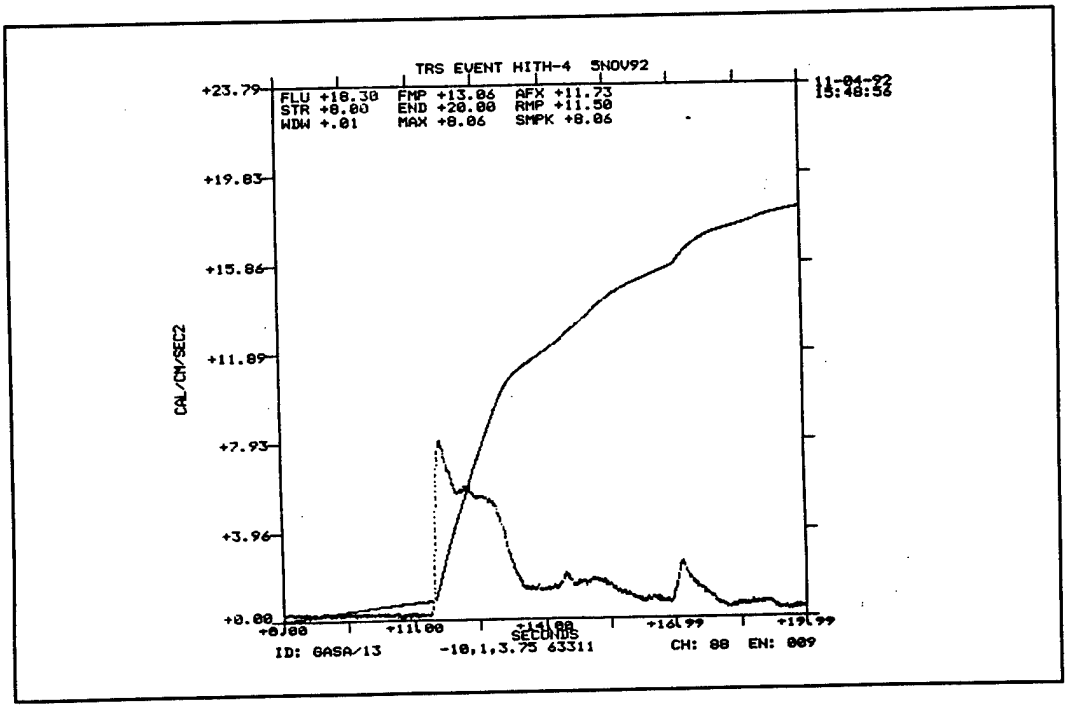

Figure D-7. Test TRS-HITH-4, radiometer at (0, 20, 3.75).

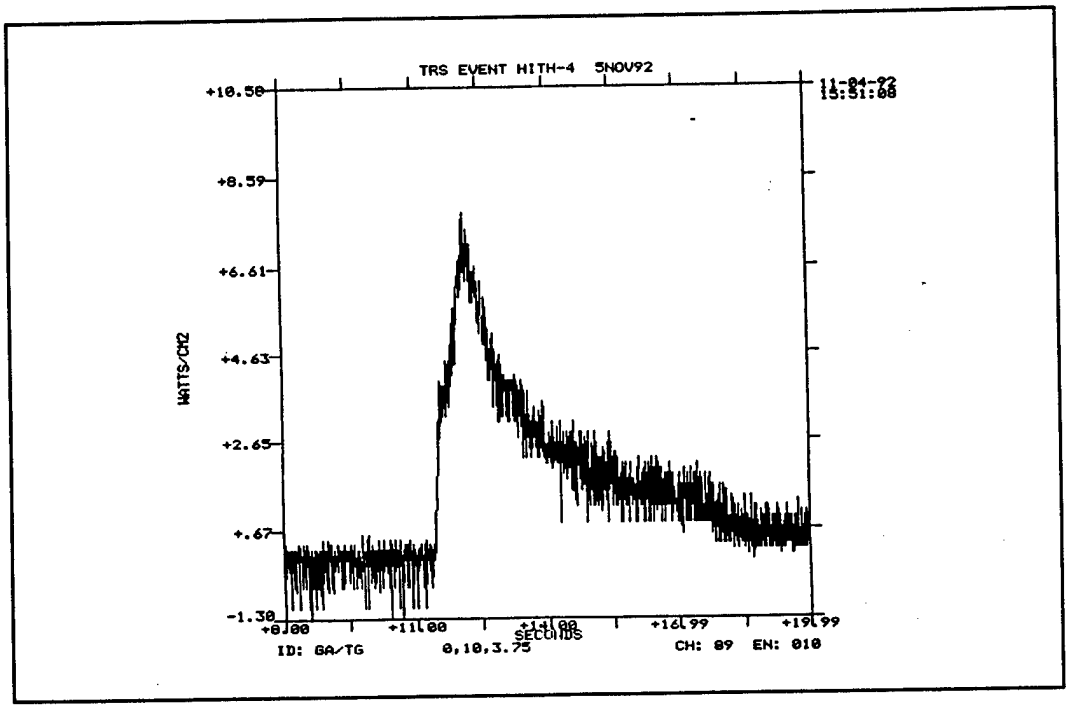

Figure D-8. Test TRS-HITH-4, radiometer at (0, -10, 3.75).

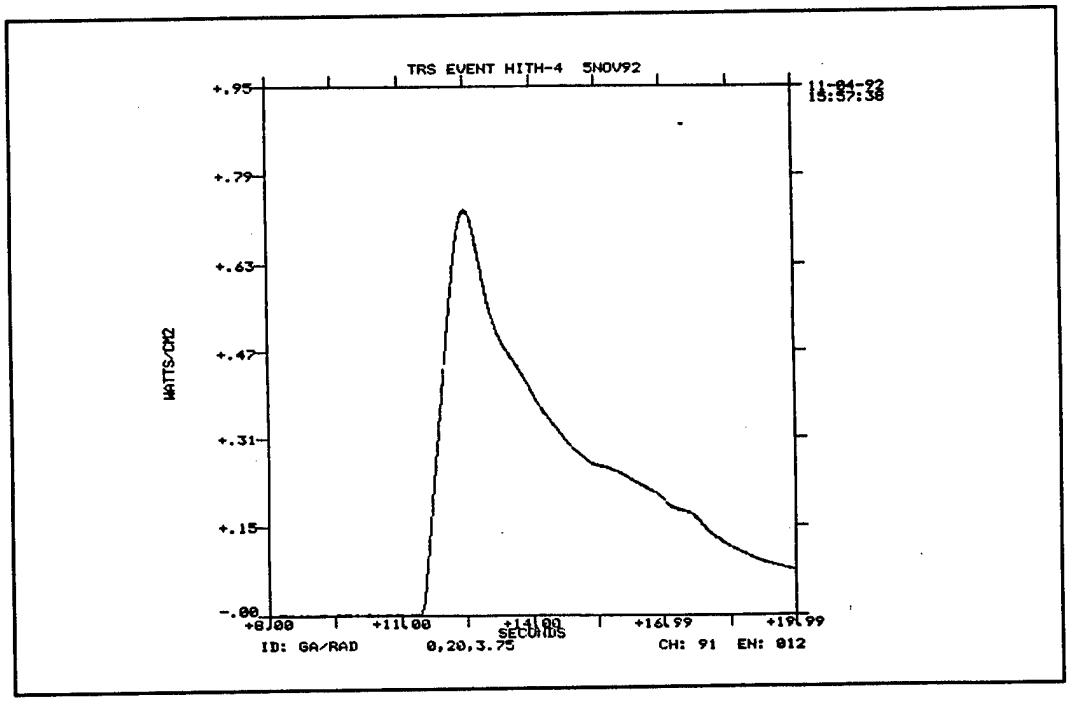

Figure D-9. Test TRS-HITH-4, radiometer at (-10, 1, 3.75).

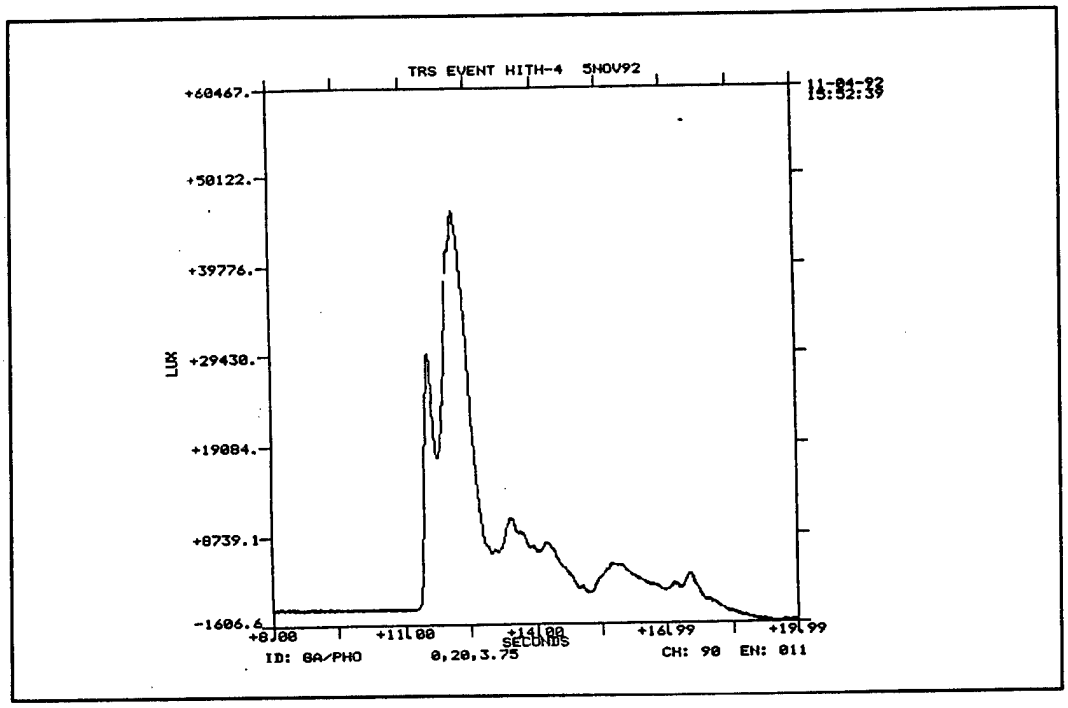

Figure D-10. Test TRS-HITH-4, GSI Thermogauge at (0, 10, 3.75).

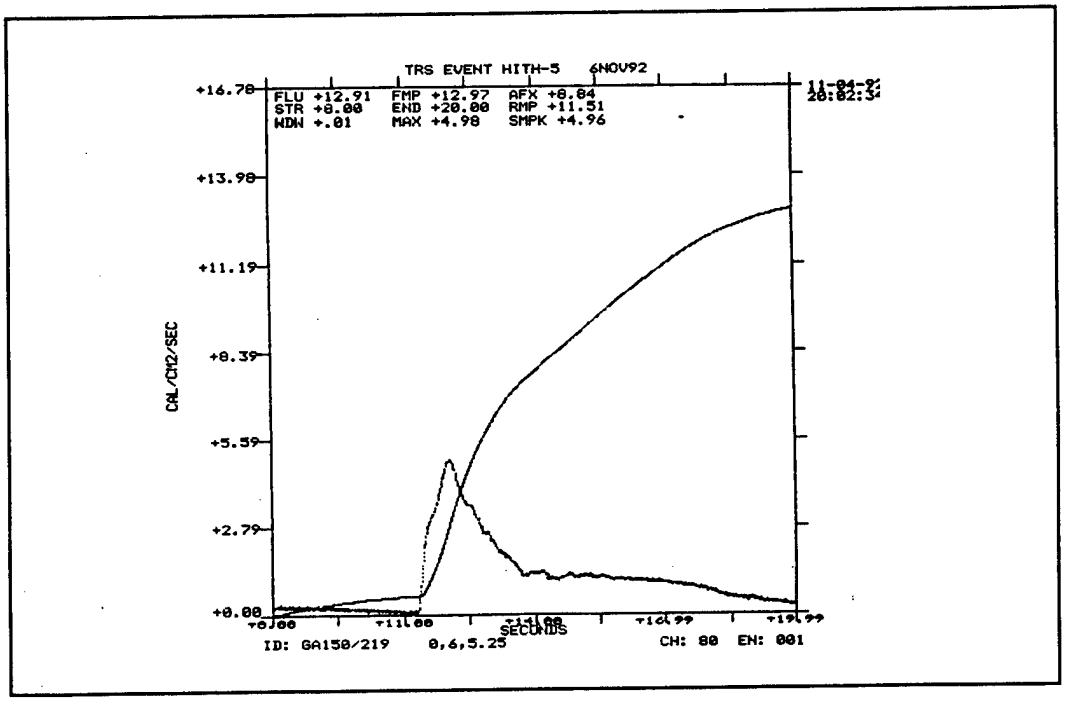

Figure D-11. Test TRS-HITH-4, GSI light probe at (0, 20, 3.75).

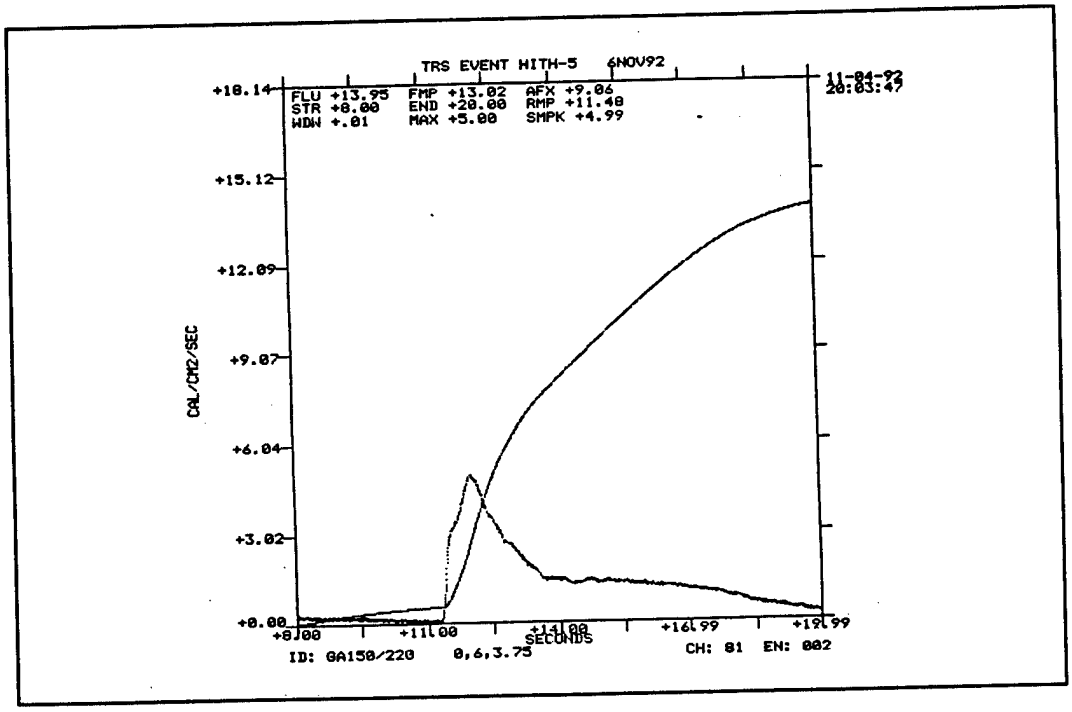

Figure D-12. Test TRS-HIHT-4, GSI radiometer at (0, 20, 3.75).

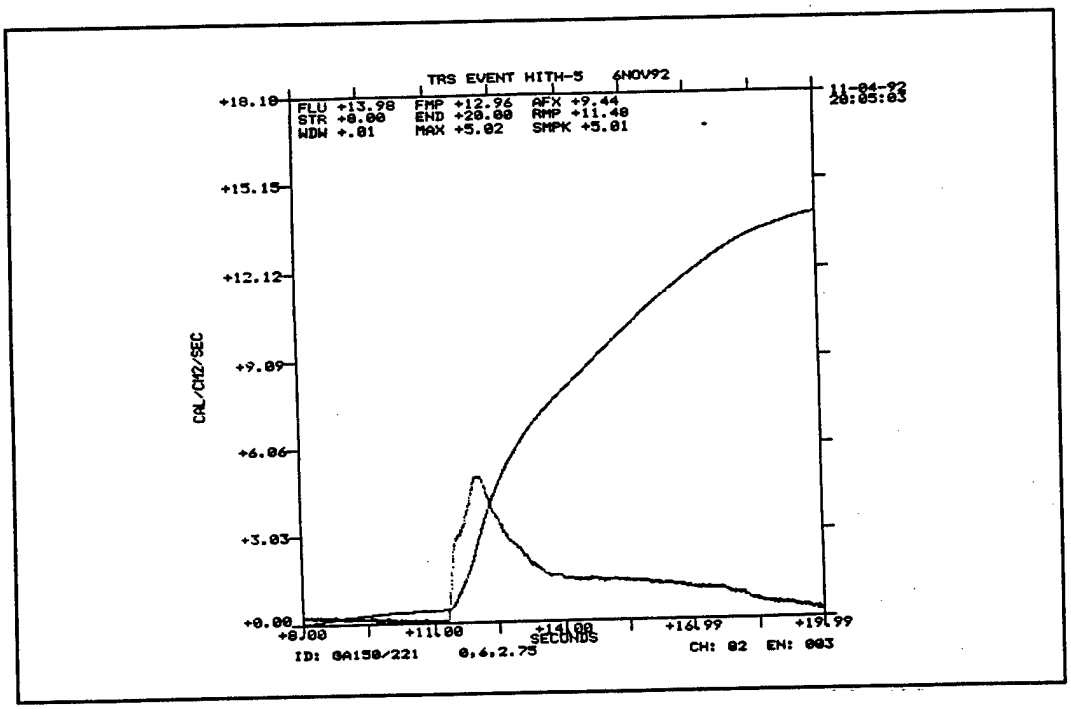

Figure D-13. Test TRS-HITH-5, Medtherm calorimeter at (0, 6, 5.25).

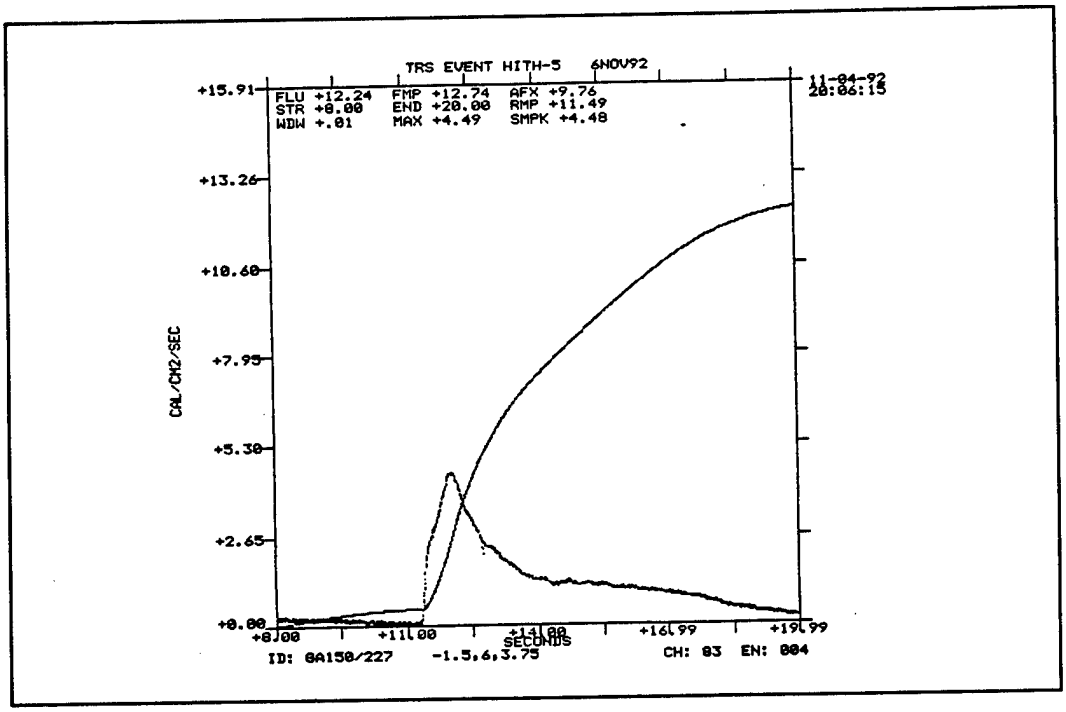

Figure D-14. Test TRS-HITH-5, Medtherm calorimeter at (0, 6, 3.75).

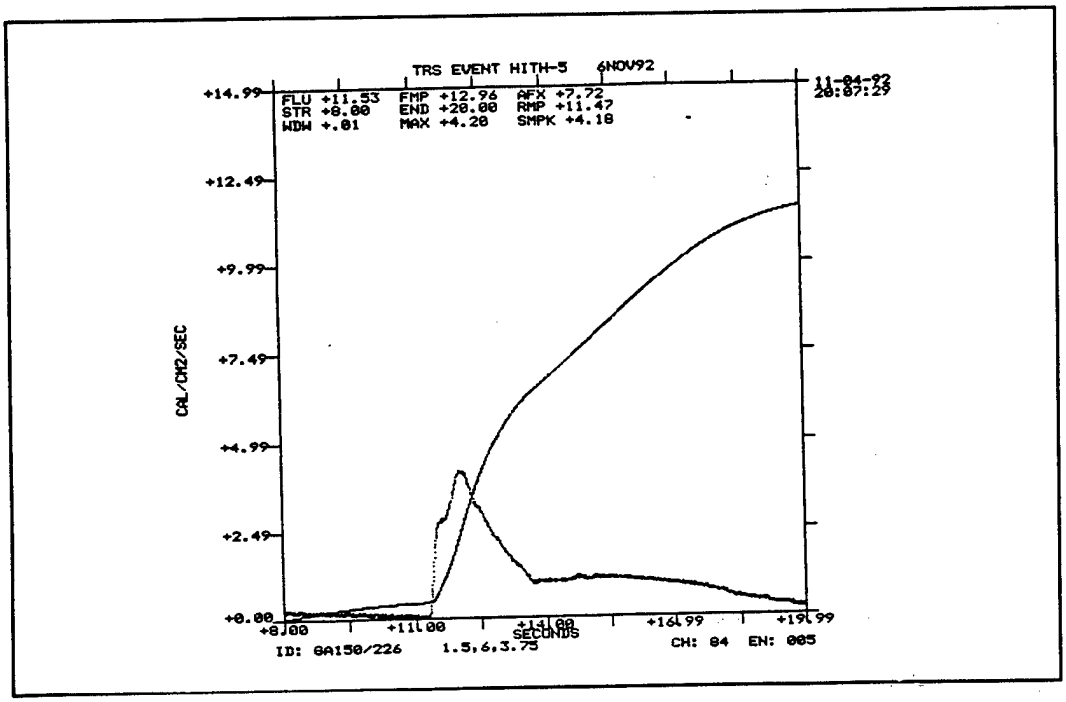

Figure D-15. Test TRS-HITH-5, Medtherm calorimeter at (0, 6, 2.75).

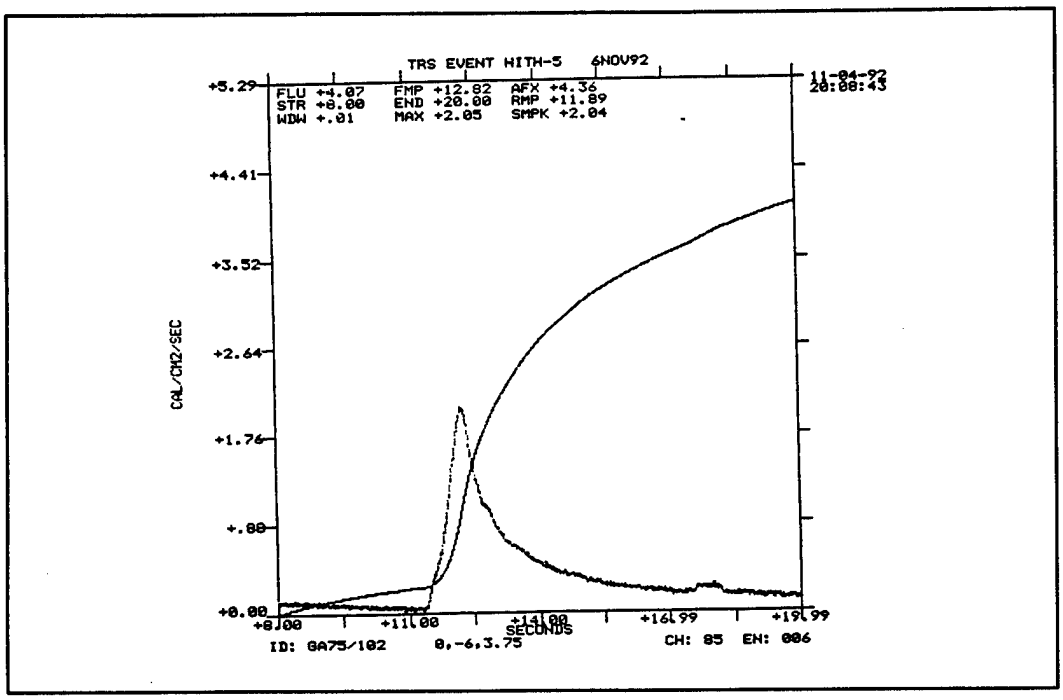

Figure D-16. Test TRS-HITH-5, Medtherm calorimeter at (-1.5, 6, 3.75).

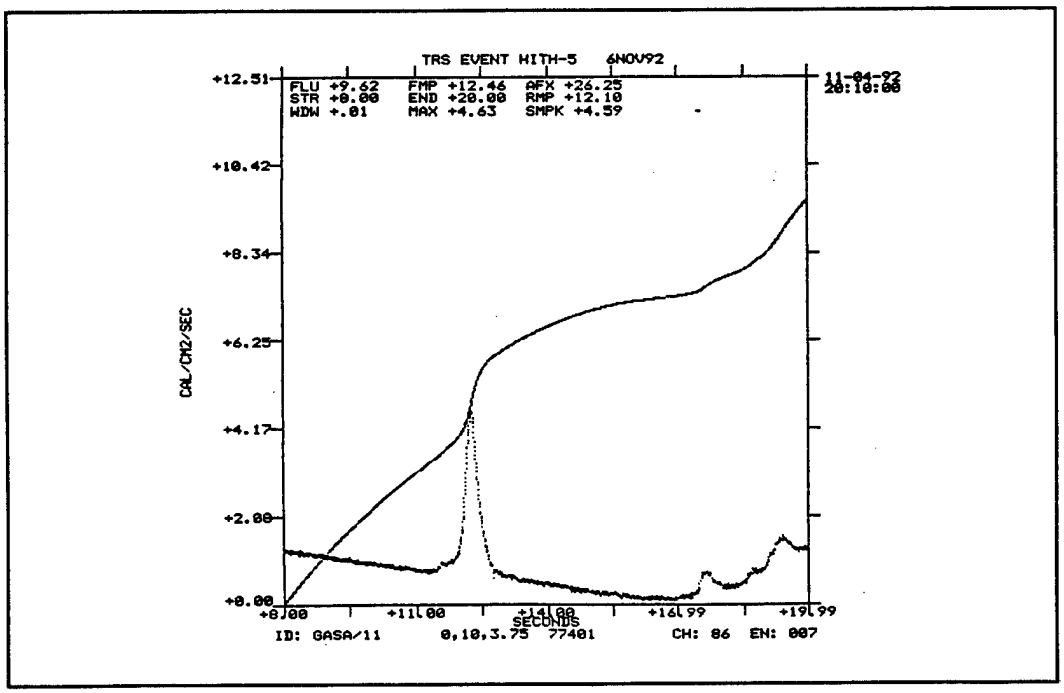

Figure D-17. Test TRS-HITH-5, Medtherm calorimeter at (1.5, 6, 3.75).

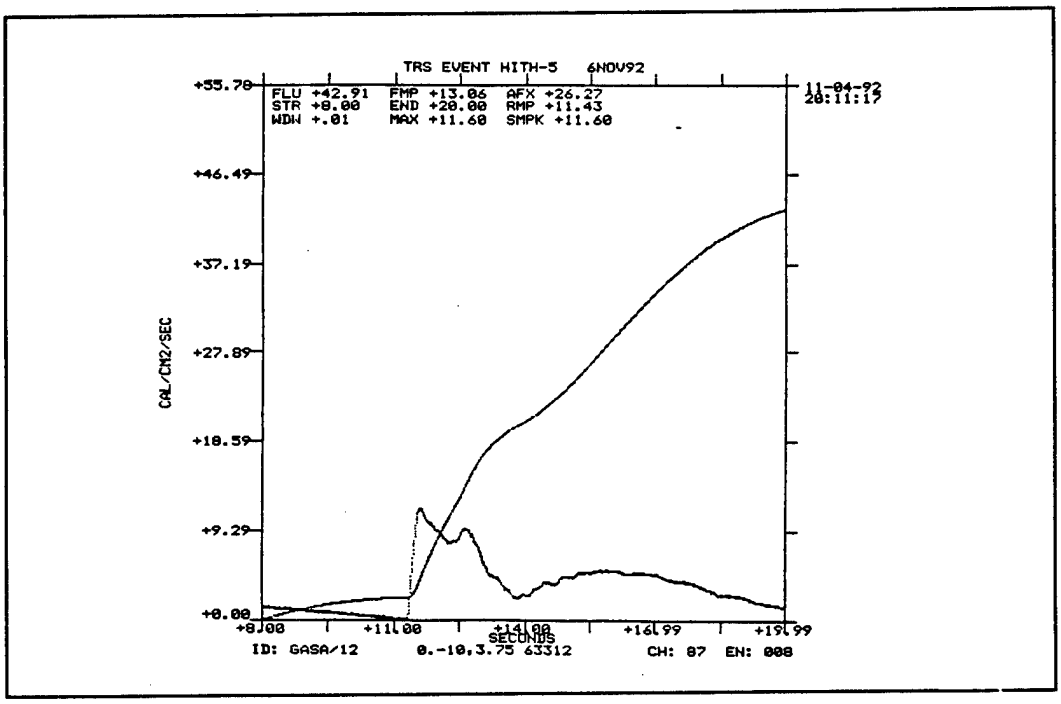

Figure D-18. Test TRS-HITH-5, Medtherm calorimeter at (0, 6, 3.75).

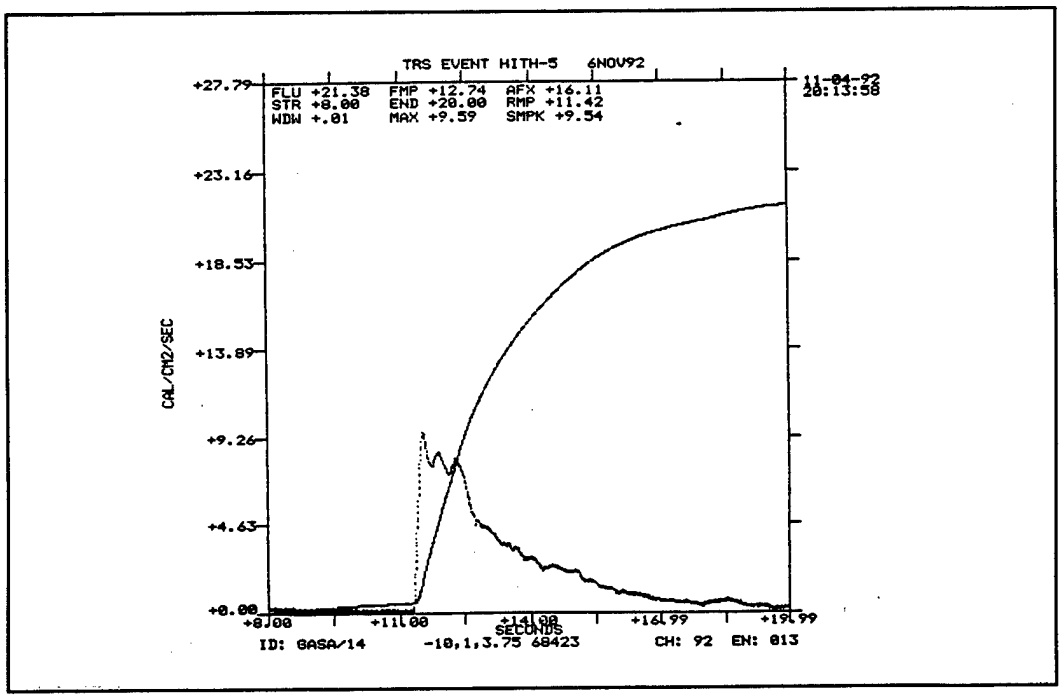

Figure D-19. Test TRS-HITH-5, radiometer at (0, 10, 3.75).

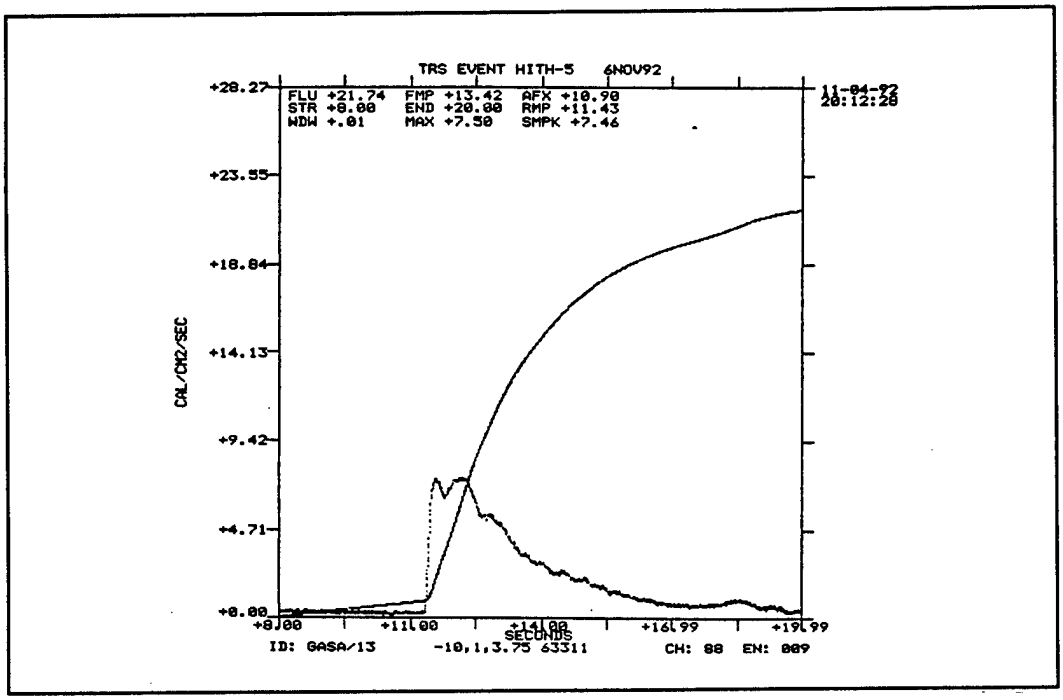

Figure D-20. Test TRS-HITH-5, radiometer at (0, -10, 3.75).

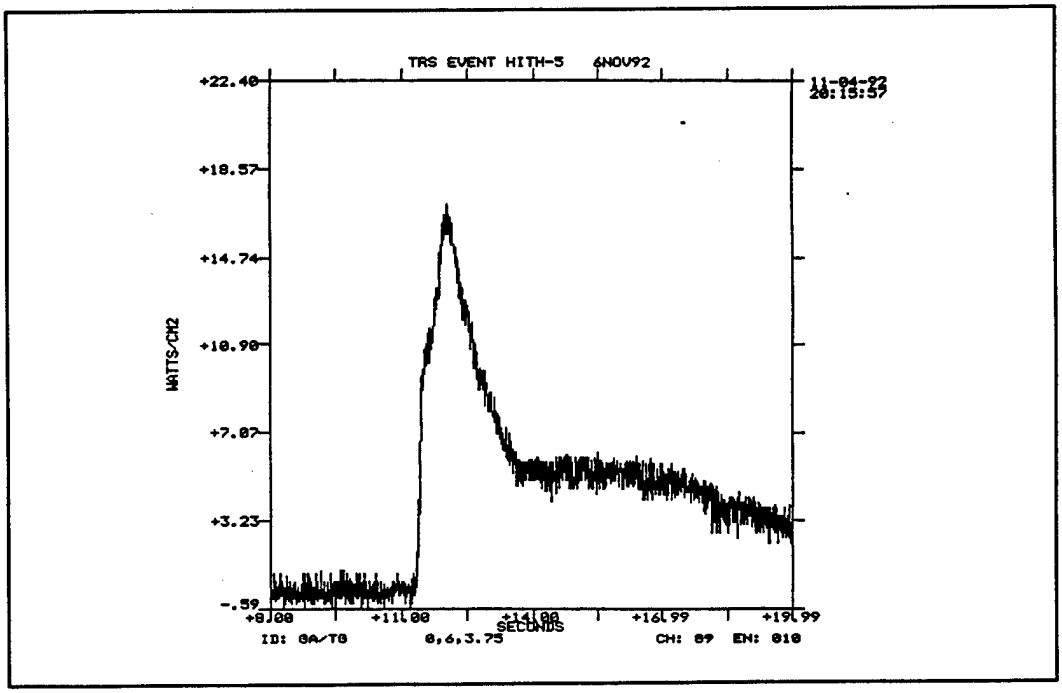

Figure D-21. Test TRS-HITH-5, radiometer at (-10, 1, 3.75).

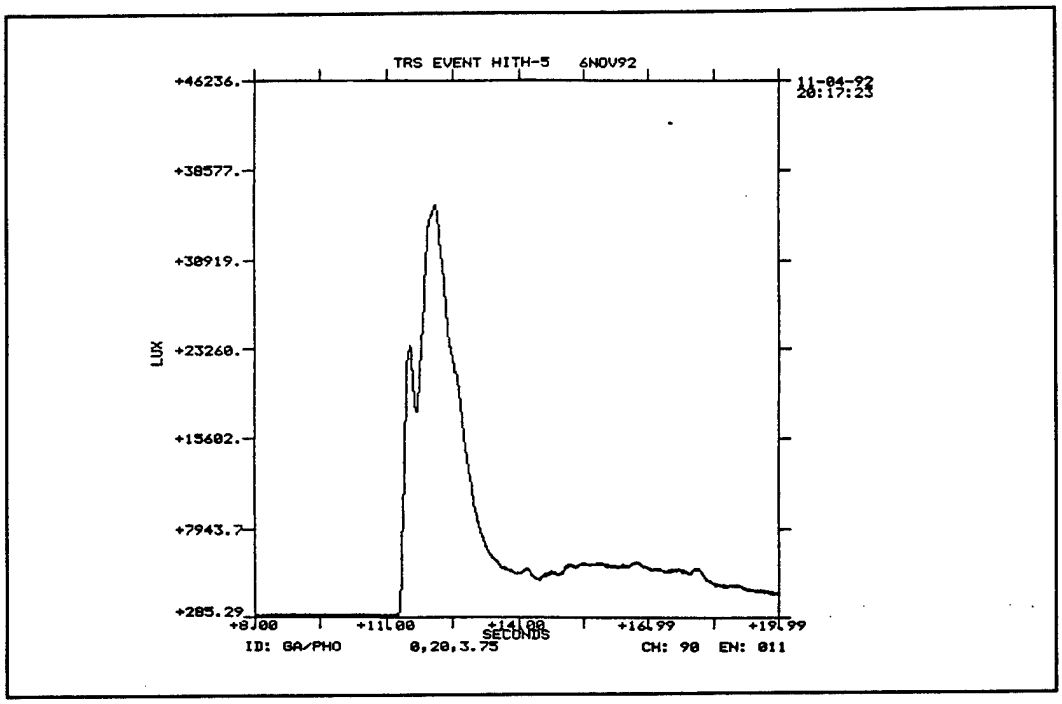

Figure D-22. Test TRS-HITH-5, radiometer at (-10, 1, 3.75).

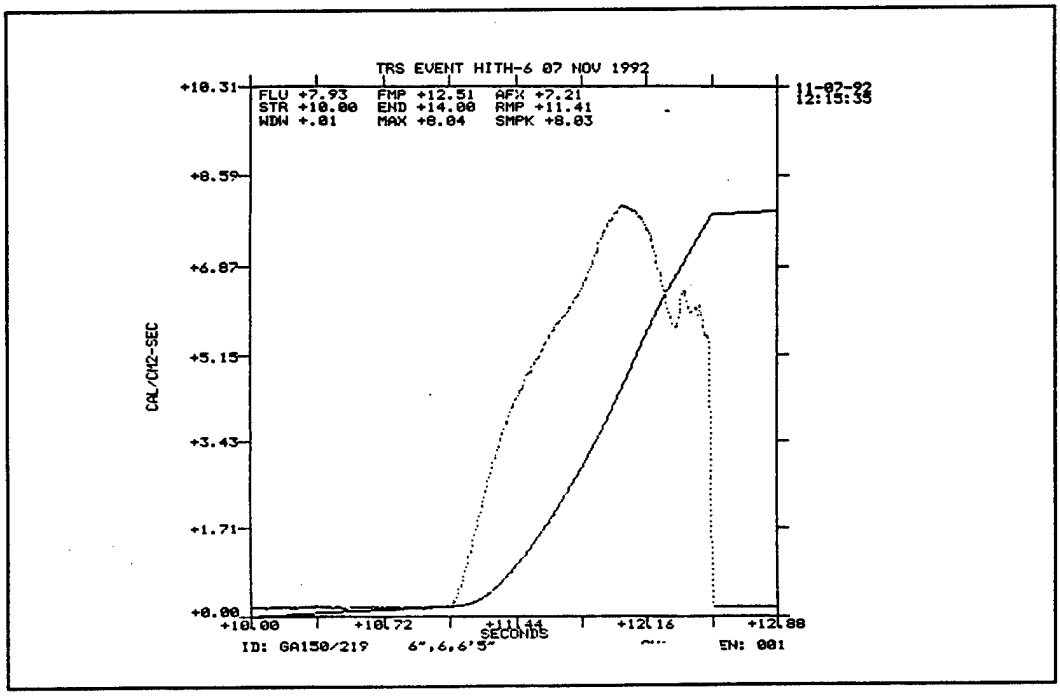

Figure D-23. Test TRS-HITH-5, GSI Thermogauge at (0, 6, 3.75).

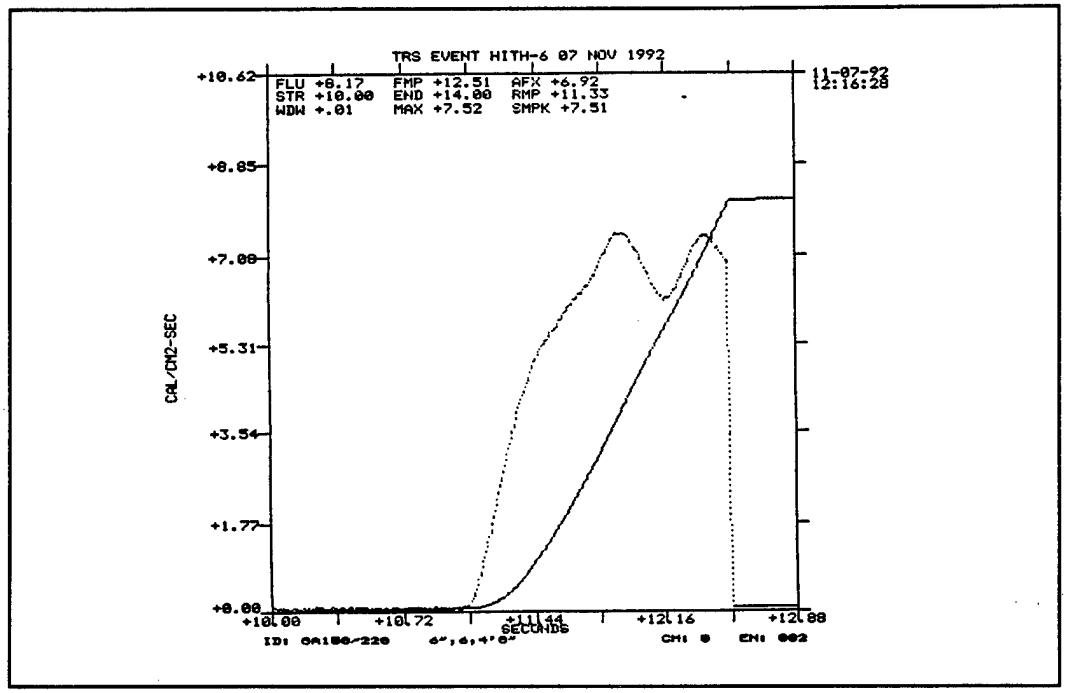

Figure D-24. Test TRS-HITH-5, GSI light probe at (0, 20, 3.75).

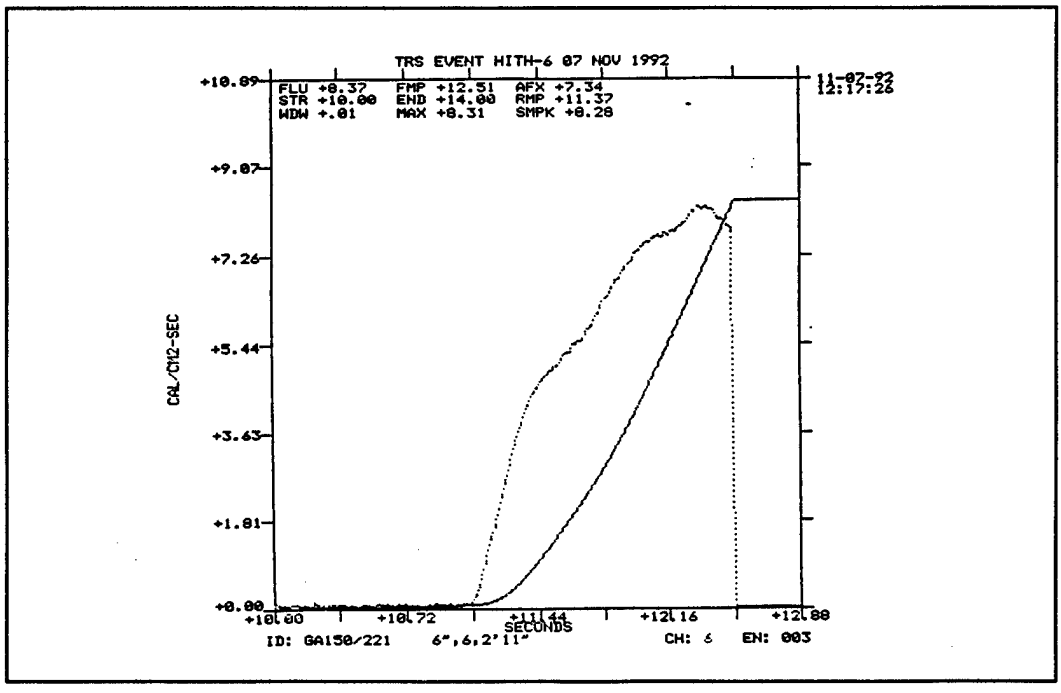

Figure D-25. Test TRS-HITH-6, Medtherm calorimeter at (0.5, 6, 6.5).

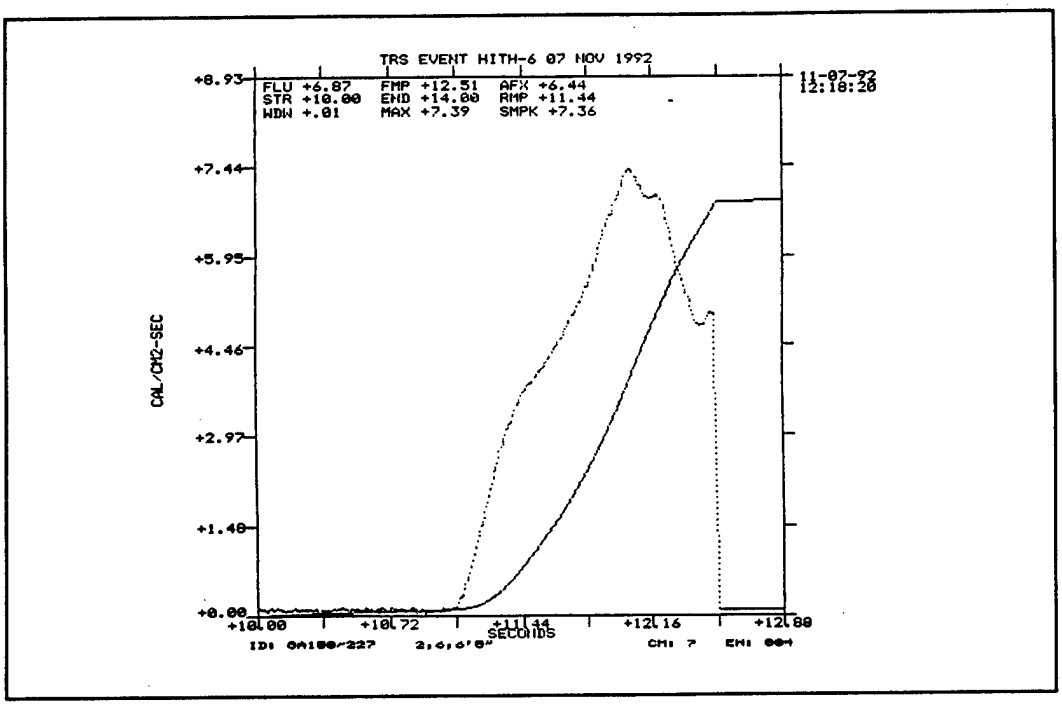

Figure D-26. Test TRS-HITH-6, Medtherm calorimeter at (0.5, 6, 4.5).

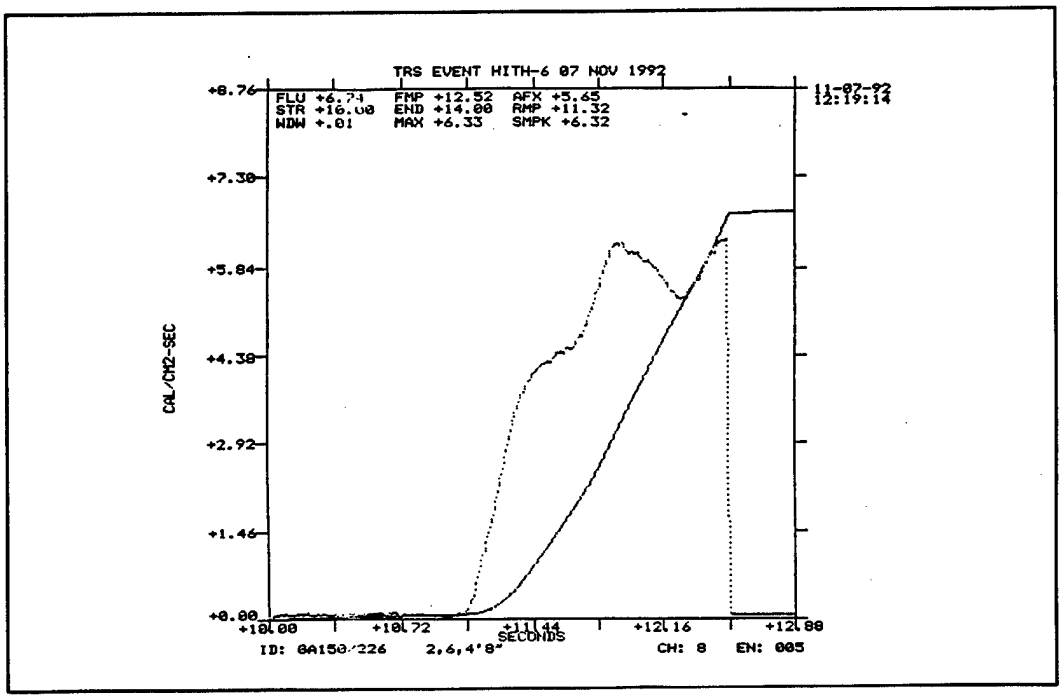

Figure D-27. Test TRS-HITH-6, Medtherm calorimeter at (0.5, 6, 2.9).

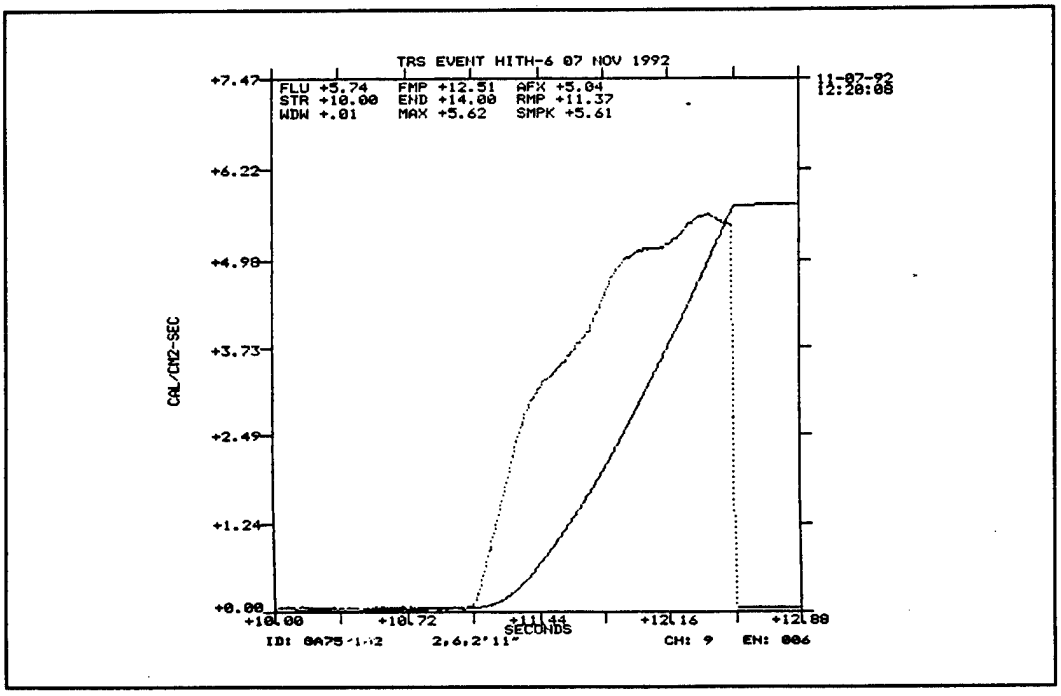

Figure D-28. Test TRS-HITH-6, Medtherm calorimeter at (2, 6, 6.4).

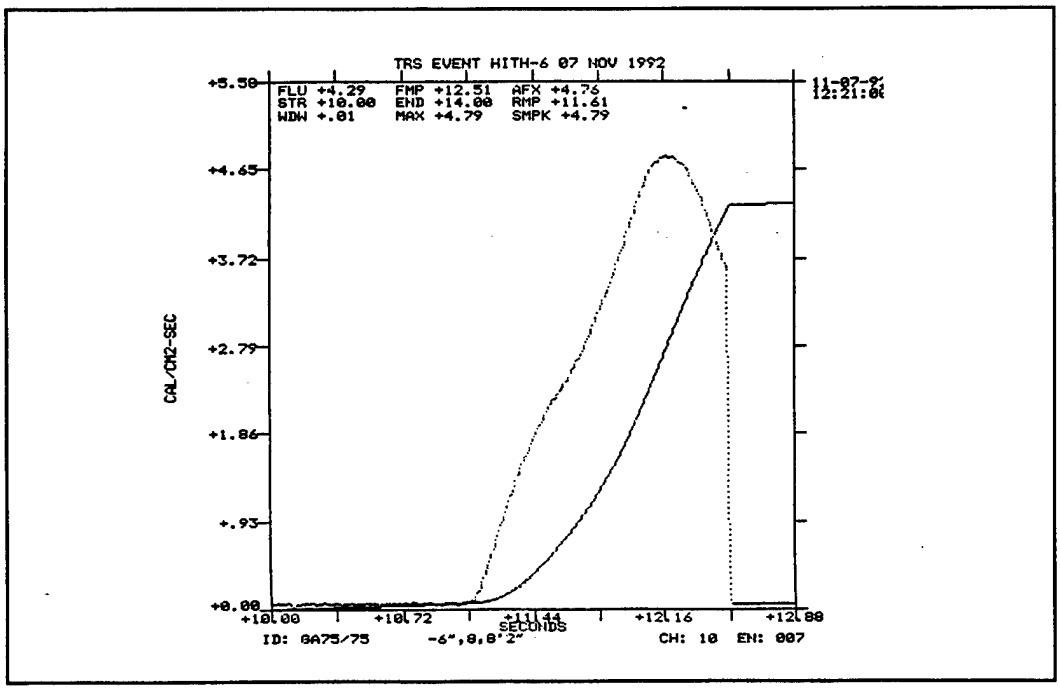

Figure D-29. Test TRS-HITH-6, Medtherm calorimeter at (2, 6, 4.7).

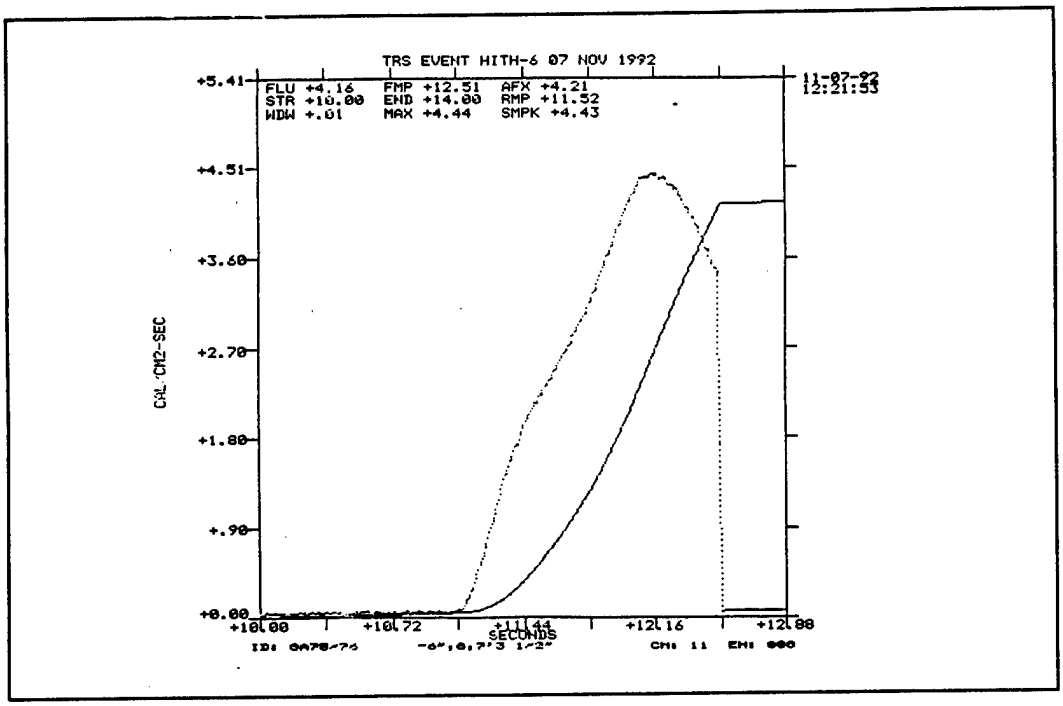

Figure D-30. Test TRS-HITH-6, Medtherm calorimeter at (2, 6, 2.9).

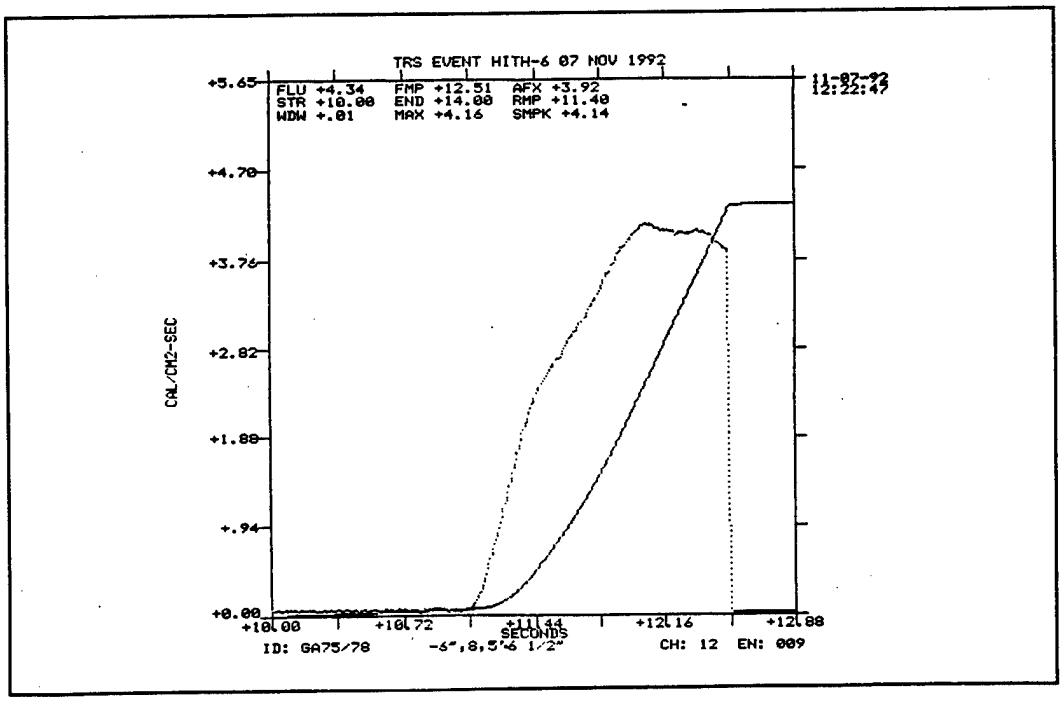

Figure D-31. Test TRS-HITH-6, Medtherm calorimeter at (-0.5, 8, 8.2).

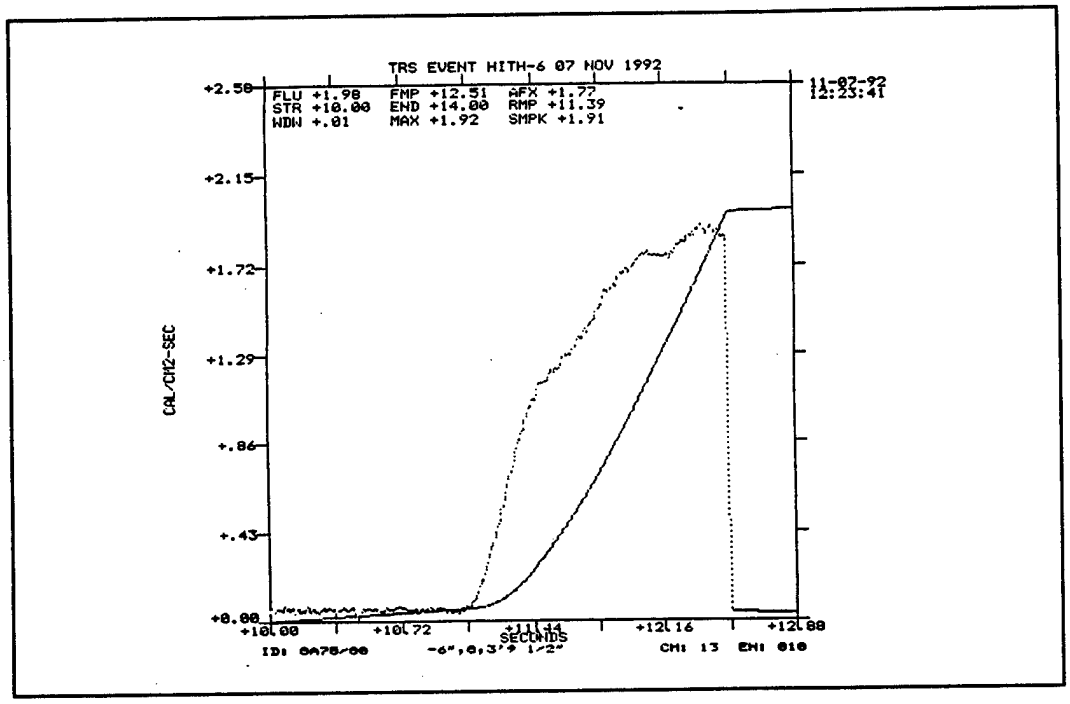

Figure D-32. Test TRS-HITH-6, Medtherm calorimeter at (-0.5, 8, 7.25).

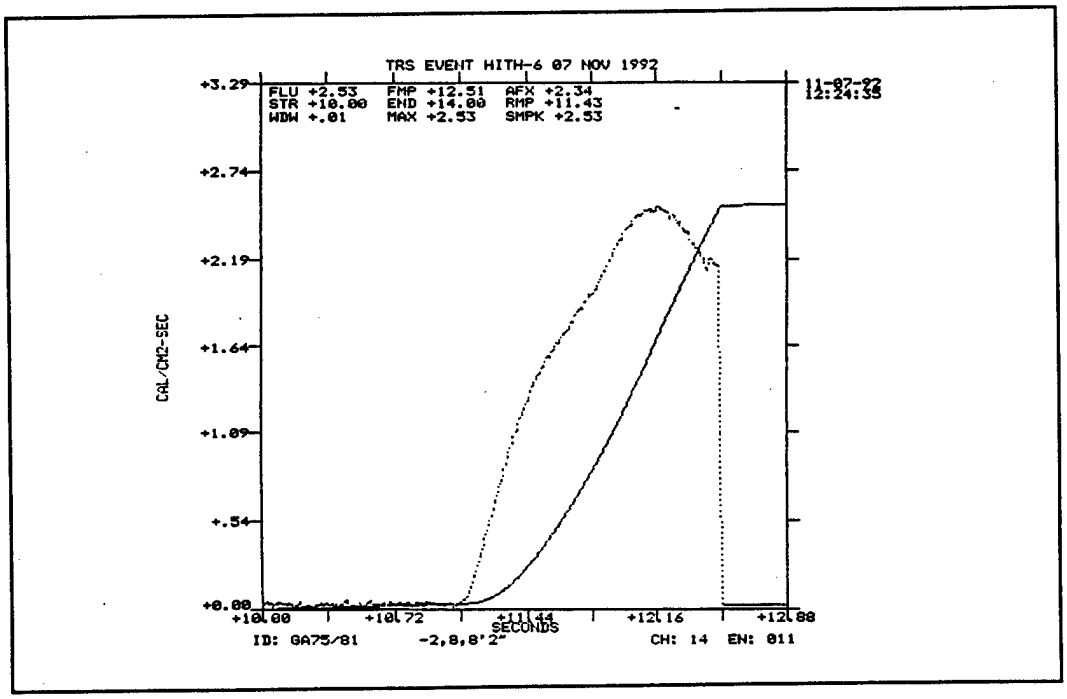

Figure D-33. Test TRS-HITH-6, Medtherm calorimeter at (-0.5, 8, 3.75).

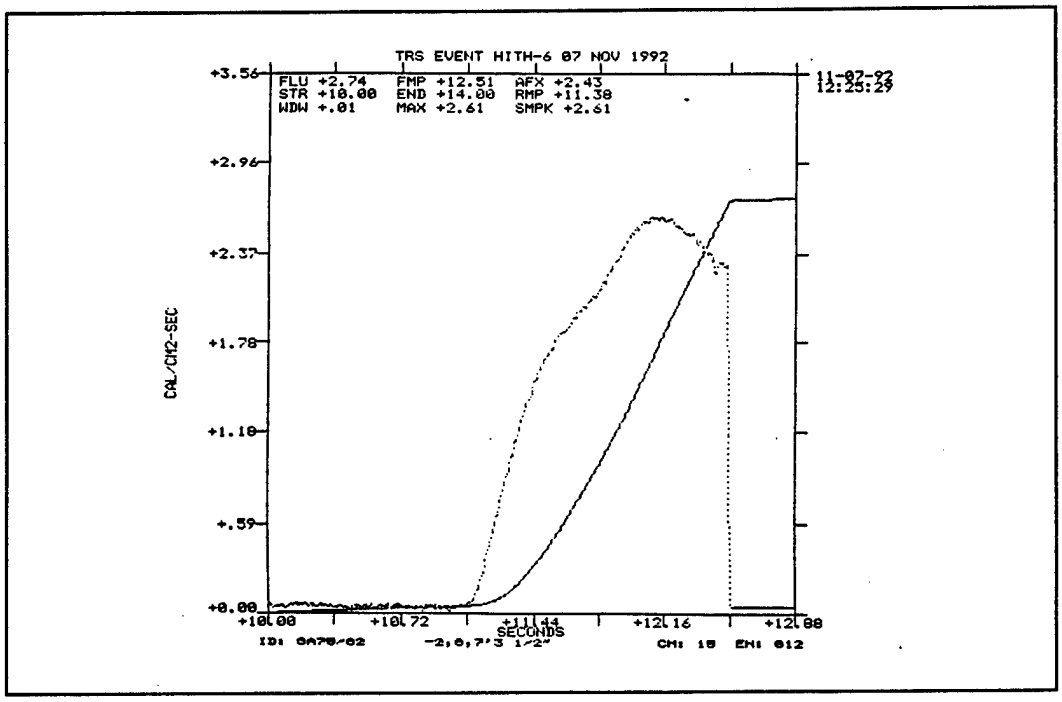

Figure D-34. Test TRS-HITH-6, Medtherm calorimeter at (-0.5, 8, 3.75).

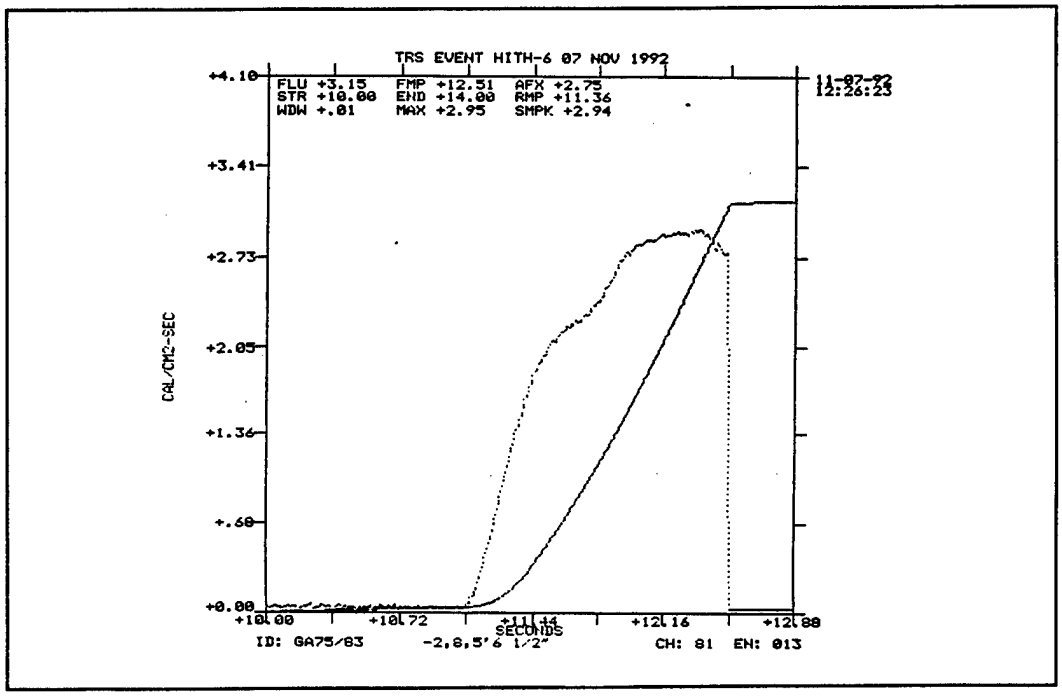

Figure D-35. Test TRS-HITH-6, Medtherm calorimeter at (-2, 8, 8.2).

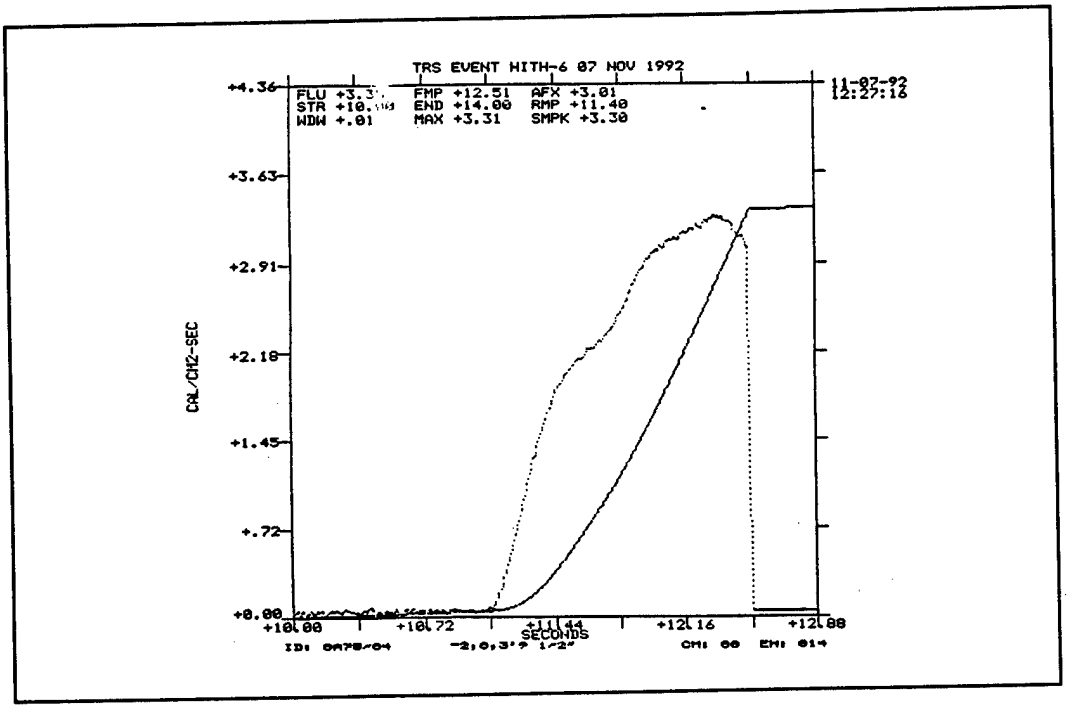

Figure D-36. Test TRS-HITH-6, Medtherm calorimeter at (-2, 6, 7.25).

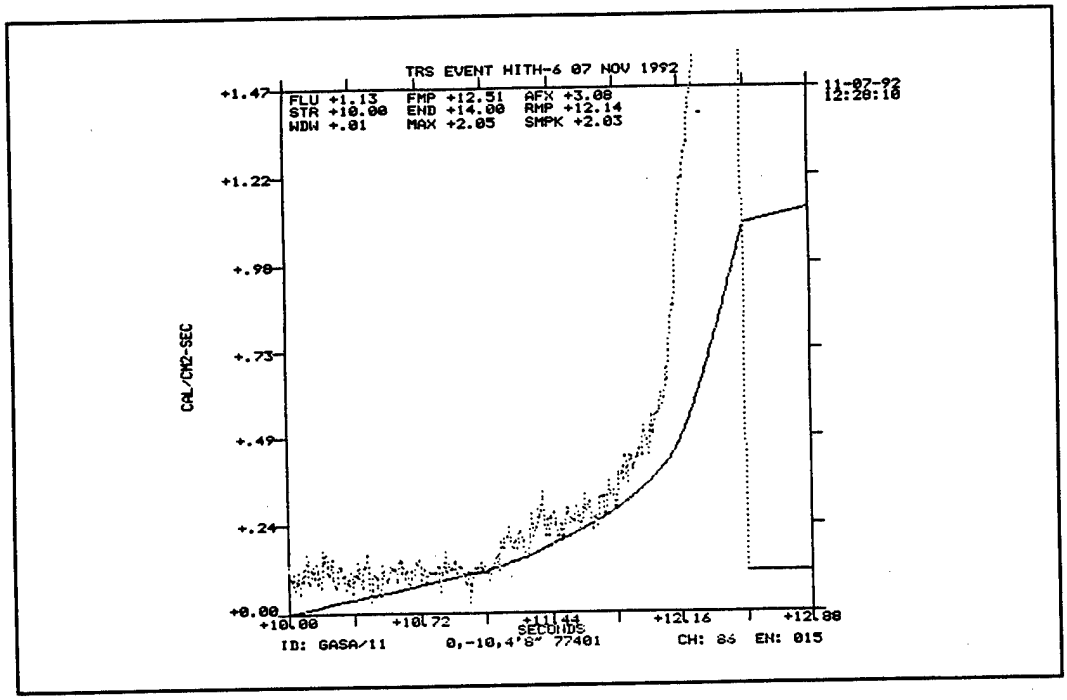

Figure D-37. Test TRS-HITH-6, Medtherm calorimeter at (-2, 8, 5.5).

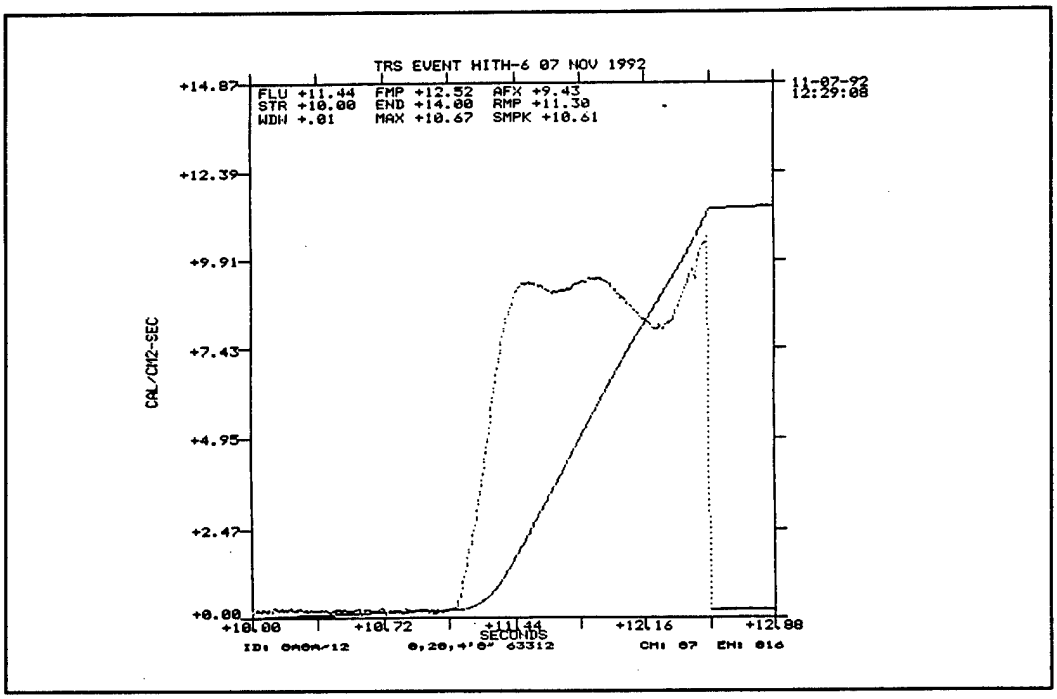

Figure D-38. Test TRS-HITH-6, Medtherm calorimeter at (-2, 8, 3.5).

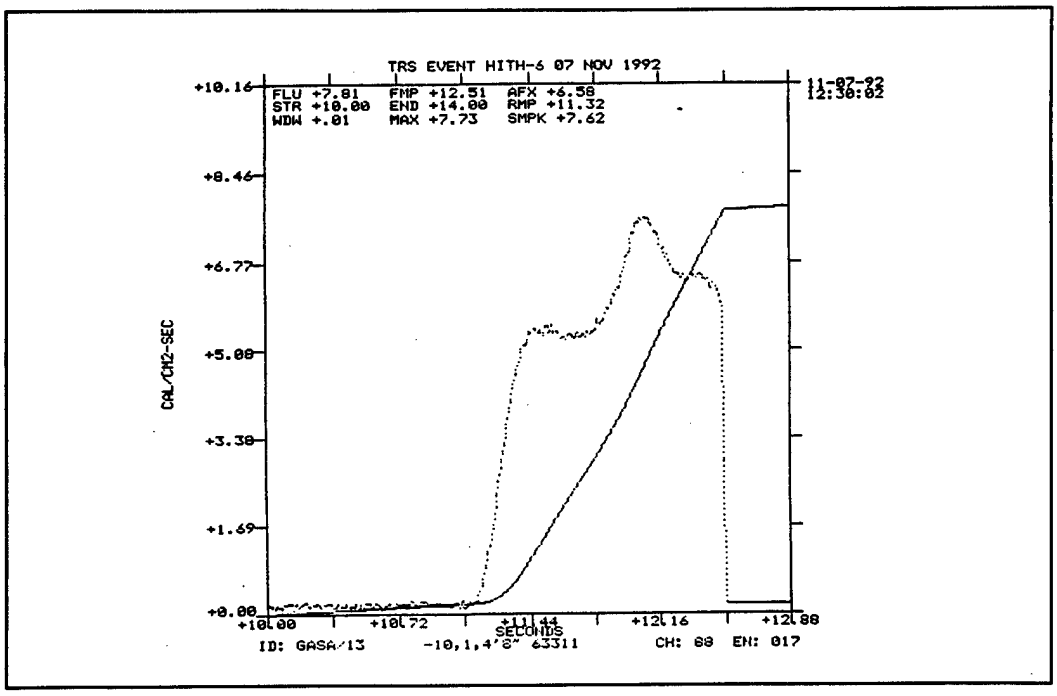

Figure D-39. Test TRS-HITH-6, radiometer at (-10, 1, 4.7).

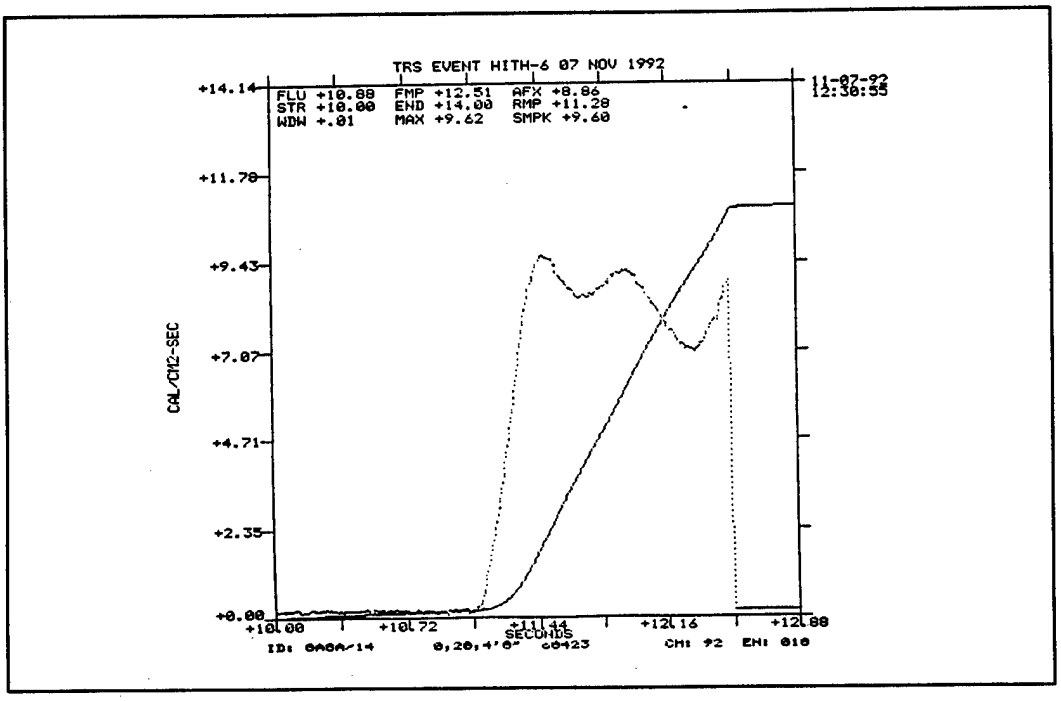

Figure D-40. Test TRS-HITH-6, radiometer at (0, 20, 4.7).

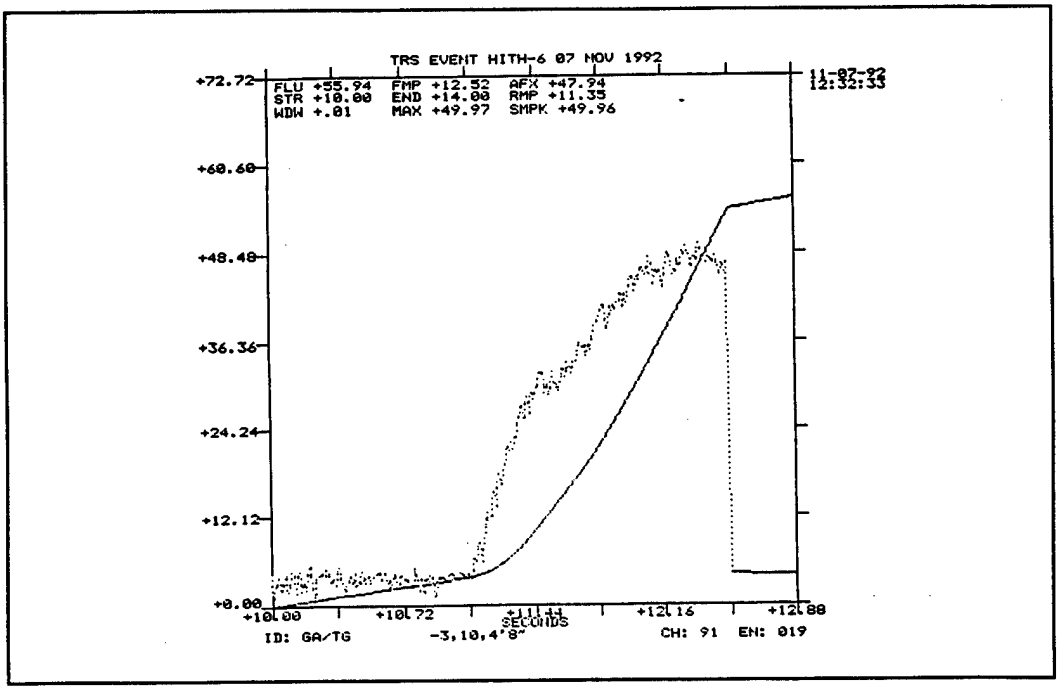

Figure D-41. Test TRS-HITH-6, GSI Thermogauge at (-3, 10, 4.7).

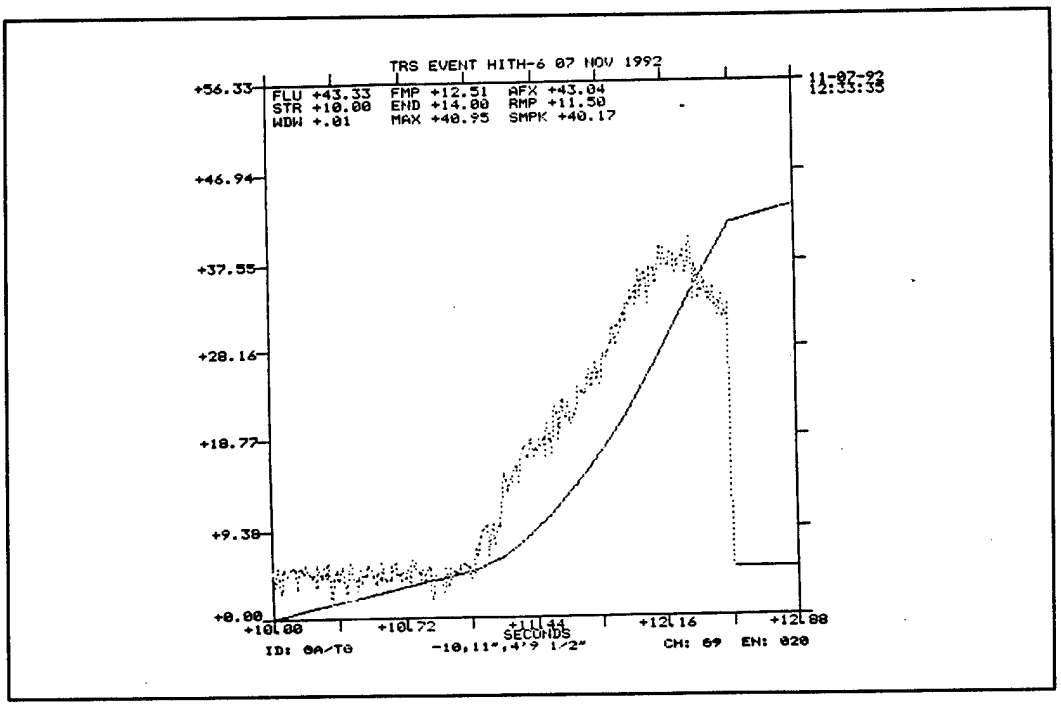

Figure D-42. Test TRS-HITH-6, GSI Thermogauge at (-10, 1, 4.7).

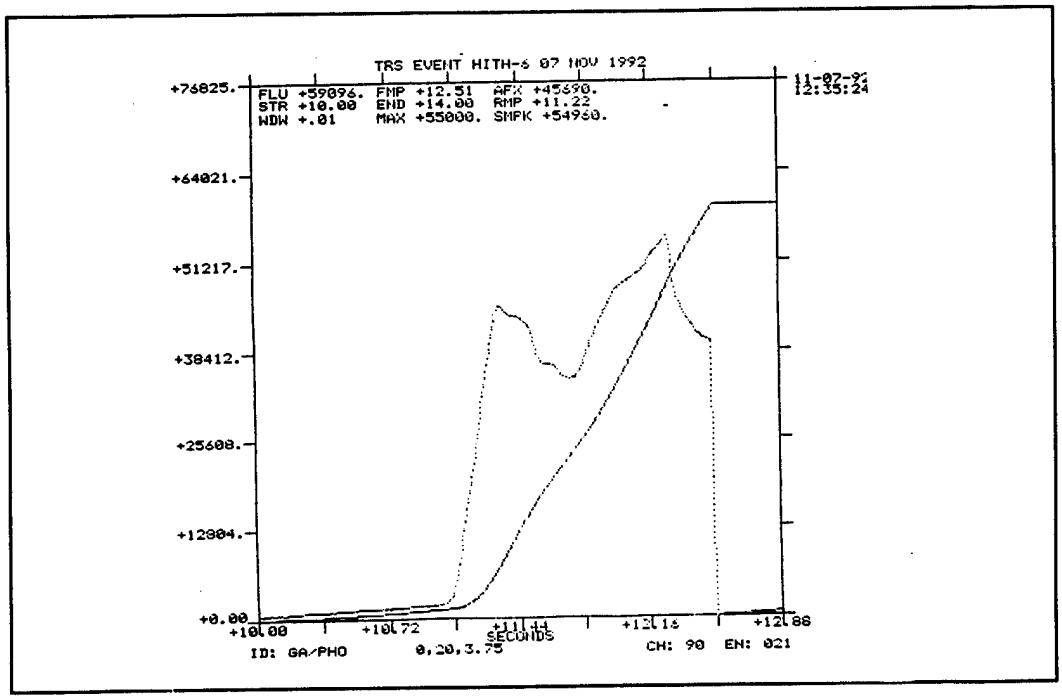

Figure D-43. Test TRS-HITH-6, GSI light probe at (0, 20, 3.75).

DISTRIBUTION LIST
DSWA TR-94-113-REV

DEPARTMENT OF DEFENSE

DEFENSE INTELLIGENCE AGENCY
ATTN: OGA-4B2
ATTN: TWJ

DEFENSE SPECIAL WEAPONS AGENCY
4 CY ATTN: ESA, LTC O'SHAUSNESSY
ATTN: ESA, W SUMMA
ATTN: EST, K WARE
2 CY ATTN: TRC
ATTN: WE
ATTN: WEL
ATTN: WEP, B PRASAD

DEFENSE TECHNICAL INFORMATION
2 CY ATTN: DTIC/OCP

FC DEFENSE SPECIAL WEAPONS AGENCY
ATTN: FCT-S, G BALADI
ATTN: FCTO
ATTN: FCTOS
ATTN: FCTTS, J JABLONSKY
ATTN: FCTTS, E MARTINEZ

DEPARTMENT OF THE ARMY

ARMY RESEARCH LABORATORIES
ATTN: TECH LIB
ATTN: ANSRL-WT-NB, MARY ABE

DEFENSE ADVANCED RSCH PROJ AGCY
ATTN: PMO

NUCLEAR EFFECTS DIVISION
ATTN: B HAMILTON
ATTN: J OKUMA
ATTN: STEWS-NE, A BRIONES
ATTN: STEWS-TR, R PENNY

U S ARMY COLD REGION RES & ENG LAB
ATTN: TECHNICAL DIRECTOR

U S ARMY ENGR WATERWAYS EXPER STATION
ATTN: CEWES-SE-R, D RICKMAN
ATTN: CEWES-SD-R, J WINDHAM
ATTN: TECHNICAL LIBRARY

U S ARMY NATIONAL GROUND INTL CTR
ATTN: IAFSTC-RMT

U S ARMY NUCLEAR & CHEMICAL AGENCY
ATTN: B PFEFFER
ATTN: G LONG

U S ARMY RESEARCH LAB
ATTN: AMSRL-SL-CM, E FIORAVANTE
ATTN: AMSRL-WT-NC, R LOCKS
ATTN: AMSRL-WT-NC, R LOTTERO
ATTN: AMSRL-WT-NC, C MERMAGAN
ATTN: AMSRL-WT-NC, STEPHEN J SCHRAML
ATTN: SLCBR-SS-T, TECH LIB
ATTN: SLCBR-TBD-B, R PEARSON

U S ARMY SPACE STRATEGIC DEFENSE CMD
ATTN: CSSD-CS
ATTN: CSSD-SA-E

U S ARMY TRADOC ANALYSIS CTR
ATTN: ATRC-WSSR

U S ENGINEERING AND SUPPORT CENTER
ATTN: HNDED-CS
ATTN: HNDED-SY

U S ARMY THAAD PROJECT OFFICE
ATTN: CSSD-H-SA

DEPARTMENT OF THE NAVY

DAVID TAYLOR RESEARCH CENTER
ATTN: P POTTER
ATTN: S BARTON

NAVAL RESEARCH LABORATORY
ATTN: CODE 5227, RESEARCH REPORT
ATTN: CODE 6180
ATTN: CODE 6795, JACOB GRUN

NAWC-WD
ATTN: CODE 473320, D HERIGSTAD

NRAD ACTIVITY PACIFIC
ATTN: CODE 250

DEPARTMENT OF THE AIR FORCE

HQ 497 IG/INOT
ATTN: INT

DEPARTMENT OF ENERGY

LOS ALAMOS NATIONAL LABORATORY
ATTN: J FRITT
ATTN: J ZAHRT
ATTN: L BRYANT
ATTN: M THOMPSON
ATTN: REPORT LIBRARY
ATTN: P WHALEN
ATTN: P GINSBERG
ATTN: S S HECKER
ATTN: W BRUNISH

SANDIA NATIONAL LABORATORIES
ATTN: B PLUMMER
ATTN: C GHANBARI
ATTN: W H BARRETT
ATTN: TECH LIB

OTHER GOVERNMENT

FEDERAL EMERGENCY MANAGEMENT AGENCY
ATTN: OFC OF CIVIL DEFENSE

DEPARTMENT OF DEFENSE CONTRACTORS

ABERDEEN RESEARCH CENTER
ATTN: N ETHERIDGE

APPLIEDD RESEARCH ASSOCIATES, INC
ATTN: J KEEFER

APTEK, INC.
ATTN: S SUTHERLAND

BERKELEY RSCH ASSOCIATES, INC.
ATTN: J ORENS

BOEING TECH & MANAGEMENT SVCS, INC.
ATTN: R BRYAN CAIRNS

CARPENTER RESEARCH CORP.
ATTN: H J CARPENTER

CHARLES NEEDHAM
ATTN: ARA
ATTN: CHARLES NEEDHAM

DAYTON, UNIVERSITY OF
ATTN: B WILT
ATTN: R SERVAIS

GENERAL SCIENCES INC
2 CY ATTN: HOWARD SEMON
2 CY ATTN: KENNETH LERNER
2 CY ATTN: L D DEDOMINICIS
2 CY ATTN: MICHAEL C MATTHEWS
2 CY ATTN: PETER D ZAVITSANOS

GEO CENTERS, INC.
ATTN: E MARRAM

GEORGIA INSTITIUTE OF TECHNOLOGY
ATTN: EES/EMSL/SOLAR SITE, C BROWN

H & H CONSULTANTS, INC
ATTN: W HALL

INFORMATION SCIENCE, INC.
ATTN: W DUDZIAK

JAYCOR
ATTN: CYRUP P KNOWLES

KAMAN SCIENCES CORP.
ATTN: D CAYNE
ATTN: LIBRARY

KAMAN SCIENCES CORP.
ATTN: A L PHILLIPS
ATTN: G PADEREWSKI
ATTN: J FANNING
ATTN: T DEUTON
ATTN: Z LAWRENCE

KAMAN SCIENCES CORP.
ATTN: D MOFFETT

KAMAN SCIENCE CORPORATION
ATTN: DASIAC
ATTN: DASIAC/DARE

KARAGOZIAN AND CASE
ATTN: J KARAGOZIAN

LOCKHEED MARTIN CORPORATION
ATTN: S SALISBURY

LOCKHEED MARTIN CORPORATIOON
ATTN: TECH INFO CTR D/COLL, D/90-11, B/106

LOGICON RDA
ATTN: BINKY LEE
ATTN: DONALD SIMONS
ATTN: LIBRARY

LOGICON RDA
ATTN: G GANONG

MAXWELL TECHNOLOGIES INC
ATTN: J BARTHEL
ATTN: K PYATT
ATTN: T PIERCE

MISSION RESEARCH CORP.
ATTN: TECH LIBRARY

NICHOLS RESEARCH CORPORATION
ATTN: R BYRN
ATTN: SDTANLEY R BERRY

PACIFICE-SIERRA RESEARCH CORP.
ATTN: H BRODE

PRIMEX PHYSICS INTERNATIONAL
ATTN: E WILLIS

SCIENCE APPLICATIONS INTL, CORP
ATTN: H WILSON
ATTN: TECHNICAL REPORT SYSTEM

SCIENCE APPLICATIONS INTL CORP
ATTN: J GUEST
ATTN: J SIMMONS
ATTN: W SCHAEFER

SCIENCE APPLICATIONS INTL CORP
ATTN: J COCKAYNE
ATTN: J D BAUM
ATTN: W CHADSEY
ATTN: W LAYSON

SCIENCE APPLICATIONS INTL CORP
ATTN: G BINNINGER

SRI INTERNATIONAL
ATTN: DR JIM GRAN
ATTN: G GREENFIELD

TELEDYNE BROWN ENGINEERING
ATTN: J RAVENSCRAFT
ATTN: MS-12 TECH LIB, P SHELTON

THE AEROSPACE CORP
ATTN: L SELZER M4/925
ATTN: LIBRARY ACQUISITION M1/199

THE BDM CORPORATION OF SAUDI ARABIA
ATTN: E DORCHAK

TITAN CORPORATION
ATTN: J THOMSEN

TITAN CORPORATION
ATTN: A FREDERICKSON

TRW SPACE & DEFENSE SECTOR SPACE &
TECH GROUP ODGEN ENG OPERATIONS
ATTN: OUT6/W WAMPLER

HEADQUARTERS
DEFENSE SPECIAL WEAPONS AGENCY
ATTN: ISA
6801 TELEGRAPH ROAD
ALEXANDRIA, VA. 22310-3398

OFFICIAL BUSINESS

107200/001

DEFENSE TECHNICAL INFORMATION CENTER
DTIC/OCP
8725 JOHN J KINGMAN RD., STE 0944
FT. BELVOIR, VA 22060-6218